Fundamental studies of microalgal biofilm formation and microalgal-bacterial membrane photobioreactors

A Thesis Submitted to the Faculty of Graduate Studies of Lakehead University

by
Yichen Liao

A dissertation submitted in fulfillment of the requirements for the degree of Doctor of Philosophy in Biotechnology

January 2024

Lakehead University, Thunder Bay, Ontario, Canada

Dedication

To my parent for their unconditional guidance and support

Abstract

Microalgae is one of the photoautotrophic microorganisms that has attracted significant attention in wastewater treatment and biofuel production. Although researchers claimed that microalgae cultivation in wastewater treatment has a very high potential for nutrient removal and economic benefit from downstream production, microalgae brought drawbacks such as extra cost and energy consumption due to diluted concentration, lower effluent quality because of suspended biomass, and risk of contamination by bacteria. Biofilm cultivation is considered an alternative to overcome the prementioned disadvantages. Furthermore, involving membrane technology in biofilm cultivation could further promote biomass harvesting efficiency and effluent quality. Thus, the new biofilm membrane bioreactors such as membrane carbonated microalgal biofilm reactor (MCMBR), and extractive membrane microalgal biofilm reactor (EMMBR) should have great prospects in sewage treatment.

In order to take full advantage of those new reactors in industrialization, a comprehensive knowledge of microalgal biofilm formation is required. For this perspective, we processed fundamental research to elucidate the microalgal biofilm formation mechanism on multiple hydrophobic membrane materials through laboratory experiments (bioreactor cultivation) and the rapid detective method (QCM-D). A model to predict microorganisms in membrane photobioreactor was also developed further to inspire the optimization of operating conditions during natural cases.

The results suggest that the contact angle (hydrophobicity), surface free energy, and free energy of cohesion of membrane materials alone could not sufficiently elucidate the selectivity of microalgae cell adhesion and biofilm formation on membrane materials surfaces, and membrane surface roughness played a dominant role in controlling biofilm formation rate, under tested

hydrodynamic conditions. Furthermore, hydrophobicity, surface free energy, free energy of cohesion, and zeta potential played an important role in controlling biofilm formation under low shear stress conditions. Under high shear stress conditions, the hydrodynamic conditions and the presence of a fraction of small particle sizes (<10 μm) of microalgae species were the dominant factors in controlling biofilm formation. In contrast, the importance of the surface properties of microalgae species was diminished. For the same microalgae species, the presence of a fraction of small particle sizes (<10 μm) of the microalgae cells/flocs played a dominant role in controlling biofilm formation under different hydrodynamic conditions. The relative importance of hydrodynamic conditions and surface and physical properties of microalgae cells in controlling biofilm formation would change under different conditions. The quartz crystal microbalance with dissipation (QCM-D) results revealed that the adhered microalgal layers exhibited viscoelastic properties. The relative importance of these mechanisms in controlling microalgae cell attachment and biofilm formation might vary, depending on the properties of specific microalgae species and hydrophobic membrane materials used. The model investigation is suggested for predicting the membrane bioreactor performance, which could shorten the experimental period spent on optimization.

The results obtained in this work replenish the fundamental knowledge of microalgal biofilm mechanisms and provide more insights into how the microalgal biofilm performance will be affected by the properties of microalgae and membrane materials. The thesis results contributed to the knowledge of the optimization of membrane bioreactor operation during laboratory or industrial cases.

Acknowledgements

Upon the completion of this thesis, I would like to express my deep appreciation to the people who helped my research and made this thesis possible.

I would like to extend my sincere gratitude to my supervisors Dr. Pedram Fatehi and Dr. Baoqiang Liao, for their guidance throughout the course of this Ph.D. study. Their rigorous research attitude and creative academic thought have inspired and benefited me a lot. I would also appreciate their kind and patient guidance on my experimental and writing works.

I would like to thank my committee members, Dr. Leila Pakzad, Dr. Ehsan Behzadfar, and Dr. Christopher Q. Lan of the University of Ottawa (external examiner) for taking the time to review my Ph.D. thesis and for their insightful comments.

Also, I acknowledge Lakehead University for international Ph.D. students in Canada and the Natural Sciences and Engineering Research Council of Canada (NSERC) for providing funding to this research. Another financial support from Lakehead University and the Government is also appreciated.

I also want to take this opportunity to thank both faculty and the staff members of the Department of Biology, Instrument Lab and Graduate Studies for their support and encouragement. I would like to take this opportunity to thank all other members of the research group, past and present, who have lent me their assistance and expertise.

Last, but not least, I would like to thank my family and friends from the bottom of my heart for their continuous support and encouragement.

Table of Contents

List of Figures

List of Tables

Chapter 1: Introduction

1.1. Overview

Microalgae are photosynthetic microorganisms that have attracted significant attention due to their potential as a sustainable source of biofuels, high-value compounds, and wastewater treatment [1]. Despite the numerous advantages of microalgae cultivation, several challenges are still associated with current applications [2]. One of the major challenges is the high cost associated with large-scale cultivation, which limits the commercial feasibility of microalgae-based products. These high costs are primarily attributed to the energy requirements for maintaining optimal growth conditions and the extra costs of harvesting diluted suspended microalgae [3]. One promising approach to cultivating microalgae is biofilm technology, where microalgae are grown on a surface in a matrix of extracellular polymeric substances, forming a cohesive community [4]. Microalgal biofilm can compensate for the deficiency of low harvesting efficiency of suspended microalgae [5, 6].

Moreover, microalgal biofilm cultivation has other advantages over traditional planktonic cultivation, such as higher productivity, lower energy requirements, and reduced bacterial contamination risks [6-8]. Microalgal biofilm cultivation can be used widely, including wastewater treatment, aquaculture, biofuels, and high-value compounds [9]. However, insufficient knowledge of the microalgal biofilm formation mechanism is still hindering the microalgal biofilm application [6, 7, 10]. In general, microalgal biofilm formation is influenced by various factors such as attached substrate properties, microalgae species, and environmental conditions, which can mainly affect the adhesion and productivity of microalgal biofilm [11, 12].

Another aspect of promoting microalgae cultivation is building a multi-species ecosystem. Co-culture of phytoplankton is suggested to address several troubles associated with microalgal

monocultures, such as harvesting efficiency and resource utilization [13]. Moreover, researchers mentioned that bacterial communities could play a crucial role in both biofilm formation and microalgae's function, as they provide essential nutrients and create a favourable environment for microalgal growth [14, 15]. Many studies revealed that the co-culture of phytoplankton combined with heterotrophic bacteria benefits all groups [16-18]. As a result, the concerns about microalgal-bacterial co-cultivation have been rising in the last decade besides individual microalgae strain cultivation. In addition, microalgae-bacteria membrane photobioreactors (MB-MPBRs) have gained significant attention in recent years as an effective approach to wastewater treatment [19]. The photobioreactors utilize a membrane separation system that facilitates the separation of community biomass from a liquid medium, thereby providing higher harvesting efficiency [20]. Furthermore, the application of MB-MPBRs has shown promise for wastewater treatment, as the microalgae and bacteria can effectively remove nutrients and contaminants from wastewater while simultaneously producing biomass for various applications [21, 22]. However, severe membrane fouling and competition between microorganism strains are current issues that influence microbial biomass production performance. Multiple studies have been conducted to explore the optimal conditions for MB-MPBR cultivation [19, 23, 24]. Models of examining microorganisms' growth kinetic are also applied prior to laboratory experiments to reduce the extra work on optimization [25-27].

Considering the techniques mentioned above, a new concept of cultivation that includes biofilm construction, microalgal-bacterial co-culture, and membrane photobioreactor can increase cost-efficiency in wastewater treatment with advantages such as large biomass production, economic benefits from further downstream production and effective pollutant removals [28, 29]. Despite microalgal-bacterial biofilm membrane photobioreactors showing promise as a

sustainable and efficient technology for microalgae cultivation, several challenges still need to be addressed to realize their full potential. One challenge is the optimization of the physical and chemical parameters that affect the growth of microorganisms in the biofilm. This includes the optimization of operation conditions, cell-substratum adhesion, as well as optimization of environmental conditions and so on [11, 30-32]. Another challenge is the development of efficient and cost-effective membrane materials that can facilitate biofilm formation and biomass retention [20]. Selecting suitable membrane materials is crucial for achieving high biomass productivity, preventing fouling, and maintaining long-term system stability [33, 34]. Furthermore, the scale-up of MB-MPBR systems remains challenging, particularly for large-scale commercial applications. This requires careful consideration of system design, energy consumption, and cost-effectiveness.

Despite these challenges, the MBB-MPBR technology has several prospects for future development and applications. One potential application is using MB-MPBR systems for wastewater treatment, where microalgae and bacteria can remove nutrients and pollutants from wastewater [24, 35, 36]. In addition, producing high-value compounds, such as bioactive molecules or pigments, using MB-MPBR technology offers a promising approach for commercial applications. Lastly, the potential of MB-MPBRs for biofuel production also presents an attractive alternative to conventional fuel sources, and ongoing research is exploring the feasibility of this technology [15, 37, 38]. Overall, the MB-MPBR technology shows great potential for sustainable and efficient microalgae cultivation. However, further research and development are necessary to overcome the current challenges and realize their full potential.

The main goal of this dissertation was to study the biofilm formation mechanism via investigation of the interaction between cell-substratum, microalgae traits, and operation

conditions of reactors. I was aiming to construct a more comprehensive fundamental knowledge for further microorganism biofilm membrane photobioreactor applications.

1.2. Novelty

The present thesis comprehensively investigated, for the first time, the impacts of membrane and microalgae surface, physical, and chemical properties on microalgae cell adhesions and biofilm formation by exploring interactions between microalgae and hydrophobic and hydrophilic membrane materials in a CDC (Centers for Disease Control and Prevention) biofilm reactor. Additionally, for the first time, advanced technologies, such as quartz crystal microbalance (QCM), were used to provide new insights into the interactions of microalgae cells and hydrophobic membrane materials. Furthermore, a fundamental mathematical model has been developed, for the first time, to predict the hydraulic and solid retention time (HRT and SRT) and influent COD/N ratio effects on the biological performance (COD, N and P removals, bacteria biomass, and microalgae biomass concentration) of microalgal-bacterial membrane separation photobioreactor (MB-MSPBR).

1.3. Objectives of the proposed study

The overall objectives of this study were to

1. investigate the surface properties of membrane materials and their role in cell adhesion and biofilm formation of microalgae in a CDC biofilm reactor;
2. investigate the surface properties of microalgae and their role in microalgal cell adhesion and biofilm formation under different hydrodynamic conditions in a CDC biofilm reactor;
3. investigate the microalgal cells' adhesion on hydrophobic membrane substrate and the effect of membrane materials and microalgae surface properties on cell adhesions by employing an emerging rapid detective technique (QCM-D);

4. construct a numerical mathematical model to simulate the microalgal-bacterial membrane photobioreactor performances in terms of HRT, SRT, and influent COD/N ratio influences.
The following chapters are presented in this thesis to address the proposed objectives.

Chapter 1 is the introduction (present chapter) that briefly discusses the importance, rationale, novelty, and objectives of this study in the thesis.

Chapter 2 briefly introduces the microalgal biofilm cultivation process and microalgae-bacterial process in the current wastewater treatment area. The literature summarized the microalgal biofilm formation mechanism research and the numerical methods for predicting microalgae-bacterial growth behaviours in past studies.

Chapter 3 investigates the influences of membrane surface properties and physical and chemical properties of *Chlorella vulgaris* cells on microalgal cell adhesion performance in a CDC biofilm reactor. *Chlorella vulgaris* cells have a high adhesive affinity on nylon substrate.

Chapter 4 reveals the effect of surface, physical, and chemical properties of different microalgal strains on cell adhesion on nylon membrane substrate under different hydrodynamic conditions in a CDC biofilm reactor.

Chapter 5 employs the quartz crystal microbalance with dissipation (QCM-D) technique to study the microalgae initial adhesion mechanism on the hydrophobic membrane substrates in real-time monitoring conditions. The effects of surface properties of different membrane materials and different microalgae species on microalgae cell adhesion were studied using QCM-D.

Chapter 6 demonstrates a numerical method to simulate the microalgae performance in membrane photobioreactors. The effects of hydraulic retention time (HRT), solid retention time (SRT), and

influent N/P ratios on the biological performance (N, P removals, and microalgae biomass growth) of MPBR were simulated using the proposed mathematical models.

Chapter 7 demonstrates a numerical method developed based on the previous chapter to simulate the biological performance of microalgal-bacterial cooperation in membrane photobioreactors. The effects of hydraulic retention time (HRT), solid retention time (SRT), and influent COD/N ratios on the biological performance (COD, N, P removals, bacteria biomass and microalgae biomass growth) of MB-MSPBR were simulated using the proposed mathematical models.

Chapter 8 summarizes conclusions and suggestions for future research.

1.4. The list of publications

Liao, Y., Bokhary, A., Maleki, E., Liao, B. (2018). A review of membrane fouling and its control in algal-related membrane processes. Bioresource Technology, 264, 343-358.

Liao, Y., Alam, N., Fatehi, P. (2022). Semitransparent films from low-substituted carboxymethylated cellulose fibers. Journal of Materials Science, 57(22), 10407-10424.

Chapter 3 has been published in the Journal of Biofouling

Liao, Y., Fatehi, P., Liao, B. (2023). Surface properties of membrane materials and their role in cell adhesion and biofilm formation of microalgae. Biofouling, 39:8, 879-895.

Chapter 5 has been published in Colloids and Surfaces B: Biointerfaces

Liao, Y., Fatehi, P., Liao, B. (2023). Microalgae cell adhesions on hydrophobic membrane substrates using Quartz crystal microbalance with dissipation. Colloids and Surfaces B: Biointerfaces, 230, 113514.

1.5. References

[1] Posten, C., Chen, S.F. (2016). Microalgae biotechnology. Springer International Publishing: Switzerland.
[2] Spolaore, P., Joannis-Cassan, C., Duran, E., Isambert, A. (2006). Commercial applications of microalgae. Journal of Bioscience and Bioengineering, 101, 87-96.
[3] Milledge, J.J., Heaven, S. (2013). A review of the harvesting of micro-algae for biofuel production. Reviews in Environmental Science and Bio/Technology, 12, 165-178.
[4] Moreno Osorio, J.H., Pollio, A., Frunzo, L., Lens, P.N.L., Esposito, G. (2021). A review of microalgal biofilm technologies: definition, applications, settings and analysis. Frontiers in Chemical Engineering, 3, 737710.
[5] Kokare, C., Chakraborty, S., Khopade, A., Mahadik, K.R. (2009). Biofilm: Importance and applications. Indian Journal of Biotechnology, 8, 159-168.
[6] Mantzorou, A., Ververidis, F. (2019). Microalgal biofilms: A further step over current microalgal cultivation techniques. Science of the Total Environment, 651, 3187-3201.
[7] Li, T., Strous, M., Melkonian, M. (2017). Biofilm-based photobioreactors: their design and improving productivity through efficient supply of dissolved inorganic carbon. FEMS Microbiology Letters, 364, fnx218.
[8] Ozkan, A., Kinney, K., Katz, L., Berberoglu, H. (2012). Reduction of water and energy requirement of algae cultivation using an algae biofilm photobioreactor. Bioresource Technology, 114, 542-548.
[9] Hu, Y., Xiao, Y., Liao, K., Leng, Y., Lu, Q. (2021). Development of microalgal biofilm for wastewater remediation: from mechanism to practical application. Journal of Chemical Technology and Biotechnology, 96, 2993-3008.
[10] Berner, F., Heimann, K., Sheehan, M. (2015). Microalgal biofilms for biomass production. Journal of Applied Phycology, 27, 1793-1804.
[11] Toyofuku, M., Inaba, T., Kiyokawa, T., Obana, N., Yawata, Y., Nomura, N. (2016). Environmental factors that shape biofilm formation. Bioscience, Biotechnology, and Biochemistry, 80, 7-12.
[12] Kesaano, M., Sims, R.C. (2014). Algal biofilm based technology for wastewater treatment. Algal Research, 5, 231-240.
[13] Wicker, R.J., Kwon, E., Khan, E., Kumar, V., Bhatnagar, A. (2022). The potential of mixed-species biofilms to address remaining challenges for economically-feasible microalgal biorefineries: A review. Chemical Engineering Journal, 451, 138481.
[14] Devi, N.D., Tiwari, R., Goud, V.V. (2023). Cultivating *Scenedesmus sp*. on substrata coated with cyanobacterial-derived extracellular polymeric substances for enhanced biomass productivity: a novel harvesting approach. Biomass Conversion and Biorefinery, 13, 2971-2983.
[15] Wang, H., Deng, L., Qi, Z., Wang, W. (2022). Constructed microalgal-bacterial symbiotic (MBS) system: Classification, performance, partnerships and perspectives. Science of The Total Environment, 803, 150082.
[16] Scognamiglio, V., Giardi, M.T., Zappi, D., Touloupakis, E., Antonacci, A. (2021). Photoautotrophs–bacteria co-cultures: Advances, challenges and applications. Materials, 14, 3027.
[17] Kwon, G., Kim, H., Song, C., Jahng, D. (2019). Co-culture of microalgae and enriched nitrifying bacteria for energy-efficient nitrification. Biochemical Engineering Journal, 152, 107385.

[18] dos Santos, V.Z., Vieira, K.R., Nass, P.P., Zepka, L.Q., Jacob-Lopes, E. (2021). Application of microalgae consortia/cocultures in wastewater treatment. Recent Advances in Microbial Degradation, Springer: Singapore, pp. 131-154.
[19] Zhang, M., Leung, K.T., Lin, H., Liao, B. (2021). Effects of solids retention time on the biological performance of a novel microalgal-bacterial membrane photobioreactor for industrial wastewater treatment. Journal of Environmental Chemical Engineering, 9, 105500.
[20] Zhao, Z., Muylaert, K., Vankelecom, I.F. (2023). Applying membrane technology in microalgae industry: A comprehensive review. Renewable and Sustainable Energy Reviews, 172, 113041.
[21] Zhang, B., Li, W., Guo, Y., Zhang, Z., Shi, W., Cui, F., Lens, P.N., Tay, J.H. (2020). Microalgal-bacterial consortia: from interspecies interactions to biotechnological applications. Renewable and Sustainable Energy Reviews, 118, 109563.
[22] Wang, H., Hill, R.T., Zheng, T., Hu, X., Wang, B. (2016). Effects of bacterial communities on biofuel-producing microalgae: stimulation, inhibition and harvesting. Critical Reviews in Biotechnology, 36, 341-352.
[23] Segredo-Morales, E., González, E., González-Martín, C., Vera, L. (2022). Secondary wastewater effluent treatment by microalgal-bacterial membrane photobioreactor at long solid retention times. Journal of Water Process Engineering, 49, 103200.
[24] Ashadullah, A., Shafiquzzaman, M., Haider, H., Alresheedi, M., Azam, M.S., Ghumman, A.R. (2021). Wastewater treatment by microalgal membrane bioreactor: evaluating the effect of organic loading rate and hydraulic residence time. Journal of Environmental Management, 278, 111548.
[25] Moreno-Grau, S., Garcia-Sanchez, A., Moreno-Clavel, J., Serrano-Aniorte, J., Moreno-Grau, M. (1996). A mathematical model for waste water stabilization ponds with macrophytes and microphytes. Ecological Modelling, 91, 77-103.
[26] Buhr, H., Miller, S. (1983). A dynamic model of the high-rate algal-bacterial wastewater treatment pond. Water Research, 17, 29-37.
[27] Papáček, Š., Jablonský, J., Petera, K. (2017). Towards Integration of CFD and Photosynthetic Reaction Kinetics in Modeling of Microalgae Culture Systems.Proceedings of the Bioinformatics and Biomedical Engineering: 5th International Work-Conference, IWBBIO 2017; April 26–28; Granada, Spain. pp. 679-690.
[28] Wang, X., Hong, Y. (2022). Microalgae biofilm and bacteria symbiosis in nutrient removal and carbon fixation from wastewater: A review. Current Pollution Reports, 8, 128-146.
[29] Derakhshan, Z., Mahvi, A.H., Ehrampoush, M.H., Ghaneian, M.T., Yousefinejad, S., Faramarzian, M., Mazloomi, S.M., Dehghani, M., Fallahzadeh, H. (2018). Evaluation of kenaf fibers as moving bed biofilm carriers in algal membrane photobioreactor. Ecotoxicology and Environmental Safety, 152, 1-7.
[30] Huang, Y., Zheng, Y., Li, J., Liao, Q., Fu, Q., Xia, A., Fu, J., Sun, Y. (2018). Enhancing microalgae biofilm formation and growth by fabricating microgrooves onto the substrate surface. Bioresource Technology, 261, 36-43.
[31] Schmidt, H., Thom, M., Wieprecht, S., Manz, W., Gerbersdorf, S.U. (2018). The effect of light intensity and shear stress on microbial biostabilization and the community composition of natural biofilms. Research and Reports in Biology, 9, 1-16.
[32] Wang, C., Tan, Y., Zhu, L., Zhou, C., Yan, X., Xu, Q., Ruan, R., Cheng, P. (2022). The intrinsic characteristics of microalgae biofilm and their potential applications in pollutants removal—A review. Algal Research, 68, 102849.

[33] Tong, C., Chang, Y.S., Ooi, B.S., Chan, D.J.C. (2021). Physico-chemistry and adhesion kinetics of algal biofilm on polyethersulfone (PES) membrane with different surface wettability. Journal of Environmental Chemical Engineering, 9, 106531.
[34] Zhang, M., Yao, L., Maleki, E., Liao, B.-Q., Lin, H. (2019). Membrane technologies for microalgal cultivation and dewatering: Recent progress and challenges. Algal Research, 44, 101686.
[35] Saini, S., Tewari, S., Dwivedi, J., Sharma, V. (2023). Biofilm Mediated Wastewater Treatment: A Comprehensive Review. Materials Advances, 4, 1415-1443.
[36] Morillas-España, A., Lafarga, T., Sánchez-Zurano, A., Acién-Fernández, F.G., González-López, C. (2022). Microalgae based wastewater treatment coupled to the production of high value agricultural products: Current needs and challenges. Chemosphere, 291, 132968.
[37] Patwardhan, S.B., Pandit, S., Ghosh, D., Dhar, D.W., Banerjee, S., Joshi, S., Gupta, P.K., Lahiri, D., Nag, M., Ruokolainen, J. (2022). A concise review on the cultivation of microalgal biofilms for biofuel feedstock production. Biomass Conversion and Biorefinery, 1-18.
[38] Moshood, T.D., Nawanir, G., Mahmud, F. (2021). Microalgae biofuels production: A systematic review on socioeconomic prospects of microalgae biofuels and policy implications. Environmental Challenges, 5, 100207.

Chapter 2: Understanding of microorganism biofilm cultivation and current photobioreactor system: a review

Abstract

Microorganism biofilm cultivation and photobioreactor systems have emerged as promising approaches for the sustainable production of biofuels, high-value compounds, and wastewater treatment. This review provides an overview of the current understanding of microorganism biofilm cultivation and photobioreactor systems, highlighting recent advancements in the field. The review discusses the importance of microbial interactions and biofilm formation for efficiently cultivating microorganisms, particularly microalgae. Developing novel photobioreactor systems, such as membrane photobioreactors, has shown promising results for improving microalgal productivity and biomass accumulation. However, much must be learned about the complex mechanisms involved in biofilm formation and bacterial-microalgal interactions and how these can be harnessed for more efficient and sustainable cultivation methods. The review also discussed the modelling development on microorganism growth and revealed its importance in membrane photobioreactor study, which could accelerate the operation optimization before experimental research. Comprehensively understanding microorganism biofilm cultivation and photobioreactor systems offers a promising path toward sustainable and environmentally friendly technologies for producing biofuels and high-value compounds.

Keywords: Microalgal biofilm, wastewater treatment, microalgae-bacteria, membrane photobioreactor, modelling

2.1. Introduction

Microalgae have earned much attention in decades, and microalgae-based products have been applied to a wide range of areas such as nourishment, cosmetics and biochemical [1-4]. Microalgae biomass also can be the feedstock of biofuel due to its high lipid content [5]. Based on this premise, some literature suggested that microalgae also could be applied to the biological process of wastewater treatment as it can consume the nutrients from wastewater while supplying biomass for biofuel production [6-8]. Conventional biological wastewater treatment is aerobic activated sludge or anaerobic technologies, primarily employing the bacteria as objective microorganisms. These traditional biological processes require high energy consumption that could occupy about 60% to 80% of the total energy consumption of the whole wastewater treatment process [9]. As a by-product of wastewater treatment, activated sludge could cause serious environmental problems even though they are currently utilized as a prominent participant in wastewater treatment [10-12]. Compared to the bacterial-based process, the microalgal process could lower the energy expenditure due to its photo-autotrophic property. In contrast, the microalgal biomass can be further supplied to more valuable downstream production [13].

However, the industrialization of microalgae wastewater treatment has been restricted by problems such as growth limited by environmental conditions (illumination, CO_2), contamination from other organisms, and high harvest cost compared to the activated sludge process [14-17]. Vandamme et al. mentioned that the biomass concentration of typical microalgal cultivation in both closed and open pond photobioreactors ranges from 0.5-5 g/L [18]. This diluted concentration requires larger land occupation for cultivation and extra harvesting to achieve the desirable biomass. Literature has been studied to optimize the operation parameter to facilitate the microalgal biomass production yield [19, 20]. However, even though more studies have been done,

suspended cultivation mode cannot fulfill the sustainable purpose of wastewater treatment. Yang et al. mentioned that water consumption in suspended cultivation could reach 200 times the amount of microalgae products [21]. As a result, the concept that culture microalgae in that form of biofilm could be a solution to improve the dilution issue [22]. Biofilm was initially considered a role that causes membrane fouling during wastewater treatment [23, 24]. In the beginning, researchers try to mitigate biofilm growth because it will shorten the life cycle of the membrane and increase the operation cost [25]. Then, the literature investigated microalgal biofilm cultivation in wastewater treatment and found that they performed better than suspended microalgae [26-28]. When microalgae are grown as biofilms attached to the substrate, the biomass concentration is concentrated, which even could reach tenfold the suspended concentration [29]. Moreover, harvesting becomes easier, lowering downstream operation costs [22]. Recently, Gao et al. suggested that wastewater treatment harvest efficiency and effluent quality could be further improved if a microfiltration membrane module was employed in the photobioreactor [30]. The separated solid retention time and hydraulic retention time can be individually controlled during the culture period, which leads to a high-level biomass concentration maintained without the effect of hydraulic loading of the reactor [31, 32]. Gao et al. investigated this membrane module and found that *Chlorella vulgaris* exhibited a higher nutrient removal in this system (4.13 mg nitrogen $L^{-1}d^{-1}$ and 0.43 mg phosphorus $L^{-1}d^{-1}$, respectively) compared to conventional photobioreactor (0.59 mg nitrogen $L^{-1}d^{-1}$ and 0.08 mg phosphorus $L^{-1}d^{-1}$, respectively) [33].

Another solution for reducing production expenses could be the utilization of the symbiosis between microorganisms, especially bacteria and microalgae. Microalgae-bacteria symbiotic interactions have advantages such as promoting microorganism growth, accelerating wastewater removal efficiency, facilitating the accumulation of carbohydrate lipid content in microalgae

biomass, and increasing the bio-flocculation between microalgae and bacteria [34]. Subashchandrabose et al. pointed out that microalgae-bacteria-based biotechnology is more promising in sustainability and industrialization than individual microorganisms-based ones [35]. However, microalgal-bacterial interactions are more complex than the individual organism because they include diverse relationships ranging from synergy to competition [36]. Microalgae and bacteria could be the mutual providers of gas and nutrients. The former supplies oxygen and organic carbon; the latter offers carbon dioxide, fixed nitrogen, and siderophores [37, 38]. In addition, research also reveals that most bacteria can accelerate the bio-flocculation of microalgae by secreting extracellular polymeric substances (EPSs), which will benefit biomass harvesting [39]. However, the antagonistic effects, such as competition among microorganisms, are also a non-negligible part of the development of microalgae and bacteria during cultivation. Microorganisms (either bacteria or microalgae) will produce inhibitors such as toxins or exotoxins to limit the growth of other organisms when the resource supplication (nutrient, living area, etc.) is insufficient [39, 40]. Thus, the optimization of operating conditions for microalgal-bacterial cultivation is required. Many experiments have been done to investigate the impact factors that influence the performance of microalgae-bacteria cultivation [41-43].

Nevertheless, the optimization of microorganism cultivation is time-consuming and usually species-dependent. Thus, more rapid research techniques to monitor real-time microorganism growth in photobioreactors are required to shorten the optimization period. As a result, the mathematical models used for studying and predicting microalgal-bacterial growth behaviour have also been developed [44]. The mathematical models are highly adaptable to examining different dynamic variables compared to the experiment. Appropriately employing a

mathematical model as the pre-testing method can facilitate optimizing the microalgal-bacterial system design.

Accordingly, a microalgal-bacterial-based membrane photobioreactor could take the most advantages in wastewater biological treatment, such as high pollutant removal, efficient biomass harvesting, and good economic benefits. The employment of mathematical models in the initial experiments could shorten the reaction optimizing stage, thus promoting the efficiency of experiments. However, the study on microalgal-bacterial based membrane photobioreactor is limited and lacks comprehensive fundamental knowledge regarding biofilm formation mechanism, the interaction among the microorganisms (bacteria and microalgae), and model fitting on simulation real-time microorganisms' activities. More experimental studies are required to construct the benchmark and fundament of this system for further industrialization.

The objective of this work is to provide a comprehensive fundamental review to discuss the different studies of microalgal biofilm cultivation in the photobioreactor, the major factors affecting the biofilm formation in the culture system and recent research on the microalgal-bacterial system in membrane photobioreactors. It also investigates the current status of applications of microalgae biofilm photobioreactors for wastewater treatment with a particular emphasis on establishing a common view for microalgal biofilm membrane photobioreactors. Further biotechnological applications of microalgal-bacterial combinations and the appropriate strategies to promote their practical applications are critically assessed. The main challenges ahead to scale up microalgal biofilm photobioreactor and the corresponding recommendations for further research are also addressed. This critical review is expected to replenish the fundamental understanding of the microalgal biofilm formation mechanisms and the microalgal-bacterial membrane photobioreactors. And guiding and inspiring researchers to solve the present

environmental problems and to motivate large-scale applications of microalgal biofilm photobioreactors in wastewater treatment.

2.2. Development of microalgae cultivation on wastewater treatment.

Microalgae are one group of photoautotrophic microorganisms that widely exist in nature and the human living environment. As previously mentioned, microalgae biomass has a wide range of applications and a high potential for the next generation of energy applications. Besides, microalgae cultivation is also considered to mitigate greenhouse gas emittance due to its ability of CO_2 fixation [45]. However, obtaining a significant amount of microalgal biomass in the natural environment is impossible except for algal bloom, which leads to severe environmental problems and harms the ecosystem [46]. As a result, photobioreactors for microalgae cultivation have been developed to obtain a considerable amount of microalgal biomasses. Initially, microalgae cultivation focused on biomass harvesting; until now, some have successfully applied it to large-scale industrialization [47, 48]. Many studies reported that microalgae could uptake the inorganic nitrogen and phosphorus and convert them into organic biomass [49]. The studies of microalgae application in wastewater treatment can be traced back to the 1950s [50]. The initial application of photobioreactors for large-scale cultivation in pollutant treatment was introduced by the Carnegie Institute in 1953 [51]. Researchers are now considering microalgal-base biological processes in wastewater treatment as next-generation technology and are still working on optimizing operating conditions [52]. Microalgae can generally be divided into two basic structures: open ponds and closed systems. In the beginning, open ponds earned many concerns due to their low cost, simple construction and easy operation [52]. However, problems such as low biomass production yield, high risk of contamination, and limitation of environmental conditions came out, followed by further studies. In order to improve these issues, the concept of closed systems was introduced to

practical applications and scientific research. Different from traditional biological approaches in wastewater treatment, microalgal-based photobioreactors require a relatively high hydraulic retention time and extra growth factors such as light and carbon dioxide [17], which could be the limitation restricting photobioreactor performance in contrary. However, current microalgae cultivation is still trapped in the diluted biomass concentration issue, and new versions or designs, such as hybrid photobioreactors, have been developed to improve their efficiency [51]. Among those emerging photobioreactors, microalgae biofilm photobioreactors are one of the most concerned systems.

2.3. Microalgae biofilm cultivation in photobioreactor system

2.3.1. Microalgae biofilm formation and cultivation systems

As an emerging concept in the last decade, microalgae biofilm cultivation has attracted more and more concerns in water treatment and biofuel/biodiesel production due to its advantages, such as high production yield and low expense [53, 54]. The formation of microalgae biofilm can be expressed as following steps: i) suspended microalgae cells adhere to the solid substrate surface by the interaction forces, such as van der Waals attraction to form an initial thin layer; ii) attached microalgae cells start to colonize which results in biofilm thickening and secreting extracellular polymeric substances (EPSs) to capture surrounded nutrients and maintain the layer matrixes; iii) Biofilm thickness became stable in a certain value due to the diffusion limitation; iv) Biofilm detaches from substrate surface because of the cell death [55, 56].

Microalgal biofilm can be classified into two main types: single-species biofilm and multiple-species biofilm. The former aims to manufacture purposes such as bio-transformations, and the latter is mainly applied to wastewater treatment [57, 58]. Monospecies biofilm could easily

control the product quality, but it is rare and requires extra purification costs [59]. Individual species biofilm earns many concerns on biotechnology due to its ease in regulating system conditions, resulting in time-saving and cost-effectiveness [60]. When it comes to multiple-species biofilm, this type can take full advantage of consuming the nutrients from polluted water due to its mixotrophic property [61].

Furthermore, multiple-species biofilms have higher environmental resistance, which can ensure their process easier regrowth undergoing a routine harvesting cycle, resulting in higher biomass productivity as the biofilm matures [62]. Nevertheless, multiple-species biofilm cultivation becomes more complicated than single species because it involves the interaction between microalgae species or even microalgae and bacteria. Besides, as Koedooder et al. mentioned, this interaction is governed by the species, leading to some compositional shift that happens when different microorganism species are grown together [63].

Microalgal biofilm bioreactors can be classified into three different types : (a) Constantly submerged biofilm reactors, (b) Partially submerged biofilm reactors, and (c) Permeated biofilm reactors (Figure 2.1). Table 2.1 shows recent research on these three types of reactors and the used parameters. The choice of reactor type usually depends on their reusability, durability, pricing, and even microalgae species [64, 65]. Submerged biofilm reactors are the simplest ones with eased operation. Still, the drawbacks of submerged biofilm reactors are high requests for dissolved carbon dioxide supplication and long-term washout, resulting in the loss of substrate/carriers [66]. For the partially submerged biofilm reactor, even though it can increase the contact of carbon dioxide, the mechanical error could be caused by long-term constant mechanical movements, which lead to a low process flexibility [22]. Regarding permeated biofilm reactors, although permeated biofilm reactors contribute to a pretty high gas transfer efficiency to the microalgal

biofilm, the thicker biofilm can instead hinder the mass transfer of nutrients [55]. Currently, the large-scale applications of microalgal biofilm photobioreactors are still invalid, which requires more fundamental knowledge to optimize the microalgae biofilm growth and to increase biomass production yield.

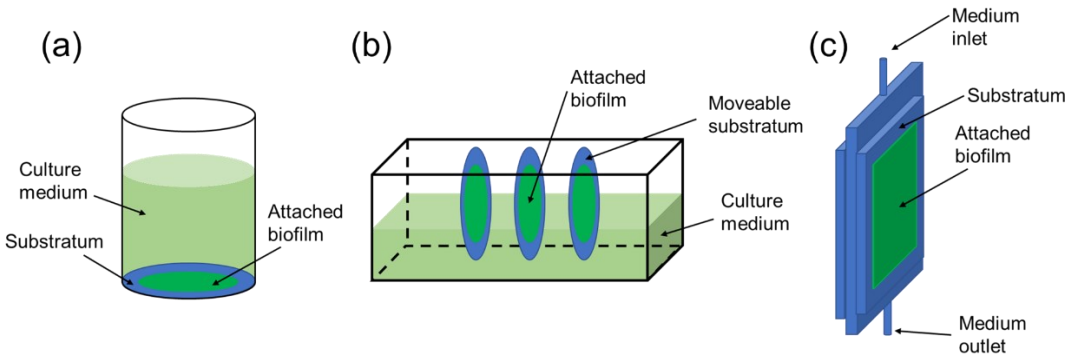

Figure 2.1. Schematic designs of the (a) constantly submerged, (b) partially submerged and (c) permeated microalgal biofilm bioreactor.

Table 2.1. Recent studies on different types of biofilm reactors.

Culture system	Area(m^2)	Substrate	Culture medium	Species	Biomass production	Ref
Constantly submerged biofilm						
Multi-layers photobioreactor	0.007	Polyethylene foam	Modified basal	*Botryococcus braunii*	34.40 $g \cdot m^{-2}$	[67]
		Glass fiber reinforced plastic			63.80 $g \cdot m^{-2}$	
Flat plate photobioreactor	0.004	Glass	CHU-10 diatom medium	*Nitzchia palea*	2.8 $g \cdot m^{-2}d^{-1}$	[68]
Partially submerged biofilm						
Rotating flat plate photobioreactor	0.036	Polyvinyl chloride	Bold's basal	*Chlorella vulgaris SAG 211-12*	3.35 $g \cdot m^{-2}$	[69]
Rocking cultivation reactor	0.019	Glass-reinforced plastic	Modified basal	*Chlorococcum sp.*	4.26 $g \cdot m^{-2}d^{-1}$	[60]
		Stainless steel		*Scenedesmus dimorphus*	0.39 $g \cdot m^{-2}d^{-1}$	

Table 2.1. (*Contd.*)

Culture system	Area(m^2)	Substrate	Culture medium	Species	Biomass production	Ref
Permeate biofilm						
Porous substrate bioreactor	0.0012	Glass fiber filter paper	BG-11	*Anabaena variabilis*	2.88 $g \cdot m^{-2} d^{-1}$	[70]
Algal biofilm photobioreactor	0.275	Concrete	BG-11	*Botryococcus braunii*	24.94 $g \cdot m^{-2}$	[71]

2.3.2. Factors that influence the microalgal biofilm reactor performance

The microalgal biofilm reactor performance can be affected by the behaviour of microalgal biofilm. The mechanism of microalgal biofilm formation is still being studied. Some literature points out that it could be attributed to three main aspects: substrate properties, microalgae properties and reactor operation conditions [72].

2.3.2.1. Properties of the substrate

As Kesaano and Sims mentioned, substrate properties play a significant role in the initial adhesion of the suspended microalgal cells [72]. Studies have been done to determine the influence of surface characteristics on biofilm formation to enhance microalgal cell attachment and biofilm growth [73-75]. The effect of substrate materials is usually attributed to physicochemical properties such as hydrophobicity, surface energy, and surface topography [76-78]. Hydrophobicity is one of the essential factors in cell-substrate interactions. Some literature noticed that microalgal cell adhesion preferred hydrophobic surfaces due to the water exclusion mechanism [79, 80]. Sekar et al. investigated attachments of multiple microalgae species (*Chlorella vulgaris, Nitzschia amphibian,* and *Chroococcus minutes*) on different material surfaces [81]. They found more extraordinary adhesion performance on hydrophobic surfaces (titanium, Perspex, and stainless steel). On the contrary, some research claimed that the hydrophilic substrate

could promote some microalgal biofilm growth due to the effective nutrient diffusion caused by its great liquid-holding capacity [77, 82, 83]. Tsavatopoulou et al. observed a similar phenomenon: *Neocholris vigensis* exhibited better biofilm attachment on the hydrophilic substrate than hydrophobic ones [84]. However, there is an argument that hydrophobicity can not solely explain the complex biofilm adhesion mechanism. Ozkan et al. pointed out that the surface hydrophobicity of material has little contribution to the adhesion strength of microalgal biofilms [74]. Another material property that could significantly affect biofilm formation is surface roughness. Rough or porous surfaces have a higher potential on remaining biofilm biomass and prevent detachment driven by hydraulic shear stress due to their larger groove area than the smooth material [59, 72]. Danaee et al. found that *S. dimorphus* gained thicker biofilm on modified polyethylene terephthalate (PET) threads due to the augment of roughness [85]. However, one drawback of rough or porous material is that microalgae harvesting becomes more challenging to remove the biomass from those microgrooves or pores from the surface [29].

Moreover, the surface charges of the substrate could also be a factor taken into account in microalgal biofilm adhesion performance. The substrate with the charged surface has more intensive positive or negative performances due to the enhanced electrostatic interaction compared to the natural ones. As is known, microalgae cells usually exhibit a negative charge due to their extracellular polymeric substance properties [86]. As a result, microalgae cells are attracted to positive charges by neutralization and repelled to negative charges due to electron repulsion. Zeng et al. also mentioned that microalgal cells have a better preference to adhere to solid substrates with positive charges [87]. Moreover, Huang et al. claimed that membrane fouling could be mitigated by the utilization of a modified membrane with a negative surface charge because of its excellent repellence of microalgae cells [88].

2.3.2.2. Properties of microalgal cells

During the thickening stage, microalgae biofilm tends to colonize to increase thickness rather than adhere to surrounding cells. As a result, the capacity of microalgal biofilm to maintain the three-dimensional matrixes is important, which will reflect in the intensity of cell-cell interaction. One dominant objective among interactions might be extracellular polymeric substances (EPS), a macromolecule secreted from microalgae cells. EPSs secreted from microalgae cells are developed into two categories: the soluble section dispersed into the culture medium, known as soluble EPSs or soluble microbial products (SMPs), and other remains surrounding cells for protection or binding purposes are called bounded EPSs [37, 89]. Cheah and Chan illustrated that EPS plays a role in maintaining biofilm structure and aggregation of nutrients from culture medium [90]. The cell-cell and cell-substrate interactions could be affected by EPSs because they generally express themselves as a cover layer outside the cells. As a result, the surface properties of the cell can be changed depending on the EPS properties [37, 89]. Some researchers mentioned that they could describe EPS-surface interaction by extended Derjaguin-Landau-Verwey-Overbeek (XDLVO) theory because the short-range thermodynamic interactions primarily controlled those interactions [91, 92]. The influences of EPS on biofilm formation can be divided into EPS production and EPS composition. Accumulation of EPS between the cell surface and substrate would enhance the microalgal biofilm adhesion strength due to the increasing affinity parts (whether hydrophilic or hydrophobic) [55]. Shen et al. investigated *B. braunii* biofilm formation on different substrates, and they found that higher attachment always came with a higher EPS concentration in the area [67].

Moreover, scientists also reveal that the biofilm adhesion is affected by the EPS constitution because they observed that microalgae biofilm showed dependence on the affinity of

the dominant part of EPSs to the substrate [93, 94]. In addition, Mühlenbruch et al. also noticed that the acidic sugar monomers like uronic acid and sulfonic acid in the EPS could also facilitate cell aggregation to promote biofilm formation [93]. Moreover, the surface properties of the microalgal cells can also be represented by the surface properties of bonded EPS in some ways due to the bonded EPS forming the outside layer of microalgae cells. For instance, Ji et al. investigated the adhesion properties of *Chlorella vulgaris* EPS on polymethyl methacrylate (PMMA) and polytetrafluoroethylene (PTFE) materials, respectively. They found that the hydrophobic fractions were dominant in bonded EPS, resulting in a higher adhesion behaviour on hydrophobic PTFE than hydrophilic PMMA [95].

Furthermore, regardless of EPS, some studies also mention that biofilm formation is affected by the microalgae species based on cell structure [96, 97], EPS formation [23, 37], and so on. Patwardhan et al. also pointed out that some microalgae species have a born affinity to adhere to solid surfaces instead of growing on a suspended medium. They mentioned that *Nitzschia palea* is a highly adherent example that could form a stronger biofilm than *Scenedesmus obliquus* [66]. Another significant factor in the microalgae aspect could be considered the morphology of individual cells (shape or size). As Gross et al. mentioned, the influence of the size of the microalgal cell on adhesion behaviour could be associated with the surface textures of the substrate [98]. And literature also mentioned that more microalgae cells would remain on the rough substrate surface if their sizes are below the ridge spacing of the microgroove on the substrate surface [99-101]. However, there is an argument that larger ridge spacing would not contribute to the adhesion of microalgae cells. Cui et al. believed that the strength of microalgae adhesion is driven by the amount of contact points between microalgal cell and substrate, and the adhesion strength would increase with the rising number of contact points [102]. Thus, they claimed that the highest

adhesion would be achieved due to the most contact points generated when the valley of the substrate surface is slightly larger but close to the microalgal cell [102].

Table 2.2 lists some recent research that focuses on the interactions between microalgae cells and substrates.

Table 2.2. Influence of interaction between microalgal cell and substrate on microalgal biofilm cultivation.

Impact factor	Bioreactor	Substrate	Culture medium	Species	Biomass production	Ref
Substrate						
Surface wettability	Flow lane incubators	Hydrophilic Polyethersulfone membrane	Sterilized f/2 + Si medium	*Cylindrotheca fusiformis*	$39.47 \pm 2.17 \times 10^9$ cells·m^{-2}	[94]
		Hydrophobic Polyethersulfone membrane			$47.64 \pm 4.03 \times 10^9$ cells·m^{-2}	
Surface wettability/roughness	Plexiglass chamber	Modified styrene-acrylic resin films	BG-11 medium	*C. vulgaris*	1.25 g·m^{-2}	[80]
		Styrene-acrylic resin films with 15 wt% perfluoroalkyl ethyl acrylate			0.45 g·m^{-2}	
Surface wettability	Rectangular reactor	Stainless steel	BG-11 medium	*Scenedesmus rubescens*	21.1 g·m^{-2}	[75]
		Silicone rubber			19.1 g·m^{-2}	
	.	Plexiglass			35.1 g·m^{-2}	
		Cork			14.9 g·m^{-2}	
		Denim			12.7 g·m^{-2}	
		Sponge towel			21.0 g·m^{-2}	
Surface roughness	micro photobioreactor	Silicone modulates with a grooved surface	BG-11 medium	*Scenedesmus obliquus*	165.84 g·m^{-2}	[103]
		Silicone modulates with a flat surface			145.11 g·m^{-2}	

Table 2.2. (*Contd.*)

Impact factor	Bioreactor	Substrate	Culture medium	Species	Biomass production	Ref
Surface wettability	Parallel plate flow chamber	Glass	BG-11 medium	*C. vulgaris*	2757 ± 74 mm^2	[74]
		Indium tin oxide-coated glass			6890 ± 92 mm^2	
Surface wettability	Cuboid container	Plain drawing paper	Sterilized f/2 + Si medium	*Cylindrotheca fusiformis*	1.16 ± 0.07 × 10^{10} cells·m^{-2}	[104]
		Polypropylene fabric			6.99 ± 0.15 × 10^9 cells·m^{-2}	
		Polyethylene plastic			5.08 ± 0.08 × 10^9 cells·m^{-2}	
		Polyvinylidene fluoride membrane			1.56 ± 0.51 × 10^8 cells·m^{-2}	
Species						
	Continuous flow chamber	Polyurethane	Bold's Basal Media	*Scenedesmus obliquus*	\	[23]
				Chlorella vulgaris	\	
Surface wettability/ Lipid content	Vertical reactor	Plexiglass	BG-11 medium	*Botryococcus braunii*	28.3 g·m^{-2}	[84]
				Neochloris vigensis	8.4 g·m^{-2}	
EPS production	Flow lane incubator	Polyvinylidene fluoride membrane	F/2 + Si medium	*Amphora coffeaeformis*	35.33*10^8 cells·m^{-2}	[105]
				Cylindrotheca fusiformis	3.78*10^8 cells·m^{-2}	
				Navicula incerta	7.78*10^8 cells·m^{-2}	

2.3.2.3. Operation conditions

The third part that influences the microalgal biofilm reactor is the operating conditions, which include hydrodynamic conditions, nutrient loading rate, temperature, pH, illumination intensity and gas supplication [103, 106-109]. For instance, research has investigated the hydrodynamic conditions such as flow rate, stirring speed and rotating rate effect on microalgae adhesion [107, 110-112]. The hydrodynamic conditions have a contradictory impact on microalgae biofilm. On the one hand, high shear stress could facilitate biofilm growth by increasing nutrient diffusion [113]. On the other hand, high shear stress could cause biofilm detachment or damage once it exceeds the biofilm limit [114]. However, studies on the influences of hydrodynamic conditions on microalgal biofilm for biomass production are still in the initial stages of laboratory experiments. Light is the energy source for microalgae photosynthesis. Microalgae biofilm growth can be inhibited by over-lighting (photo-inhibition) or insufficient illumination (photo limitation) [115, 116]. The suitable illumination intensity varies among the species and could also be affected by the growth conditions. Literature has been done to determine the saturated illumination of different microalgae biofilms, such as periphyton-based [117], benthic algae-based [118], and freshwater microalgae-based [119]. Regardless of the light saturation, the microalgal biofilm growth under illumination has a higher algal density than that grown in the dark [120]. One bottleneck in applying microalgae biofilm in large quantities of wastewater treatment is limiting climate-dependent natural sunlight. The solar irradiance mentioned by Kesaano and Sims can easily exceed 2000 $\mu mol \cdot m^{-2} \cdot s^{-1}$ in summer but very low in the winter (below 100 $\mu mol \cdot m^{-2} \cdot s^{-1}$) [72]. And it is not an economical and sustainable option to employ artificial light on biofilm growth due to its high energy consumption.

Like other biological wastewater treatment, temperature shifts also affect microalgae-biofilm performance [121]. As Adetunji and Odetokun mentioned, microbial activities such as metabolism controlled by enzymes have feedback on temperature fluctuation [122]. As a result, biofilm growth will be promoted when it is under the appropriate temperature. Fica and Sims reported that increasing the influent temperature to 27 ℃ (suitable for microalgal cell growth) has a significant positive effect on the productivity of the biofilm system [123]. Compared to conventional algal open ponds, microalgae biofilm systems require less water [71]. However, Posadas et al. pointed out that biofilm cultivation under a thin water layer is more sensitive to temperature fluctuation than suspended ones [124]. Consequently, most of the water is lost to evaporation, which causes water waste, water chemistry, and cell desiccation [71, 72]. Similar to solar irradiance, temperatures are also limited by seasons. A thermal model for microalgal biofilm photobioreactor predicted evaporative losses of 6.0, 7.3, 3.4, and 1.0 $Lm^{-2}d^{-1}$ in spring, summer, fall and winter, respectively [125]. Low temperatures can reduce the water evaporated loss but lead to weak cell activities [59, 72]. Thus, thermal control in wastewater-based microalgal biofilm systems should be considered to minimize temperature fluctuations and balance the water-evaporated losses and temperature suitable for biofilm growth.

Besides, the influence of nutrients on biofilm growth, biofilm formation, and species composition are also reported in some studies [21, 120, 126]. The nutrient tolerance of biofilm is dependent on the type of species. Generally, a microalgal-based biofilm (phototrophic) system rather grows in a medium with light and inorganic nutrients, while microalgal-bacterial-based (heterotrophic) biofilms prefer concentrated biodegradable organic matter [127, 128]. Moreover, there is a universal knowledge that insufficient nutrients could restrict microalgae growth and lead to low biofilm productivity [129, 130]. Carbon, nitrogen, and phosphorus are primary elements

during microalgae cultivation [65]. According to nutrient requirement variety among different microorganisms, nutrient concentration adjustment could control the biofilm organism composition [56]. Literature mentioned that the Redfield ratio (C: N: P 106:16:1 molar basis) was proposed as a typical optimal ratio for microalgae growth [131, 132]. This indicates that microalgal biofilm growth could be facilitated by maintaining the nutrient ratio around that range. Choi and Lee reported that *Chlorella vulgaris* productivity reached a maximum of 2.97 $g \cdot L^{-1} \cdot day^{-1}$ by increasing the N/P ratio to about 10 [133]. Furthermore, a low organic/inorganic carbon ratio in culture medium could promote microalgae occupied a high fraction in microalgal-bacterial based biofilm [134, 135]. Table 2.3 exhibited the studies investigating the operating conditions affecting microalgae production.

Table 2.3. Influence of operation conditions on microalgal biofilm cultivation.

Operation conditions	Bioreactor	Substrate	Setting parameter	Species	Biomass production	Ref
Hydrodynamic shear	3-channel flow-cells	Glass	1.0 m Pa	*Chlorella vulgaris*	5.2 $\mu m^3 \cdot \mu m^{-2}$	[107]
			6.5 m Pa		6.4 $\mu m^3 \cdot \mu m^{-2}$	
			11.0 m Pa		8 $\mu m^3 \cdot \mu m^{-2}$	
Light intensity	Single layer vertical plate attached photobioreactor	Glass	0 $\mu mol \cdot m^{-2} \cdot s^{-1}$	*S. obliquus*	0.7 $g \cdot m^{-2} \cdot d^{-1}$	[119]
			150 $\mu mol \cdot m^{-2} \cdot s^{-1}$		10 $g \cdot m^{-2} \cdot d^{-1}$	

Table 2.3. (*Contd.*)

Operation conditions	Bioreactor	Substrate	Setting parameter	Species	Biomass production	Ref
Temperature	twin-layer porous substrate photobioreactor	Polyvinylidene fluoride membrane	17 ℃	*S. microadriaticum*	72.7 $g \cdot m^{-2}$	[136]
			22 ℃		66.4 $g \cdot m^{-2}$	
			27 ℃		34.2 $g \cdot m^{-2}$	
pH	Parallel plate flow chamber	polyvinyl chloride	pH = 5.5	*Chlorella sp.*	1600 $cells \cdot mm^{-2}$	[137]
			pH = 6.8		1550 $cells \cdot mm^{-2}$	
			pH = 8.1		1400 $cells \cdot mm^{-2}$	
Nutrient			TN = 100 $mg \cdot L^{-1}$ TP = 8 $mg \cdot L^{-1}$	*Chlorella vulgaris*	9×10^7 $cells \cdot cm^{-2}$	[138]
			TN = 50 $mg \cdot L^{-1}$ TP = 4 $mg \cdot L^{-1}$		7×10^7 $cells \cdot cm^{-2}$	
			TN = 25 $mg \cdot L^{-1}$ TP = 2 $mg \cdot L^{-1}$		5×10^7 $cells \cdot cm^{-2}$	

In summary, the factors that influence biofilm performance are various, and they mostly have synergic interaction. Much research noticed that predicting biofilm performance by an individual element is impossible. The synergic impact between factors should be considered when dealing with such a complicated system.

2.4. Recent microalgal-bacterial process in membrane photobioreactor- experiment and modelling

As previously mentioned, mono-species microalgal cultivation is rare in the open system, and multiple-species cultivation could promote nutrient removal and production yield [23, 61].

Moreover, microalgae-based cultivation has drawbacks such as diluted suspension concentrations, low organic matter removal efficiency, and ease of contamination [41, 139]. On the other hand, traditional biological technologies for wastewater treatment, such as aerobic activated sludge or anaerobic technologies, have downsides, such as high energy consumption due to technical limitations and inferior nutrient removal. As a result, the microalgae-bacterial combined process is suggested as a sustainable alternative for wastewater treatment as it shows a lower energy demand for gas supply (both carbon dioxide and oxygen) while guaranteeing effective pollutants removal (organic matter, nutrients) and resource recovery [34, 43]. The microalgae-bacterial cooperated system relies on the symbiotic relationship among the microorganisms (Figure 2.2). On the one hand, microalgae uptake nutrients such as nitrogen and phosphorus to convert inorganic carbon into organic carbon by photosynthesis and generate oxygen for bacteria growth. On the other hand, bacteria activities can produce carbon dioxide, which will benefit microalgal biomass growth. However, this synergic interaction is complicated and could change to competition mode if the balance is broken. Zhang et al. mention that some bacteria could produce toxic components to impede microalgae growth while the microalgae also could release exotoxins to inhibit bacterial activities[140]. Some literature suggested that the synergic relationship can be promoted by adding beneficial bacteria species in microalgae cultivation, such as nitrifying bacteria [141] and *Brevundimonas diminuta* [142]. General, microalgae-bacteria systems can be classified into the following categories based on the existing state of microalgae and bacteria in the bioreactor: suspended microalgal-bacterial system (SMB), immobilized microalgal-bacterial system (IMB), respectively. SMB system was utilized initially for nutrient removal during microalgal processing. In this system, microalgae and bacteria are suspended in the aqueous culture medium in a weak synergic interaction, which proved later would lead to a mediocre removal performance and

settleability [39, 143, 144]. The IBM system aims to enhance the aggregation of microalgae and bacteria to form a consortium, either floc/cluster or biofilm, which can facilitate the symbiotic relationship between them [35, 145]. The IMB system can be classified into two constitutions based on their accumulation mechanism: a) biofilm and b) self-flocculation.

The former will supply a solid substrate as carriers or membranes for microalgae and bacteria to attach to form a thick mixotrophic biofilm layer. The latter mostly relies on the interaction between microalgae and bacteria, such as cell-cell aggregation or bio-flocculation [145]. Compared to the SMB system, the IMB system exhibits better performance in biomass production and removal of pollutants because the aggregation of microorganisms strengthens symbiosis [146]. For example, bio-flocculation could happen between microalgae and bacteria and present as microalgal-bacterial bio-flocs under the aggregative force driven by the extracellular polymeric substance (EPS) [145, 147]. Table 2.4 exhibits the pros and cons between SMB and IMB. The bio flocs show a uniform structure with small volume and low stability, which would benefit from achieving the growth balance and interaction between microorganisms [41].

Moreover, the reactor performance could be further boosted when it comes to the biofilm-based IMB system. As the previous section mentioned, biofilm-based cultivation has advantages such as cost-efficiency, low energy consumption and high production yield. Table 2.5 lists recent microalgae-bacterial system experiments on membrane photobioreactors.

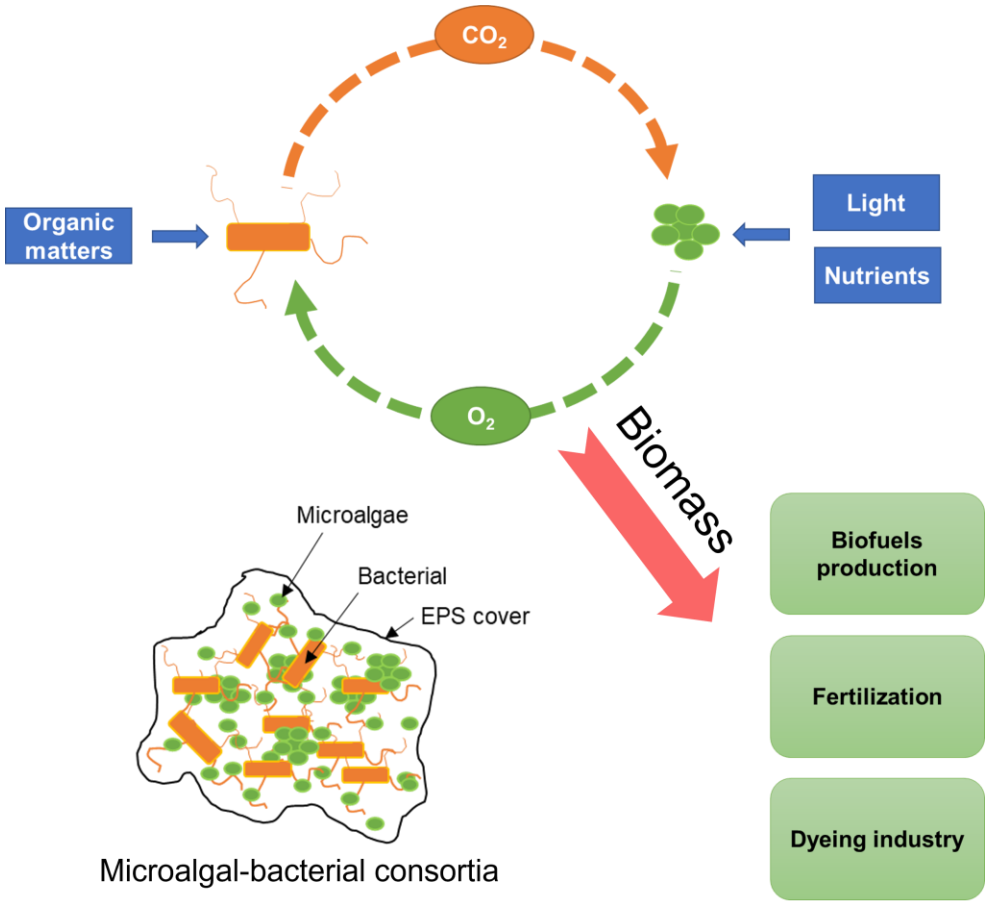

Figure 2.2. Mechanism of wastewater treatment by means of microalgae-bacterial processes and resource recovery.

Table 2.4. Comparison of SMB and IMB cultivation systems.

Cultivation	Pro	Cons
SMB	Offsetting Greenhouse gas emission	Extra harvesting cost
	Enhanced microalgal growth	Low and dynamic cell concentration
	Easier harvesting	Large space requirement
IMB		
	Higher biomass productivity	Harvesting may be limited
	Low space requirement	Extra cost on carrier/substrate
	Efficiency wastewater removal	
	Shorter hydraulic retention time	
	No extra harvesting	

Table 2.5. Laboratory experiments of the microalgal-bacterial system in the membrane photobioreactor.

Microalgae	Bacteria	Medium	Growth Promotion Effect	Factor	Performance	Ref
Chlorella sp. *Scenedesmus sp.* *Nitzschia sp.* *Navicula sp.*	Activated sludge Cyanobacteria	Secondary wastewater	Biomass production increased	Solid retention time	Up to 2250 $mg \cdot L^{-1}$ compared to control 200 $mg \cdot L^{-1}$	[148]
Chlorella vulgaris	Activated sludge	Synthetic wastewater	Increased TP removal Increased biomass concentration	Solid retention time	Up to 3.41 ± 0.12 $g \cdot L^{-1}$ at SRT = 30 days	[149]
Chlorella *Nitzschia*		Primary settled wastewater	2.5 folds of inorganic nitrogen removal enhanced	Carbon loading raters (CLRs)	Up to 994 ± 63 $mg \cdot L^{-1}$ at high CLR	[150]
Chlorella vulgaris	Activated sludge	Urine		Illumination period	TN removal: 20.43 ± 13.38 mg $N \cdot L^{-1}$ TP removal: 15.65 ± 15.01 mg $P \cdot L^{-1}$	[151]
Chlorella vulgaris	Activated sludge	wastewater	Mixed cellulose ester membrane	/	COD removal up to 54.3 % NH_4 removal up to 94.35 % $P\text{-}PO_4^-$ removal up to 74.32 %	[152]

Instead of laboratory experiments, modelling is a time-saving alternative to predict the microalgal-bacterial performance in the photobioreactor system. Mathematical models are an effective tool to analyze insight into complicated systems such as microalgal-bacterial interaction. Furthermore, mathematically modelling the activity of microalgal-bacterial consortia before the actual experiment starts can predict their behaviour and give more views for optimization of the design of the photobioreactor. Mechanistic bacterial mathematical models for traditional wastewater treatment systems have been successfully developed and validated and are currently widely accepted and applied over decades [153]. And that was followed by a considerable amount of the simple model for steady-state microalgae. These steady-state models assume that microalgae

growth will maintain the factor values constant over time, initially designed to investigate microalgae performance changing with a single variable [154, 155]. Recently, more complex dynamics models of microalgae involving multiple physical factors have been studied based on Droop's or Monod's kinetics [44, 156-158]. In this case, the values of elements could be dynamic over time.

Compared to the individual kind of microorganism model (either activated sludge or microalgae), the microalgae-bacteria model requests a higher complicated degree of mathematic derivation because it considers influences of multiple factors and interactions between organisms in wastewater treatment. The first mathematical model to describe the growth of microalgae and bacteria in high-rate algal ponds (HRAPs) was produced by Buhr and Miller [154]. In this model, microalgal growth was limited by carbon dioxide, total inorganic nitrogen, and illumination, while bacterial activities were restricted by organic substrate, dissolved oxygen and nitrogen. Afterward, more and more complex models were derived based on the augment of features and processes. For example, Reichert et al. developed a mechanistic model known as River Water Quality Model 1 (RWQM1) that involves nitrogen and phosphorous variables in microalgal and bacterial growth [159]. The limitation of this model is that they hadn't taken the inorganic carbon influence, which would be the majority role in the microorganism growth, account into the system. Moreover, the following model developed by Sah et al. started to include more nutrients and physical or environmental factors (aeration, solar intensity, and temperature) in microalgal-bacterial processes [160]. These models mentioned below are generally based on Monod kinetics, and the microalgae-bacteria interactions are expressed in a matrix format with kinetics and stoichiometric coefficients.

Moreover, some dynamic models of microalgae and bacteria combining processes were designed for different purposes. Moreno Grau et al. developed a model for predicting the dynamics

of microalgae, bacteria and zooplankton in waste stabilization ponds (WSPs) [155]. The microalgae growth in their model relied on ammonia and phosphorus Monod functions, and the illumination and temperature were limited by the Steel function and Arrhenius equations, respectively [44]. Beran and Kargi investigated the flowing quality of WSPs through the model considering variables such as microorganism biomass, soluble chemical oxygen demand, dissolved oxygen and nutrient concentrations [161]. The microalgae growth in this model followed Liebig's "Law of the Minimum," which allows only one substrate to be restricted simultaneously. However, most integrated microalgal-bacterial models do not consider the synergic effects of those impact factors (light intensity, pH, gas concentration, etc.) in the entire system. Thereby, Solimeno et al. developed a new integral mechanistic model called BIO_ALGAW to conquer the limitations of past microalgae-bacteria mathemetic models [44].

In the past 20 years, more complex microalgae-bacteria mechanistic models were developed by promoting increasing concern on applications of microalgae biomass in emerging bioproduct or biofuel areas. These models give a view on understanding the interaction between microalgae and bacteria and the optimization of experiment design. Table 2.6 shows some of these mathematical models applied to the synergy process of the microalgae-bacteria system in the membrane photobioreactor.

Table 2.6. Mathematical model of the microalgal-bacterial system in the membrane photobioreactor.

Description	Model formula	Nomenclature	Ref
Nitrite inhibition model	$ETR = \Phi_{PS\ II} \cdot E \cdot 0.5$ $\frac{\nu}{\nu_{MAX}} = \frac{K_I}{K_I + I}$ $\frac{\nu}{\nu_{MAX}} = \frac{K_I^n}{K_I^n + I^n}$	$\Phi_{PS\ II}$: quantum yield of PS II E: irradiance of the actinic light ($\mu mol \cdot m^{-2} \cdot s^{-1}$) ν / ν_{MAX} – relative photosynthesis activity rate ν_{MAX}-non-inhibited photosynthesis activity rate I- photon concentration K_I-50% inhibitor concentration n-Hill coefficient	[162]

Table 2.6. (*Contd.*)

Description	Model formula	Nomenclature	Ref
Light utilization evaluation model	$I_{(x)} = I_0 exp(-kX_T x)$ $I_{av} = \frac{I_0}{kX_T L}(1 - exp(-kX_T x))$ Output=$\frac{I_{av}}{I_s} exp(1 - \frac{I_{av}}{I_s})$ Efficiency =$\frac{Output}{Input}$= $\frac{I_{av}}{I_s I_0} exp(1 - \frac{I_{av}}{I_s})$ $I_{(x)} = I_0 exp(-(k_a X_a + k_b X_b + C)x)$	I_0: initial light intensity, μmol·m^2·s^{-1} $I_{(x)}$: light intensity at location x meter away from the light source k: extinction coefficient, m^{-1}·g^{-1}TSS X_T: total suspended solid (TSS) concentration, g TSS·m^{-3} L: length of the light pathway inside the reactor, m I_s: saturation light intensity, μmol·m^2·s^{-1} I_{av}: average light intensity, μmol·m^2·s^{-1} x: distance from the light source, m k_a: extinction coefficient for microalgae, cm^{-1}g^{-1}TSS k_b: extinction coefficient for bacteria, cm^{-1}g^{-1}TSS X_a: microalgae concentration, g^{-1} TSS X_b: bacteria concentration, g^{-1} TSS C: constant, cm^{-1}	[163]

2.5. Future developments and challenges

2.5.1. Scale-up of microalgal-based photobioreactor

Biotechnologies such as biofilm cultivation, membrane filtration, and multiple species could promote microalgae photobioreactor performance, such as pollutants removal, biomass harvesting, microorganism growth, and biomass production co-cultivation (microalgae-bacteria) [8, 13, 59]. In addition, previous studies also provided evidence that the benefits could reflect on the industrial market and the natural environment [4, 6, 43, 164]. In assumption, a large-scale microalgal-bacterial biofilm membrane photobioreactor could take full advantage of the wastewater treatment areas and offer a considerable amount of biomass to downstream applications such as biofuel, pigment and nourishment fields. However, the conflict between maintaining cost-efficiency and marketing profit hinders the scale-up of the microalgal biofilm bioreactor from the lab to the industrial level [14, 61, 164], which is mostly attributed to the

technological limitation and the lack of comprehensive fundamental knowledge of the interactions among microorganisms and substrates. Further studies of the impact factors affecting microalgal biofilm bioreactors are required for further development.

2.5.2. The effects of operation condition on the accumulation of lipid content

The previous section mentioned that one primary reason that microalgal-based biotechnologies received more and more concerns was due to the considerable prospects of microalgal feedstocks on biofuel production [20, 165, 166]. However, the high expenses during the lipid extraction process block the development of microalgae in biofuel applications [164, 165, 167]. Literature provides evidence that the lipid content of microalgae in the attached biofilm system exhibited a higher value than the suspended system [168]. However, as Shen et al. mentioned, microalgae produce 5-15% lower lipid content in wastewater than in a culture medium [67]. Studies show that operation conditions such as temperature, pH, and illumination could be optimized to maximize the lipid production yield [169]. As the study of optimization lipid content on microalgal biofilm membrane photobioreactor through operation parameters is limited, comprehensive knowledge is required to fill the gap between biofuel application and microalgal-based wastewater treatment.

2.5.3. The potential applications

The presented microalgae process focuses on the downstream product of the cultivation, mainly in the cosmetic, nutrient, and fertilizer industries [47, 169, 170]. Despite having a high potential for wastewater treatment, they haven't been applied to substitute the traditional aerobic activated sludge and anaerobic technologies due to limitations such as low harvesting efficiency, poor organic matter removal, and low tolerance to harsh conditions [41, 134, 145, 146].

Microalgal biofilm membrane bioreactor guarantees concentrated biomass harvest, replenishing the drawback of diluted microalga suspension [33, 109, 171]. Microalgal biofilm membrane photobioreactor has very high potential in applications that require a large amount of microalgal biomass, such as biofuel production [20, 108]. Microalgae can produce multiple times more biomass per unit of land area than terrestrial plants due to their higher photosynthetic efficiency [172, 173]. In addition, Microalgae have shorter growth periods and can undergo more frequent biomass harvesting compared to terrestrial plants that only allow harvesting in their respective seasons, such as crops [174].

Biological wastewater treatment plays a significant role in the water treatment plant, and the conventional method requires high operation and maintenance costs during the daily procedure. These increased expenses can be mitigated by introducing the microalgal biofilm photobioreactor technology. Using microalgae biofilm systems to treat wastewater is energy-effective and makes it easy to harvest the bioproduct with high marketing potential. These bioproducts produced from microalgae cultivation are highly required in other areas, thus creating revenue for wastewater treatment infrastructure and energy requirements of operations [49, 59]. Moreover, employing a microalgae biofilm system for wastewater reveals that it successfully removes 30-100% of nutrients from the wastewater [175, 176].

As known, biofuel production is one of the downstream processes of microalgae cultivation. Microalgal biofilm photobioreactors can benefit biodiesel production due to their extremely high production yield [65]. Moreover, incorporating bacteria can further strengthen the biofilm photobioreactor [41]. Compared to the monospecies microalgal system, microalgal-bacterial based biofilm photobioreactor has the following advantages: 1) Better microalgae growth promoted by the phytohormones, or macro/micro-nutrient produced by bacteria [34, 39, 177]; 2) High potential

bio-flocculation facilitated by bacteria which enhance microalgae aggregation for better harvest efficiency [36]; 3) easier biodiesel or bioethanol conversion processes because anaerobic bacteria activities contribute to the microalgal recalcitrant cell wall break down [40, 178, 179]. Moreover, Saba et al. investigated a novel biotechnological device called photosynthetic algae microbial fuel cells (PAMFC) that combines photosynthetic microalgae and electrochemically active bacteria, which could convert solar energy [180]. Besides, this technology can also benefit from contaminant removal from wastewater and has high adaptability at a wide range of light wavelengths and intensities for power generation [181, 182].

2.6. Conclusions

In conclusion, understanding microorganism biofilm cultivation and the current photobioreactor system has advanced significantly in recent years. The research has revealed the importance of microbial interactions and biofilm formation for the efficient cultivation of microorganisms, particularly for microalgae in wastewater treatment and for producing biofuels and high-value compounds.

In addition, developing novel photobioreactor systems, such as membrane photobioreactors, has shown promising results for improving microalgal productivity and biomass accumulation. However, much must be learned about the complex mechanisms involved in biofilm formation and bacterial-microalgal interactions and how these can be harnessed for more efficient and sustainable cultivation methods.

Future research should focus on integrating interdisciplinary approaches, including molecular biology and detective techniques on a micro-scale, further to unravel the complex interactions between microorganisms in biofilm cultivation. Moreover, efforts should be made to optimize the photobioreactor systems and develop cost-effective and scalable solutions for

commercial applications. Overall, understanding microorganism biofilm cultivation and the current photobioreactor system offers a promising path toward sustainable and environmentally friendly technologies for producing biofuels and high-value compounds.

2.7. References

[1] Milledge, J.J. (2011). Commercial application of microalgae other than as biofuels: a brief review. Reviews in Environmental Science and Bio/Technology, 10, 31-41.
[2] Priyadarshani, I., Rath, B. (2012). Commercial and industrial applications of micro algae–A review. Journal of Algal Biomass Utilization, 3, 89-100.
[3] Bhalamurugan, G.L., Valerie, O., Mark, L. (2018). Valuable bioproducts obtained from microalgal biomass and their commercial applications: A review. Environmental Engineering Research, 23, 229-241.
[4] Khanra, S., Mondal, M., Halder, G., Tiwari, O., Gayen, K., Bhowmick, T.K. (2018). Downstream processing of microalgae for pigments, protein and carbohydrate in industrial application: A review. Food and Bioproducts Processing, 110, 60-84.
[5] Moshood, T.D., Nawanir, G., Mahmud, F. (2021). Microalgae biofuels production: A systematic review on socioeconomic prospects of microalgae biofuels and policy implications. Environmental Challenges, 5, 100207.
[6] Nagappan, S., Devendran, S., Tsai, P.C., Dahms, H.U., Ponnusamy, V.K. (2019). Potential of two-stage cultivation in microalgae biofuel production. Fuel, 252, 339-349.
[7] Jaiswal, K.K., Banerjee, I., Singh, D., Sajwan, P., Chhetri, V. (2020). Ecological stress stimulus to improve microalgae biofuel generation: a review. Octa Journal of Biosciences, 8, 48-54.
[8] Baldev, E., Ali, D.M., Pugazhendhi, A., Thajuddin, N. (2021). Wastewater as an economical and ecofriendly green medium for microalgal biofuel production. Fuel, 294, 120484.
[9] Clarens, A.F., Resurreccion, E.P., White, M.A., Colosi, L.M. (2010). Environmental life cycle comparison of algae to other bioenergy feedstocks. Environmental Science & Technology, 44, 1813-1819.
[10] Mujtaba, G., Lee, K. (2017). Treatment of real wastewater using co-culture of immobilized *Chlorella vulgaris* and suspended activated sludge. Water Research, 120, 174-184.
[11] Otieno, B., Apollo, S., Kabuba, J., Naidoo, B., Simate, G., Ochieng, A. (2019). Ozonolysis pre-treatment of waste activated sludge for solubilization and biodegradability enhancement. Journal of Environmental Chemical Engineering, 7, 102945.
[12] Wang, D., He, D., Liu, X., Xu, Q., Yang, Q., Li, X., Liu, Y., Wang, Q., Ni, B.J., Li, H. (2019). The underlying mechanism of calcium peroxide pretreatment enhancing methane production from anaerobic digestion of waste activated sludge. Water Research, 164, 114934.
[13] Wollmann, F., Dietze, S., Ackermann, J.U., Bley, T., Walther, T., Steingroewer, J., Krujatz, F. (2019). Microalgae wastewater treatment: Biological and technological approaches. Engineering in Life Sciences, 19, 860-871.
[14] Abdelfattah, A., Ali, S.S., Ramadan, H., El-Aswar, E.I., Eltawab, R., Ho, S.H., Elsamahy, T., Li, S., El-Sheekh, M.M., Schagerl, M. (2023). Microalgae-based wastewater treatment:

Mechanisms, challenges, recent advances, and future prospects. Environmental Science and Ecotechnology, 13, 100205.
[15] Li, K., Liu, Q., Fang, F., Luo, R., Lu, Q., Zhou, W., Huo, S., Cheng, P., Liu, J., Addy, M. (2019). Microalgae-based wastewater treatment for nutrients recovery: A review. Bioresource Technology, 291, 121934.
[16] Morillas-España, A., Lafarga, T., Sánchez-Zurano, A., Acién-Fernández, F.G., González-López, C. (2022). Microalgae based wastewater treatment coupled to the production of high value agricultural products: Current needs and challenges. Chemosphere, 291, 132968.
[17] Lutzu, G.A., Ciurli, A., Chiellini, C., Di Caprio, F., Concas, A., Dunford, N.T. (2021). Latest developments in wastewater treatment and biopolymer production by microalgae. Journal of Environmental Chemical Engineering, 9, 104926.
[18] Vandamme, D., Foubert, I., Muylaert, K. (2013). Flocculation as a low-cost method for harvesting microalgae for bulk biomass production. Trends in Biotechnology, 31, 233-239.
[19] Verma, R., Kumar, R., Mehan, L., Srivastava, A. (2018). Modified conventional bioreactor for microalgae cultivation. Journal of Bioscience and Bioengineering, 125, 224-230.
[20] Ghazvini, M., Kavosi, M., Sharma, R., Kim, M. (2022). A review on mechanical-based microalgae harvesting methods for biofuel production. Biomass and Bioenergy, 158, 106348.
[21] Yang, J., Xu, M., Zhang, X., Hu, Q., Sommerfeld, M., Chen, Y. (2011). Life-cycle analysis on biodiesel production from microalgae: water footprint and nutrients balance. Bioresource Technology, 102, 159-165.
[22] Hoh, D., Watson, S., Kan, E. (2016). Algal biofilm reactors for integrated wastewater treatment and biofuel production: a review. Chemical Engineering Journal, 287, 466-473.
[23] Irving, T.E., Allen, D.G. (2011). Species and material considerations in the formation and development of microalgal biofilms. Applied Microbiology and Biotechnology, 92, 283-294.
[24] Krishnan, M., Dahms, H.U., Seeni, P., Gopalan, S., Sivanandham, V., Jin-Hyoung, K., James, R.A. (2017). Multi metal assessment on biofilm formation in offshore environment. Materials Science and Engineering: C, 73, 743-755.
[25] Golberg, K., Emuna, N., Vinod, T., Van Moppes, D., Marks, R.S., Arad, S.M., Kushmaro, A. (2016). Novel Anti‐Adhesive Biomaterial Patches: Preventing Biofilm with Metal Complex Films (MCF) Derived from a Microalgal Polysaccharide. Advanced Materials Interfaces, 3, 1500486.
[26] Craggs, R.J., Adey, W.H., Jenson, K.R., John, M.S.S., Green, F.B., Oswald, W.J. (1996). Phosphorus removal from wastewater using an algal turf scrubber. Water Science and Technology, 33, 191-198.
[27] Schumacher, G., Sekoulov, I. (2002). Polishing of secondary effluent by an algal biofilm process. Water Science and Technology, 46, 83-90.
[28] Vymazal, J., Sládeček, V., Stach, J. (2001). Biota participating in wastewater treatment in a horizontal flow constructed wetland. Water Science and Technology, 44, 211-214.
[29] Johnson, M.B., Wen, Z. (2010). Development of an attached microalgal growth system for biofuel production. Applied Microbiology and Biotechnology, 85, 525-534.
[30] Gao, F., Yang, Z.H., Li, C., Zeng, G.M., Ma, D.H., Zhou, L. (2015). A novel algal biofilm membrane photobioreactor for attached microalgae growth and nutrients removal from secondary effluent. Bioresource Technology, 179, 8-12.
[31] Honda, R., Boonnorat, J., Chiemchaisri, C., Chiemchaisri, W., Yamamoto, K. (2012). Carbon dioxide capture and nutrients removal utilizing treated sewage by concentrated microalgae cultivation in a membrane photobioreactor. Bioresource Technology, 125, 59-64.

[32] Bilad, M., Discart, V., Vandamme, D., Foubert, I., Muylaert, K., Vankelecom, I.F. (2014). Coupled cultivation and pre-harvesting of microalgae in a membrane photobioreactor (MPBR). Bioresource Technology, 155, 410-417.
[33] Gao, F., Yang, Z.H., Li, C., Wang, Y., Jin, W., Deng, Y. (2014). Concentrated microalgae cultivation in treated sewage by membrane photobioreactor operated in batch flow mode. Bioresource Technology, 167, 441-446.
[34] Ramanan, R., Kim, B.H., Cho, D.H., Oh, H.M., Kim, H.S. (2016). Algae–bacteria interactions: evolution, ecology and emerging applications. Biotechnology Advances, 34, 14-29.
[35] Subashchandrabose, S.R., Ramakrishnan, B., Megharaj, M., Venkateswarlu, K., Naidu, R. (2011). Consortia of cyanobacteria/microalgae and bacteria: biotechnological potential. Biotechnology Advances, 29, 896-907.
[36] Fuentes, J.L., Garbayo, I., Cuaresma, M., Montero, Z., González-del-Valle, M., Vílchez, C. (2016). Impact of microalgae-bacteria interactions on the production of algal biomass and associated compounds. Marine Drugs, 14, 100.
[37] Xiao, R., Zheng, Y. (2016). Overview of microalgal extracellular polymeric substances (EPS) and their applications. Biotechnology Advances, 34, 1225-1244.
[38] Buchan, A., LeCleir, G.R., Gulvik, C.A., González, J.M. (2014). Master recyclers: features and functions of bacteria associated with phytoplankton blooms. Nature Reviews Microbiology, 12, 686-698.
[39] Wang, H., Hill, R.T., Zheng, T., Hu, X., Wang, B. (2016). Effects of bacterial communities on biofuel-producing microalgae: stimulation, inhibition and harvesting. Critical Reviews in Biotechnology, 36, 341-352.
[40] Demuez, M., González-Fernández, C., Ballesteros, M. (2015). Algicidal microorganisms and secreted algicides: new tools to induce microalgal cell disruption. Biotechnology Advances, 33, 1615-1625.
[41] Wang, H., Deng, L., Qi, Z., Wang, W. (2022). Constructed microalgal-bacterial symbiotic (MBS) system: Classification, performance, partnerships and perspectives. Science of The Total Environment, 803, 150082.
[42] Xie, B., Tang, X., Ng, H.Y., Deng, S., Shi, X., Song, W., Huang, S., Li, G., Liang, H. (2020). Biological sulfamethoxazole degradation along with anaerobically digested centrate treatment by immobilized microalgal-bacterial consortium: performance, mechanism and shifts in bacterial and microalgal communities. Chemical Engineering Journal, 388, 124217.
[43] Mojiri, A., Zhou, J.L., Nazari, M., Rezania, S., Farraji, H., Vakili, M. (2022). Biochar enhanced the performance of microalgae/bacteria consortium for insecticides removal from synthetic wastewater. Process Safety and Environmental Protection, 157, 284-296.
[44] Solimeno, A., Parker, L., Lundquist, T., García, J. (2017). Integral microalgae-bacteria model (BIO_ALGAE): Application to wastewater high rate algal ponds. Science of the Total Environment, 601, 646-657.
[45] Posten, C., Chen, S.F. (2016). Microalgae biotechnology. Springer International Publishing: Switzerland.
[46] Maso, M., Garcés, E. (2006). Harmful microalgae blooms (HAB); problematic and conditions that induce them. Marine Pollution Bulletin, 53, 620-630.
[47] Singh, R., Sharma, S. (2012). Development of suitable photobioreactor for algae production–A review. Renewable and Sustainable Energy Reviews, 16, 2347-2353.
[48] Gupta, P.L., Lee, S., Choi, H. (2015). A mini review: photobioreactors for large scale algal cultivation. World Journal of Microbiology and Biotechnology, 31, 1409-1417.

[49] Sathinathan, P., Parab, H., Yusoff, R., Ibrahim, S., Vello, V., Ngoh, G. (2023). Photobioreactor design and parameters essential for algal cultivation using industrial wastewater: A review. Renewable and Sustainable Energy Reviews, 173, 113096.
[50] Oswald, W.J., Golueke, C.G. (1960). Biological transformation of solar energy. Advances in Applied Microbiology, Academic Press: Cambridge, pp. 223-262.
[51] Vo, H.N.P., Ngo, H.H., Guo, W., Nguyen, T.M.H., Liu, Y., Liu, Y., Nguyen, D.D., Chang, S.W. (2019). A critical review on designs and applications of microalgae-based photobioreactors for pollutants treatment. Science of the Total Environment, 651, 1549-1568.
[52] Ting, H., Haifeng, L., Shanshan, M., Zhang, Y., Zhidan, L., Na, D. (2017). Progress in microalgae cultivation photobioreactors and applications in wastewater treatment: A review. International Journal of Agricultural and Biological Engineering, 10, 1-29.
[53] Berner, F., Heimann, K., Sheehan, M. (2015). Microalgal biofilms for biomass production. Journal of Applied Phycology, 27, 1793-1804.
[54] Fanesi, A., Paule, A., Bernard, O., Briandet, R., Lopes, F. (2019). The architecture of monospecific microalgae biofilms. Microorganisms, 7, 352.
[55] Moreno Osorio, J.H., Pollio, A., Frunzo, L., Lens, P.N.L., Esposito, G. (2021). A review of microalgal biofilm technologies: definition, applications, settings and analysis. Frontiers in Chemical Engineering, 3, 737710.
[56] Hu, Y., Xiao, Y., Liao, K., Leng, Y., Lu, Q. (2021). Development of microalgal biofilm for wastewater remediation: from mechanism to practical application. Journal of Chemical Technology and Biotechnology, 96, 2993-3008.
[57] Wang, C., Tan, Y., Zhu, L., Zhou, C., Yan, X., Xu, Q., Ruan, R., Cheng, P. (2022). The intrinsic characteristics of microalgae biofilm and their potential applications in pollutants removal—A review. Algal Research, 68, 102849.
[58] Mantzorou, A., Ververidis, F. (2019). Microalgal biofilms: A further step over current microalgal cultivation techniques. Science of the Total Environment, 651, 3187-3201.
[59] Saini, S., Tewari, S., Dwivedi, J., Sharma, V. (2023). Biofilm Mediated Wastewater Treatment: A Comprehensive Review. Materials Advances, 4, 1415-1443.
[60] Shen, Y., Xu, X., Zhao, Y., Lin, X. (2014). Influence of algae species, substrata and culture conditions on attached microalgal culture. Bioprocess and Biosystems Engineering, 37, 441-450.
[61] Wicker, R.J., Kwon, E., Khan, E., Kumar, V., Bhatnagar, A. (2022). The potential of mixed-species biofilms to address remaining challenges for economically-feasible microalgal biorefineries: A review. Chemical Engineering Journal, 451, 138481.
[62] Zhang, T., Hu, H., Wu, Y., Zhuang, L., Xu, X., Wang, X., Dao, G. (2016). Promising solutions to solve the bottlenecks in the large-scale cultivation of microalgae for biomass/bioenergy production. Renewable and Sustainable Energy Reviews, 60, 1602-1614.
[63] Koedooder, C., Stock, W., Willems, A., Mangelinckx, S., De Troch, M., Vyverman, W., Sabbe, K. (2019). Diatom-bacteria interactions modulate the composition and productivity of benthic diatom biofilms. Frontiers in Microbiology, 10, 1255.
[64] Vasilieva, S., Lobakova, E., Lukyanov, A., Solovchenko, A. (2016). Immobilized microalgae in biotechnology. Moscow University Biological Sciences Bulletin, 71, 170-176.
[65] Wang, J., Liu, W., Liu, T. (2017). Biofilm based attached cultivation technology for microalgal biorefineries—a review. Bioresource Technology, 244, 1245-1253.
[66] Patwardhan, S.B., Pandit, S., Ghosh, D., Dhar, D.W., Banerjee, S., Joshi, S., Gupta, P.K., Lahiri, D., Nag, M., Ruokolainen, J. (2022). A concise review on the cultivation of microalgal biofilms for biofuel feedstock production. Biomass Conversion and Biorefinery, 1-18.

[67] Shen, Y., Zhang, H., Xu, X., Lin, X. (2015). Biofilm formation and lipid accumulation of attached culture of *Botryococcus braunii*. Bioprocess and Biosystems Engineering, 38, 481-488.
[68] Schnurr, P.J., Espie, G.S., Allen, D.G. (2013). Algae biofilm growth and the potential to stimulate lipid accumulation through nutrient starvation. Bioresource Technology, 136, 337-344.
[69] Melo, M., Fernandes, S., Caetano, N., Borges, M.T. (2018). *Chlorella vulgaris* (SAG 211-12) biofilm formation capacity and proposal of a rotating flat plate photobioreactor for more sustainable biomass production. Journal of Applied Phycology, 30, 887-899.
[70] Murphy, T.E., Berberoglu, H. (2014). Flux balancing of light and nutrients in a biofilm photobioreactor for maximizing photosynthetic productivity. Biotechnology Progress, 30, 348-359.
[71] Ozkan, A., Kinney, K., Katz, L., Berberoglu, H. (2012). Reduction of water and energy requirement of algae cultivation using an algae biofilm photobioreactor. Bioresource Technology, 114, 542-548.
[72] Kesaano, M., Sims, R.C. (2014). Algal biofilm based technology for wastewater treatment. Algal Research, 5, 231-240.
[73] Cao, J., Yuan, W., Pei, Z., Davis, T., Cui, Y., Beltran, M. (2009). A preliminary study of the effect of surface texture on algae cell attachment for a mechanical-biological energy manufacturing system. Journal of Manufacturing Science and Engineering, 131, 064505.
[74] Ozkan, A., Berberoglu, H. (2011). Adhesion of *Chlorella vulgaris* on hydrophilic and hydrophobic surfaces.Proceedings of the ASME International Mechanical Engineering Congress and Exposition; pp. 169-178.
[75] Tsavatopoulou, V.D., Manariotis, I.D. (2020). The effect of surface properties on the formation of *Scenedesmus rubescens* biofilm. Algal Research, 52, 102095.
[76] Ozkan, A., Berberoglu, H. (2013). Physico-chemical surface properties of microalgae. Colloids and Surfaces B: Biointerfaces, 112, 287-293.
[77] Genin, S.N., Aitchison, J.S., Allen, D.G. (2014). Design of algal film photobioreactors: material surface energy effects on algal film productivity, colonization and lipid content. Bioresource Technology, 155, 136-143.
[78] Cui, Y., Yuan, W. (2013). Thermodynamic modeling of algal cell–solid substrate interactions. Applied Energy, 112, 485-492.
[79] Zhang, X., Yuan, H., Jiang, Z., Lin, D., Zhang, X. (2018). Impact of surface tension of wastewater on biofilm formation of microalgae *Chlorella sp*. Bioresource Technology, 266, 498-506.
[80] Tang, J., Liu, B., Gao, L., Wang, W., Liu, T., Su, G. (2021). Impacts of surface wettability and roughness of styrene-acrylic resin films on adhesion behavior of microalgae *Chlorella sp*. Colloids and Surfaces B: Biointerfaces, 199, 111522.
[81] Sekar, R., Venugopalan, V., Satpathy, K., Nair, K., Rao, V. (2004). Laboratory studies on adhesion of microalgae to hard substrates. Hydrobiologia, 512, 109-116.
[82] Zhang, L., Chen, L., Wang, J., Chen, Y., Gao, X., Zhang, Z., Liu, T. (2015). Attached cultivation for improving the biomass productivity of *Spirulina platensis*. Bioresource Technology, 181, 136-142.
[83] Zhuang, L., Yu, D., Zhang, J., Liu, F., Wu, Y., Zhang, T., Dao, G., Hu, H. (2018). The characteristics and influencing factors of the attached microalgae cultivation: a review. Renewable and Sustainable Energy Reviews, 94, 1110-1119.

[84] Tsavatopoulou, V.D., Aravantinou, A.F., Manariotis, I.D. (2021). Comparison of *Botryococcus braunii* and *Neochloris vigensis* Biofilm Formation on Vertical Oriented Surfaces. Biointerface Research in Applied Chemistry, 11, 12843-12857.
[85] Danaee, S., Ofoghi, H., Heydarian, S.M. (2021). Acceleration of microalgal biofilm formation on PET by surface engineering. Korean Journal of Chemical Engineering, 38, 2500-2509.
[86] Kwak, D.-H., Kim, M.-S. (2015). Flotation of algae for water reuse and biomass production: role of zeta potential and surfactant to separate algal particles. Water Science and Technology, 72, 762-769.
[87] Zeng, W., Li, P., Huang, Y., Xia, A., Zhu, X., Zhu, X., Liao, Q. (2022). How Interfacial Properties Affect Adhesion: An Analysis from the Interactions between Microalgal Cells and Solid Substrates. Langmuir, 38, 3284-3296.
[88] Huang, R., Liu, Z., Yan, B., Li, Y., Li, H., Liu, D., Wang, P., Cui, F., Shi, W. (2020). Layer-by-layer assembly of high negatively charged polycarbonate membranes with robust antifouling property for microalgae harvesting. Journal of Membrane Science, 595, 117488.
[89] Babiak, W., Krzemińska, I. (2021). Extracellular polymeric substances (EPS) as microalgal bioproducts: A review of factors affecting EPS synthesis and application in flocculation processes. Energies, 14, 4007.
[90] Cheah, Y.T., Chan, D.J.C. (2021). Physiology of microalgal biofilm: a review on prediction of adhesion on substrates. Bioengineered, 12, 7577-7599.
[91] Teng, J., Wu, M., Chen, J., Lin, H., He, Y. (2020). Different fouling propensities of loosely and tightly bound extracellular polymeric substances (EPSs) and the related fouling mechanisms in a membrane bioreactor. Chemosphere, 255, 126953.
[92] Wu, M., Chen, Y., Lin, H., Zhao, L., Shen, L., Li, R., Xu, Y., Hong, H., He, Y. (2020). Membrane fouling caused by biological foams in a submerged membrane bioreactor: Mechanism insights. Water Research, 181, 115932.
[93] Mühlenbruch, M., Grossart, H.P., Eigemann, F., Voss, M. (2018). Mini-review: Phytoplankton-derived polysaccharides in the marine environment and their interactions with heterotrophic bacteria. Environmental Microbiology, 20, 2671-2685.
[94] Tong, C., Chang, Y.S., Ooi, B.S., Chan, D.J.C. (2021). Physico-chemistry and adhesion kinetics of algal biofilm on polyethersulfone (PES) membrane with different surface wettability. Journal of Environmental Chemical Engineering, 9, 106531.
[95] Ji, C., Zhou, H., Deng, S., Chen, K., Dong, X., Xu, X., Cheng, L. (2021). Insight into the adhesion propensities of extracellular polymeric substances (EPS) on the abiotic surface using XDLVO theory. Journal of Environmental Chemical Engineering, 9, 106563.
[96] Wimpenny, J., Manz, W., Szewzyk, U. (2000). Heterogeneity in biofilms. FEMS Microbiology Reviews, 24, 661-671.
[97] Kokare, C., Chakraborty, S., Khopade, A., Mahadik, K.R. (2009). Biofilm: Importance and applications. Indian Journal of Biotechnology, 8, 159-168.
[98] Gross, M., Zhao, X., Mascarenhas, V., Wen, Z. (2016). Effects of the surface physico-chemical properties and the surface textures on the initial colonization and the attached growth in algal biofilm. Biotechnology for biofuels, 9, 1-14.
[99] Scardino, A., Harvey, E., De Nys, R. (2006). Testing attachment point theory: diatom attachment on microtextured polyimide biomimics. Biofouling, 22, 55-60.
[100] Scardino, A., Guenther, J., De Nys, R. (2008). Attachment point theory revisited: the fouling response to a microtextured matrix. Biofouling, 24, 45-53.

[101] Hoipkemeier-Wilson, L., Schumacher, J.F., Carman, M.L., Gibson, A.L., Feinberg, A.W., Callow, M.E., Finlay, J.A., Callow, J.A., Brennan, A.B. (2004). Antifouling potential of lubricious, micro-engineered, PDMS elastomers against zoospores of the green fouling alga *Ulva (Enteromorpha)*. Biofouling, 20, 53-63.
[102] Cui, Y., Yuan, W., Cao, J. (2013). Effects of surface texturing on microalgal cell attachment to solid carriers. International Journal of Agricultural and Biological Engineering, 6, 44-54.
[103] Huang, Y., Zheng, Y., Li, J., Liao, Q., Fu, Q., Xia, A., Fu, J., Sun, Y. (2018). Enhancing microalgae biofilm formation and growth by fabricating microgrooves onto the substrate surface. Bioresource Technology, 261, 36-43.
[104] Tong, C., Derek, C. (2021). The role of substrates towards marine diatom *Cylindrotheca fusiformis* adhesion and biofilm development. Journal of Applied Phycology, 33, 2845-2862.
[105] Tong, C., Lew, J., Derek, C. (2022). Algal extracellular organic matter pre-treatment enhances microalgal biofilm adhesion onto microporous substrate. Chemosphere, 307, 135740.
[106] Belohlav, V., Zakova, T., Jirout, T., Kratky, L. (2020). Effect of hydrodynamics on the formation and removal of microalgal biofilm in photobioreactors. Biosystems Engineering, 200, 315-327.
[107] Fanesi, A., Lavayssière, M., Breton, C., Bernard, O., Briandet, R., Lopes, F. (2021). Shear stress affects the architecture and cohesion of *Chlorella vulgaris* biofilms. Scientific Reports, 11, 4002.
[108] Guo, C., Duan, D., Sun, Y., Han, Y., Zhao, S. (2019). Enhancing *Scenedesmus obliquus* biofilm growth and CO_2 fixation in a gas-permeable membrane photobioreactor integrated with additional rough surface. Algal Research, 43, 101620.
[109] Zhao, Z., Muylaert, K., Szymczyk, A., Vankelecom, I.F. (2021). Enhanced microalgal biofilm formation and facilitated microalgae harvesting using a novel pH-responsive, crosslinked patterned and vibrating membrane. Chemical Engineering Journal, 410, 127390.
[110] Park, A., Jeong, H., Lee, J., Kim, K., Lee, C. (2011). Effect of shear stress on the formation of bacterial biofilm in a microfluidic channel. BioChip Journal, 5, 236-241.
[111] Fernández, I., Bravo, J., Mosquera-Corral, A., Pereira, A., Campos, J., Méndez, R., Melo, L. (2014). Influence of the shear stress and salinity on Anammox biofilms formation: modelling results. Bioprocess and Biosystems Engineering, 37, 1955-1961.
[112] Azevedo, N., Pinto, A., Reis, N., Vieira, M., Keevil, C. (2006). Shear stress, temperature, and inoculation concentration influence the adhesion of water-stressed Helicobacter pylori to stainless steel 304 and polypropylene. Applied and Environmental Microbiology, 72, 2936-2941.
[113] Schmidt, H., Thom, M., Wieprecht, S., Manz, W., Gerbersdorf, S.U. (2018). The effect of light intensity and shear stress on microbial biostabilization and the community composition of natural biofilms. Research and Reports in Biology, 9, 1-16.
[114] Zakova, T., Jirout, T., Kratky, L., Belohlav, V. (2019). Hydrodynamics as a tool to remove biofilm in tubular photobioreactor. Chemical Engineering Transactions, 76, 451-456.
[115] Wolf, G., Picioreanu, C., van Loosdrecht, M.C. (2007). Kinetic modeling of phototrophic biofilms: the PHOBIA model. Biotechnology and Bioengineering, 97, 1064-1079.
[116] Serôdio, J., Vieira, S., Cruz, S. (2008). Photosynthetic activity, photoprotection and photoinhibition in intertidal microphytobenthos as studied in situ using variable chlorophyll fluorescence. Continental Shelf Research, 28, 1363-1375.
[117] Hill, W.R., Fanta, S.E. (2008). Phosphorus and light colimit periphyton growth at subsaturating irradiances. Freshwater Biology, 53, 215-225.

[118] Hill, W.R., Fanta, S.E., Roberts, B.J. (2009). Quantifying phosphorus and light effects in stream algae. Limnology and Oceanography, 54, 368-380.
[119] Liu, T., Wang, J., Hu, Q., Cheng, P., Ji, B., Liu, J., Chen, Y., Zhang, W., Chen, X., Chen, L. (2013). Attached cultivation technology of microalgae for efficient biomass feedstock production. Bioresource Technology, 127, 216-222.
[120] Sekar, R., Nair, K., Rao, V., Venugopalan, V. (2002). Nutrient dynamics and successional changes in a lentic freshwater biofilm. Freshwater Biology, 47, 1893-1907.
[121] Zimmo, O., Van der Steen, N., Gijzen, H. (2004). Nitrogen mass balance across pilot-scale algae and duckweed-based wastewater stabilisation ponds. Water Research, 38, 913-920.
[122] Adetunji, V.O., Odetokun, I.A. (2012). Biofilm formation in human and tropical foodborne isolates of Listeria strains. American Journal of Food Technology, 7, 517-531.
[123] Fica, Z.T., Sims, R.C. (2016). Algae-based biofilm productivity utilizing dairy wastewater: effects of temperature and organic carbon concentration. Journal of Biological Engineering, 10, 1-7.
[124] Posadas, E., García-Encina, P.-A., Soltau, A., Domínguez, A., Díaz, I., Muñoz, R. (2013). Carbon and nutrient removal from centrates and domestic wastewater using algal–bacterial biofilm bioreactors. Bioresource Technology, 139, 50-58.
[125] Murphy, T.E., Berberoğlu, H. (2012). Temperature fluctuation and evaporative loss rate in an algae biofilm photobioreactor. Journal of Solar Energy Engineering, 134, 011002.
[126] Kebede‐westhead, E., Pizarro, C., Mulbry, W.W., Wilkie, A.C. (2003). Production and nutrient removal by periphyton grown under different loading rates of anaerobically digested flushed dairy manure 1. Journal of Phycology, 39, 1275-1282.
[127] Olapade, O.A., Leff, L.G. (2006). Influence of dissolved organic matter and inorganic nutrients on the biofilm bacterial community on artificial substrates in a northeastern Ohio, USA, stream. Canadian Journal of Microbiology, 52, 540-549.
[128] Hillebrand, H., Kahlert, M., Haglund, A.L., Berninger, U.G., Nagel, S., Wickham, S. (2002). Control of microbenthic communities by grazing and nutrient supply. Ecology, 83, 2205-2219.
[129] Xin, L., Hong-Ying, H., Ke, G., Ying-Xue, S. (2010). Effects of different nitrogen and phosphorus concentrations on the growth, nutrient uptake, and lipid accumulation of a freshwater microalga *Scenedesmus sp*. Bioresource Technology, 101, 5494-5500.
[130] Li, T., Strous, M., Melkonian, M. (2017). Biofilm-based photobioreactors: their design and improving productivity through efficient supply of dissolved inorganic carbon. FEMS Microbiology Letters, 364, fnx218.
[131] Razaghi, A., Godhe, A., Albers, E. (2014). Effects of nitrogen on growth and carbohydrate formation in *Porphyridium cruentum*. Open Life Sciences, 9, 156-162.
[132] Redfield, A.C. (1958). The biological control of chemical factors in the environment. American Scientist, 46, 230A-221.
[133] Choi, H.J., Lee, S.M. (2015). Effect of the N/P ratio on biomass productivity and nutrient removal from municipal wastewater. Bioprocess and Biosystems Engineering, 38, 761-766.
[134] Unnithan, V.V., Unc, A., Smith, G.B. (2014). Mini-review: a priori considerations for bacteria–algae interactions in algal biofuel systems receiving municipal wastewaters. Algal Research, 4, 35-40.
[135] Schnurr, P.J., Allen, D.G. (2015). Factors affecting algae biofilm growth and lipid production: A review. Renewable and Sustainable Energy Reviews, 52, 418-429.

[136] Tsirigoti, A., Tzovenis, I., Koutsaviti, A., Economou-Amilli, A., Ioannou, E., Melkonian, M. (2020). Biofilm cultivation of marine dinoflagellates under different temperatures and nitrogen regimes enhances DHA productivity. Journal of Applied Phycology, 32, 865-880.
[137] Yuan, H., Zhang, X., Jiang, Z., Wang, X., Chen, X., Cao, L., Zhang, X. (2019). Analyzing the effect of pH on microalgae adhesion by identifying the dominant interaction between cell and surface. Colloids and Surfaces B: Biointerfaces, 177, 479-486.
[138] Yang, Y., Zhuang, L.L., Yang, T., Zhang, J. (2022). Recognition of key factors on attached microalgae growth from the internal sight of biofilm. Science of The Total Environment, 811, 151417.
[139] Subramanian, S., Huiszoon, R.C., Chu, S., Bentley, W.E., Ghodssi, R. (2020). Microsystems for biofilm characterization and sensing–a review. Biofilm, 2, 100015.
[140] Zhang, B., Li, W., Guo, Y., Zhang, Z., Shi, W., Cui, F., Lens, P.N., Tay, J.H. (2020). Microalgal-bacterial consortia: from interspecies interactions to biotechnological applications. Renewable and Sustainable Energy Reviews, 118, 109563.
[141] Karya, N., Van der Steen, N., Lens, P. (2013). Photo-oxygenation to support nitrification in an algal–bacterial consortium treating artificial wastewater. Bioresource Technology, 134, 244-250.
[142] Sforza, E., Pastore, M., Sanchez, S.S., Bertucco, A. (2018). Bioaugmentation as a strategy to enhance nutrient removal: Symbiosis between *Chlorella protothecoides* and *Brevundimonas diminuta*. Bioresource Technology Reports, 4, 153-158.
[143] Ma, X., Zhou, W., Fu, Z., Cheng, Y., Min, M., Liu, Y., Zhang, Y., Chen, P., Ruan, R. (2014). Effect of wastewater-borne bacteria on algal growth and nutrients removal in wastewater-based algae cultivation system. Bioresource Technology, 167, 8-13.
[144] Park, J., Jin, H.F., Lim, B.R., Park, K.Y., Lee, K. (2010). Ammonia removal from anaerobic digestion effluent of livestock waste using green alga *Scenedesmus sp*. Bioresource Technology, 101, 8649-8657.
[145] Quijano, G., Arcila, J.S., Buitrón, G. (2017). Microalgal-bacterial aggregates: applications and perspectives for wastewater treatment. Biotechnology Advances, 35, 772-781.
[146] Abinandan, S., Subashchandrabose, S.R., Venkateswarlu, K., Megharaj, M. (2018). Microalgae–bacteria biofilms: a sustainable synergistic approach in remediation of acid mine drainage. Applied Microbiology and Biotechnology, 102, 1131-1144.
[147] Wang, H., Qi, B., Jiang, X., Jiang, Y., Yang, H., Xiao, Y., Jiang, N., Deng, L., Wang, W. (2019). Microalgal interstrains differences in algal-bacterial biofloc formation during liquid digestate treatment. Bioresource Technology, 289, 121741.
[148] Segredo-Morales, E., González, E., González-Martín, C., Vera, L. (2022). Secondary wastewater effluent treatment by microalgal-bacterial membrane photobioreactor at long solid retention times. Journal of Water Process Engineering, 49, 103200.
[149] Zhang, M., Leung, K.T., Lin, H., Liao, B. (2021). Effects of solids retention time on the biological performance of a novel microalgal-bacterial membrane photobioreactor for industrial wastewater treatment. Journal of Environmental Chemical Engineering, 9, 105500.
[150] Segredo-Morales, E., González-Martín, C., Vera, L., González, E. (2023). Performance of a novel rotating membrane photobioreactor based on indigenous microalgae-bacteria consortia for wastewater reclamation. Journal of Industrial and Engineering Chemistry, 119, 586-597.
[151] Bui, X., Nguyen, T., Nguyen, H., Vo, T., Ngo, T. (2019). Evaluating nutrients removal and membrane fouling of membrane photobioreactor using urine as substrate and microalgae-bacteria

as co-cultures under two light-dark cycles.Proceedings of the Basic Research in “Earth and Environmental Sciences”; November; Ho Chi Minh. pp. 531-533.
[152] Chaleshtori, S.N., Shamskilani, M., Babaei, A., Behrang, M. (2022). Municipal wastewater treatment and fouling in microalgal-activated sludge membrane bioreactor: Cultivation in raw and treated wastewater. Journal of Water Process Engineering, 49, 103069.
[153] Van Loosdrecht, M., Ekama, G., Wentzel, M., Hooijmans, C., Lopez-Vazquez, C., Meijer, S., Brdjanovic, D. (2015). Introduction to modelling of activated sludge processes. Applications of activated sludge models, IWA Publishing: London, pp. 1-68.
[154] Buhr, H., Miller, S. (1983). A dynamic model of the high-rate algal-bacterial wastewater treatment pond. Water Research, 17, 29-37.
[155] Moreno-Grau, S., Garcia-Sanchez, A., Moreno-Clavel, J., Serrano-Aniorte, J., Moreno-Grau, M. (1996). A mathematical model for waste water stabilization ponds with macrophytes and microphytes. Ecological Modelling, 91, 77-103.
[156] Bello, M., Ranganathan, P., Brennan, F. (2017). Dynamic modelling of microalgae cultivation process in high rate algal wastewater pond. Algal Research, 24, 457-466.
[157] Eze, V.C., Velasquez-Orta, S.B., Hernández-García, A., Monje-Ramírez, I., Orta-Ledesma, M.T. (2018). Kinetic modelling of microalgae cultivation for wastewater treatment and carbon dioxide sequestration. Algal Research, 32, 131-141.
[158] Papáček, Š., Jablonský, J., Petera, K. (2017). Towards Integration of CFD and Photosynthetic Reaction Kinetics in Modeling of Microalgae Culture Systems.Proceedings of the Bioinformatics and Biomedical Engineering: 5th International Work-Conference, IWBBIO 2017; April 26–28; Granada, Spain. pp. 679-690.
[159] Reichert, P., Borchardt, D., Henze, M., Rauch, W., Shanahan, P., Somlyódy, L., Vanrolleghem, P. (2001). River water quality model no. 1 (RWQM1): II. Biochemical process equations. Water Science and Technology, 43, 11-30.
[160] Sah, L., Rousseau, D.P., Hooijmans, C.M., Lens, P.N. (2011). 3D model for a secondary facultative pond. Ecological Modelling, 222, 1592-1603.
[161] Beran, B., Kargi, F. (2005). A dynamic mathematical model for wastewater stabilization ponds. Ecological Modelling, 181, 39-57.
[162] Aparicio, S., Robles, Á., Ferrer, J., Seco, A., Falomir, L.B. (2022). Assessing and modeling nitrite inhibition in microalgae-bacteria consortia for wastewater treatment by means of photo-respirometric and chlorophyll fluorescence techniques. Science of The Total Environment, 808, 152128.
[163] Yang, J., Li, Z., Lu, L., Fang, F., Guo, J., Ma, H. (2020). Model-based evaluation of algal-bacterial systems for sewage treatment. Journal of Water Process Engineering, 38, 101568.
[164] Mishra, N., Mishra, S., Prasad, R. (2021). Current Status and Challenges of Microalgae as an Eco-Friendly Biofuel Feedstock: A Review. Present Environment & Sustainable Development, 15, 179-189.
[165] Peng, L., Fu, D., Chu, H., Wang, Z., Qi, H. (2020). Biofuel production from microalgae: a review. Environmental Chemistry Letters, 18, 285-297.
[166] Williams, P.J.L.B., Laurens, L.M. (2010). Microalgae as biodiesel & biomass feedstocks: Review & analysis of the biochemistry, energetics & economics. Energy & Environmental Science, 3, 554-590.
[167] Lam, M.K., Lee, K.T. (2012). Microalgae biofuels: a critical review of issues, problems and the way forward. Biotechnology Advances, 30, 673-690.

[168] Lee, S., Oh, H., Jo, B., Lee, S., Shin, S., Kim, H., Lee, S., Ahn, C. (2014). Higher biomass productivity of microalgae in an attached growth system, using wastewater. Journal of Microbiology and Biotechnology, 24, 1566-1573.
[169] Singh, G., Patidar, S. (2021). Development and applications of attached growth system for microalgae biomass production. BioEnergy Research, 14, 709-722.
[170] Lutzu, G.A., Zhang, L., Zhang, Z., Liu, T. (2017). Feasibility of attached cultivation for polysaccharides production by *Porphyridium cruentum*. Bioprocess and Biosystems Engineering, 40, 73-83.
[171] Derakhshan, Z., Mahvi, A.H., Ehrampoush, M.H., Ghaneian, M.T., Yousefinejad, S., Faramarzian, M., Mazloomi, S.M., Dehghani, M., Fallahzadeh, H. (2018). Evaluation of kenaf fibers as moving bed biofilm carriers in algal membrane photobioreactor. Ecotoxicology and Environmental Safety, 152, 1-7.
[172] Sayre, R. (2010). Microalgae: the potential for carbon capture. Bioscience, 60, 722-727.
[173] Melis, A. (2009). Solar energy conversion efficiencies in photosynthesis: minimizing the chlorophyll antennae to maximize efficiency. Plant Science, 177, 272-280.
[174] Benedetti, M., Vecchi, V., Barera, S., Dall'Osto, L. (2018). Biomass from microalgae: the potential of domestication towards sustainable biofactories. Microbial Cell Factories, 17, 1-18.
[175] Christenson, L.B., Sims, R.C. (2012). Rotating algal biofilm reactor and spool harvester for wastewater treatment with biofuels by-products. Biotechnology and Bioengineering, 109, 1674-1684.
[176] Zamalloa, C., Vulsteke, E., Albrecht, J., Verstraete, W. (2011). The techno-economic potential of renewable energy through the anaerobic digestion of microalgae. Bioresource Technology, 102, 1149-1158.
[177] Cho, D.H., Ramanan, R., Heo, J., Lee, J., Kim, B.H., Oh, H.M., Kim, H.S. (2015). Enhancing microalgal biomass productivity by engineering a microalgal–bacterial community. Bioresource Technology, 175, 578-585.
[178] Goh, B.H.H., Ong, H.C., Cheah, M.Y., Chen, W.H., Yu, K.L., Mahlia, T.M.I. (2019). Sustainability of direct biodiesel synthesis from microalgae biomass: A critical review. Renewable and Sustainable Energy Reviews, 107, 59-74.
[179] Lee, S.Y., Cho, J.M., Chang, Y.K., Oh, Y.K. (2017). Cell disruption and lipid extraction for microalgal biorefineries: A review. Bioresource Technology, 244, 1317-1328.
[180] Saba, B., Christy, A.D., Yu, Z., Co, A.C. (2017). Sustainable power generation from bacterio-algal microbial fuel cells (MFCs): an overview. Renewable and Sustainable Energy Reviews, 73, 75-84.
[181] Lee, D.J., Chang, J.S., Lai, J.Y. (2015). Microalgae–microbial fuel cell: a mini review. Bioresource Technology, 198, 891-895.
[182] Ren, J.L., Zhang, A.H., Kong, L., Wang, X.J. (2018). Advances in mass spectrometry-based metabolomics for investigation of metabolites. RSC Advances, 8, 22335-22350.

Chapter 3: Surface Properties of Membrane Materials and Their Role in Cell Adhesion and Biofilm Formation of Microalgae

Abstract

This study investigated the effects of surface properties of membrane materials on microalgae cell adhesion and biofilm formation using *Chlorella vulgaris* and five different types of membrane materials under hydrodynamic conditions. The results suggest that the contact angle (hydrophobicity), surface free energy, and free energy of cohesion of membrane materials alone could not sufficiently elucidate the selectivity of microalgae cell adhesion and biofilm formation on membrane materials surfaces, and membrane surface roughness played a dominant role in controlling biofilm formation rate, under tested hydrodynamic conditions. A lower level of biofilm EPS production was generally associated with a larger amount of biofilm formation. The Zeta potential of membrane materials could enhance initial microalgae cell adhesion and biofilm formation through salt bridging or charge neutralization mechanisms.

Keywords: Membrane carbonated biofilm reactor; extractive membrane microalgal biofilm reactor; microalgal biofilm, membrane material, membrane surface properties, extracellular polymeric substances.

3.1. Introduction

Microalgae are photosynthetic microorganisms widely used in many areas, including food, cosmetics, pharmaceutics, and wastewater treatment [1]. Microalgae have attracted much attention in wastewater purification in recent years because of their high potential for nitrogen and phosphorus nutrient removals, which can make up for the insufficient nutrient removal in conventional activated sludge wastewater treatment for organic pollutants removal [2, 3]. The microalgal biomass outlet can be the biofuel or biodiesel production feedstock because of its high lipid content [4-6]. However, one of the major shortcomings of microalgae application is that the suspended microalgae in the culture medium have a low biomass concentration (0.5-6 g/L) [7-9]. Furthermore, the conventional harvesting methods to concentrate the suspended microalgae, such as filtration, gravity sedimentation, flocculation, and centrifugation, require significant energy consumption, chemical usage, or land occupancy, which can occupy about 30% of the total production cost [10, 11].

Compared to conventional suspended cultivation, an immobilized method known as algal biofilm cultivation has been recommended to enhance the cost-effectiveness of microalgae harvesting and wastewater treatment [9, 12-14]. Briefly, some research found that microalgae cells have an affinity to some substrates and tend to aggregate on the substrate surface to form biofilm [15, 16]. The microalgal biofilm can lead to concentrated biomass, and the biofilm biomass is more accessible to harvest than the suspended microalgae [10]. As a result, the algal biofilm reactor that can prolong microalgae's attachment has received much attention over the last decade [17]. An algal biofilm reactor can satisfy the wastewater treatment requirement and the microalgal biomass harvesting efficiency [18]. However, conventional microalgal biofilm reactors have faced the

challenges of CO_2 transfer due to increased biomass concentration and growth and limited penetration distance of CO_2 in biofilm.

Furthermore, a settler is needed to separate the detached biofilm from treated effluent. Thus, the concepts of membrane carbonated microalgal biofilm reactor (MCMBR) and extractive membrane microalgal biofilm reactor (EMMBR) are proposed to overcome the CO_2 transfer limitation and/or biomass separation problems in conventional microalgal biofilm reactors. The MCMBR utilizes hydrophobic membranes to transfer molecule CO_2 to the microalgal biofilm formed on the outer side of the membrane. In contrast, the nutrients (N and P) from wastewater are transferred into the microalgal biofilm from an opposite direction in a counter-current approach, which is different from the conventional microalgal biofilm that has a co-current approach for CO_2 and nutrients (N and P) deliveries. It is anticipated that the counter-current approach has a much higher process efficiency for microalgal biofilm growth and nutrient removal than the co-current approach. On the other hand, the EMMBR uses the hydrophilic membrane as a substrate to support biofilm formation on the membrane surface for nutrient uptake and serve as a separation barrier to permeate the treated effluent from the biofilm and get a zero-solids permeate and thus solve the biomass separation problem from treated effluent. Both MCMBR and EMMBR, as novel and emerging technologies, are highly desirable for exploration.

Furthermore, a comprehensive understanding of microalgal biofilm's characteristics is the premise of microalgal biofilm reactors efficiently applied in industrial applications and wastewater treatment. As Zhuang et al. (2018) mentioned, microalgal biofilm formation can be affected by microalgae species, substrate properties, and cultivation environment [14]. One of the major factors is the adhesion of microalgae cells for biofilm formation, which can be classified into two main aspects: microalgal properties and substrate properties [19, 20]. Some literature has studied

the different microalgae adhesion performances on different material substrates [9, 20-23]. Talluri et al. (2020) found that hydrophilic materials such as glass could bind water molecules via hydrogen bonding or electrostatic interaction, which could hinder microorganism cell adhesion [24]. Thus, Shen et al. (2016) mentioned that the hydrophobic material could be a good attached substrate for microalgae due to its high affinity [16].

Moreover, employing a porous substrate as a biofilm carrier has been suggested because the porous substrate (like a membrane), contains advantages such as high gas and liquid transfer efficiency thus increasing the microalgal biofilm productivity [9, 10, 25]. Literature also mentioned that the algal biofilm formed more easily on the porous substrate [14]. As a result, microalgal biofilm cultivation on a hydrophobic porous substrate seems to be an optimum option for microalgal biofilm reactor applications and MCMBR development. Even though much research has been done on the adhesion of microalgae and microalgal biofilm formation on various surfaces, no study is still focused on hydrophobic membrane materials for MCMBR development. And the exact factors that affect biofilm development on hydrophobic membrane material are still unclear. A study of microalgal biofilm attachment performance on hydrophobic membrane materials is required to fill the knowledge gap of microalgal formation performance and investigate the satisfactory membrane substrates for further microalgal biofilm reactor application for wastewater treatment.

As the first step in developing the novel MCMBR and EMMBR technology, the most efficient and suitable membrane materials for fast CO_2 delivery and/or fast microalgal biofilm formation should be identified. This study aimed to study the influences of five membrane materials with different surface roughness and hydrophobicity on cell adhesion and microalgal biofilm formation. This was done by examining the dynamic microalgal biofilm cultivation using

a CDC biofilm photobioreactor (Biosurface Technologies Corporation, Montana, USA). The change in biofilm quantity and biofilm formation with experimental time was monitored. The contact angle, surface energy, zeta potential, surface roughness of membrane materials coupons and extracellular polymeric substance properties of microalgal biofilm were characterized. The impact of membrane surface properties, microalgal biofilm properties, and floc properties on microalgal cell adhesion and biofilm formation was systematically assessed and explored. An improved fundamental understanding of the roles of membrane materials and biofilm properties on cell adhesion and microalgal biofilm formation rate was achieved.

As compared to previous studies on microalgae cell adhesion and biofilm formation on substrates in the literature, this study distinguished itself from the studies in the literature with novelties in three aspects: (1) this study used membrane materials (for emerging membrane microalgal biofilm photobioreactor development) rather than conventional substrates, such as plastic rings and clay pellets etc., for cell adhesion and biofilm formation, (2) a comprehensive characterization of the surface properties, including contact angles, zeta potential, and surface roughness of membrane materials, which are not found for such a complete surface characterization in the studies in the literature for conventional substrates; and (3) this study was conducted in a CDC biofilm reactor under hydrodynamic conditions similar to the industrial application.

3.2. Materials and methods

3.2.1. Microalgae strains and culture medium

Chlorella vulgaris (CPCC 90) was obtained from the Canadian Phycological Culture Centre at the University of Waterloo, ON, Canada. Microalgae were precultured in a 1.5 L plastic

reactor with BG-11 medium, followed by previous literature [26-28]. The element constitution and concentration of BG-11 medium were shown on supplementary material (Table 3.1). The plastic reactor was illuminated by fluorescent light (94.85 μmol/m^2/s) with constant aeration (1.0 L/min) and placed in a walk-in incubator room under controlled environmental conditions at room temperature. The total suspended solids quantified the microalgal biomass concentration (g/L).

Table 3.1. Element constitution and concentration of BG-11 medium.

Component	Concentration g/L
$NaNO_3$	1.5
K_2HPO_4	0.03
$MgSO_4 \cdot 7H_2O$	0.075
$CaCl_2 \cdot 2H_2O$	0.036
Citric Acid	0.006
$Na_2EDTA \cdot 2H_2O$	0.001
Na_2CO_3	0.02
Trace element	
H_3BO_3	0.00286
$MnCl_2 \cdot 4H_2O$	0.00181
$ZnSO_4 \cdot 7H_2O$	0.000222
$NaMoO_4 \cdot 2H_2O$	0.00039
$CuSO_4 \cdot 5H_2O$	0.000079
$Co(NO_3)_2 \cdot 6H_2O$	0.0000494

Algal biofilm productivity P_b (g/m^2) was calculated as follows:

$$P_b = \frac{W_t - W_0}{2A_s} \quad (3.1)$$

W_t and W_0 are the dried weight of the membrane materials coupons harvested on a certain day (t) and before cultivation, respectively, and A_s = 0.000127 m^2 is the effective surface of each side of each tested coupon (diameter: 12.7 mm).

3.2.2. Materials

Sodium nitrate, dipotassium hydrogen phosphate, citric acid, magnesium sulfate heptahydrate, calcium chloride, ethylenediaminetetraacetic acid tetrasodium salt dihydrate,

sodium carbonate, boric acid, manganese chloride tetrahydrate, cobaltous nitrate hexahydrate, zinc sulfate heptahydrate, sodium molybdate dihydrate, sodium chloride, copper sulfate pentahydrate, and sodium hydroxide were obtained from Sigma-Aldrich. The concentrations of these inorganic nutrients in the feed are listed in Table 3.1 in the supplemental materials. Hydrochloric acid (36.5%) obtained from Sigma-Aldrich was diluted to 3.65% wt. before use. CDC biofilm reactor and 5 different membrane material coupons (Polypropylene (PP), Polyurethane rubber (PU), Silicone rubber (Si), Polytetrafluoroethylene (PTFE), and Nylon) were purchased from Biosurface Technologies Corporation (Montana, USA) for adhesion and biofilm formation test.

3.2.3. Experimental set-up

The experimental set-up utilized a CDC biofilm reactor (Biosurface Technologies Corporation, USA) to build an immersed vertical microalgal biofilm system (Figure 3.1). The effective volume of the CDC biofilm reactor used was 360 mL. Five types of membrane materials coupons, Nylon, polypropylene (PP), polytetrafluoroethylene (PTFE), polyurethane rubber (PU) and silicone rubber (Si) were used; they were selected based on their suitability as membrane materials and high availability and affordable cost. All the membrane materials coupons were circular (0.0127 m × 0.0038 m, diameter × thickness). The coupons were rinsed with deionized water and dried in the oven at 44 °C for two days. Each coupon was weighed before microalgae cultivation. A total of 24 of the same type of coupons were immersed into the CDC biofilm reactor in each experimental run with a stirring speed of 125 rpm for 16 days of cultivation. The CDC biofilm reactor was in a semi-continuous phase; a 45 mL BG-11 culture medium (TN: 250 mg/L, TP: 5 mg/L) was pumped into the reactor, and the same 45 mL suspension was drained from the reactor daily. This gave a hydraulic retention time (HRT) of 8 days. Air with an aeration intensity of 1.0 L/min was provided to the CDC biofilm reactor to provide CO_2 for microalgal growth. A

magnetic stirring speed of 125 rpm for the shaft of the membrane materials coupons (24 coupons) assembly (which was immersed vertically in the suspension) was provided to control the hydrodynamic conditions. The suspended microalgal mixed liquor was collected for further measurements (zeta potential, EPS extraction, and biomass concentration measurement). Four fluorescent lamps were installed around the CDC biofilm reactor, providing an illuminating intensity of 94.85 µmol/m^2/s. The membrane materials coupons were removed from the CDC biofilm reactor after 2, 4, 6, 8, 10, 12, 14 and 16 days of cultivation. The attached microalgal biomass was collected for EPS extraction and biofilm attachment measurement. Zeta potential, pH, and suspended microalgal mixed liquor cell concentration were determined. Three coupons were removed from the CDC Biofilm reactor each time for biofilm characterization.

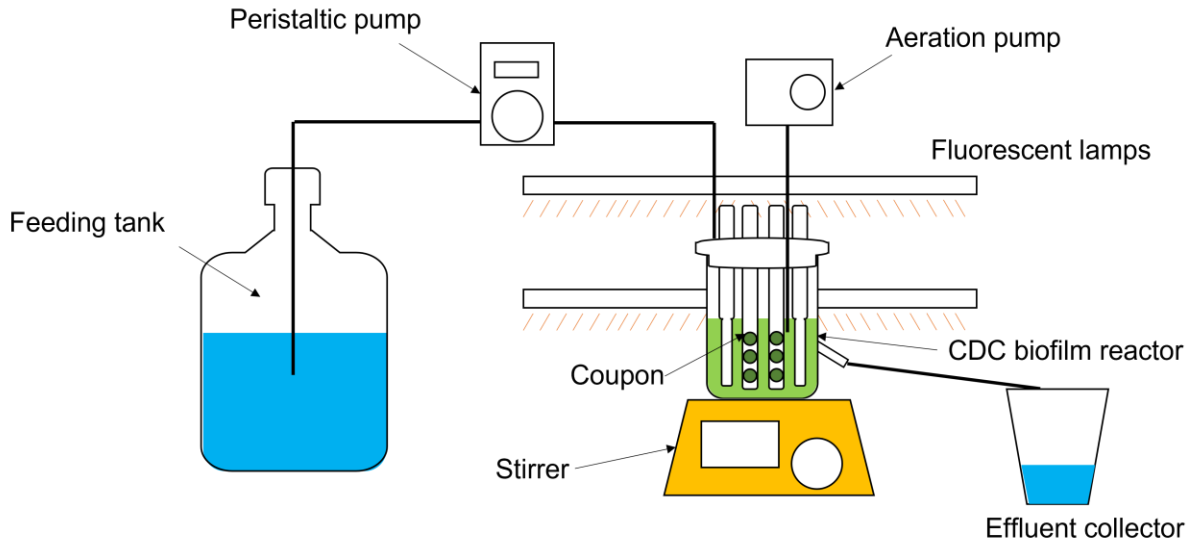

Figure 3.1. Experimental set-up of the CDC biofilm reactor for different material coupons.

3.2.4. Contact angle

The contact angle of the five types of membrane materials coupons and *Chlorella vulgaris* cells was determined using the optical tensiometer instrument (Theta Lite, Biolin Scientific, USA) accoutred with a camera followed by a sessile drop method in Attension software. Briefly, 5 µL of

droplets from three reference liquids (distilled water, formamide and diiodomethane) were dropped onto the surface of the membrane materials, respectively. The average results of three independent tests were reported. Before contact angle measurement, the *Chlorella vulgaris* cell layer was prepared as a lawn constructed by vacuum-filtering with the 0.45 μm mixed cellulose esters (MCE) filter membrane (47 mm diameter, Merck Millipore Ltd, Ireland).

3.2.5. Surface free energy (SFE)

The SFE of the membrane materials and *Chlorella vulgaris* were determined through Young's equation combined with contact angle [19]:

$$\gamma_{\zeta}=\gamma_L \cos\theta + \gamma_{SL} \quad (3.2)$$

where the γ_{ζ} is the SFE (mJ/m^2) of the solid material, γ_L is the surface energy (mJ/m^2) of the liquid, θ is the contact angle, and γ_{SL} is the interfacial energy (mJ/m^2) between solid and liquid. According to Tsavatopoulou and Manariotis (2020), the interfacial energy between solid and liquid $_{SL}$ can be obtained by the Good thermodynamic approach, which mentions that γ_{SL} is composed of polar and non-polar components [8]:

$$\gamma_{SL} = \gamma_{SL}^{P} + \gamma_{SL}^{LW} \quad (3.3)$$

Moreover, polar and non-polar components can be determined by the positive and negative interfacial tensions by the Van Oss equation [8]:

$$\gamma_{SL}^{P} = 2(\sqrt{\gamma_S^+} - \sqrt{\gamma_L^+})(\sqrt{\gamma_S^-} - \sqrt{\gamma_L^-}) \quad (3.4)$$

$$\gamma_{SL}^{LW} = (\sqrt{\gamma_S^{LW}} - \sqrt{\gamma_L^{LW}})^2 \quad (3.5)$$

where γ_{S^+} and γ_{S^-} are the acid and base interactions of the solid, and γ_{L^+}, γ_{L^-} are the acid and base interactions of the liquid, γ_S^{LW} and γ_L^{LW} are Lifshitz-van der Waals forces/interactions for solid and liquid, respectively. The liquid properties (γ_{L^+}, γ_{L^-} and γ_L^{LW}) can be obtained from the liquid reference list [29, 30], and the solid properties can be calculated by the van Oss-Chaudhury-Good Equation [31]:

$$(1+\cos\theta)\,\gamma_L = 2\left(\sqrt{\gamma_S^{LW}\cdot\gamma_L^{LW}} + \sqrt{\gamma_S^{+}\cdot\gamma_L^{-}} + \sqrt{\gamma_S^{-}\cdot\gamma_L^{+}}\right) \qquad (3.6)$$

By choosing a non-polar diiodomethane to Equation (3.6), acid and base interactions of the liquid are equal to zero, and Equation (3.6) will change to:

$$(1+\cos\theta)\,\gamma_L = 2\sqrt{\gamma_S^{LW}\cdot\gamma_L^{LW}} \qquad (3.7)$$

Thus, the γ_S^{LW} can be obtained. Then, further applying two other polar liquids (DI water and formamide) to Equation (3.6), the two remaining γ_{S^+} and γ_{S^-} can be determined. Therefore, the SFE can be calculated through Equation (3.2) based on the known factors. Moreover, as van Oss et al. (1988) mentioned, the hydrophobicity of the microalgae cell or substrate surface can also be determined by their free energy of cohesion (ΔG_{coh}) with the following equation [32]:

$$\Delta G_{coh} = -2\left(\sqrt{\gamma_S^{LW}} - \sqrt{\gamma_L^{LW}}\right)^2 - \left[4\left(\sqrt{\gamma_S^{+}\cdot\gamma_S^{-}} + \sqrt{\gamma_L^{+}\cdot\gamma_L^{-}} - \sqrt{\gamma_S^{+}\cdot\gamma_L^{-}} - \sqrt{\gamma_S^{-}\cdot\gamma_L^{+}}\right)\right] \qquad (3.8)$$

3.2.6. Extracellular Polymeric Substances (EPS) Extraction and Measurement

The EPS extraction was modified according to Tong and Derek [21]. This study classified the microalgal organic matter extraction into two sections: soluble EPS from the microalgal medium in the CDC biofilm reactor and bounded EPS, which adhered to the microalgal cells. The microalgae biofilm biomass was gently scrapped off from the coupons and extracted with 20 mL

of 1.5 M sodium chloride at 30 ℃ for 1 h in the water bath with 120 rpm oscillation to extract the tightly bounded EPS from the microalgal cells. Both the collected samples were centrifuged at 2500 ×g for 15 minutes. Then the soluble EPS and bounded EPS supernatant were filtered through a 0.45 µm MCE filter membrane (47 mm diameter, Merck Millipore Ltd, Ireland) to avoid the effect of cell debris on composition analysis. The EPS supernatant was then measured total carbohydrate and protein through a modified spectrometric detection method followed by Gaudy and Wolfe, and Lowry et al., respectively [33, 34]. Glucose and bovine serum albumin (BSA) were used as the standard for carbohydrates and protein measurement, respectively. Both absorbances of EPS sample for carbohydrate and protein were read on a UV spectrophotometer (Genesys 10S UV-Vis, Thermo, USA).

3.2.7. Nutrient measurement

The total nitrogen (TN) and total phosphorus (TP) were quantified with the alkaline persulfate digestion-UV spectrophotometric method and ammonium molybdate spectrophotometry, respectively [35]. Duplicate measurements of TN and TP were conducted for each sample, and the average values were reported. Both absorbances of the sample for total nitrogen and phosphorus were read on a UV spectrophotometer (Genesys 10S UV-Vis, Thermo, USA).

3.2.8. Zeta potential

A NanoBrook Zeta PALS (Brookhaven Instruments Corp, USA) was employed to analyze the zeta potential of the microalgae suspension. 1 mL of microalgae suspension was added to 5 mL of prefiltered 1mM KCl solution for zeta potential measurement. The zeta potential of the membrane material coupons was gauged through a surface zeta potential electrode BI-SZP

(Brookhaven Instruments Corp, USA) applied in the culture medium (Table 3.1) of the microalgae growth. All zeta potential experiments were conducted at room temperature at a constant electric field (8.4 V/cm), and the average number of three independent measurements was reported.

3.2.9. Particle size distribution (PSD)

The particle size distribution of microalgae cells was determined by a Mastersizer Micro Plus 3000 (Malvern Instrument, Worcestershire, UK) in the range of 0.01 μm to 3500 μm. The suspended samples were stirred at 360 rpm to obtain adequate dispersed suspension before measuring the particle sizes.

3.2.10. Surface roughness

Three-dimensional (3D) images of the membrane materials coupon surface topography and roughness parameters were carried out by using an MFP-3D origin+ atomic force microscope (AFM) (Oxford Instruments, UK). The surface of coupons was scanned in a contact mode on the area of 20 × 20 μm^2 with a scan rate of 1 Hz. Silicone AC160TS-R3 cantilevers (Oxford Instruments, UK) with nominal force constant 26 N/m and resonance frequency 300 kHz were employed to image the coupon surface during AFM measurement. The image and data were collected and processed by Asylum Research software across scanned areas 20 × 20 μm.

3.2.11. Statistical analyses

The experiment data were examined using a one-way ANOVA test and Spearman correlations conducted from the Origin software for significant difference analysis ($p < 0.05$).

3.3. Result and discussion

3.3.1. Microalgae biofilm growth analysis

In this study, the cell adhesion and biofilm formation of the *Chlorella vulgaris* strain were tested for a total of about 100 days of cultivation, including five materials phases (Nylon, PP, PU, PTFE, and Si) in the CDC biofilm reactor. As shown in Figure 3.2a, during the 100 days of cultivation, the suspended microalgae biomass concentration was maintained at around 1.63 g/L. The pH of the microalgae culture medium was stable at around 9.16. Figure 3.2b shows the zeta potential of microalgae suspension in the culture medium over 100 days was around -22 mV, which is similar to the literature value [36]. Figure 3.2c shows that the TN and TP concentrations in the microalgae culture medium were around 145.18 mg/L and 0.52 mg/L, respectively. The ANOVA test revealed that the population means were not significantly different among the five membrane materials coupon phases at the 0.05 level (ANOVA, $p>0.05$), which means that the conditions of the suspended microalgae in the reactor were relatively stable during the experimental time. Moreover, Table 3.2 shows the TN and TP removal efficiencies over the five membrane material coupon phases. The TP removal of the CDC biofilm reactor during all five phases was above 85%, and the TN removal ranged from 36% to 48 %. The moderate removal of the TN could be explained by the high nitrogen/phosphorus ratio (50:1) in influent, resulting in a low efficiency for nitrogen consumption due to phosphorus limitation [37]. Xin et al. (2010) also observed the nitrogen removal of *Scenedesmus sp.* dropped to 45% when the nitrogen/phosphorus ratio of the culture medium reached 20:1 [38]. However, the ANOVA test of either TN or TP removal revealed that the population means were not significantly different in the five membrane materials coupon phases at the 0.05 level (ANONA, $p > 0.05$). The reason for no statistically significant difference between the nutrient consumption among the five phases might be owing to the fact that the

quantity of biofilm on the membrane materials coupon surface was not large enough to cause a significant change in the nutrient consumption compared to the suspended microalgae. Moreover, Figure 3.3 exhibits the particle size distribution of the suspended microalgal culture medium on the 1st day and the 16th day. The particle size distribution showed that the microalgae cells or flocs were also under the similar particle size ranges, which indicated that particle size had no significant effects on biofilm formation in this study. Thus, it could be assumed that all the microalgae mediums of different membrane material coupon phases were under similar conditions.

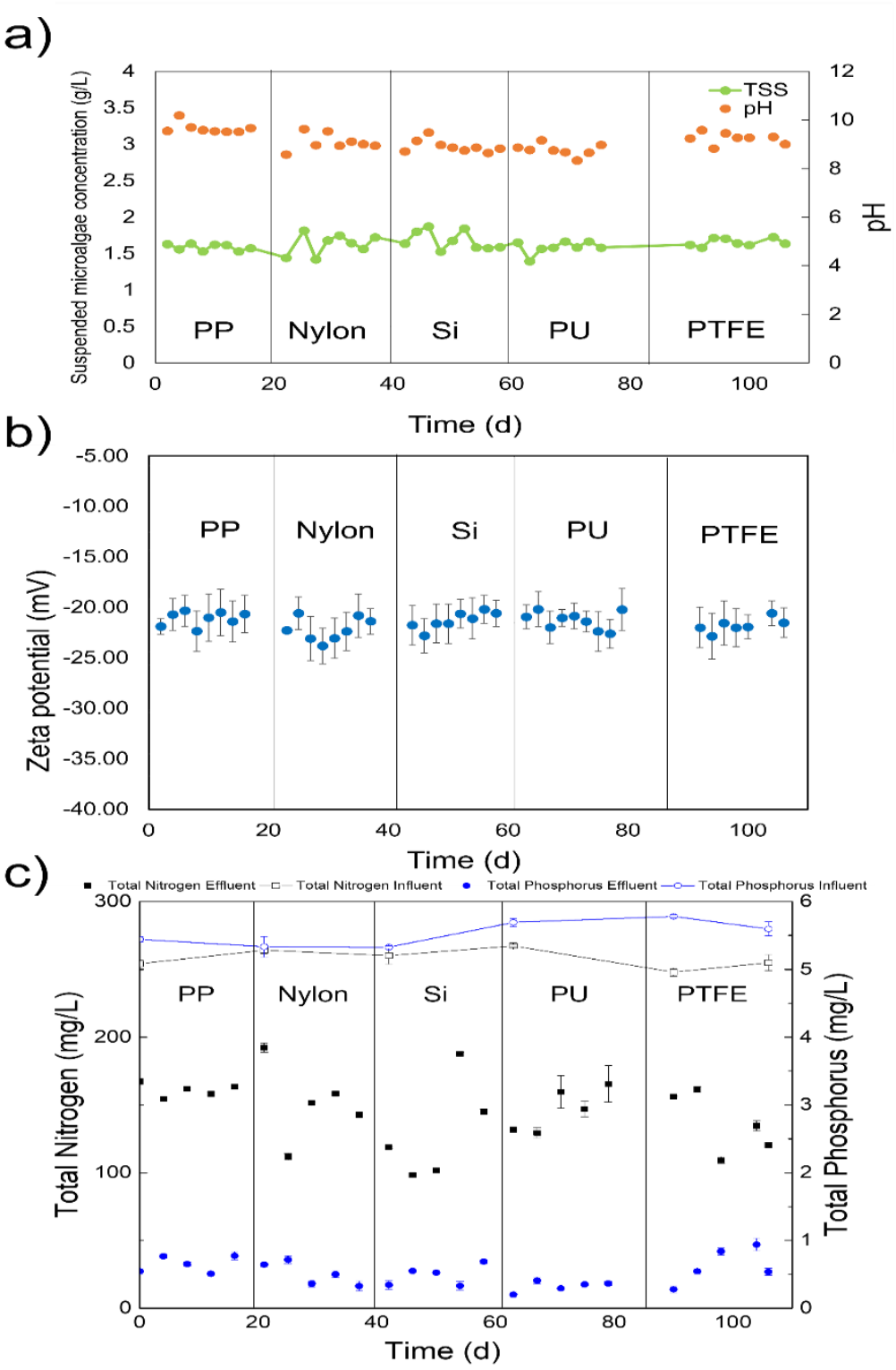

Figure 3.2. a) Biomass concentration and pH of the microalgal culture medium, b) Zeta potential of microalgal culture medium, and c) Nutrient concentration of influent and effluent of CDC reactor at different material coupon phases.

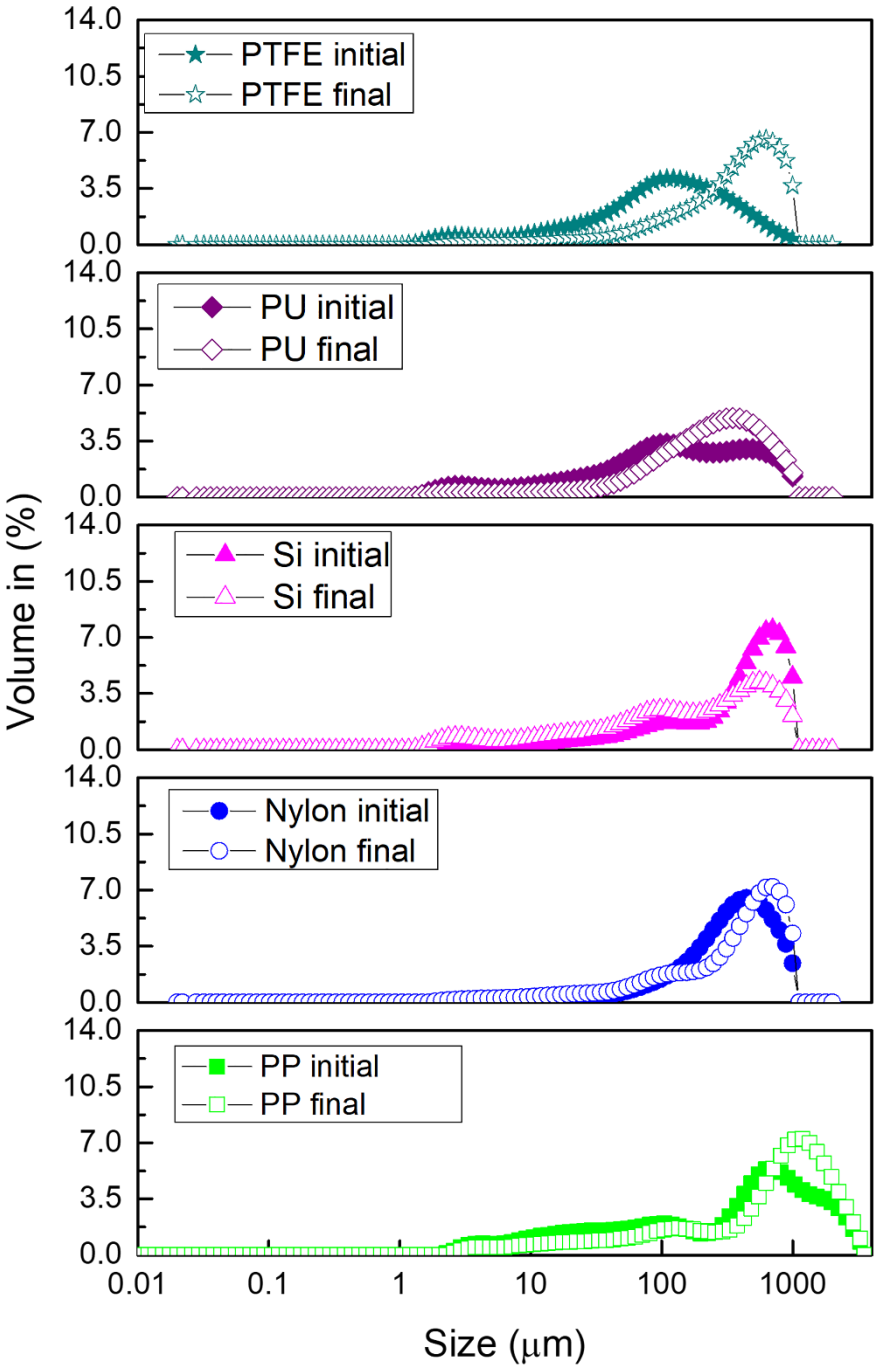

Figure 3.3. Particle size distribution of microalgal culture medium in different material phases.

Table 3.2. Nutrient removal of CDC reactor at different material coupon phases.

	PP	Nylon	PU	Si	PTFE
Nitrogen (TN) removal	36% ± 2%	39% ± 12%	48% ± 15%	41% ± 6%	45% ± 9%
Phosphorus (TP) removal	87% ± 2%	90% ± 3%	90% ± 3%	94% ± 2%	87% ± 5%

3.3.2. Membrane material morphology

The coupons made with different membrane materials were designed with the same dimensions (12.7 mm diameter disc coupon) (Figure 3.4). The differences among membrane material coupons were not only the materials' composition but also the materials' surface properties, including hydrophobicity, zeta potential, surface roughness, and so on. Compared to the silicone rubber (Si) and polyurethane (PU) rubber coupons, the rest three coupons (polypropylene (PP), nylon, and Polytetrafluoroethylene (PTFE)) had different forms on the surface of the coupon. Figure 3.5 shows the photograph of these two types of membrane material coupons. As shown in Figure 3.5, there is a ring texture structure on the polypropylene (PP) coupon but not on the silicone rubber (Si) coupon surface, which may affect biofilm attachment. Thus, the impact of surface roughness was also considered in this study and will be discussed in the following sections.

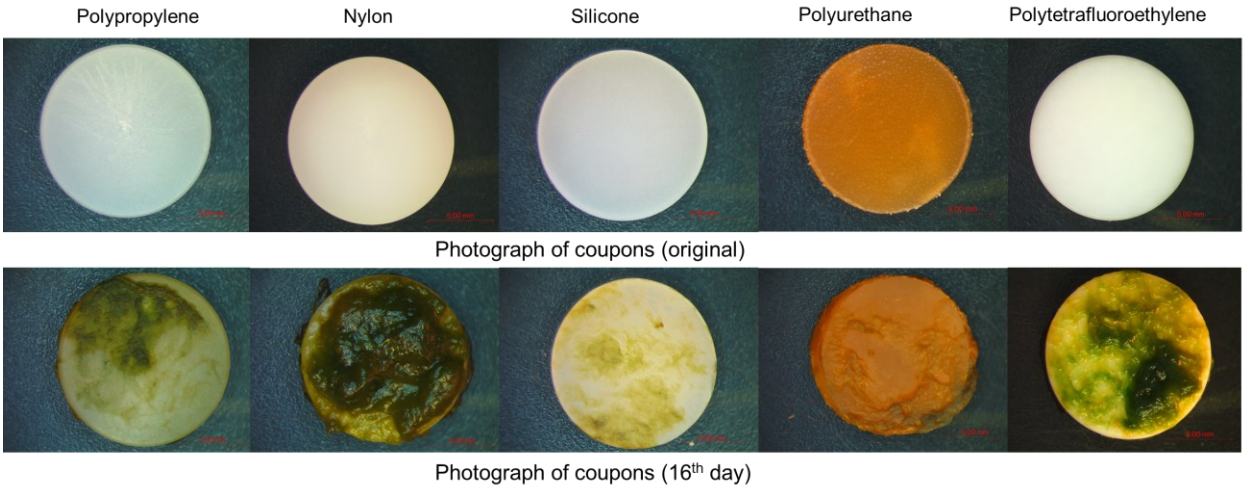

Figure 3.4. Photograph of different material coupons before cultivation and after 16 days of cultivation.

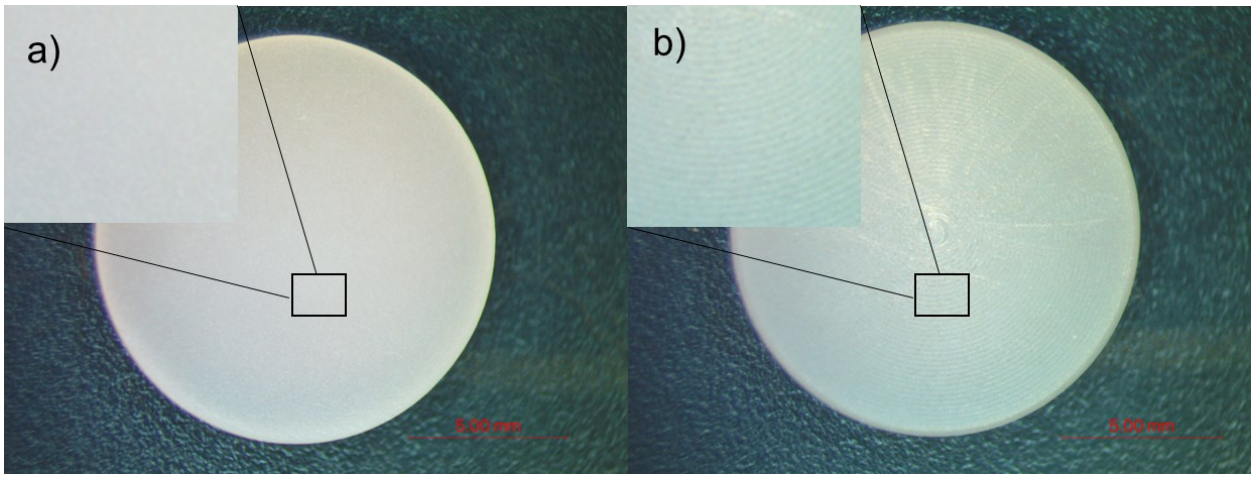

Figure 3.5. Photograph of smooth a) silicone rubber coupon and rough b) polypropylene coupon.

3.3.3. Microalgal biofilm production

Figure 3.6 exhibits the wet biomass amount of *Chlorella vulgaris* biofilm after 1 hour of drying at ambient temperature after being taken out from the CDC biofilm reactor every two days over the cultivation period (16 days). The highest biofilm attachment reached 514.3 g/m^2 on the Nylon coupon on the 16th day (growth rate: 32.14 g/m^2/d). The second largest amount of wet biofilm attachment was on PTFE coupons (113.65 g/m^2). The wet biofilm attachments of PP (28.61 g/m^2), PU (12.07 g/m^2), and Si (6.43 g/m^2) coupons were all below 30 g/m^2.

Furthermore, the photograph of the attached biofilm on membrane material coupons also showed that the Nylon coupon has the thickest biofilm (Figure 3.4). Thus, based on the attachment performance, Nylon was the best material for fast *Chlorella vulgaris* biofilm cultivation under tested hydrodynamic conditions. The following sections will further investigate the factors affecting the biofilm formation rates observed in this study.

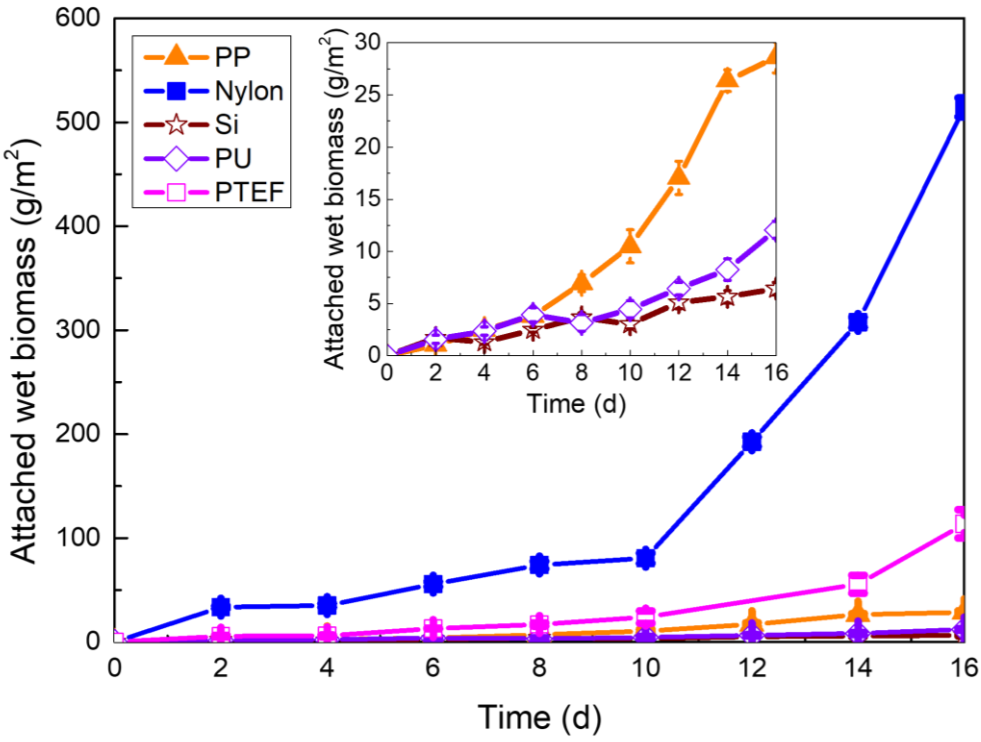

Figure 3.6. Wet biofilm attachment profiles of different material coupons undergo 16 days period.

3.3.4. Factors affecting cell adhesion and biofilm formation rate

Multiple factors could influence biofilm development: surface properties of the attached substrate, microalgae species, and environmental conditions such as pH, hydrodynamic conditions, temperature, and light intensity [39-41]. According to the previous microalgae growth analysis, the effect of environmental conditions was insignificant here, as the temperature and pH were relatively stable from the beginning to the end of the experiments. Furthermore, the hydrodynamic conditions were maintained the same. Thus, the surface properties of *Chlorella vulgaris* and the membrane material coupons were the majority factors that controlled the cell adhesion and biofilm formation rates in this study.

3.3.4.1. Influence of biofilm biomass EPS

Figure 3.7a shows the EPS concentration of biofilm on different membrane materials over 16 days of cultivation. On the 16th day, the biofilm on Nylon coupons contained the lowest total EPS content, about 67.29 mg/g biofilm. The highest total EPS can reach 239.96 mg/g biofilm achieved on the surface of silicone rubber (Si) coupons. The values of biofilm EPS production are not reported here for the early stage (2, 4 days), due to the limited amount of cell adhesion as biofilm and thus below the detection and analytical limits of EPS extraction and analysis. Figure 3.8 exhibits the change in EPS productivity (mg EPS/g biofilm) on biofilm formation for the last three days of biofilm sampling (days 12, 14 and 16). In general, lower EPS quantities (mg EPS/g biofilm) of biofilms on Nylon, PTEF and PP, as compared to the larger EPS quantities of biofilms on PU and Si (Figure 3.7a), were associated with a larger amount of biofilm formation (Figure 3.6). This may suggest that under carbon source and light penetration limitation for thicker biofilm (a larger amount of biofilm), the secreted EPS of biofilm might serve as a carbon source for cell maintenance and growth in the inner layer of the thicker biofilm. Thus the total amount of EPS (mg EPS/g biofilm) decreased with an increase in the biofilm quantity on the membrane materials and experimental time (Figure 3.8) [42, 43]. Shen et al. (2015) also observed a similar trend during *B.brauinii* cultivation, and they found the EPS/biofilm concentration reduced from 85 mg/g to 45 mg/g after 20 days of cultivation [44].

However, as Cheah and Chan (2021) described, EPS are biomolecules produced by microalgal cells and are a binding agent contributing to the aggregation of the microalgae cells on the attached substrates [39]. They also mentioned that EPS accumulation on the substrate surface would increase the adhesion strength between the cells and substrates. The microorganisms in the biofilm will tend to increase the secretion of EPS to maintain the biofilm matrix structure during

the later biofilm thickening period [39, 40]. The EPS production profiles did not support their claim, indicating that EPS production was not the significant or dominant factor influencing this study's *Chlorella vulgaris* biofilm adhesion. Similar arguments were claimed by Devi et al. (2021) that the EPS amount is not the main dependent factor of cell adhesion strength [45]. Rather, as they illustrated, the biochemical composition diversity and EPS age play a more important role in biofilm adhesion behaviour than EPS amount. Figure 3.7b exhibits microalgal biofilm EPS's carbohydrate and protein fraction on different material coupons. In this study, the protein had a higher fraction than that of the carbohydrates fraction in some phases. Some membrane materials' protein content can reach almost four-fold of the carbohydrates (79% protein vs. 21% carbohydrate of Nylon coupon on the 16^{th} day). The low carbohydrate fraction of EPS in this study might also verify the previous suggestion that the microalgae biofilm consumed the EPS as a carbon sink to replenish the carbon shortage, which phenomenon also mentioned by some literature [21, 46, 47].

Moreover, Ji et al. (2021) also illustrated that the hydrophobicity of the EPS influences the initial adhesion performance [48]. They found that the EPS of *Chlorella vulgaris* with the dominant hydrophobic fraction preferred to adhere to the hydrophobic PTFE surface rather than the hydrophilic polymethyl methacrylate (PMMA) surface. Thus, the effect of the varieties of EPS biochemical compositions and physicochemical properties should also be considered in future work.

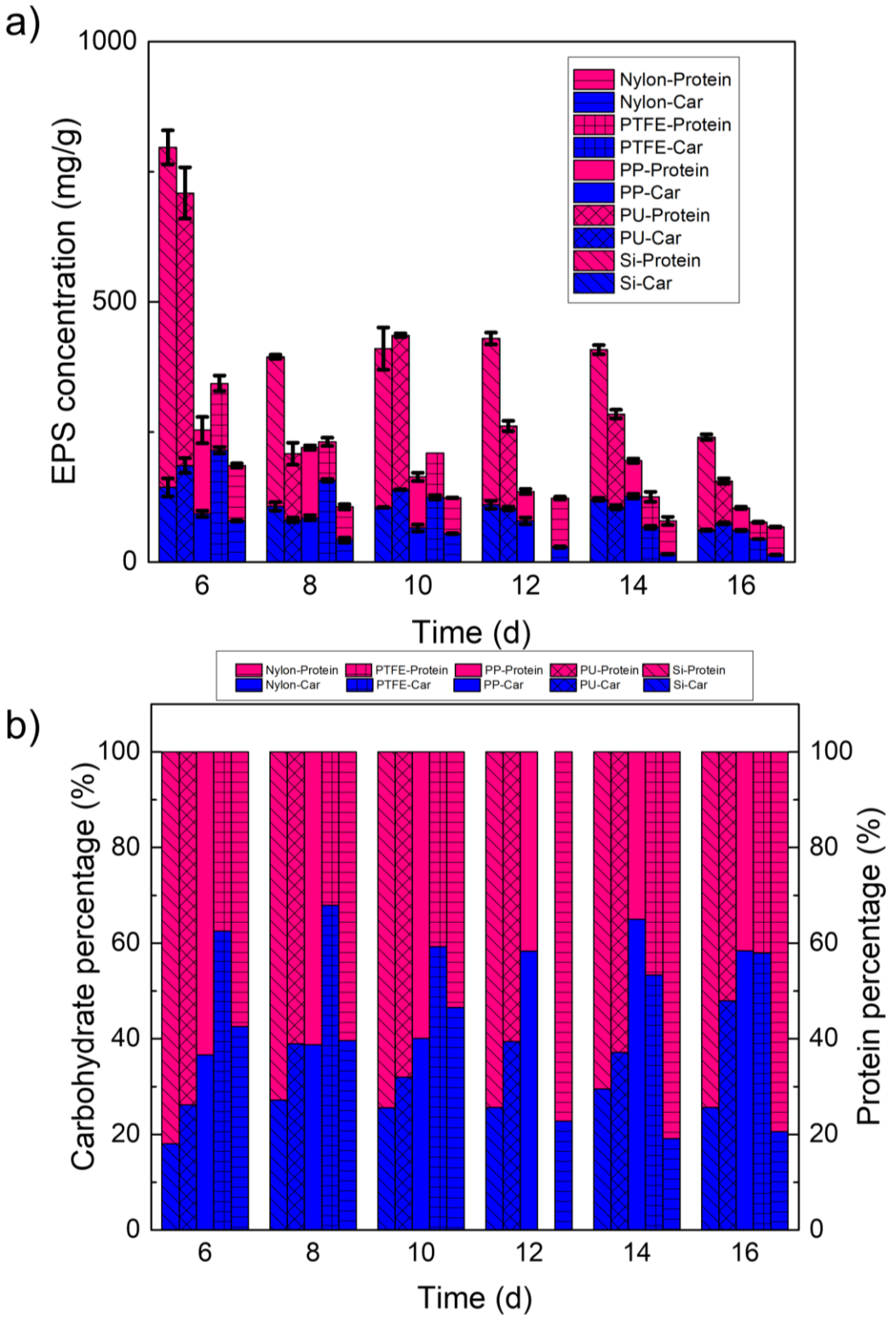

Figure 3.7. The bounded EPS a) concentration and b) composition proportion of C. V biofilms at different coupon phases (the EPS of the 12th day of the PTFE membrane material was not measured due to unexpected laboratory closure of that day).

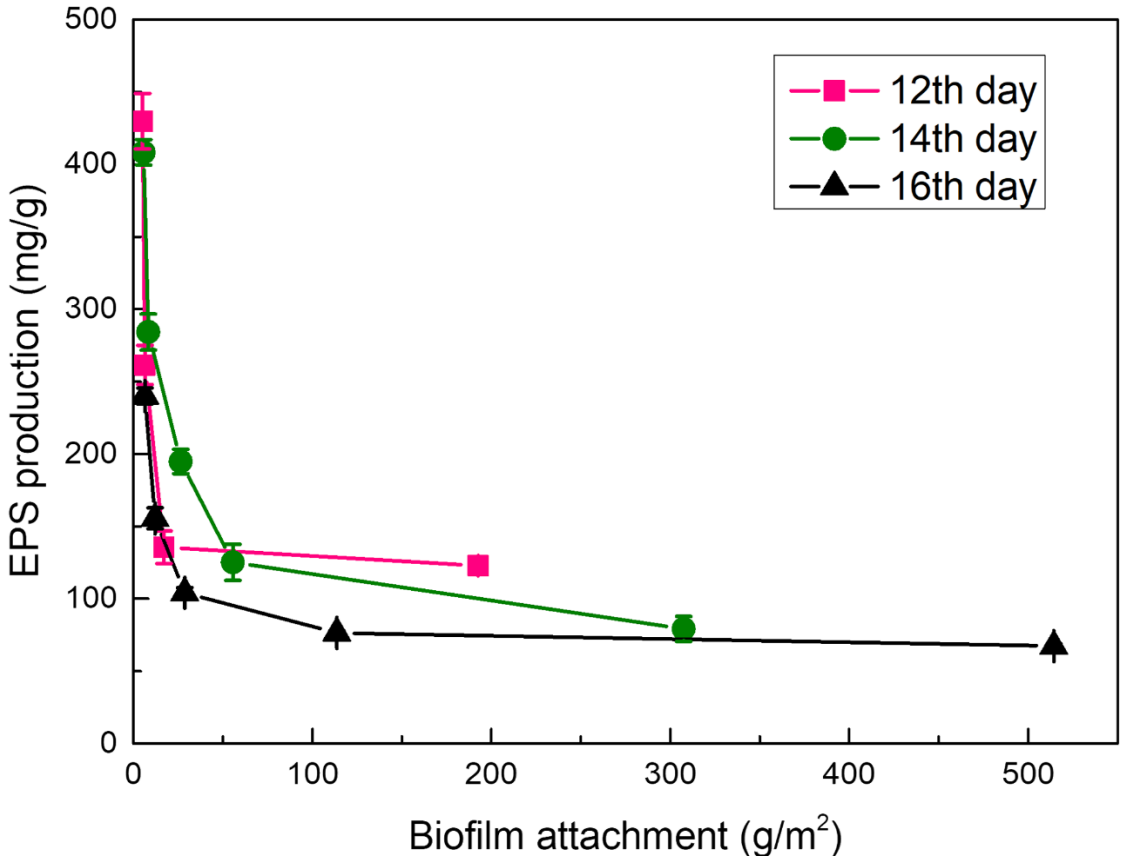

Figure 3.8. Changing of EPS productivity (mg EPS/g biofilm) on biofilm formation for the 12th, 14th, and 16th day.

3.3.4.2. Influence of membrane surface properties

Tables 3.3 and 3.4 summarize the surface properties of the membrane materials and microalgae species (contact angles, surface free energy (SFE), free energy of cohesion (ΔG_{coh}), and zeta potential) and the surface roughness of the membrane materials, respectively. These five membrane materials' hydrophobicity range (the order from hydrophobic to hydrophilic) was Si > PTFE > PU > PP > Nylon. Except for Si and PTFE coupons, the PU, PP, and Nylon coupons exhibited hydrophilic properties based on water contact angle results. The SFE of the materials and microalgae ranged from 23.79 to 47.66 mJ/m^2. The ΔG_{coh} value of membrane materials ranged from -42.11 to -89.20 mJ/m^2, and these ΔG_{coh} had a similar trend with the water contact angle on hydrophobicity consequence: a more hydrophobic membrane material usually exhibited a high

ΔG_{coh}. As Table 3.3 shows, the zeta potential of the different coupons and *Chlorella vulgaris*. The zeta potential value of the coupons ranged from -11.37 mV to 4.77 mV, and the absolute value of zeta potential followed the trend: Nylon > PTFE > PU > PP > Si coupons. The Nylon and Si coupons exhibited negative potential, and the rest of the coupons showed a positive surface potential. As Table 3.4 displayed, R_a is the arithmetic roughness average of the coupons' surface, and R_q is the root mean square along the sampling length. The roughness of the membrane material coupons followed the sequence of Nylon > PTFE > PP > Si > PU. The 3D surface topography images (Figure 3.9) also reflected the same tendency of the materials' surface roughness.

Figure 3.10 shows the correlations between the quantity of microalgal cell adhesion and biofilm formation and the water contact angle, zeta potential, difference of SFE between microalgae and substrate material, free energy cohesion (ΔG_{coh}), and surface roughness. It is clear that the absolute zeta potential (Figure 3.10b) and surface roughness (Figure 3.10e) exhibited positive correlations ($r_s = 0.9$, $p < 0.05$ and $r_s = 1$, $p < 0.05$; respectively) with the quantity of biofilm formation while the difference of SFE between microalgae and materials (Figure 3.10c) showed a negative correlation ($r_s = -0.9$, $p < 0.05$) to the quantity of biofilm formation. On the other hand, water contact angle (Figure 3.10a) ($r_s = -0.7$, $p = 0.188 > 0.05$) and free energy of cohesion (Figure 3.10d) ($r_s = 0$, $p = 1 > 0.05$) had no statistically significant correlation to the quantity of biofilm formation. These results suggest that the surface roughness, the magnitude of zeta potential and the differences in SFE of membrane materials would play an important role in controlling microalgal cell adhesion and biofilm formation. The role of each parameter is discussed in-depth in the following sections.

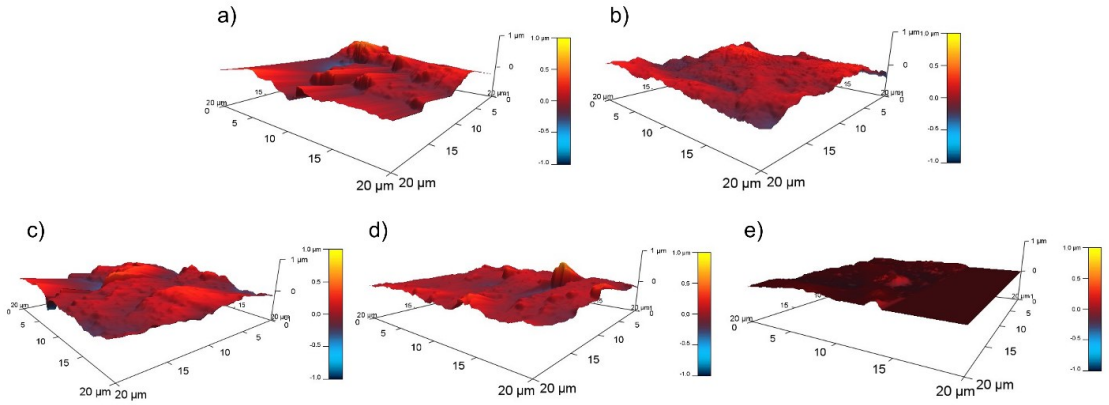

Figure 3.9. 3D surface topography of a) Nylon, b) Polytetrafluoroethylene (PTFE), c) Polypropylene (PP), d) Silicone Rubber (Si), and e) Polyurethane (PU) coupon

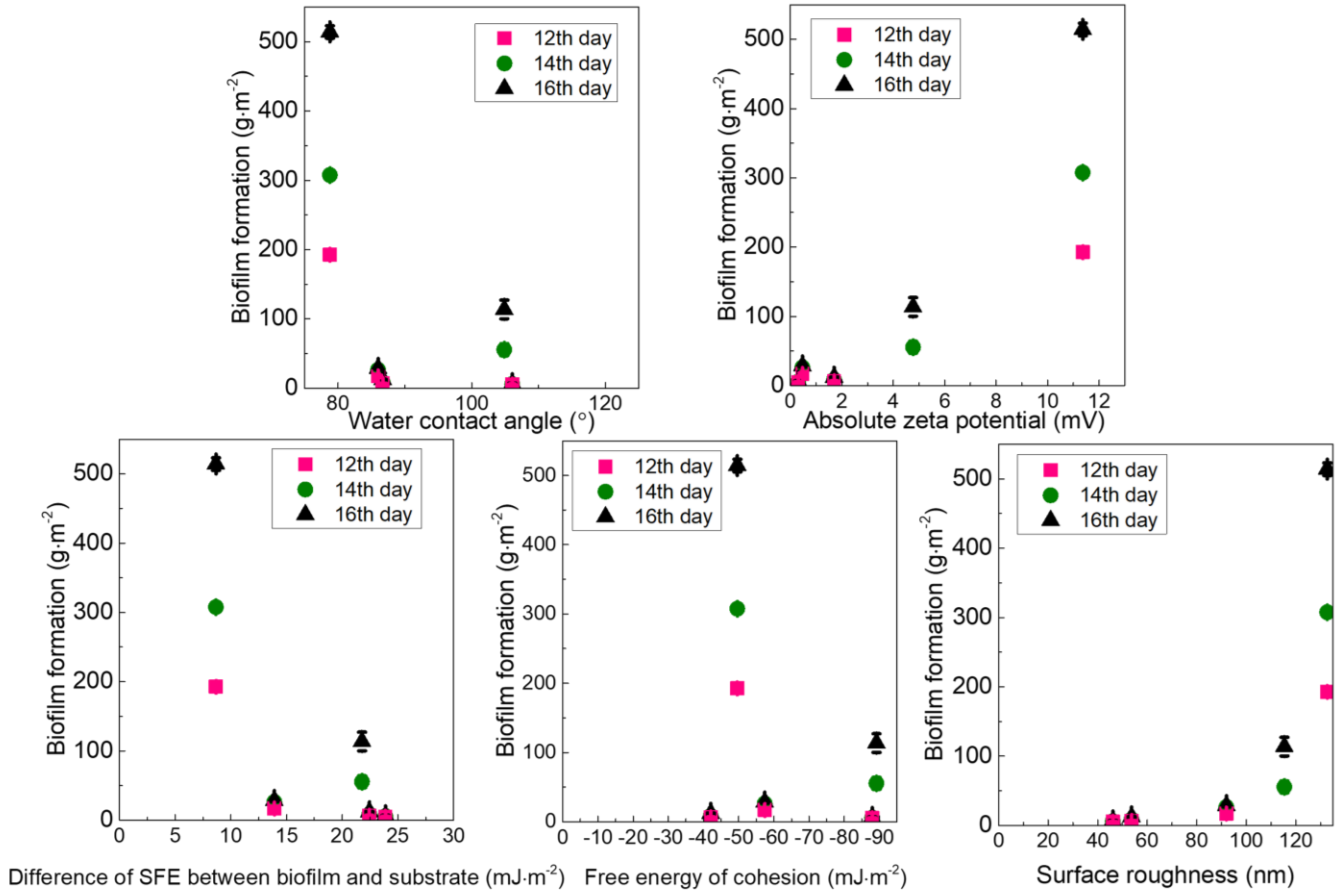

Figure 3.10. Correlations profiles between the quantity of microalgal biofilm formation and the a) contact angle, b) zeta potential, c) Difference of SFE, d) free energy cohesion (ΔG_{coh}), and e) surface roughness.

Table 3.3. Contact angle and surface energy of different material coupons.

Materials	Contact angle (◦)			Surface energy γ_s (mJ/m^2)	ΔG_{coh} (mJ/m^2)	Zeta potential (mV)
	Water	Formamide	Diiodomethane			
Nylon	78.8 ± 1.5	44.8 ± 2.9	50.8 ± 3.4	39.00	-49.60	-11.37 ± 3.6
Polypropylene	86.0 ± 1.9	67.4 ± 4.1	52.3 ± 4.6	33.75	-57.41	0.47 ± 0
Polyurethane Rubber	86.7 ± 4.8	76.6 ± 1.9	66.0 ± 2.2	25.23	-42.11	1.70 ± 0.21
Polytetrafluoroethylene	104.9 ± 1.3	82.7 ± 6.2	64.7 ± 0.4	25.88	-89.20	4.77 ± 0.10
Silicone Rubber	106.1 ± 1.2	83.7 ±1.3	68.7 ± 4.7	23.79	-87.96	-0.3 ± 0.18
Chlorella vulgaris	33.2 ± 1.5	33.4 ± 1.6	34.4 ± 3	47.66	26.52	-21.51 ± 0.92

Table 3.4. Surface roughness of the membrane materials measured at a scanning area of 400 µm^2.

Material	R_a (nm)	R_q (nm)
Polyurethane rubber (PU)	46.14 ± 19.78	63.26 ± 20.83
Silicone rubber (Si)	53.65 ± 7.90	91.03±13.53
Polypropylene (PP)	91.98 ± 20.64	118.16 ± 22.69
Polytetrafluoroethylene (PTFE)	115.33 ± 26.70	149.60 ± 37.76
Nylon	132.64 ±49.04	184.02 ± 60.14

The free energy of cohesion (ΔG_{coh}) is another parameter that reflects the hydrophobicity of the material [13, 49]. Basically, when solid-solid interactions are stronger than solid-water, a positive ΔG_{coh} represents hydrophilicity, while a negative ΔG_{coh} indicates hydrophobicity. Moreover, Table 3.3 also shows the ΔG_{coh} for the membrane materials in contact with the water liquid. Although the culture medium was not the same as water, it could also reflect the hydrophobicity somehow since most of the culture medium is water. As shown in Table 3.3, the ΔG_{coh} value of *Chlorella vulgaris* was positive, which indicated the hydrophilicity of microalgal cells in the culture medium. Different from the contact angle, the ΔG_{coh} of membrane materials

were all negative, which indicated that they all exhibited hydrophobicity in contact with the culture medium. The most hydrophobic membrane material was the PTFE coupons and the lowest was the PU coupons. The literature indicated that microalgal cells had better adhesion on hydrophobic substrate surfaces [50-52]. In this study, the *Chlorella vulgaris* adhesion did not follow this trend; the highest biofilm attachment (i.e. the highest biofilm formation rate) was achieved in the most hydrophilic nylon coupons. Some studies also argue that the influence of hydrophobicity on microalgae adhesion is insignificant [12, 22, 24, 39]. Genin et al. (2014) study found that the hydrophobicity did not correlate with either biomass augment or decrease for a multi-microorganism biofilm [53]. Irving and Allen (2011) also illustrated that it was impossible to predict biofilm growth by hydrophobicity alone after examining *Scenedesmus obliquus* and *Chlorella vulgaris* biofilm developments on different hydrophobic materials [54].

On the other hand, Zeriouh et al. (2017) pointed out that SFE is a parameter presenting the available energy generated from the interaction of a solid surface when the functional group, atoms or molecules approach the solid surface [49]. They argue that SFE is an important physicochemical property that could account for the influence of the interaction between microorganisms and the surface. As Zhang et al. (2015) hypothesized, a decrease in the difference in SFE between microbial and solid surfaces would result in a larger degree of microbial adhesion [55]. Their later experiment proved this hypothesis by examining the adhesion behaviours of different bacterial strains (*Pseudomonas putida*, *Salmonella Typhimurium*, and *Escherichia coli*) on thoroughly cleaned microscopy glass and salinized glass slides. As displayed in Table 3.3, the Nylon coupon (39 mJ/m^2) had the smallest difference to *Chlorella vulgaris* (47.66 mJ/m^2) but had the thickest microalgal biofilm, and the silicone rubber (23.79 mJ/m^2) had the thinnest biofilm due to the largest difference of SFE to the microalgae. However, the PP coupons did not follow this trend.

The PP coupon had less biofilm biomass than the PTFE coupon, even though it had a closer SFE to *Chlorella vulgaris*. Similar to Tsavatopoulou et al. (2021) study, they also found that the geotextile and silicone rubber didn't exhibit the best adhesion performance even though they had the lowest difference to the SFE of *B.braunii* and *N.vigensis*, respectively [22]. The SFE alone played an important role but could not explain the biofilm adhesion in all cases studied.

As Tong and Derek (2021a) mentioned, microalgae are easier to adhere to the substrate with the opposite charges [21]. However, the attachment performance of *Chlorella vulgaris* showed a similar trend as the absolute value of the substrate's zeta potential, which was Nylon > PTFE > PP > PU > Si coupons. Basically, the substrate with a positive charge can facilitate the negative microalgae cells' adhesion, while the negatively charged substrate could limit the adhesion because of electrostatic repulsion [56]. For the material with the negative charge, Nylon with the highest negative zeta potential (-11.37 mV) exhibited a higher biofilm adhesion behaviour than those materials with positive zeta potential (PTFE, PP, and PU). This might suggest metal ions, like Ca^{2+}, bridging mechanism between the negatively charged microalgae cells and Nylon played a significant role in the highest biofilm formation. On the other hand, the positive charge (the second largest absolute value of zeta potential, 4.77 mV) of the PTFE membrane materials could enhance biofilm formation (the 2nd largest amount of biofilm quantity) through charge neutralization. Based on the DLVO theory, the surface potential of both microalgae and membrane material substrate corresponds to the electrostatic interaction energy (G^{EL}), which is one of the energy components of total interaction energy (G^{T}) [57]. As Zeng et al. (2022) mentioned, when the solid substrate possesses negative surface charges, the decrease of the absolute value of the potential contributes to the augment of the G^{T} [58]. The change tendency of the surface properties is the opposite of the total interaction energy when the solid substrate possesses a positive surface

charge. This study found the opposite trend between the materials with negative charges. The higher zeta potential Nylon (-11.37 mV) exhibited higher adhesion performance than Si (-0.3 mV). This fact indicated that the electrostatic interaction is not dominant in adhesion. Some research also found a similar phenomenon that microalgae achieved more significant attachment on the substratum with more negative charges [59-61]. For the positive zeta potential case, the PP coupons achieved a higher biofilm attachment than PU coupons due to their lower absolute zeta potential value (0.47 mV to 1.70 mV). The PTFE coupon exhibited better microalgae biofilm adhesion than PP coupons. This could be due to higher positive (PTFE) and negative (cells) charge neutralization. One explanation could be that the zeta potential is not the primary factor affecting the adhesion of microalgae cells since the G^{EL} influence on G^{T} will be negligible at longer separation distances [58]. These results might suggest that different dominant mechanisms of microalgal biofilm formation existed among different membrane materials, such as salt bridging and charge neutralization.

Some studies mentioned that surface roughness could promote the attachment of the algal cell to the substrate [62, 63]. In this study, the largest, second largest, and third largest biofilm formation was achieved on the Nylon, PETF, and PP membrane material coupon, which had the roughest (R_a=132.64 nm) and the second roughest (R_a=115.33 nm), and the third largest roughest (R_a=91.98 nm) surface, respectively. These results indicated that the surface roughness of the membrane materials positively correlated to the microalgal biofilm formation rate and played a crucial role in controlling the microalgal biofilm formation. This phenomenon could be explained by the accumulation caused by the extra asperities and flow-stagnant areas on the rougher surface compared to the smoother ones [23]. When the suspended microalgae flowed above those surfaces, more microalgae cells could be detained and remain in those areas, thus exhibiting a higher biofilm

formation performance. When it came to the PP and PTFE coupons in SFE, despite the PP coupon having smaller differences in SFE to that of *Chlorella vulgaris,* the biofilm attachment in the PP was lower than the PTFE coupon (PP: 28.61 g/m^2 vs. PTFE: 113.65 g/m^2). This is because the PP coupon (R_a=91.98 nm) had lower surface roughness than the PTFE coupon (R_a=115.33 nm), enabling PTFE coupons to intercept more suspended microalgal cells for biofilm formation. The same tendencies were found in Zhang et al. (2020) research [23]. They discovered that *Chlorella vulgaris* exhibited a higher adhesion strength on rougher pine sawdust carriers than on smoother rice husk carriers.

Moreover, the surface roughness could explain the conflict between this study and Ozkan and Berberoglu's research (2011) that *Chlorella vulgaris* prefers adhering to the more hydrophobic material surface [51]. In this study, the low microalgal cells' attachment to more hydrophobic material (such as PU and Si coupons), compared to Nylon coupons, could be attributed to their considerably low surface roughness (46.14 nm and 53.65 nm, respectively). However, the SFE had the same significant influence on the adhesion behaviour of *Chlorella vulgaris* in this research as the surface roughness had. For instance, the explanation of adhesion behaviour between the PU and Si coupons is more reasonable by the SFE theory than surface roughness. Most of the adhesion increased with the smaller difference of SFE between the material and microalgae, even though some exhibited some changes under the surface roughness influence as well. This phenomenon revealed that biofilm formation was not driven by only a single influence factor but by multiple elements, such as surface roughness, zeta potential, hydrophobicity, and SFE. Different dominant mechanisms of controlling biofilm formation were observed in this study for different membrane materials. Thus, the synergy between the multiple affecting factors must also be considered during the microalgae biofilm formation mechanism study.

3.3.5. Implication to the development of membrane carbonated microalgal biofilm reactor and extractive membrane microalgal biofilm reactor

The results from this study suggest that the surface roughness, SFE, zeta potential, and hydrophobicity of the membrane materials all played a certain role in controlling the microalgal biofilm formation rate in MCMBR and EMMBR; it is a combination of the roles of these properties that determines the biofilm formation with the surface roughness as a dominant factor in all the cases. The nylon and PTFE membrane materials are the best membrane materials properties that promote a fast biofilm formation for wastewater treatment from the view of microalgal biofilm formation.

In the development of MCMBR and EMMBR, emerging technologies for wastewater treatment (nutrient removal), it would be expected that the membranes should have the capability of quickly forming a microalgal biofilm for stable nutrient removal and biofilm production in order to reduce the time between the cyclic operation (biofilm removal at the end and biofilm formation at the beginning) and having a high permeability of CO_2 (for MCMBR). Thus, PTFE appears to be the most suitable membrane material for MCMBR development, considering its capability for quick microalgal biofilm formation and high CO_2 permeability. At the same time, Nylon is an excellent membrane material for the development of EMMBR, considering its capability of the highest microalgal biofilm formation rate and excellent permeability of treated effluent. It is anticipated that the results from this study have identified two excellent membrane materials (PTFE and Nylon) for the further development of MCMBR and EMMBR, respectively. Further studies should optimize the conditions, such as microalgal species, process and environmental conditions to develop MCMBR and EMMBR.

3.4. Conclusion

The experimental work presented herein investigated the role of different physicochemical surface properties of a group of membrane materials in controlling the adhesion of microalgae and biofilm formation using a CDC Biofilm reactor under a dynamic condition. Among the five tested materials (Nylon, polypropylene, polyurethane rubber, polytetrafluoroethylene, and silicone rubber), Nylon exhibited the highest wet biofilm attachment of *Chlorella vulgaris*, reaching up to 514.3 g/m^2 over 16 days of cultivation. The hydrophilic *Chlorella vulgaris* did not adhere better to the highest hydrophobic silicone rubber. These results revealed that membrane surface roughness played a dominant role in determining microalgal cell adhesion and biofilm formation. A rougher membrane surface was positively correlated to higher microalgal cell adhesion and biofilm formation rate under tested hydrodynamic conditions. The contact angle and hydrophobicity did not play the main role in the cell attachment of *Chlorella vulgaris*.

Moreover, bounded EPS positively impacted the initial adhesion of microalgae biofilm and served a role in maintaining the biofilm matrix in the thickening period. As a result, bounded EPS productivity (mg EPS/mg biofilm) decreased with biofilm growth. For almost all membrane materials (except polypropylene), SFE played a significant role in biofilm adhesion. Furthermore, the zeta potential (positive and negative) of these membrane materials could play an important role as well through charge neutralization or salt-bridging mechanisms.

Furthermore, the biofilm formation mechanism was complicated and influenced by multiple factors. The relative importance of these mechanisms could change depending on the specific microalgae species and membrane materials involved and tested hydrodynamic conditions. The synergy between the multiple affecting factors also needs to be further studied in the future. The thickest biofilm is achieved on Nylon coupons with the lowest difference between the SFE

and the *Chlorella vulgaris* cells. Based on these findings, Nylon and PTFE come first in membrane material selection for further development of the novel and emerging EMMBR and MCMBR technologies for wastewater treatment.

3.5. Reference

[1] Wang, J., Zhang, M., Fang, Z. (2019). Recent development in efficient processing technology for edible algae: A review. Trends in Food Science & Technology, 88, 251-259.
[2] Posten, C., Chen, S.F. (2016). Microalgae biotechnology. Springer International Publishing: Switzerland.
[3] Wollmann, F., Dietze, S., Ackermann, J.U., Bley, T., Walther, T., Steingroewer, J., Krujatz, F. (2019). Microalgae wastewater treatment: Biological and technological approaches. Engineering in Life Sciences, 19, 860-871.
[4] Benedetti, M., Vecchi, V., Barera, S., Dall'Osto, L. (2018). Biomass from microalgae: the potential of domestication towards sustainable biofactories. Microbial Cell Factories, 17, 1-18.
[5] Johansen, M.N. (2012). Microalgae: biotechnology, microbiology, and energy. Nova Science Publisher's: New York.
[6] Williams, P.J.L.B., Laurens, L.M. (2010). Microalgae as biodiesel & biomass feedstocks: Review & analysis of the biochemistry, energetics & economics. Energy & Environmental Science, 3, 554-590.
[7] Chen, C.Y., Yeh, K.L., Aisyah, R., Lee, D.J., Chang, J.S. (2011). Cultivation, photobioreactor design and harvesting of microalgae for biodiesel production: a critical review. Bioresource Technology, 102, 71-81.
[8] Tsavatopoulou, V.D., Manariotis, I.D. (2020). The effect of surface properties on the formation of *Scenedesmus rubescens* biofilm. Algal Research, 52, 102095.
[9] Zhao, Z., Muylaert, K., Szymczyk, A., Vankelecom, I.F. (2021). Enhanced microalgal biofilm formation and facilitated microalgae harvesting using a novel pH-responsive, crosslinked patterned and vibrating membrane. Chemical Engineering Journal, 410, 127390.
[10] Dalirian, N., Najafabadi, H.A., Movahedirad, S. (2021). Surface attached cultivation and filtration of microalgal biofilm in a ceramic substrate photobioreactaor. Algal Research, 55, 102239.
[11] Lee, S., Oh, H., Jo, B., Lee, S., Shin, S., Kim, H., Lee, S., Ahn, C. (2014). Higher biomass productivity of microalgae in an attached growth system, using wastewater. Journal of Microbiology and Biotechnology, 24, 1566-1573.
[12] Kesaano, M. (2015). Characterization and performance of algal biofilms for wastewater treatment and industrial applications [Doctoral dissertation]. Utah State University.
[13] Ozkan, A., Berberoglu, H. (2013). Physico-chemical surface properties of microalgae. Colloids and Surfaces B: Biointerfaces, 112, 287-293.
[14] Zhuang, L., Yu, D., Zhang, J., Liu, F., Wu, Y., Zhang, T., Dao, G., Hu, H. (2018). The characteristics and influencing factors of the attached microalgae cultivation: a review. Renewable and Sustainable Energy Reviews, 94, 1110-1119.
[15] Ozkan, A., Berberoglu, H. (2013). Adhesion of algal cells to surfaces. Biofouling, 29, 469-482.

[16] Shen, Y., Zhu, W., Chen, C., Nie, Y., Lin, X. (2016). Biofilm formation in attached microalgal reactors. Bioprocess and Biosystems Engineering, 39, 1281-1288.
[17] Gross, M.A. (2015). Development and optimization of biofilm based algal cultivation [Doctoral dissertation]. Iowa State University.
[18] Christenson, L. (2011). Algal biofilm production and harvesting system for wastewater treatment with biofuels by-products [Master thesis]. Utah State University.
[19] Yuan, H., Zhang, X., Jiang, Z., Chen, X., Zhang, X. (2018). Quantitative criterion to predict cell adhesion by identifying dominant interaction between microorganisms and abiotic surfaces. Langmuir, 35, 3524-3533.
[20] Yuan, H., Zhang, X., Jiang, Z., Wang, X., Chen, X., Cao, L., Zhang, X. (2019). Analyzing the effect of pH on microalgae adhesion by identifying the dominant interaction between cell and surface. Colloids and Surfaces B: Biointerfaces, 177, 479-486.
[21] Tong, C., Derek, C. (2021). Biofilm formation of benthic diatoms on commercial polyvinylidene fluoride membrane. Algal Research, 55, 102260.
[22] Tsavatopoulou, V.D., Aravantinou, A.F., Manariotis, I.D. (2021). Comparison of *Botryococcus braunii* and *Neochloris vigensis* Biofilm Formation on Vertical Oriented Surfaces. Biointerface Research in Applied Chemistry, 11, 12843-12857.
[23] Zhang, Q., Yu, Z., Jin, S., Liu, C., Li, Y., Guo, D., Hu, M., Ruan, R., Liu, Y. (2020). Role of surface roughness in the algal short-term cell adhesion and long-term biofilm cultivation under dynamic flow condition. Algal Research, 46, 101787.
[24] Talluri, S.N., Winter, R.M., Salem, D.R. (2020). Conditioning film formation and its influence on the initial adhesion and biofilm formation by a cyanobacterium on photobioreactor materials. Biofouling, 36, 183-199.
[25] Podola, B., Li, T., Melkonian, M. (2017). Porous substrate bioreactors: a paradigm shift in microalgal biotechnology? Trends in Biotechnology, 35, 121-132.
[26] George, B., Pancha, I., Desai, C., Chokshi, K., Paliwal, C., Ghosh, T., Mishra, S. (2014). Effects of different media composition, light intensity and photoperiod on morphology and physiology of freshwater microalgae *Ankistrodesmus falcatus*–A potential strain for bio-fuel production. Bioresource Technology, 171, 367-374.
[27] Rippka, R., Deruelles, J., Waterbury, J.B., Herdman, M., Stanier, R.Y. (1979). Generic assignments, strain histories and properties of pure cultures of cyanobacteria. Microbiology, 111, 1-61.
[28] Yang, C.C., Wen, R.C., Shen, C.R., Yao, D.J. (2015). Using a microfluidic gradient generator to characterize BG-11 medium for the growth of cyanobacteria *Synechococcus elongatus* PCC7942. Micromachines, 6, 1755-1767.
[29] Ma, K., Chung, T.S., Good, R.J. (1998). Surface energy of thermotropic liquid crystalline polyesters and polyesteramide. Journal of Polymer Science Part B: Polymer Physics, 36, 2327-2337.
[30] Rudawska, A., Jacniacka, E. (2018). Evaluating uncertainty of surface free energy measurement by the van Oss-Chaudhury-Good method. International Journal of Adhesion and Adhesives, 82, 139-145.
[31] Wang, W., Shen, A., Yang, X., Guo, Y., Zhao, T. (2020). Surface free energy method for evaluating the effects of anti-stripping agents on the moisture damage to asphalt mixtures. Journal of Adhesion Science and Technology, 34, 1947-1970.
[32] Van Oss, C., Good, R., Chaudhury, M. (1988). Additive and nonadditive surface tension components and the interpretation of contact angles. Langmuir, 4, 884-891.

[33] Gaudy, E., Wolfe, R. (1962). Composition of an extracellular polysaccharide produced by Sphaerotilus natans. Applied Microbiology, 10, 200-205.
[34] Lowry, O., Rosebrough, N., Farr, A.L., Randall, R. (1951). Protein measurement with the Folin phenol reagent. Journal of Biological Chemistry, 193, 265-275.
[35] China, E. (2002). Monitoring and analysis methods for water and wastewater. China Environmental Science Press: Beijing, pp. 232-235.
[36] Matho, C., Schwarzenberger, K., Eckert, K., Keshavarzi, B., Walther, T., Steingroewer, J., Krujatz, F. (2019). Bio-compatible flotation of *Chlorella vulgaris*: Study of zeta potential and flotation efficiency. Algal Research, 44, 101705.
[37] Choi, H.J., Lee, S.M. (2015). Effect of the N/P ratio on biomass productivity and nutrient removal from municipal wastewater. Bioprocess and Biosystems Engineering, 38, 761-766.
[38] Xin, L., Hong-Ying, H., Ke, G., Ying-Xue, S. (2010). Effects of different nitrogen and phosphorus concentrations on the growth, nutrient uptake, and lipid accumulation of a freshwater microalga *Scenedesmus sp*. Bioresource Technology, 101, 5494-5500.
[39] Cheah, Y.T., Chan, D.J.C. (2021). Physiology of microalgal biofilm: a review on prediction of adhesion on substrates. Bioengineered, 12, 7577-7599.
[40] Mantzorou, A., Ververidis, F. (2019). Microalgal biofilms: A further step over current microalgal cultivation techniques. Science of the Total Environment, 651, 3187-3201.
[41] Wang, J.H., Zhuang, L.L., Xu, X.Q., Deantes-Espinosa, V.M., Wang, X.X., Hu, H.Y. (2018). Microalgal attachment and attached systems for biomass production and wastewater treatment. Renewable and Sustainable Energy Reviews, 92, 331-342.
[42] Hwang, J.H., Cicek, N., Oleszkiewicz, J.A. (2010). Achieving biofilm control in a membrane biofilm reactor removing total nitrogen. Water Research, 44, 2283-2291.
[43] Taşkan, B., Hasar, H., Lee, C.H. (2020). Effective biofilm control in a membrane biofilm reactor using a quenching bacterium (*Rhodococcus sp*. BH4). Biotechnology and Bioengineering, 117, 1012-1023.
[44] Shen, Y., Zhang, H., Xu, X., Lin, X. (2015). Biofilm formation and lipid accumulation of attached culture of *Botryococcus braunii*. Bioprocess and Biosystems Engineering, 38, 481-488.
[45] Devi, N.D., Tiwari, R., Goud, V.V. (2023). Cultivating *Scenedesmus sp*. on substrata coated with cyanobacterial-derived extracellular polymeric substances for enhanced biomass productivity: a novel harvesting approach. Biomass Conversion and Biorefinery, 13, 2971-2983.
[46] Flemming, H.C., Wingender, J. (2010). The biofilm matrix. Nature Reviews Microbiology, 8, 623-633.
[47] Xiao, R., Zheng, Y. (2016). Overview of microalgal extracellular polymeric substances (EPS) and their applications. Biotechnology Advances, 34, 1225-1244.
[48] Ji, C., Zhou, H., Deng, S., Chen, K., Dong, X., Xu, X., Cheng, L. (2021). Insight into the adhesion propensities of extracellular polymeric substances (EPS) on the abiotic surface using XDLVO theory. Journal of Environmental Chemical Engineering, 9, 106563.
[49] Zeriouh, O., Reinoso-Moreno, J.V., López-Rosales, L., Cerón-García, M.D.C., Sánchez-Mirón, A., García-Camacho, F., Molina-Grima, E. (2017). Biofouling in photobioreactors for marine microalgae. Critical Reviews in Biotechnology, 37, 1006-1023.
[50] Cui, Y., Yuan, W. (2013). Thermodynamic modeling of algal cell–solid substrate interactions. Applied Energy, 112, 485-492.
[51] Ozkan, A., Berberoglu, H. (2011). Adhesion of *Chlorella vulgaris* on hydrophilic and hydrophobic surfaces.Proceedings of the ASME International Mechanical Engineering Congress and Exposition; pp. 169-178.

[52] Ozkan, A., Berberoglu, H. (2013). Cell to substratum and cell to cell interactions of microalgae. Colloids and Surfaces B: Biointerfaces, 112, 302-309.
[53] Genin, S.N., Aitchison, J.S., Allen, D.G. (2014). Design of algal film photobioreactors: material surface energy effects on algal film productivity, colonization and lipid content. Bioresource Technology, 155, 136-143.
[54] Irving, T.E., Allen, D.G. (2011). Species and material considerations in the formation and development of microalgal biofilms. Applied Microbiology and Biotechnology, 92, 283-294.
[55] Zhang, X., Zhang, Q., Yan, T., Jiang, Z., Zhang, X., Zuo, Y.Y. (2015). Quantitatively predicting bacterial adhesion using surface free energy determined with a spectrophotometric method. Environmental Science & Technology, 49, 6164-6171.
[56] Hoshiba, T., Yoshikawa, C., Sakakibara, K. (2018). Characterization of initial cell adhesion on charged polymer substrates in serum-containing and serum-free media. Langmuir, 34, 4043-4051.
[57] Tong, C., Derek, C. (2021). The role of substrates towards marine diatom *Cylindrotheca fusiformis* adhesion and biofilm development. Journal of Applied Phycology, 33, 2845-2862.
[58] Zeng, W., Li, P., Huang, Y., Xia, A., Zhu, X., Zhu, X., Liao, Q. (2022). How Interfacial Properties Affect Adhesion: An Analysis from the Interactions between Microalgal Cells and Solid Substrates. Langmuir, 38, 3284-3296.
[59] Parreira, P., Magalhães, A., Gonçalves, I.C., Gomes, J., Vidal, R., Reis, C.A., Leckband, D.E., Martins, M.C.L. (2011). Effect of surface chemistry on bacterial adhesion, viability, and morphology. Journal of Biomedical Materials Research Part A, 99, 344-353.
[60] Tang, J., Liu, B., Gao, L., Wang, W., Liu, T., Su, G. (2021). Impacts of surface wettability and roughness of styrene-acrylic resin films on adhesion behavior of microalgae *Chlorella sp*. Colloids and Surfaces B: Biointerfaces, 199, 111522.
[61] Teixeira, P., Oliveira, R. (1999). Influence of surface characteristics on the adhesion of *Alcaligenes denitrificans* to polymeric substrates. Journal of Adhesion Science and Technology, 13, 1287-1294.
[62] Huang, Y., Zheng, Y., Li, J., Liao, Q., Fu, Q., Xia, A., Fu, J., Sun, Y. (2018). Enhancing microalgae biofilm formation and growth by fabricating microgrooves onto the substrate surface. Bioresource Technology, 261, 36-43.
[63] Sekar, R., Venugopalan, V., Satpathy, K., Nair, K., Rao, V. (2004). Laboratory studies on adhesion of microalgae to hard substrates. Hydrobiologia, 512, 109-116.

Chapter 4: Surface and physical and chemical properties of microalgae and their role on microalgal cell adhesion and biofilm formation under different hydrodynamic conditions

Abstract

Extractive membrane microalgal biofilm photobioreactors (EM-MBPBR) are one of the emerging and novel bioreactor systems for microalgae cultivation and wastewater treatment. In this study, three microalgae species (*Phormidium tenue*, *Monoraphidium braunii*, and *Ankistrodesmus falcatus*) with different surface and physical and chemical properties were examined in a CDC biofilm bioreactor with Nylon as the membrane material for biofilm formation under different hydrodynamic conditions. Physicochemical and surface properties of these microalgae species, including contact angle, surface energy, zeta potential, particle sizes, and extracellular polymeric substances (EPS), were examined to clarify their role in controlling microalgal cell adhesion and biofilm formation on Nylon membrane material under different hydrodynamic conditions. The results showed that under low shear stress conditions, hydrophobicity, surface free energy, free energy of cohesion, and zeta potential played an important role in controlling biofilm formation. Under high shear stress conditions, the hydrodynamic conditions and the presence of a fraction of small particle sizes (<10 μm) of microalgae species were the dominant factors in controlling biofilm formation. In contrast, the importance of the surface properties of microalgae species was diminished. For the same microalgae species, the presence of a fraction of small particle sizes (<10 μm) of the microalgae cells/flocs played a dominant role in controlling biofilm formation under different hydrodynamic conditions. The results suggest that the relative importance of

hydrodynamic conditions and surface and physical properties of microalgae cells in controlling biofilm formation would change under different conditions.

Keywords: Extractive membrane microalgal biofilm reactor; microalgal biofilm; microalgae species; hydrodynamic conditions; surface properties.

4.1. Introduction

Microalgal biofilm cultivation has recently attracted much attention [1-3]. Compared to conventional suspended microalgae cultivation, microalgal biofilm cultivation can achieve condensed algal biofilm, thus reducing the constructive area and cost of the harvesting procedures. Although there are a number of advantages of the microalgal biofilm technology, the wide application of the microalgal biofilm technology is limited by CO_2 transfer and the need for a settler for the detached biofilm separation from treated effluent. Thus, novel microalgal biofilm technology to overcome these challenges is highly desirable. Among the emerging microalgal biofilm technologies being developed, extractive membrane microalgal biofilm photobioreactor (EMMBPBR) is a promising approach to overcome the challenge of sloughed biofilm separation from treated effluent and obtain a superior quality of effluent (permeate) with zero-solids. The EMMBPBR uses a hydrophilic membrane as both the support media for biofilm attachment and the filtration medium to allow treated effluent from the biofilm to permeate through the membrane. There is no report of microalgal studies on this emerging EMMBPBR technology in the literature. To develop this novel type of EMMBPBR, the first step is to screen a suitable membrane material for this application. In our previous study, we identified Nylon, a widely used hydrophilic membrane material for wastewater purification, as an excellent membrane material for fast microalgal biofilm formation [4] and thus suitable for EMMBPBR development.

The mechanisms of microalgal biofilm formation reveal that a number of factors such as the physical, chemical and surface properties of the attached substrate, microalgae species, the hydrodynamic condition in biofilm reactor, culture media composition and concentration, and the mechanism of interaction between microorganism cell and substrate, etc. [5, 6]. These factors play a vital role in controlling the rate of microalgal biofilm formation or biomass amount of biofilm. Thus, fundamental studies on the role of these factors in controlling microalgal biofilm formation are highly desirable.

In order to fulfill the fundamental knowledge of the microalgae cell adhesion and biofilm formation mechanism, and particularly for the EMMBPBR development, the study of the microalgae-substrate (membrane) interaction is required. Based on membrane properties, one of the prerequisites that confirm microalgal biofilm cultivation application is the affinity of the microalgal cells to the membrane, which is reflected by the dynamic change of harvested biomass of microalgal biofilm. Some literature mentioned that different microalgae species result in different biofilm formation behaviours, which could be traced back to the EPS composition, surface properties, and physical-chemical properties of the microorganism cells [7-9]. Tsavatopoulou et al. claimed that microalgae strain played an indispensable role during microalgal cell attachment [7]. They found that *Botryococcus braunii* and *Neochloris vigensis* exhibited different behaviours on the same substrate.

Moreover, *Botryococcus braunii* performed the best on plexiglass, while the sponge towel exhibited the highest attachment in *Neochloris bigensis* case [7]. The effect of microalgae species on biofilm formation has been studied for decades. However, the fundamental knowledge of microalgae-membrane interactions is still limited due to the abundant diversity of microalgae species. The most important is, as Zhuang et al. mentioned, the selection of microalgae species for

biomass production needs to fulfill industrial demands such as high productivity, ease of adhesion, and high value of by-products [6, 10]. Thus, studies on the role of microalgae species' effects on microalgae biofilm cultivation are always required to complement the fundamental knowledge of microalgae cultivation.

Literature also mentioned that the hydrodynamic conditions in the biofilm reactor, such as liquid flow velocity, aeration rate or shear stress, would influence the microalgae biofilm growth, even biofilm formation in bioreactors [11, 12]. Zeriouh et al. noticed that the shear stress caused by fluid-dynamic conditions also played a role in the *N. gaditana* cell attachment on the bioreactor wall beside the extended Derjaguin, Landau, Verwey, Overbeek (XDLVO) forces [13]. Zhang et al. revealed that surface roughness positively affected *Chlorella vulgaris* cell adhesion by creating ambient hydrodynamic conditions [14]. Although these studies all observed that the hydrodynamic condition influenced microalgal cell adhesion, researchers discussed less about that since it is not their main objective. For instance, despite Cheah and Chan pointing out that fluid flow velocity and shear stress have an effect on cell adhesion, hydrodynamic conditions were not considered in the extensively used XDLVO model to predict cell adhesion [15]. Thus, studying hydrodynamic conditions under a real cultivation environment is limited and urgently needed. Considering the reality of industrial application and the aim to open a further view of biofilm research, the effect of the shear stress on microalgal biofilm cultivation in the continuous submerged biofilm reactor is highly desirable.

The overall goal of this study was to evaluate the role of different surface and physical and chemical properties of microalgae species on cell adhesion and biofilm formation on a widely used hydrophilic Nylon membrane material to develop an emerging EMMBPBR technology for wastewater purification. The objectives of this study were to (i) investigate the biofilm formation

of different microalgae strains and study the factors that affect biofilm formation mechanisms among the microalgae strains; (ii) characterize the surface, physical, and chemical properties of microalgae cells; and (iii) investigate the role of different hydrodynamic conditions that influence the biofilm formation of different strains of microalgae and fulfill the fundamental knowledge of the microalgal biofilm cultivation. For the previous paper, Nylon was identified as the optimal attachment membrane material for the *Chlorella vulgaris* biofilm formation to further develop the novel EMMBPBR technology for wastewater treatment. Therefore, three different microalgae species (*Phormidium tenue*, *Monoraphidium braunii*, and *Ankistrodesmus falcatus*) were employed and cultured in a CDC biofilm reactor at 16 days (each run) under different hydrodynamic conditions (two different rotation speeds of the magnetic stirrer). The physical and chemical properties, such as hydrophobicity, zeta potential, and EPS concentration and composition, of the microalgal strains were measured, and their role in controlling microalgal biofilm formation was identified and discussed.

4.2. Materials and methods

4.2.1. Microalgae strains and preculture

Phormidium tenue (CPCC 424), *Monoraphidium braunii* (CPCC 625), and *Ankistrodesmus falcatus* (CPCC 669) were obtained from the Canadian Phycological Culture Centre at the University of Waterloo, ON, Canada. Algal precultures were prepared with BG-11 medium [16] in 1.5 L plastic bottle reactors. The aeration (1.0 L/min) and LED illumination (94.85 μmol/m^2/s) were continuously provided to ensure microalgae growth before the biofilm formation experiment.

4.2.2. Materials

Sodium nitrate, dipotassium hydrogen phosphate, magnesium sulfate heptahydrate, calcium chloride, citric acid, ethylenediaminetetraacetic acid tetrasodium salt dihydrate, sodium carbonate, boric acid, manganese chloride tetrahydrate, zinc sulfate heptahydrate, sodium molybdate dihydrate, copper sulfate pentahydrate and cobaltous nitrate hexahydrate were obtained from Sigma-Aldrich and used as received. Hydrochloric acid (36.5%) obtained from Sigma-Aldrich was diluted to 3.65% wt. before use. Nylon disc coupons were used in this study.

4.2.3. Experimental set-up

A CDC biofilm reactor (Biosurface Technologies Corporation, USA) with an effective volume of 360 mL was used to assess the role of the surface properties of microalgae species and hydrodynamic conditions on microalgal cell adhesion and biofilm formation. Briefly, twenty-four nylon coupons were immersed into the CDC biofilm reactor for 16-day cultivation in BG-11 medium at stirring speeds of 125 rpm and 60 rpm, respectively, for each run. An aeration intensity of 1.0 L/min and LED illumination of 94.85 μmol/m^2/s were provided to the CDC biofilm reactor for microalgae cultivation and biofilm formation. Daily, 45 mL of effluent was withdrawn from the CDC biofilm reactor and 45 mL of influent (BG-11 medium) was added to the CDC biofilm reactor. This is equivalent to a reaction time (or hydraulic retention time) of 8 days for the high-strength nutrients wastewater.

Biomass growth was monitored by measuring total suspended solids (TSS). The attached biofilm biomass was determined and collected for EPS extraction and attachment measurement. Zeta potential, pH, particle size distribution and cell concentration were determined in the liquid each time when three coupons were sampled.

4.2.4. Analytical methods

4.2.4.1. Contact angle

The contact angle of the sample and material was determined by using the optical tensiometer instrument (Theta Lite, Biolin Scientific, USA) equipped with a camera followed by a sessile drop method in Attension software. The average results of three independent tests were reported. The microalgae were prepared as a lawn of 0.0003 g/mm^2, modified from the Zeriouh et al. study before contact angle measurement [13]. Briefly, microalgae were washed triple times with DI water and centrifuged to remove supernatants. The final centrifuges were resuspended in 10 mL DI water and then filtered through a 0.45 μm mixed cellulose esters (MCE) filter membrane (47 mm diameter, Merck Millipore Ltd, Ireland). Next, the microalgal lawn remaining on the filter membrane was immersed in 1% agar (w/v) prepared in 10% v/v glycerol water solution for 30 mins to stabilize the moisture content. The surface free energy of microalgae was determined through Young's equation combined with contact angle, which is the same as the former studies [17-20].

4.2.4.2. Other routine analysis

The total nitrogen (TN) and total phosphorus (TP) were measured with the alkaline potassium persulfate digestion-UV spectrophotometric method and ammonium molybdate spectrophotometry, respectively [21, 22]. The EPS extraction and measurement were followed by the previous study [23]. Glucose and bovine serum albumin (BSA) were used as the standard for carbohydrates and protein measurement, respectively [24, 25]. The absorbance of the sample for spectrometric methods was read on a UV spectrophotometer (Genesys 10S UV-Vis, Thermo, USA). Zeta potential measurement was analyzed by a NanoBrook Zeta PALS (Brookhaven

Instruments Corp, USA) by using 1 mM KCl solution as a buffer solution. Particle size distribution measurement was achieved by a Mastersizer Micro Plus 3000 (Malvern Instrument, Worcestershire, UK).

4.2.5. Statistical analysis

The experiment data were examined through an ANOVA test conducted from Origin software to examine the statistically significant difference ($p < 0.05$) between phases. The Pearson correlations between surface properties and biofilm formation were also examined by the Origin software. All the results were satisfied with statistical analysis and were expressed as mean ± standard deviation.

4.3. Result and Discussion

4.3.1. Microalgae growth analysis

Figure 4.1 shows the microalgae growth profile during the different species in about 32 days under different hydrodynamic conditions (125 rpm and 60 rpm). Figure 4.1a shows that the biomass concentration of the three species (*Phormidium tenue*, *Monoraphidium braunii*, and *Ankistrodesmus falcatus*) is maintained at around 0.25 ± 0.08 g/L. The ANOVA test showed that the suspended biomass concentration is not significantly different at the 0.05 level ($p > 0.05$). Thus, the effect of the potential differences in suspended biomass concentration could be neglected. Moreover, the pH of these three species is also not statistically significantly different at level 0.05 ($p > 0.05$), which indicates that the pH effect would not be considered in this study (Figure 4.1b). On the other hand, Figure 4.1c reflects the average zeta potential of three species during the cultivation periods significantly differ from each other at the 0.05 level (*Phormidium tenue*: -38.66

± 2.85 mV, *Monoraphidium braunii*: -36.95 ± 3.70 mV, and *Ankistrodesmus falcatus*: -35.33 ± 1.74 mV) ($p < 0.05$). As a result, the zeta potential effect of microalgae on microalgal cell adhesion and biofilm formation will be discussed in the next section. Figure 4.2 shows the effluent total nitrogen and phosphorus concentrations in the different microalgae culture mediums. The effluent of *Phormidium tenue* has the highest total nitrogen concentration (184.03 ± 13.52 mg/L), followed by the *Monoraphidium braunii* (146.63 ± 20.55 mg/L), and the lowest total TN was found in *Ankistrodesmus falcatus* (140.54 ± 24.90 mg/L). The total phosphorus of these three species was 3.49 ± 0.76 mg/L (*Phormidium tenue*), 3.01 ± 1.17 mg/L (*Monoraphidium braunii*), and 3.07 ± 0.66 mg/L (*Ankistrodesmus falcatus*), respectively. Moreover, Table 4.1 shows the TN and TP removal efficiencies over three microalgae phases. The TN removal of the CDC reactor during phases was around 26% ± 5% to 44% ± 10%, and the TP removal ranged from 30 % ± 15% to 40 % ± 23%. The nutrient removal follows the trend of *Ankistrodesmus falcatus* > *Monoraphidium braunii* > *Phormidium tenue*. In this study, the nutrient removals of all microalgae are below 50%, which could be ascribed to the low suspended biomass concentration limitation and high nutrient concentrations in the influent (TN = 250 mg/L; TP = 6 mg/L). Furthermore, the nutrient removal was most achieved by suspended microalgae (*Phormidium tenue*: 81.15% ± 5.40%, *Monoraphidium braunii*: 82.99% ± 3.34%, and *Ankistrodesmus falcatus*: 82.16% ± 3.86%, respectively) compared to microalgae biofilm (*Phormidium tenue*: 8.70% ± 6.08%, *Monoraphidium braunii*: 6.64% ± 3.76%, and *Ankistrodesmus falcatus*: 7.57% ± 4.34%, respectively) since it contained the greatest number of microalgae cells.

Figure 4.3 shows the particle size distribution of these three microalgae species in the CDC bioreactor on the 16th day of cultivation under stirring speeds of 125 rpm and 60 rpm, respectively. Under 125 rpm, *Monoraphidium braunii* exhibited the biggest particle size (Dx (0.5): 225 μm),

followed by the *Phormidium tenue* (Dx (0.5): 118 µm). *Ankistrodesmus falcatus* is the smallest one (Dx (0.5): 99.6 µm). Except for *Phormidium tenue*, *Monoraphidium braunii* and *Ankistrodesmus falcatus* showed larger particle sizes under the lower stirring speed (60 rpm), which can be explained by more large microalgal flocs formation and less floc breakages under a smaller applied shear stress. The results of particle size distribution, as shown in Figure 4.3, indicate that *Monoraphidium braunii* and *Ankistrodesmus falcatus* were sensitive to the change of shear stress. An increase in shear stress (stirring speed) led to the breakage of large flocs and smaller floc sizes. In contrast, an increase in shear stress (stirring speed from 60 to 125 rpm) did not cause a significant change in floc sizes (except for a slight rise in the number of small flocs in the size range of 1-10 µm) of *Phormidium tenue,* indicating that *Phormidium tenue* had a higher tolerance for shear stress, compared to the other two microalgae. The morphology (Figure 4.4) of these microalgae species under an inverted optical microscope verified the observations of the particle size analysis (*Phormidium tenue*: diameter 2 µm; *Monoraphidium braunii*: width 2.5 µm, length 15 µm; and *Ankistrodesmus falcatus*: width 1.5 µm, length 12 µm, respectively). As Michels et al. mentioned, the higher shear stress could facilitate the intercellular junction's separation and cause a chain, reducing microalgal clusters. They observed that the number of smaller floc of *Skeletonema costatum* increased when the applied shear stress level increased from 0.26 Pa to 5.4 Pa [26]. The results from this study are consistent with those of Michels et al. [26].

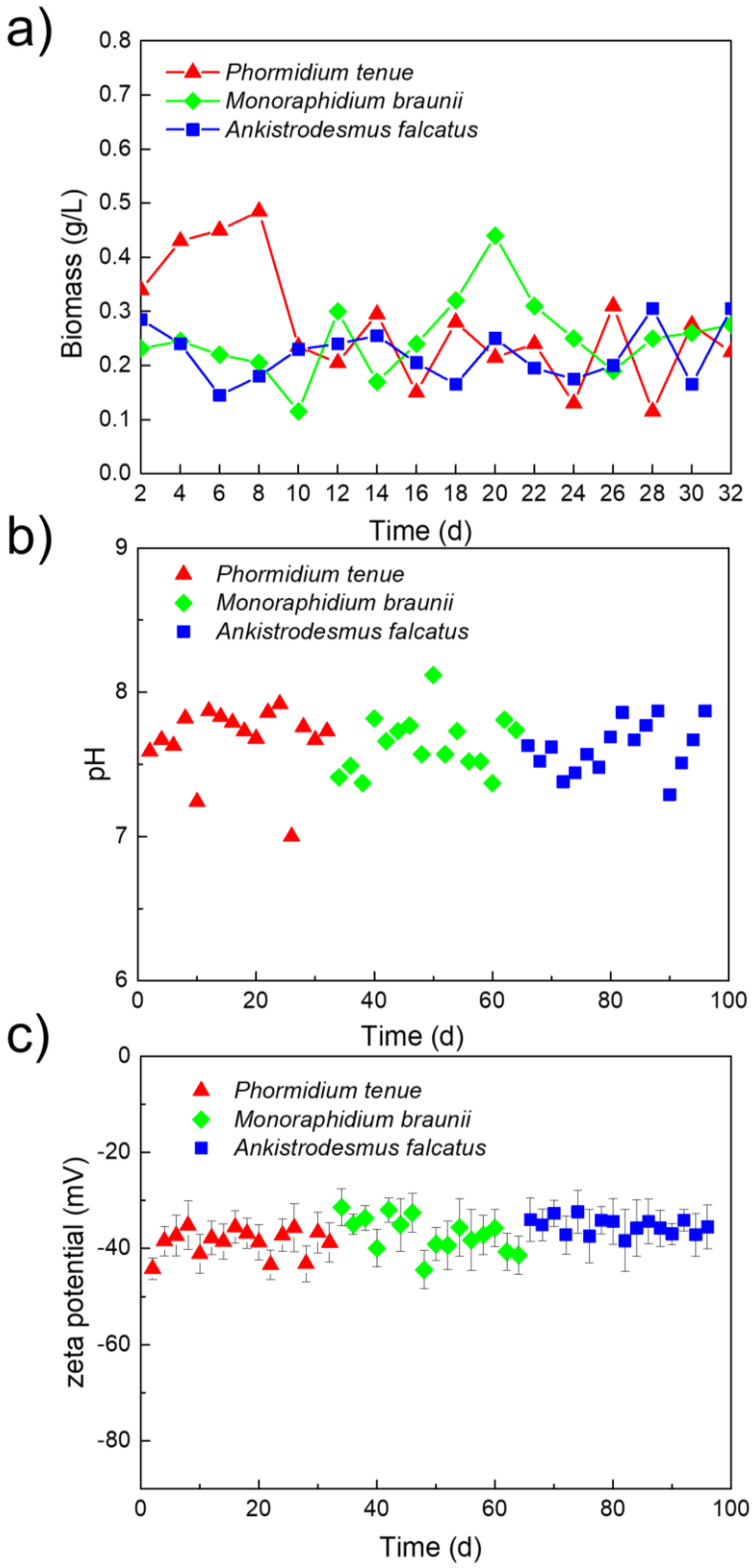

Figure 4.1. a) Biomass concentration, b) pH, and c) Zeta potential of microalgal culture medium in CDC reactor effluent at different microalgae species phases (Results = mean ± standard deviation, n= 6 each data point for zeta potential).

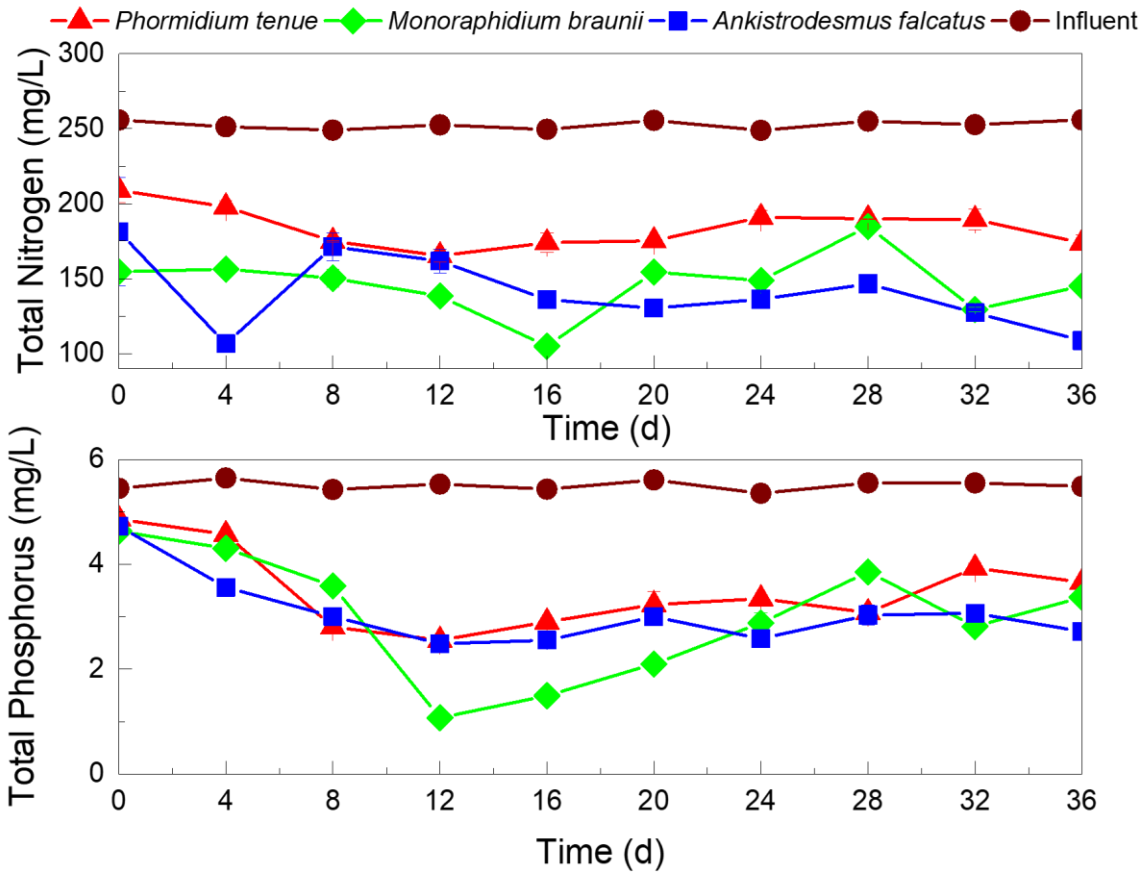

Figure 4.2. Total nitrogen and total phosphorus of effluent of CDC biofilm reactor in different microalgal species phases (Results = mean ± standard deviation, n= 2).

Table 4.1. Nutrient removal of CDC reactor at different microalgae phases (Results = mean ± standard deviation).

	Phormidium tenue	*Monoraphidium braunii*	*Ankistrodesmus falcatus*
Nitrogen (TN) removal	26 % ± 5 %	41 % ± 8 %	44 % ± 10 %
Phosphorus (TP) removal	30 % ± 15 %	40 % ± 23 %	39 % ± 13 %

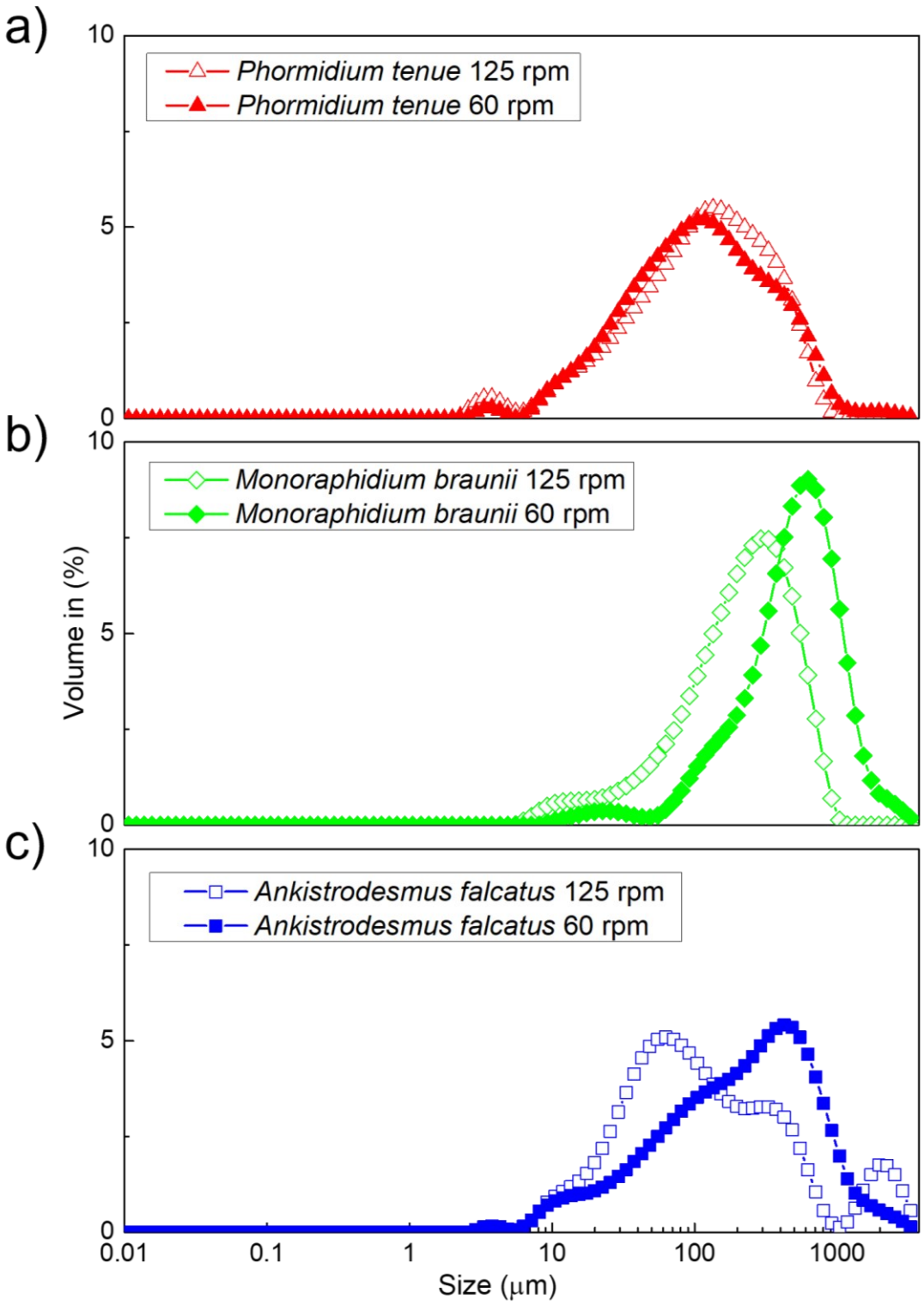

Figure 4.3. Particle size distribution of a) *Phormidium tenue*, b) *Monoraphidium braunii*, and c) *Ankistrodesmus falcatus* under different hydrodynamic conditions on the 16th day of biofilm cultivation.

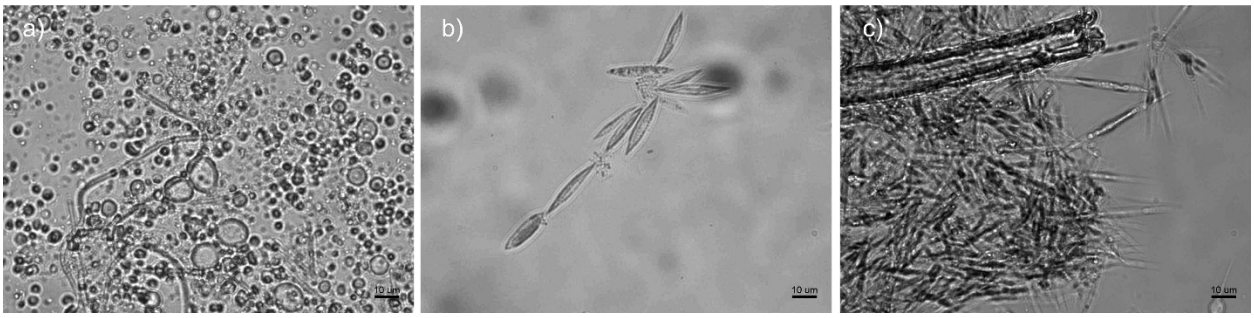

Figure 4.4. Optical microscope of a) *Phormidium tenue*, b) *Monoraphidium braunii*, and c) *Ankistrodesmus falcatus*.

4.3.2. Microalgal biofilm attachment

Figure 4.5 exhibits the wet biomass amount of different microalgal biofilms after 1 hour of taking it out from the reactor every two days over the cultivation period, under the hydrodynamic conditions of 125 rpm and 60 rpm, respectively. At 125 rpm, the highest biomass attachment was observed on *Monoraphidium braunii* biofilm, which reached 187.40 ± 10.57 g/m^2 on the Nylon coupon on the 16th day. The second largest attachment was on *Ankistrodesmus falcatus* biofilm (73.10 ± 1.38 g/m^2). The *Phormidium tenue* biofilm had the lowest attach performance, which is 66.80 ± 6.79 g/m^2. When the reactor was under 60 rpm, the highest attach behaviour was found on *Ankistrodesmus falcatus* biofilm (144.23 ± 6.52 g/m^2), and the lowest attachment was achieved on *Phormidium tenue* biofilm (24.02 ± 0.39 g/m^2).

Furthermore, the photograph of the different microalgal biofilms on nylon coupons also indicated that the thickest biofilms were *Monoraphidium braunii* at 125 rpm and *Ankistrodesmus falcatus* at 60 rpm, respectively (Figure 4.6). Multiple factors affected biofilm formation, including substrate properties, environmental conditions, and microalgae species [2, 15, 27]. This study will further investigate and discuss these two aspects: microalgae species and hydrodynamic conditions.

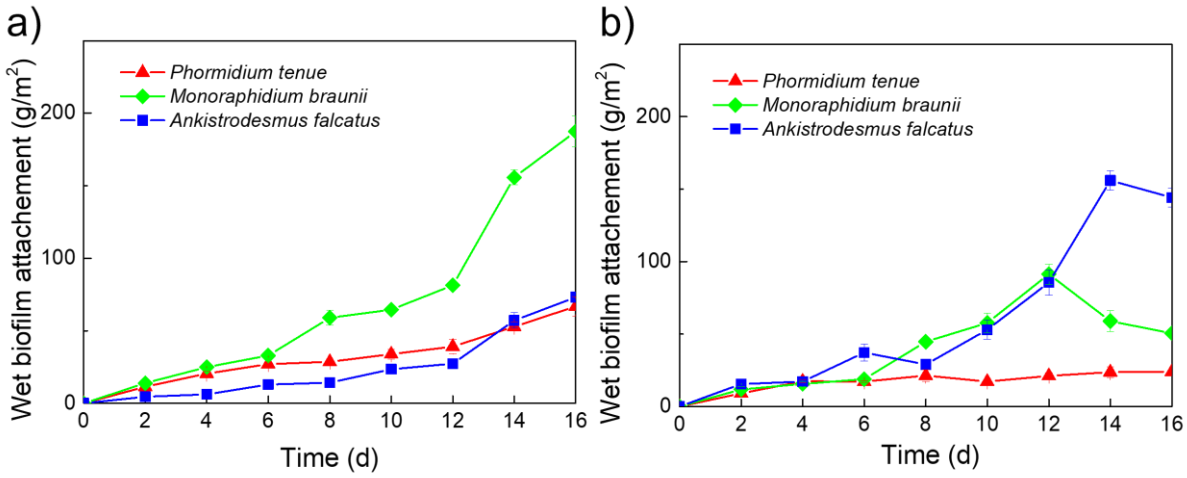

Figure 4.5. Wet biofilm attachment of different microalgae species at a) 125 rpm and b) 60 rpm

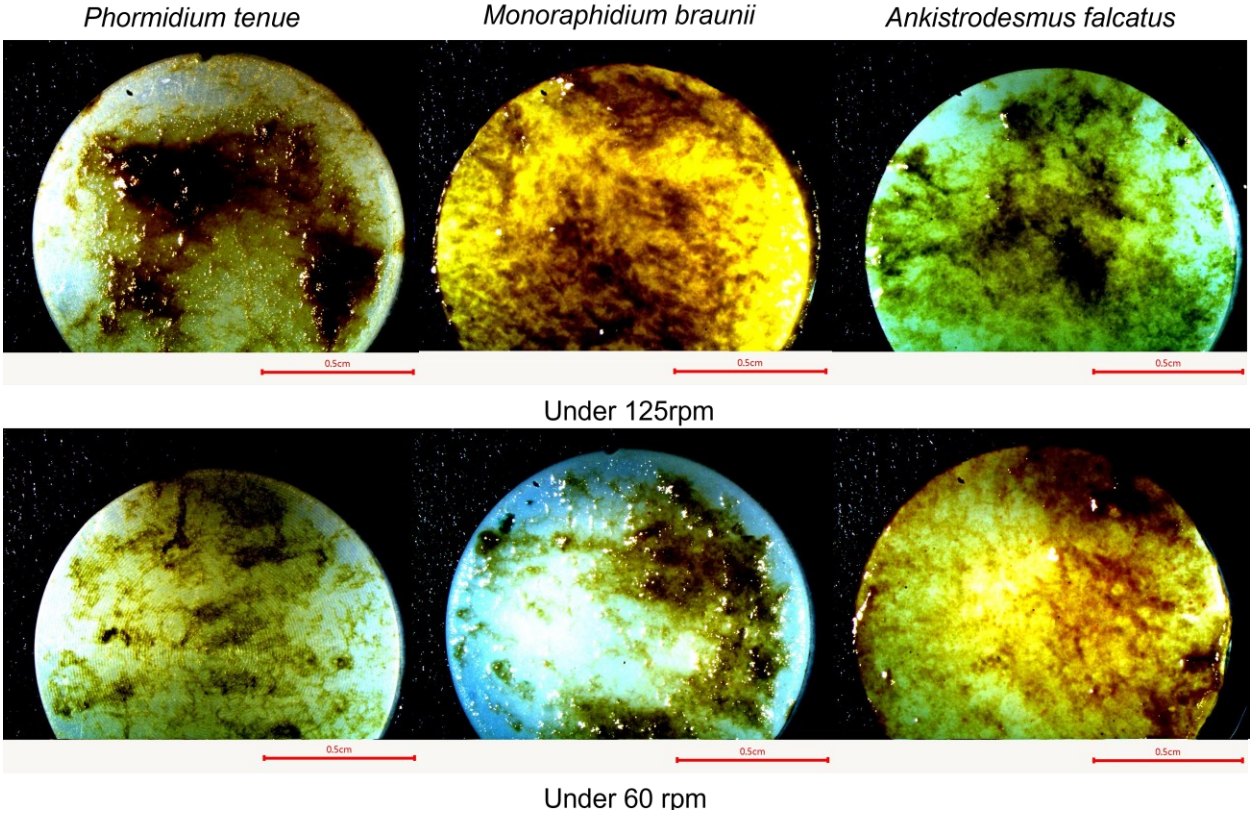

Figure 4.6. Photograph of different biofilm species on nylon coupons 16 days of cultivation under different stirring speeds.

4.3.3. Influence factors on biofilm attachment

4.3.3.1. Influence of biofilm biomass EPS

Figure 4.7a shows the EPS concentration of different microalgal biofilms on nylon coupons over 16 days of cultivation under 125 rpm. The early period EPS concentration was not reported due to the limited amount of cell adhesion as biofilm and thus below the detection and analytical limits of EPS extraction and analysis. On the 16th day, the *Monoraphidium braunii* biofilm on nylon coupons contains the lowest total EPS content, about 65.46 mg/g biofilm. The highest total EPS can reach 134.53 mg/g biofilm achieved on *Phormidium tenue* biofilm (125 rpm). The EPS profiles of different microalgal biofilms under 60 rpm conditions are also reported in this study, which exhibited a similar trend with the changing of EPS concentration (Figure 4.7b). The EPS concentration decreased, followed by the augment of biofilm biomass, which was also reported in a previous study [28]. As the literature mentioned, EPS concentration decreased during cultivation due to a higher microalgal biomass growth rate [28-30]. One possible explanation for the trend could be as follows: The increased biofilm thickness during the growth period limited the CO_2 and light transfer efficiency to the inner side of the microalgal biofilm [31, 32]. As a result, the EPS will be consumed as a carbon resource to maintain the growth of microalgae cells in the biofilm's inner side, leading to the EPS concentration decreasing with the biofilm biomass increasing (Figure 4.5 and Figure 4.7). Similar phenomena are also reported and mentioned in some literature [23, 30, 33]. Unlike the general suggestions that EPS has positive effects on biofilm adhesion (EPS concentration increases with the biofilm biomass increase) [15, 34], the EPS results in this study indicated that EPS had no significant influence on biofilm formation which was consistent with the point made by Devi et al.[35].

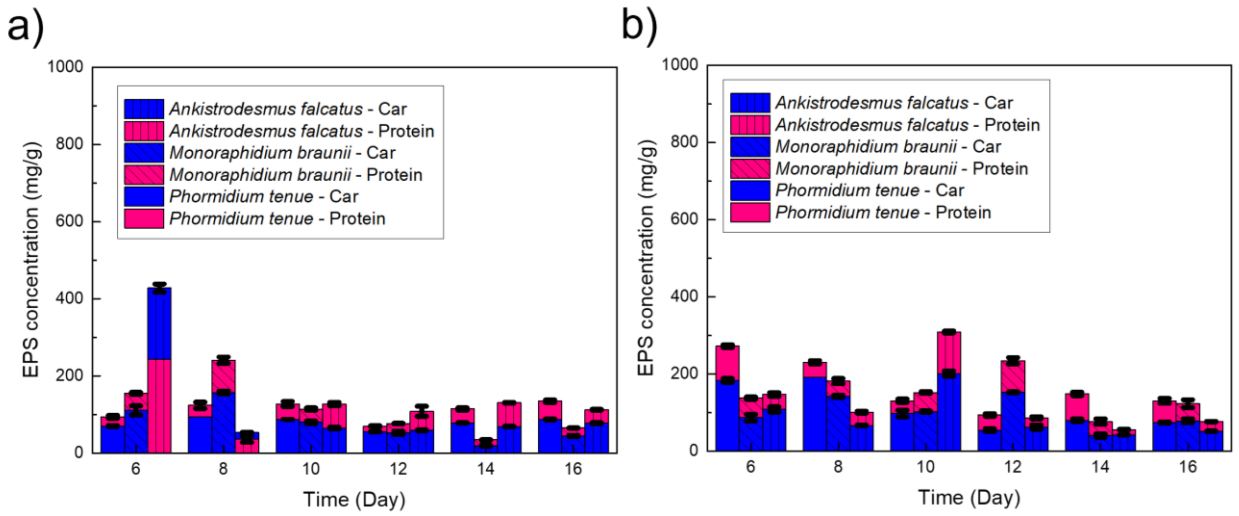

Figure 4.7. EPS concentration of different microalgae species in the hydrodynamic condition of a) 125 rpm and b) 60 rpm.

4.3.3.2. Influence of surface properties

Table 4.2 shows the surface properties of microalgae and Nylon material (Contact angle, surface free energy, free energy of cohesion, and zeta potential). Based on the contact angle result, all these three microalgae and Nylon are considered hydrophilic (< 90°), and the contact angle of microalgae followed the trend: *Ankistrodesmus falcatus* > *Monoraphidium braunii* > *Phormidium tenue*. Table 4.2 also shows the zeta potential value of the different microalgae and nylon coupons. The zeta potential value of the microalgae ranges from -35.33 ± 1.74 mV to -38.66 ± 2.85 mV, and the absolute value of zeta potential follows the trend: *Phormidium tenue* > *Monoraphidium braunii* > *Ankistrodesmus falcatus*. Both the microalgae and Nylon material exhibited negative zeta potential. Moreover, the total surface free energy (γ^{Tol}) of these three microalgae ranges from 30.84 mJ/m^2 to 48.69 mJ/m^2, which followed the trend: *Phormidium tenue* > *Monoraphidium braunii* > *Ankistrodesmus falcatus*. Research claims the hydrophobic material is suitable for microalgal biofilm formation due to the water exclusion mechanism and hydrophobic attraction [36]. However, literature also reported that some hydrophilic microalgae prefer to adhere to

hydrophilic materials with an excellent liquid-holding capacity [37-39]. Table 4.2 shows three hydrophilic microalgae (*Phormidium tenue*, *Monoraphidium braunii* and *Ankistrodesmus falcatus*) formed biofilm on the hydrophilic Nylon material surface. As Shen et al. mentioned, this occurrence can be attributed to the promotion of initial attachment caused by hydrophilic materials' high dispersive surface energy [40]. As a result, the formation of microalgae biofilms was observed on the Nylon material surface. Nevertheless, as some literature mentioned, the free energy of cohesion (ΔG_{coh}) can also be an index to determine the hydrophilicity and hydrophobicity of the microalgal or material surface [13, 41]. The hydrophilic surface presents a positive free energy of cohesion ($\Delta G_{coh} > 0$), and vice versa is hydrophobic ($\Delta G_{coh} < 0$) [42]. Regardless of the contact angle, as Table 4.2 shows, the Nylon surface was considered hydrophobic due to the negative ΔG_{coh}. The positive ΔG_{coh} of three microalgae indicated that their surfaces were hydrophilic. Thereby, the hydrophobic property verified by ΔG_{coh} might be why higher attachment is achieved on more hydrophobic microalgae (*Monoraphidium braunii* and *Ankistrodesmus falcatus*) instead of more hydrophilic *Phormidium tenue*. Thereby, this preference based on ΔG_{coh} results could be ascribed to the water exclusion mechanism [36, 43]. Also, the XDLVO theory illustrated that the hydrophobic attraction driven by acid-base interaction force would occur between the microalgae and hydrophobic material [44]. The more hydrophobic microalgae cells are, the higher adhesion on the hydrophobic substrate was observed [23]. From this point of view, the biofilm formation in this study might be positively affected by hydrophobic attraction. However, the adhesion results at 125 rpm (Figure 4.5a) did not obey the trend below. The highest attachment was not achieved by the most (*Phormidium tenue*) or least (*Ankistrodesmus falcatus*) hydrophilic microalgae. Instead, *Monoraphidium braunii,* with moderate hydrophilicity, accomplished the highest biofilm attachment. Tong et al. also found that the highest attachment on pristine polyvinylidene fluoride

membrane was achieved on *A.coffeaeformis* with moderate hydrophilicity [45]. This occurrence proves that surface wettability might not be the only dominant factor in controlling microalgae biofilm formation under 125 rpm. Furthermore, Alexander and Williams also argued that hydrophilicity (water contact angle) is not the most suitable predictor of cell-substrate interactions due to the complicated material surface chemistry [46].

Table 4.2. Contact angle and surface energy of different microalgae species.

Materials	Contact angle (◦)			Surface energy (mJ/m^2)					ΔG_{coh} (mJ/m^2)	Zeta potential (mV)
	Water	Formamide	Diiodomethane	γ^{LW}	γ^{AB}	γ^{+}	γ^{-}	γ^{Tol}		
Nylon	78.8 ± 1.5	44.8 ± 2.9	50.8 ± 3.4	33.82	5.19	3.18	2.11	39.00	-49.60	-11.37 ± 3.6
Phormidium tenue	31.8 ± 1.9	32.7 ± 3	48.7 ± 3.8	35.00	13.69	0.99	47.17	48.69	26.36	-38.66 ± 2.85
Monoraphidium braunii	35.4 ± 2.8	47.7 ± 4.1	50.1 ± 1.0	34.22	1.78	0.01	57.11	36.00	46.68	-36.95 ± 3.70
Ankistrodesmus falcatus	36.7 ± 0.1	51.4 ± 2.1	53.9 ± 4.9	32.07	0.59	0.001	59.49	32.66	51.41	-35.33 ± 1.74

Surface free energy is another surface property affecting the microalgae biofilm adhesion [47]. As Ozkan and Berberoglu claimed, the Lifshitz van der Waals (LW) component (γ^{LW}) represents the polarity of the cell surface [48]. The higher value of the LW component results in a higher apolar surface, leading to a higher attachment to material due to the lower affinity for polar water [48]. The LW component of the microalgae ranged from 32.07 to 35.00 mJ/m^2, which occupied above 70% of the total surface free energy. The high ratio of LW components in total surface free energy also proves that LW interaction probably contributed the most among those interaction forces in the low-energy surface material. However, the microalgae with the highest

LW component did not exhibit the highest biofilm attachment, which indicates that the LW component of the surface free energy or polarity might not be the only factor affecting microalgae biofilm formation in this study. As Barros et al. mentioned, the AB component would represent a measure of hydrophilic repulsion when the microalgae exhibited a hydrophilic character ($\Delta G_{coh} > 0$) [49]. Thus, a higher value of the AB component is supposed to observe less biofilm attachment due to the higher hydrophilic repulsion. This may be one probable reason why *Phormidium tenue* shows the worst biofilm behaviour. Von Fraunhofer mentioned that surface free energy is an important index to measure the wettability of a solid surface [50]. Low surface free energy results in poor molecular attraction, which leads to a low biofilm formation [51]. When it comes to total surface free energy in this study, the highest biofilm amount was not achieved on either the species with the highest value or lowest value of the total surface free energy, which indicates that the relationship between total surface free energy and microalgal adhesion may not be linear under 125 rpm. Some studies indicated that adhesion performance also corresponds to the difference in total surface free energy between microalgae strain and attached substrate [19, 52]. Regardless of the species and substrate types, Zhang et al. argued that the degree of the microorganism adhesion would linearly increase with the reduction of surface free energy difference [52]. They found *P. putida* exhibited the best adhesion performance due to the lowest surface free energy difference between the cell and substrate [52]. As Table 4.2 shows, the *Monoraphidium braunii* biofilm (35.47 mJ/m^2) has the lowest difference between nylon coupon (39.00 mJ/m^2) reached the highest attachment (187.40 ± 10.57 g/m^2). The *Phormidium tenue* (48.69 mJ/m^2) has the thinnest biofilm with the largest difference to the nylon surface free energy under the hydrodynamic condition of 125 rpm (Figure 4.5a). The Dupré equation could explain this. As Baldan mentioned, the adhesion strength can be described by the work of adhesion (W_A), which is equal to the sum of surface free

energies of two solid phases (γ_1 and γ_2, respectively) minus their interfacial tension ($\gamma_{1,2}$) [53]. The closer the surface free energies of the two solid phases, the closer the interfacial tension ($\gamma_{1,2}$) is to zero [54]. Thereby, a higher work of adhesion was obtained, leading to a higher adhesion performance.

Hwang et al. claimed that material with negative charges is generally unfavourable to negative microalgae biofilm formation due to electrostatic repulsion [31]. However, in this study, all three microalgae (*Phormidium tenue*, *Monoraphidium braunii*, and *Ankistrodesmus falcatus*) generated biofilm on the Nylon coupon surface. This observation could be attributed to the ionic bridging. Negative microalgal cells can be bridged with other negative particles or even substrate with negative charges with the existence of cationic particles (Ca^{2+} and Zn^{2+}) [55]. In general, the less the absolute value of zeta potential, the less repulsion force was obtained, leading to higher adhesion should be observed [56, 57]. The attachment performance of the microalgae did not show a similar trend in this study, which indicates that the electrostatic interaction might not be the decisive factor in biofilm formation. In the next section, further discussion will focus on the effect of hydrodynamic conditions.

4.3.3.3. Influence of hydrodynamic conditions

Figure 4.8 displays the microalgal biofilm performance under different hydrodynamic conditions. Some literature mentioned that hydrodynamic conditions such as shear stress or rotation speed would influence biofilm activity by affecting biofilm architecture or cell growth [58, 59]. In the *Phormidium tenue* and *Monoraphidium braunii* biofilm cases, the biofilm attachment decreased (from 66.8 ± 6.79 g/m^2 to 24.02 ± 0.39 g/m^2 and 187.40 ± 10.57 g/m^2 to 50.52 ± 2.77 g/m^2, respectively) when the stirring speed changed from 125 rpm to 60 rpm. However, the *Ankistrodesmus falcatus* biofilm shows the opposite behaviour to formers, increasing from 73.10

± 1.38 g/m^2 to 144.23 ± 6.52 g/m^2. This change can be attributed to the effect of the hydrodynamic conditions because the stirring speed was the only variable in this case. In general, shear stress might increase the detachment potential of biofilm once the shear force suppresses the adhesion force of microalgae cells [60]. As a result, intensive shear stress applications were usually suggested for the anti-biofouling of the membrane for removing undesirable microorganism biofilm [61, 62]. So, the augment of *Ankistrodesmus falcatus* biofilm attachment, when the stirring speed changed from 125 rpm to 60 rpm, might be due to less detachment occurring under lower shear stress.

Nevertheless, researchers also argued that applying a higher surface shear stress could improve biofilm biomass by increasing nutrient diffusion for biofilm growth [63]. Therefore, the opposite results from *Phormidium tenue* and *Monoraphidium braunii* biofilm might be considered that lower hydrodynamic strength could not provide sufficient nutrient diffusion for biofilm growth, leading to less biofilm biomass. This study's contradictory phenomena among microalgae indicated that the hydrodynamic condition influencing biofilm formation might be species-dependent. As the literature mentioned, there is a tolerance limitation for microalgae biofilm on shear stress, which is the critical value of the interaction between shear force and adhesion [64, 65]. Below this critical value, the adhesion force is higher than the shear force; thus microalgae cells exhibit adhesion on the substrate surface. As a result, higher shear stress below this microalgae tolerance limitation could increase nutrient diffusion and transfer, leading to better biofilm performance [66, 67]. However, once the applied shear stress exceeds the critical value, the detachment occurs and reduces biofilm [68]. Belohlav et al. claimed that the critical value of wall shear stress could be a processing parameter to control the stability of microalgal biofilm [69]. They also reported that no biofilm was observed when the flow rate of the culture medium

exceeded the critical value [69]. In this study, for the case of *Phormidium tenue* and *Monoraphidium braunii*, biofilm attachment decreases with the stirring speed decrease. One reasonable explanation is that the stirring speed is not large enough (125 rpm) to cause a significant biofilm detachment. Thus, the interaction of the dissolved nutrients and biofilm has less efficiency, resulting in lower growth under lower stirring speed (60 rpm). When it comes to the *Ankistrodesmus falcatus* case in which a higher stirring speed results in lower biofilm attachment, higher shear speed enhances biofilm detachment. The higher stirring speed increasing the scouring to the *Ankistrodesmus falcatus* biofilm surface resulted in reduced biofilm biomass.

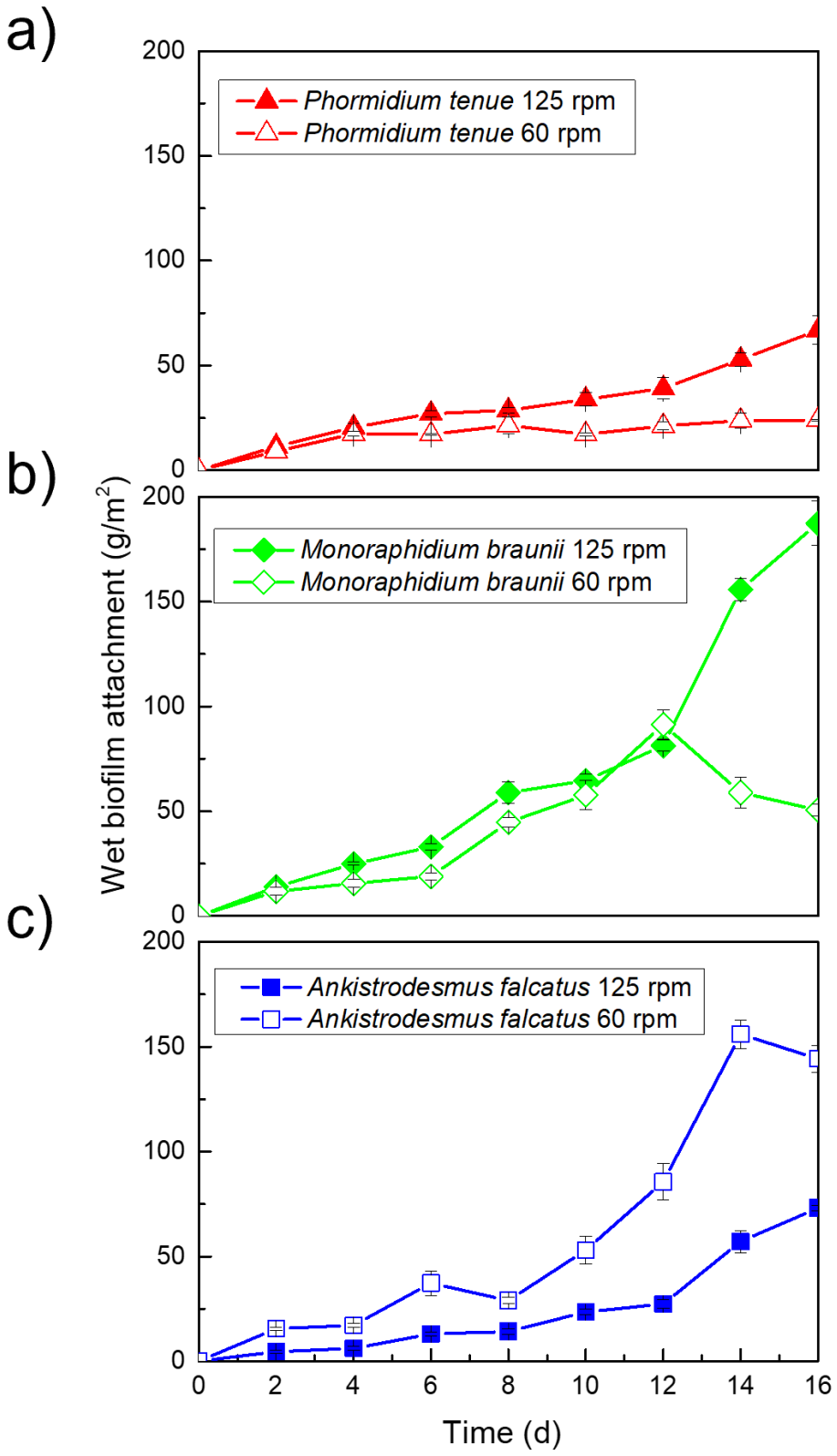

Figure 4.8. a) *Phormidium tenue*, b) *Monoraphidium braunii*, and c) *Ankistrodesmus falcatus* biofilm formation at different hydrodynamic conditions.

Moreover, the presence of a fraction of small particle (microalgal cell or flocs) sizes (< 10 or 20 μm) played an important role in controlling the microalgae biofilm formation; the increase in the quantity and formation rate of biofilm for both *Phormidium tenue* and *Monoraphidium braunii* under the higher stress (125 rpm) (Figure 4.8)) is correlated to the presence of a larger fraction of small particle sizes (<10 or 20 μm), as compared to that under lower shear stress (60 rpm) (Figure 4.3a) and 4.3b)). Similarly, the higher quantity and formation rate of *Ankistrodesmus falcatus* biofilm under a lower shear stress (60 rpm) is correlated to the presence of a fraction of small particle sizes (< 6 μm) of microalgal cells/flocs (Figure 4.3c), as compared to that under the higher shear stress (125 rpm). This is because smaller cells and flocs have a higher tendency or higher affinity to attach to membrane surfaces for biofilm formation [70, 71].

4.3.4. Correlation of impact factors on biofilm formation

Figure 4.9 exhibited the Pearson correlation between the impact factors (Contact angle, zeta potential, free energy of cohesion (ΔG_{coh}), surface free energy (SFE), and floc/cell size of microalgae) and microalgal biofilm formation under different hydrodynamic conditions (125 rpm and 60 rpm, respectively). It is evident that the floc/cell size showed a significant positive correlation with biofilm formation ($r = 0.99734$, $p < 0.05$ on the 12^{th} day) under 125 rpm, while the rest factors didn't exhibit a strong correlation ($r < 0.8$) at the 0.05 level. Regarding the lower shear stress (60 rpm), the factor of floc/cell size exhibited a very poor correlation with biofilm formation ($r < 0.5$, $p > 0.05$). Instead, the contact angle, zeta potential and free energy of cohesion (ΔGcoh) of microalgae showed a positive correlation ($r > 0.8$), while the SFE of microalgae exhibited a negative correlation (r = -0.96299 on the 12th day) with biofilm formation.

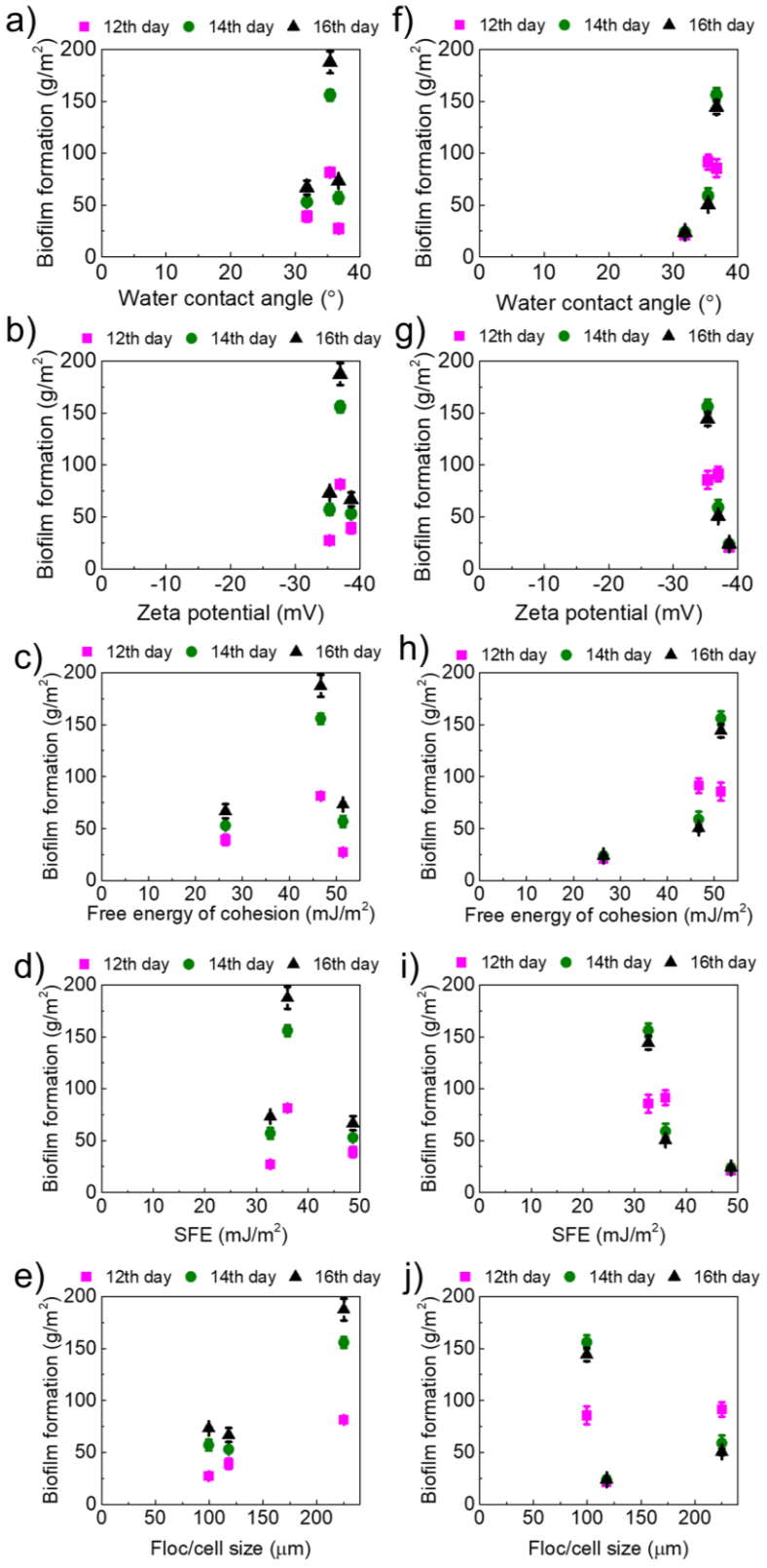

Figure 4.9. Correlation profiles between impact factors and biofilm formation under 125 rpm (a, b, c, d, and e) and under 60 rpm (f, g, h, i, and j), respectively.

In summary, the biofilm formation could be controlled by the surface and physical and chemical properties of microalgae cells under low hydrodynamic conditions. As some literature revealed, the microalgae species have their own critical shear stress during cultivation [69-71]. When the hydrodynamic condition is below the critical value, the shear strength is not lower than the adhesion strength driven by microalgae cells. As a result, the biofilm formation was dominant by the attractive force caused by the microalgae properties (contact angle, zeta potential, free energy of cohesion, and surface free energy). Once the shear force is stronger than the adhering force of the biofilm, biofilm formation might be significantly affected by the hydrodynamic conditions. As a result, the biofilm formation was dominated by the factor (the size of microalgae cells/flocs) which highly correlates to the high-level shear stress. Thus, choosing microalgae species and shear stress are vital during the algal biofilm cultivation period, especially at the initial stage.

4.3.5. Implication to the Development of Extractive Membrane Microalgal Biofilm Photobioreactor (EMMPBR)

The results from this study reveal that the surface properties of microalgae, including SFE, zeta potential, and hydrophobicity, play a crucial role in controlling the rate of microalgal biofilm formation in EMMBR. The combination of these properties determines the biofilm formation, with hydrodynamic conditions being the dominant factor in all cases. Higher hydrodynamic conditions promote nutrient diffusion, but if the conditions exceed the critical value of microalgae, biofilm formation may be hindered. In developing EMMBR, an emerging technology for wastewater treatment, especially in nutrient removal, it is important to select microalgae species that can form biofilms quickly and recover effectively after harvesting to reduce the time between cyclic operations. A suitable hydrodynamic condition can also promote biofilm formation by increasing

mass transfer and nutrient diffusion, which shortens the growth period. These findings provide guidance for the selection and screening of microalgae species and hydrodynamic conditions to facilitate rapid microalgal biofilm formation in EMMPBR technology development. Moreover, the study shows that the relative importance of surface hydrophobicity, zeta potential, and surface free energy, which determine biofilm formation and biological performance, changes under different circumstances. Therefore, it is recommended to integrate the analysis of all these properties and their relative importance in controlling microalgae cell adhesion and biofilm formation.

4.4. Conclusion

The experimental work presented here investigated the role of surface and physical properties of different microalgae strains in controlling microalgae cell adhesion and biofilm formation on the membrane material surfaces (Nylon) under different hydrodynamic conditions. The following conclusions could be made:

1.) Under a low shear stress condition (60 rpm), the hydrophobicity (water contact angle), zeta potential, and free energy of cohesion (ΔG_{coh}) of the microalgae species were positively correlated to the quantity and biofilm formation rate. In contrast, the surface free energy of microalgae species was negatively correlated to the biofilm's quantity and formation rate, indicating the importance of surface properties in controlling microalgae cell adhesion and biofilm formation.

2. Under a high shear stress, the hydrodynamic conditions and the presence of a fraction of small particle sizes of microalgae cells/flocs played a dominant role, over the surface properties of microalgae species, in controlling the quantity and formation rate of microalgal biofilm.

3. For the same microalgae species, the presence of a fraction of small particle sizes of microalgae cells/flocs played an important role in controlling biofilm's quantity and formation rate under different hydrodynamic conditions.

4.) The relative importance of the hydrodynamic conditions and surface and physical properties of microalgae species in controlling biofilm's quantity and formation rate would vary, depending on specific experimental conditions and microalgae species used.

4.5. References

[1] Saini, S., Tewari, S., Dwivedi, J., Sharma, V. (2023). Biofilm Mediated Wastewater Treatment: A Comprehensive Review. Materials Advances, 4, 1415-1443.
[2] Mantzorou, A., Ververidis, F. (2019). Microalgal biofilms: A further step over current microalgal cultivation techniques. Science of the Total Environment, 651, 3187-3201.
[3] Fica, Z.T., Sims, R.C. (2016). Algae-based biofilm productivity utilizing dairy wastewater: effects of temperature and organic carbon concentration. Journal of Biological Engineering, 10, 1-7.
[4] Gross, M., Zhao, X., Mascarenhas, V., Wen, Z. (2016). Effects of the surface physico-chemical properties and the surface textures on the initial colonization and the attached growth in algal biofilm. Biotechnology for biofuels, 9, 1-14.
[5] Zhao, Z., Muylaert, K., Szymczyk, A., Vankelecom, I.F. (2021). Enhanced microalgal biofilm formation and facilitated microalgae harvesting using a novel pH-responsive, crosslinked patterned and vibrating membrane. Chemical Engineering Journal, 410, 127390.
[6] Zhuang, L., Yu, D., Zhang, J., Liu, F., Wu, Y., Zhang, T., Dao, G., Hu, H. (2018). The characteristics and influencing factors of the attached microalgae cultivation: a review. Renewable and Sustainable Energy Reviews, 94, 1110-1119.
[7] Tsavatopoulou, V.D., Aravantinou, A.F., Manariotis, I.D. (2021). Comparison of *Botryococcus braunii* and *Neochloris vigensis* Biofilm Formation on Vertical Oriented Surfaces. Biointerface Research in Applied Chemistry, 11, 12843-12857.
[8] Romeu, M.J.L., Domínguez-Pérez, D., Almeida, D., Morais, J., Campos, A., Vasconcelos, V., Mergulhao, F.J. (2020). Characterization of planktonic and biofilm cells from two filamentous cyanobacteria using a shotgun proteomic approach. Biofouling, 36, 631-645.
[9] Shen, Y., Xu, X., Zhao, Y., Lin, X. (2014). Influence of algae species, substrata and culture conditions on attached microalgal culture. Bioprocess and Biosystems Engineering, 37, 441-450.
[10] Lutzu, G.A., Zhang, L., Zhang, Z., Liu, T. (2017). Feasibility of attached cultivation for polysaccharides production by *Porphyridium cruentum*. Bioprocess and Biosystems Engineering, 40, 73-83.
[11] Wang, J., Zhang, M., Fang, Z. (2019). Recent development in efficient processing technology for edible algae: A review. Trends in Food Science & Technology, 88, 251-259.

[12] Banerjee, S., Dasgupta, S., Das, D., Atta, A. (2020). Influence of photobioreactor configuration on microalgal biomass production. Bioprocess and Biosystems Engineering, 43, 1487-1497.
[13] Zeriouh, O., Reinoso-Moreno, J.V., López-Rosales, L., Cerón-García, M.D.C., Sánchez-Mirón, A., García-Camacho, F., Molina-Grima, E. (2017). Biofouling in photobioreactors for marine microalgae. Critical Reviews in Biotechnology, 37, 1006-1023.
[14] Zhang, Q., Yu, Z., Jin, S., Liu, C., Li, Y., Guo, D., Hu, M., Ruan, R., Liu, Y. (2020). Role of surface roughness in the algal short-term cell adhesion and long-term biofilm cultivation under dynamic flow condition. Algal Research, 46, 101787.
[15] Cheah, Y.T., Chan, D.J.C. (2021). Physiology of microalgal biofilm: a review on prediction of adhesion on substrates. Bioengineered, 12, 7577-7599.
[16] Yang, C.C., Wen, R.C., Shen, C.R., Yao, D.J. (2015). Using a microfluidic gradient generator to characterize BG-11 medium for the growth of cyanobacteria *Synechococcus elongatus* PCC7942. Micromachines, 6, 1755-1767.
[17] Tsavatopoulou, V.D., Manariotis, I.D. (2020). The effect of surface properties on the formation of *Scenedesmus rubescens* biofilm. Algal Research, 52, 102095.
[18] Yuan, H., Zhang, X., Jiang, Z., Chen, X., Zhang, X. (2018). Quantitative criterion to predict cell adhesion by identifying dominant interaction between microorganisms and abiotic surfaces. Langmuir, 35, 3524-3533.
[19] Wang, W., Shen, A., Yang, X., Guo, Y., Zhao, T. (2020). Surface free energy method for evaluating the effects of anti-stripping agents on the moisture damage to asphalt mixtures. Journal of Adhesion Science and Technology, 34, 1947-1970.
[20] Van Oss, C., Good, R., Chaudhury, M. (1988). Additive and nonadditive surface tension components and the interpretation of contact angles. Langmuir, 4, 884-891.
[21] Zhang, M., Leung, K., Lin, H., Liao, B. (2022). Evaluation of membrane fouling in a microalgal-bacterial membrane photobioreactor: Effects of SRT. Science of The Total Environment, 839, 156414.
[22] Zhang, M., Leung, K.T., Lin, H., Liao, B. (2020). The biological performance of a novel microalgal-bacterial membrane photobioreactor: Effects of HRT and N/P ratio. Chemosphere, 261, 128199.
[23] Tong, C., Derek, C. (2021). Biofilm formation of benthic diatoms on commercial polyvinylidene fluoride membrane. Algal Research, 55, 102260.
[24] Gaudy, E., Wolfe, R. (1962). Composition of an extracellular polysaccharide produced by Sphaerotilus natans. Applied Microbiology, 10, 200-205.
[25] Lowry, O., Rosebrough, N., Farr, A.L., Randall, R. (1951). Protein measurement with the Folin phenol reagent. Journal of Biological Chemistry, 193, 265-275.
[26] Michels, M.H., Van der Goot, A.J., Vermuë, M.H., Wijffels, R.H. (2016). Cultivation of shear stress sensitive and tolerant microalgal species in a tubular photobioreactor equipped with a centrifugal pump. Journal of Applied Phycology, 28, 53-62.
[27] Wang, J.H., Zhuang, L.L., Xu, X.Q., Deantes-Espinosa, V.M., Wang, X.X., Hu, H.Y. (2018). Microalgal attachment and attached systems for biomass production and wastewater treatment. Renewable and Sustainable Energy Reviews, 92, 331-342.
[28] Shen, Y., Zhang, H., Xu, X., Lin, X. (2015). Biofilm formation and lipid accumulation of attached culture of *Botryococcus braunii*. Bioprocess and Biosystems Engineering, 38, 481-488.

[29] Babiak, W., Krzemińska, I. (2021). Extracellular polymeric substances (EPS) as microalgal bioproducts: A review of factors affecting EPS synthesis and application in flocculation processes. Energies, 14, 4007.
[30] Xiao, R., Zheng, Y. (2016). Overview of microalgal extracellular polymeric substances (EPS) and their applications. Biotechnology Advances, 34, 1225-1244.
[31] Hwang, G., Ahn, I.S., Mhin, B.J., Kim, J.Y. (2012). Adhesion of nano-sized particles to the surface of bacteria: mechanistic study with the extended DLVO theory. Colloids and Surfaces B: Biointerfaces, 97, 138-144.
[32] Taşkan, B., Hasar, H., Lee, C.H. (2020). Effective biofilm control in a membrane biofilm reactor using a quenching bacterium (*Rhodococcus sp*. BH4). Biotechnology and Bioengineering, 117, 1012-1023.
[33] Flemming, H.C., Wingender, J. (2010). The biofilm matrix. Nature Reviews Microbiology, 8, 623-633.
[34] Ji, C., Zhou, H., Deng, S., Chen, K., Dong, X., Xu, X., Cheng, L. (2021). Insight into the adhesion propensities of extracellular polymeric substances (EPS) on the abiotic surface using XDLVO theory. Journal of Environmental Chemical Engineering, 9, 106563.
[35] Devi, N.D., Tiwari, R., Goud, V.V. (2023). Cultivating *Scenedesmus sp*. on substrata coated with cyanobacterial-derived extracellular polymeric substances for enhanced biomass productivity: a novel harvesting approach. Biomass Conversion and Biorefinery, 13, 2971-2983.
[36] Sekar, R., Venugopalan, V., Satpathy, K., Nair, K., Rao, V. (2004). Laboratory studies on adhesion of microalgae to hard substrates. Hydrobiologia, 512, 109-116.
[37] Genin, S.N., Aitchison, J.S., Allen, D.G. (2014). Design of algal film photobioreactors: material surface energy effects on algal film productivity, colonization and lipid content. Bioresource Technology, 155, 136-143.
[38] Zhang, L., Chen, L., Wang, J., Chen, Y., Gao, X., Zhang, Z., Liu, T. (2015). Attached cultivation for improving the biomass productivity of *Spirulina platensis*. Bioresource Technology, 181, 136-142.
[39] Ji, C., Wang, H., Cui, H., Zhang, C., Li, R., Liu, T. (2023). Characterization and evaluation of substratum material selection for microalgal biofilm cultivation. Applied Microbiology and Biotechnology, 107, 2707-2721.
[40] Shen, Y., Zhu, W., Chen, C., Nie, Y., Lin, X. (2016). Biofilm formation in attached microalgal reactors. Bioprocess and Biosystems Engineering, 39, 1281-1288.
[41] Ozkan, A., Berberoglu, H. (2013). Physico-chemical surface properties of microalgae. Colloids and Surfaces B: Biointerfaces, 112, 287-293.
[42] Rosmahadi, N.A., Leong, W.H., Rawindran, H., Ho, Y.C., Mohamad, M., Ghani, N.A., Bashir, M.J., Usman, A., Lam, M.K., Lim, J.W. (2021). Assuaging microalgal harvesting woes via attached growth: A critical review to produce sustainable microalgal feedstock. Sustainability, 13, 11159.
[43] Yuan, H., Zhang, X., Jiang, Z., Wang, X., Chen, X., Cao, L., Zhang, X. (2019). Analyzing the effect of pH on microalgae adhesion by identifying the dominant interaction between cell and surface. Colloids and Surfaces B: Biointerfaces, 177, 479-486.
[44] Ozkan, A., Berberoglu, H. (2011). Adhesion of *Chlorella vulgaris* on hydrophilic and hydrophobic surfaces.Proceedings of the ASME International Mechanical Engineering Congress and Exposition; pp. 169-178.

[45] Tong, C., Chua, M., Tan, W.H., Derek, C. (2023). Microalgal extract as bio-coating to enhance biofilm growth of marine microalgae on microporous membranes. Chemosphere, 315, 137712.
[46] Alexander, M.R., Williams, P. (2017). Water contact angle is not a good predictor of biological responses to materials. Biointerphases, 12, 02C201(201-206).
[47] Yongabi, D., Khorshid, M., Gennaro, A., Jooken, S., Duwé, S., Deschaume, O., Losada-Pérez, P., Dedecker, P., Bartic, C., Wübbenhorst, M. (2020). QCM-D study of time-resolved cell adhesion and detachment: Effect of surface free energy on eukaryotes and prokaryotes. ACS Applied Materials & Interfaces, 12, 18258-18272.
[48] Ozkan, A., Berberoglu, H. (2013). Cell to substratum and cell to cell interactions of microalgae. Colloids and Surfaces B: Biointerfaces, 112, 302-309.
[49] Barros, A.C., Gonçalves, A.L., Simões, M. (2019). Microalgal/cyanobacterial biofilm formation on selected surfaces: the effects of surface physicochemical properties and culture media composition. Journal of Applied Phycology, 31, 375-387.
[50] Von Fraunhofer, J.A. (2012). Adhesion and cohesion. International Journal of Dentistry, 2012, 1-8.
[51] Woitschach, F., Kloss, M., Schlodder, K., Rabes, A., Mörke, C., Oschatz, S., Senz, V., Borck, A., Grabow, N., Reisinger, E.C. (2021). The use of zwitterionic methylmethacrylat coated silicone inhibits bacterial adhesion and biofilm formation of *staphylococcus aureus*. Frontiers in Bioengineering and Biotechnology, 9, 686192.
[52] Zhang, X., Zhang, Q., Yan, T., Jiang, Z., Zhang, X., Zuo, Y.Y. (2015). Quantitatively predicting bacterial adhesion using surface free energy determined with a spectrophotometric method. Environmental Science & Technology, 49, 6164-6171.
[53] Baldan, A. (2012). Adhesion phenomena in bonded joints. International Journal of Adhesion and Adhesives, 38, 95-116.
[54] Petean, P., Aguiar, M. (2015). Determining the adhesion force between particles and rough surfaces. Powder Technology, 274, 67-76.
[55] Li, N., Wang, P., Wang, S., Wang, C., Zhou, H., Kapur, S., Zhang, J., Song, Y. (2022). Electrostatic charges on microalgae surface: mechanism and applications. Journal of Environmental Chemical Engineering, 10, 107516.
[56] Zheng, Y., Huang, Y., Xia, A., Qian, F., Wei, C. (2019). A rapid inoculation method for microalgae biofilm cultivation based on microalgae-microalgae co-flocculation and zeta-potential adjustment. Bioresource Technology, 278, 272-278.
[57] Ma, C., Wang, G., Liu, X., Li, Y., Huang, J., Zhang, P., Chu, X., Wang, L., Zhao, B., Zhang, Z. (2022). A novel gravity sedimentation-Forward osmosis hybrid technology for microalgal dewatering. Chemosphere, 308, 136300.
[58] Wang, C., Lan, C.Q. (2018). Effects of shear stress on microalgae–A review. Biotechnology Advances, 36, 986-1002.
[59] Fanesi, A., Lavayssière, M., Breton, C., Bernard, O., Briandet, R., Lopes, F. (2021). Shear stress affects the architecture and cohesion of *Chlorella vulgaris* biofilms. Scientific Reports, 11, 4002.
[60] Romeu, M.J., Domínguez-Pérez, D., Almeida, D., Morais, J., Araújo, M.J., Osório, H., Campos, A., Vasconcelos, V., Mergulhão, F.J. (2022). Hydrodynamic conditions affect the proteomic profile of marine biofilms formed by filamentous cyanobacterium. npj Biofilms and Microbiomes, 8, 80.

[61] Vanysacker, L., Boerjan, B., Declerck, P., Vankelecom, I.F. (2014). Biofouling ecology as a means to better understand membrane biofouling. Applied Microbiology and Biotechnology, 98, 8047-8072.
[62] Du, X., Wang, Y., Leslie, G., Li, G., Liang, H. (2017). Shear stress in a pressure-driven membrane system and its impact on membrane fouling from a hydrodynamic condition perspective: a review. Journal of Chemical Technology & Biotechnology, 92, 463-478.
[63] Fernández, I., Bravo, J., Mosquera-Corral, A., Pereira, A., Campos, J., Méndez, R., Melo, L. (2014). Influence of the shear stress and salinity on Anammox biofilms formation: modelling results. Bioprocess and Biosystems Engineering, 37, 1955-1961.
[64] Greener, J., Harvey, W.Y., Gagné-Thivierge, C., Fakhari, S., Taghavi, S.M., Barbeau, J., Charette, S.J. (2022). Critical shear stresses of Pseudomonas aeruginosa biofilms from dental unit waterlines studied using microfluidics and additional magnesium ions. Physics of Fluids, 34, 021902.
[65] Chen, X., Zhang, C., Paterson, D.M., Townend, I.H., Jin, C., Zhou, Z., Gong, Z., Feng, Q. (2019). The effect of cyclic variation of shear stress on non-cohesive sediment stabilization by microbial biofilms: the role of 'biofilm precursors'. Earth Surface Processes and Landforms, 44, 1471-1481.
[66] Rochex, A., Godon, J.-J., Bernet, N., Escudié, R. (2008). Role of shear stress on composition, diversity and dynamics of biofilm bacterial communities. Water Research, 42, 4915-4922.
[67] Liu, Y., Tay, J.-H. (2002). The essential role of hydrodynamic shear force in the formation of biofilm and granular sludge. Water Research, 36, 1653-1665.
[68] Tang, Y., Valocchi, A.J., Werth, C.J., Liu, H. (2013). An improved pore-scale biofilm model and comparison with a microfluidic flow cell experiment. Water Resources Research, 49, 8370-8382.
[69] Belohlav, V., Zakova, T., Jirout, T., Kratky, L. (2020). Effect of hydrodynamics on the formation and removal of microalgal biofilm in photobioreactors. Biosystems Engineering, 200, 315-327.
[70] Sun, J., Yu, Z., Yang, L., Chu, H., Jiang, S., Zhang, Y., Zhou, X. (2023). New insight in algal cell adhesion and cake layer evolution in algal-related membrane processes: Size-fractioned particles, initial foulant seeds and EDEM simulation. Environmental Research, 220, 115162.
[71] Alzahrani, S., Mohammad, A.W., Hilal, N., Abdullah, P., Jaafar, O. (2013). Identification of foulants, fouling mechanisms and cleaning efficiency for NF and RO treatment of produced water. Separation and Purification Technology, 118, 324-341.

Chapter 5: Microalgae cell adhesions on hydrophobic membrane substrates using Quartz crystal microbalance with dissipation

Abstract

Microalgal cell adhesion and biofilm formation are affected by interactions between microalgae strains and membrane materials. Variations of surface properties of microalgae and membrane materials are expected to affect cell-membranes and cell-cell interactions and, thus, initial microalgal cell adhesion and biofilm formation rates. Hence, it should be possible to identify the dominant mechanisms controlling microalgal cell adhesion and biofilm formation. The effects of surface properties of three different microalgae strains and three different types of membrane materials on microalgal cell adhesion and biofilm formation were systematically investigated in real-time by monitoring changes in the oscillation frequency and dissipation of the quartz crystal resonator (QCM-D). The results revealed that, in general, a higher surface free energy, more negative zeta potential, and higher surface roughness of membrane materials positively correlated with a larger quantity of microalgae cell deposition, while more hydrophilic microalgae with a larger negative zeta potential preferred to attach to a more hydrophobic membrane material. The adhered microalgal layers exhibited viscoelastic properties. The relative importance of these mechanisms in controlling microalgae cell attachment and biofilm formation might vary, depending on the properties of specific microalgae species and hydrophobic membrane materials used.

Keywords: QCM, Biofilm, Interaction, Microalgae species, Membrane material, Surface properties

5.1. Introduction

Microalgal biofilm cultivation is a promising technology for wastewater treatment [1]. Microalgal biofilm cultivation aims to increase aerated carbon dioxide utilization efficiency and microalgae biomass production yield [2, 3]. A successful initial stage is an essential prerequisite for microalgal biofilm formation [4, 5]. Fast adhesion of microalgal cells on the substrate can reduce the cultivation time and the cost [6, 7]. Conventional cell adhesion measurements are based on cell counting or activity assays [8]. However, researchers pointed out that those approaches usually involve mechanical or fluorescence procedures such as atomic force microscopy (AFM), hydrodynamic assays, and traction force microscopy, which are considered invasive and can result in changes in cell adhesion performance due to the applied force breaking the cell physiology [8].

Furthermore, the abovementioned measurements do not satisfy real-time monitoring under natural environmental conditions [9-11]. Huang et al. argued they have difficulty achieving fast-tracking (monitoring rate range from s^{-1} to min^{-1}) on the underlying interaction because of the intrinsic ex-situ nature [12]. The current detective method for minor changes on surface attachment is limited. Kreis et al. employed a micropipette force spectroscopy measurement to detect the adhesion behaviour of the single *Chlamydomonas* cell on the model substrate, such as silicon and magnesium oxide [13]. Their study offers new insight into the microalgal cell adhesion mechanism on a micro-scale rather than general bioreactor observation. However, although Kreis et al. studied the individual *Chlamydomonas* cell interaction and revealed its universal adhesion mechanism on the abiotic surface, they didn't consider the interaction between the cells or the cells matrix, and the diversity of individual cells as well [13].

On the other hand, most microalgal biofilm studies currently focus on the biofilm thickening stage observed from bioreactor cultivation [14-16]. Although the observation based on

bioreactor cultivation can give a clear view of cell attachment performance after a certain period of time, it is time-consuming, and the interfacial contact between suspended microalgal cells and the substrate is difficult to observe due to the small amount of initial adhesion. Thus, a more rapid, safer, more comprehensive, and ultrasensitive technology is required to scrutinize the microalgae cell attachment in the initial stage of microalgal biofilm formation.

Quartz crystal microbalance with dissipation (QCM-D) is an acoustic sensing measurement that can monitor the cell-substrate real-time adhesive interaction. As an emerging technology, QCM has received much attention in cell biologies, such as disease diagnosis and bacterial cell adhesion, due to its non-invasive and unlabeled capacity in recent years [8, 17]. The QCM-D technique can obtain more specific details of initial microalgal cell adhesion because it considers the viscoelastic behaviour of the microorganism biofilm [18]. Schofield et al. suggested that QCM-D is a convenient real-time method to analyze the viscoelastic properties of biofilm when monitoring the *S. mutans* biofilm attachment behaviours [19]. Furthermore, the interaction mechanism between inorganic/organic adhesives and attached substrates could also be determined by QCM research. Walkowiak et al. utilized the QCM-D technique to analyze the proteins' adhesion mechanisms on the synthesis polyelectrolyte brush surface [20]. Peng's group investigated the influence of Rhamnolipid in the *Thiobacillus denitrificans* biofilm formation on sulphur-based biofilter surface by the QCM-D technique [4]. Yongabi et al. studied the influences of ionic strength on the adhesion mechanism of *S. cerevisiae* in long-term interaction [9]. The bacterial biofilm formation mechanisms have been well studied in the last decade. Researchers suggested that the QCM-D method is a suitable technique because it can supply the adhesion data on micro dimensions [10], which is also suitable for the microalgae biofilm formation study. Still, fewer studies have been reported in this area. Moreover, another advantage of QCM-D for

microalgae biofilm formation study is that it can simulate the adhesion measurement in aquatic conditions similar to that in a bioreactor environment. Nevertheless, limited study focuses on microalgal biofilm formation through QCM measurement. Thus, comprehensive knowledge of microalgal biofilm formation is urgently needed.

This study investigated the initial cell attachment behaviours between different microalgae strains and hydrophobic membrane materials employing a quartz crystal microbalance with dissipation monitoring (QCM-D) as a rapid, non-invasive and effective method. The physicochemical and surface properties, such as surface roughness, zeta potential, contact angle, interactions of microalgae strains and attached hydrophobic membrane material substrates were taken into account to explain the interfacial cell adhesion mechanism in micro-scale, which would provide new enlightenment for enhancing the microalgal biofilm formation in novel microalgal biofilm bioreactor development, including the emerging membrane carbonated microalgal biofilm photobioreactor (MCMBPBR) technology development and application.

5.2. Material and methodologies

5.2.1. Microalgae cultivation and microalgal suspension preparation

The microalgae stains (*Phormidium tenue* (CPCC 424), *Monoraphidium braunii* (CPCC 625), and *Ankistrodesmus falcatus* (CPCC 669)) were obtained from Canadian Phycological Culture Centre at the University of Waterloo, ON, Canada and pre-cultivated with BG-11 medium [21, 22] in 1.5 L plastic bottle reactors, respectively. Aeration and illumination were continuously provided to ensure microalgae growth during pre-cultivation. The composition of the BG-11 and the cultivation conditions were all followed by a previous study [22]. Before QCM measurement, the cultivated microalgae suspension was centrifugated for 15 min at 5000 xg prior to washing

with Mili-Q water. The washing procedure was undergone three times, then the supernatant was drained, and the centrifuged biomass was stored in BG-11 culture medium at a 0.2 g/L suspension for QCM-D experiments.

5.2.2. Analytical methods

5.2.2.1. QCM

The microalgal initial adhesion on the different hydrophobic membrane materials was investigated using a Quartz crystal microbalance with dissipation (QCM-D 401, E1, Qsense Inc. Gothenborg, Sweden). The QCM sensors coated with selected hydrophobic membrane materials (polytetrafluoroethylene (PTFE, QSX 331), polydimethylsiloxane (PDMS, QSX 900) and polyurethane (PUR, QSX 999)) were purchased from Biolin Scientific. In this series of experiments, the new sensors coated with these membrane materials were rinsed with fresh Mili-Q water and then dried with nitrogen gas before measurement. The flow rate of the involved solutions was maintained at 0.15 mL/min, and the entire experiment was operated at 22 ℃. The adhesion experiments of microalgal cells on PTFE, PDMS and PUR surfaces were conducted in a BG-11 medium. QCM-D measurement data was collected by a Q-Tools software (Q-sense, Gothenburg, Sweden) to obtain the frequency shift (Δf) and energy dissipation shift (ΔD) curves. The third overtone was used to determine the adhered mass. The QCM-D cell adhesion experiment was repeated three times under each tested condition (each species + each membrane material)

5.2.2.2. Other routine analysis

An optical tensiometer instrument performed the contact angle measurement of the microalgae cell layers and QCM sensors (Theta Lite, Biolin Scientific, USA). Before testing, the

microalgae lawn was prepared as described in previous studies [23]. NanoBrook Zeta PALS (Brookhaven Instruments Corp, USA) was employed for analyzing the zeta potential profile of microalgae. Before the zeta potential test, the microalgae strain was washed thrice with Mili-Q water. The zeta potential of the hydrophobic membrane materials is from the literature [24-29] due to the challenges of directly measuring the zeta potential of these QCM sensors. Three-dimensional (3D) topography images and the surface roughness of QCM sensors were measured by employing an MFP-3D origin+ atomic force microscope (AFM) (Oxford Instruments, UK).

5.2.3. Surface free energy (SFE)

The SFE was calculated based on Young's equation in the previous study [30]. So as to discuss the interactions between microalgae and the QCM sensor, the interaction energies were also calculated. As Hoek et al. mentioned, the total interaction energy (ΔG^{Tol}, mJ/m^2) between the microalgae and attached substrate in the aqueous system could consist of Lifshitz-van der Waals (LW) (ΔG^{LW}, mJ/m^2), electrostatic repulsive double layer (EL) (ΔG^{EL}, mJ/m^2) and Lewis acid-base (AB) interactions (ΔG^{AB}, mJ/m^2) [31]. According to extended Derjaguin, Landau, Verwey and Overbeek (XDLVO) theory, those interactions can be displayed as interaction energy per unit area between two infinite planar surfaces based on the following equations [31].

$$\Delta G^{Tol} = \Delta G^{LW} + \Delta G^{AB} + \Delta G^{EL} \quad (5.1)$$

$$\Delta G_{l_0}^{LW} = -2\left(\sqrt{\gamma_S^{LW}} - \sqrt{\gamma_W^{LW}}\right)\left(\sqrt{\gamma_M^{LW}} - \sqrt{\gamma_W^{LW}}\right) \quad (5.2)$$

$$\Delta G_{l_0}^{EL} = \frac{\varepsilon\varepsilon_0\kappa}{2}\left(\zeta_M^2 + \zeta_S^2\right)\left[1 - \coth(\kappa l_0) + \frac{2\zeta_M\zeta_S}{\zeta_M^2+\zeta_S^2}\operatorname{csch}(\kappa l_0)\right] \quad (5.3)$$

$$\Delta G_{l_0}^{AB} = 2\left[\sqrt{\gamma_W^+}\left(\sqrt{\gamma_M^-} + \sqrt{\gamma_S^-} - \sqrt{\gamma_W^-}\right) + \sqrt{\gamma_W^-}\left(\sqrt{\gamma_M^+} + \sqrt{\gamma_S^+} - \sqrt{\gamma_W^+}\right) - \sqrt{\gamma_M^+\gamma_S^-} - \sqrt{\gamma_M^-\gamma_S^+}\right] \quad (5.4)$$

The subscripts M, S and W of the surface tension γ represent microalgae, substrate, and water, respectively; γ^{LW}, γ^{+} and γ^{-} are the LW, electron-acceptor and electron-donor components of surface tension, respectively; l is the distance between the microalgae and substrate surfaces (l_0 is the minimum distance between these two surfaces); ε (78.5) and ε_0 (8.854×10^{-2} CV^{-1}/m) are the dielectric constant of water and the vacuum, respectively [32]; ζ_M and ζ_S are the surface zeta potentials of microalgae and substrate, respectively; $\Delta G_{l_0}^{LW}$, $\Delta G_{l_0}^{EL}$ and $\Delta G_{l_0}^{AB}$ are interaction components mentioned in the former section at the distance l_0 [33];κ is the inverse Debye length [34].

5.2.4. Statistical analyses

The experiment data were examined using a one-way ANOVA test conducted from the Origin software for significant difference analysis ($p<0.05$) of the results obtained under different testing.

5.3. Result and discussion

5.3.1. Morphology and surface properties of microalgae and QCM sensors

Figure 5.1 exhibits the morphology and sizes of microalgae cells obtained from the optical compound microscope. *Phormidium tenue* is unicellular with an oval or spherical shape, while *Monoraphidium braunii* and *Ankistrodesmus falcatus* were straight cells. The difference between *Monoraphidium braunii* and *Ankistrodesmus falcatus* is that the end of the former cells are rounded, and the latter cells are needled. In addition, Figure 5.1 also shows that *Ankistrodesmus falcatus* cells have smaller sizes than *Monoraphidium braunii* cells. Table 5.1 shows the surface properties of the sensors and microalgae species. As Table 5.1 shows, the hydrophobicity of the sensors

follows the order from hydrophobic to less hydrophobic by QSX 900 (PDMS) > QSX 999 (PUR) > QSX 331 (PTFE). Besides contact angle, the hydrophilicity and hydrophobicity are also verified by the free energy of cohesion (ΔG_{coh}) [35]. The negative ΔG_{coh} indicates the membrane materials (PTFE, PDMS, and PUR) were hydrophobic, and positive ΔG_{coh} of microalgae certified their hydrophilic surface (Table 5.1). The SFE of the sensors ranges from 21.66 mJ/m^2 to 43.23 mJ/m^2 (QSX 331 (PTFE)> QSX 999 (PUR)> QSX 900(PDMS)), which is in the opposite trend with the contact angle. That means a more hydrophobic surface is associated with a smaller SFE. The zeta potential of the microalgae species in 1 mM KCl ranges from -43.87 mV to -27.92 mV. These zeta potentials followed the order from more negative charge to less negative charge: *Phormidium tenue* > *Monoraphidium braunii* > *Ankistrodesmus falcatus*. The zeta potential of membrane materials is also shown in Table 5.1, obtained from the literature [24-29]. The zeta potential of QCM sensors could not be measured directly due to the concern of preventing sensor damage from the measurement. Based on the result from the literature, the zeta potential of the hydrophobic membrane materials was all negative and ranged from -58 mV to -13.4 mV [24-29]. The zeta potential of the hydrophobic membrane materials follows the order from more negative charge to less negative charge: PTFE > PDMS > PUR.

Table 5.2 shows the surface roughness parameters of the QCM sensors' surfaces, R_a is the arithmetic roughness average of the coupons' surface, and Rq is the root mean square along the sampling length. The sensors' surface roughness followed the order from high to low: the QSX 900 (PDMS) > QSX 999 (PUR) > QSX 331 (PTFE). The roughest sensor was QSX 900 (PDMS) (R_a=36.85 nm), and the smoothest one was QSX 331 (PTFE) (R_a=3.53 nm) in this study, respectively. The 3D surface topography images (Figure 5.2) also reflect the same tendency of the hydrophobic membrane materials' surface roughness.

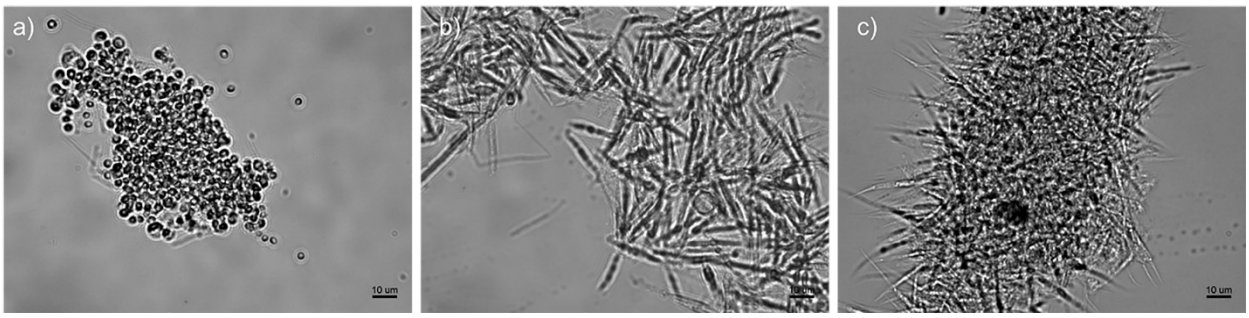

Figure 5.1. Optical microscope images of a) *Phormidium tenue*, b) *Monoraphidium braunii*, and c) *Ankistrodesmus falcatus*.

Table 5.1. Surface properties of QCM sensors and microalgae.

Materials	Contact angle (◦)			Surface energy γ (mJ·m^{-2})	ΔG_{coh} (mJ·m^{-2})	Zeta potential (mV)[a]
	Water	Formamide	Diiodomethane			
QSX 331 (PTFE)	74.1 ± 3.1	49.0 ± 2.5	41.6 ± 2.7	43.23	-46.58	-46 ~ -58[24, 25]
QSX 900 (PDMS)	92.9 ± 4.6	80.8 ± 2.8	75.4 ± 1.2	21.66	-50.68	-31 ~ -39[26, 27]
QSX 999 (PUR)	85.1 ± 5.9	62.7 ± 4.4	45.7 ± 3.9	37.69	-62.94	-13.4 ~ -20[28, 29]
Phormidium tenue [b]	31.8 ± 1.9	32.7 ± 3.0	48.7 ± 3.8	48.69	26.36	-43.87 ± 1.17
Monoraphidium braunii [b]	35.4 ± 2.8	47.7 ± 4.1	50.1 ± 1.0	36.00	46.68	-38.32 ± 7.91
Ankistrodesmus falcatus [b]	36.7 ± 0.1	51.4 ± 2.1	53.9 ± 4.9	32.66	51.41	-27.92 ± 2.64

a: Zeta potential of membrane materials obtained from literature with the concern to prevent the damage of QCM sensors from zeta potential measurement

b: Microalgae have been washed before zeta measurements.

Table 5.2. Surface roughness of the QCM sensors.

Material	R_a (nm)	R_q (nm)
Polytetrafluoroethylene (PTFE, QSX 331)	3.53 ± 0.02	10.08 ± 5.06
Polydimethylsiloxane (PDMS, QSX 900)	36.85 ± 14.57	65.71±23.25
Polyurethane (PUR, QSX 999)	3.72 ± 0.45	9.60 ± 4.67

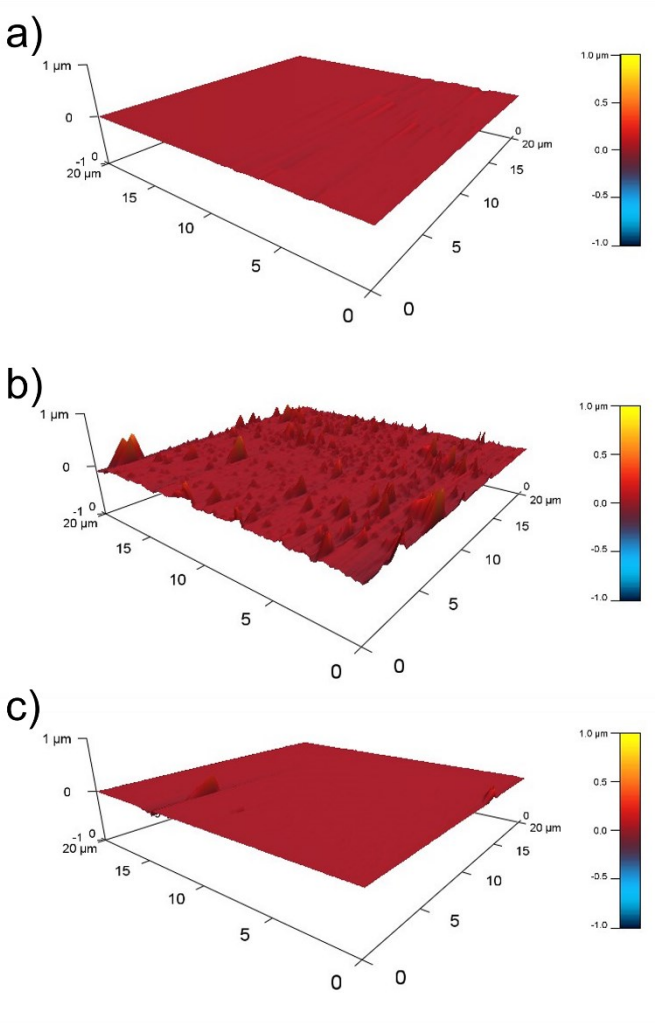

Figure 5.2. 3D surface topography images of a) PTFE, b) PDMS, and c) PUR QCM sensors.

5.3.2. Initial adhesion of microalgae cells

Figure 5.3 shows the frequency shift during the attachment of different microalgae species to the polytetrafluoroethylene (PTFE, QSX 331), polydimethylsiloxane (PDMS, QSX 900) and polyurethane (PU, QSX 999) QCM sensors. The deposition of suspended microalgal cells on the hydrophobic membrane materials substrate surface in an initial contact stage is the foundation for forming biofilms [12, 36]. A higher initial adhesion can contribute to facilitating biofilm thickening. As illustrated in Figure 5.3a, the adhesion of *Phormidium tenue* on the PTFE surface reached equilibrium at around 17.79 ± 1.31 Hz, corresponding to the highest deposition. The

secondary highest deposition was achieved on *Monoraphidium braunii* adhesion of 9.99 ± 1.13 Hz. The *Ankistrodesmus falcatus* exhibited the lowest deposition rate on the PTFE sensor, with the lowest deposition of 2.04 ± 0.28 Hz. In Figure 5.3b, when the microalgae attached to the PDMS surface, the *Phormidium tenue* achieved the highest deposition and reached equilibrium at 19.09± 0.47 Hz. *Ankistrodesmus falcatus* became the second-highest deposition of 10.16 ± 1.52 Hz but with a lower adhesion rate than *Monoraphidium braunii* (8.88 ± 0.10 Hz). Moreover, as Figure 5.3c shows, the deposition on the PUR surface follows the trends of *Phormidium tenue* (17.29 ± 1.75 Hz) > *Monoraphidium braunii* (5.80 ± 0.57 Hz) > *Ankistrodesmus falcatus* (2.02 ± 0.24 Hz).

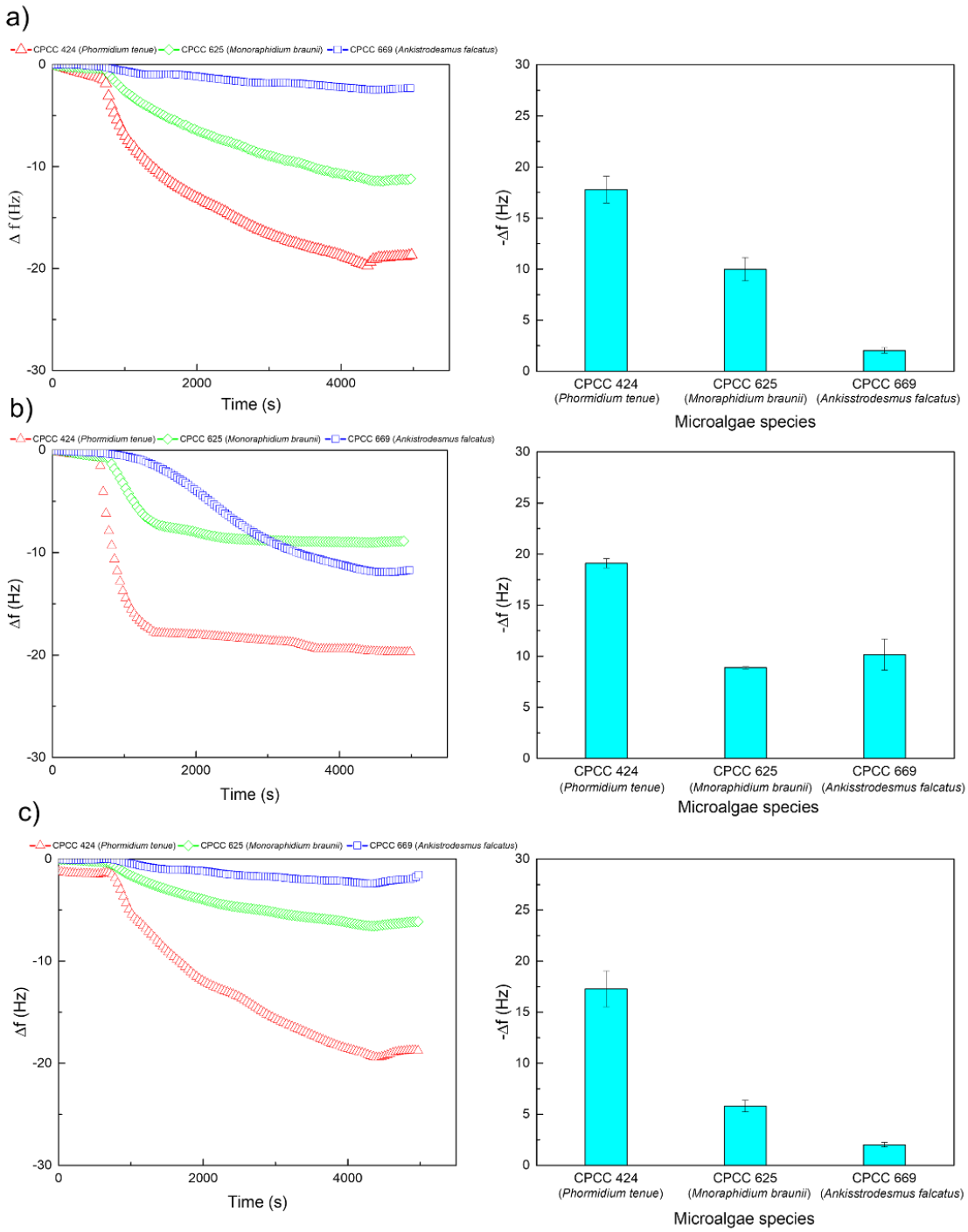

Figure 5.3. Deposition frequency shifts and variations of different microalgae species on a) PTFE, b) PDMS, and c) PUR QCM sensors at 22 ℃.

For the same senor with different microalgae species, the PTFE and PU-coated sensors showed the same order of initial cell deposition from high to low: *Phormidium tenue* >

Monoraphidium braunii > *Ankistrodesmus falcatus* (ANOVA, $p < 0.05$), while the PDMS coated sensor showed a slightly different order from high to low: *Phormidium tenue* > *Ankistrodesmus falcatus* > *Monoraphidium braunii* (ANOVA, $p < 0.05$). However, the difference was small between *Ankistrodesmus falcatus* (10.16 ± 1.52 Hz) and *Monoraphidium braunii* (8.88 ± 0.10 Hz) for the PDMS sensor. Furthermore, for the same microalgae with different sensors, both *Phormidium tenue* and *Ankistrodesmus falcatus* showed similar order of the initial microalgae cell deposition from high to low: PDMS > PTFE > PU (ANOVA, $p < 0.05$), while *Monoraphidium braunii* had a slightly different order of the initial microalgae cell deposition from high to low: PTFE > PDMS > PU (ANOVA, $p < 0.05$).

5.3.3. Effect of surface properties on adhesion of microalgae cells

5.3.3.1. Effect of hydrophobicity and zeta potential of microalgae species on adhesion of microalgae cells

Table 5.1 shows that the microalgae employed in this study were all hydrophilic. Ozkan and Berberoglu claimed that the total interaction energy is governed by the attractive AB interaction between hydrophilic green algae and the substrate [37]. As a result, higher hydrophobicity of hydrophilic green algae could enhance the cell-substrate adhesion because of higher AB attraction (hydrophobic attraction). They found that microalgae with higher hydrophobicity attached more to the hydrophobic substrate [35]. However, the microalgae adhesion in this study didn't follow the hydrophobicity mechanism because the highest attachment was achieved on the most hydrophilic *Phormidium tenue*. Similarly, Ji et al. found that more hydrophilic *S.dimorphus* exhibited higher attachment to hydrophobic polypropylene membrane than *T.minus* [38].

Moreover, the only phenomenon that may relate to the hydrophobic attraction is that higher adhesion of the *Ankistrodesmus falcatus* with more hydrophobicity than more hydrophilic *Monoraphidium braunii* on the PDMS surface was observed. Nevertheless, this phenomenon may also be caused by the fact that the PDMS sensor has a rougher surface compared to the rest of the sensors, which will promote more adhesion on smaller *Ankistrodesmus falcatus* cells (width: 2.5-4.5 μm) compared to *Monoraphidium braunii* (width: 2-8 μm) [39, 40]. The above observations illustrate that hydrophilicity/hydrophobicity might not be the only pivotal factor in controlling microalgae attachment.

Besides hydrophobicity, the zeta potential of microalgae also plays a critical role during the adhesion on the solid substrate. As Table 5.1 displayed, all the microalgae and hydrophobic membrane materials in this study exhibited negative zeta potential under tested conditions. Hoshiba et al. mentioned that microalgae cells had trouble attaching to negatively charged substrates because they usually contain the same charges, leading to electrostatic repulsion [41]. On the contrary, all the microalgae (*Phormidium tenue*, *Monoraphidium braunii*, and *Ankistrodesmus falcatus*) adhered to those three negatively charged materials (PTFE, PDMS and PUR). One possible mechanism might be attributed to ionic bridging. Positive particles (such as Ca^{2+} and Zn^{2+} ions) can bind partly or entirely to microalgal cells and membrane materials through ionic bridging [42]. When the microalgal biofilm formation occurs with the existence of those particles, negative microalgal cells can be bridged with other negative particles or even substrates with negative charges. For macromolecules and colloidal particles, as Hanaor et al. illustrated, a high zeta potential resists particle aggregation, while a low zeta potential leads to flocculation due to the attractive forces surpassing the electrostatic repulsion [43]. As a result, microalgae seem easier to attach to the substrate with a low zeta potential when the substrate and microalgae bring

the same polar charges. In this study, the *Phormidium tenue* with the highest absolute value of zeta potential (-43.87 mV) showed the highest adhesion over three materials (PTFE, PDMS, and PUR), which the electrostatic interaction mechanism cannot explain. Thus, in this case, the adhesion was not dominated by direct electrostatic repulsive interactions between the microalgal cells and hydrophobic membrane substrates. Other mechanisms, such as ionic bridging, might play an important role for cell adhesion to the QCM sensors and typically more negative charges of both the microalgae species and QCM sensors provided more ionic bridging sites and thus enhanced the microalgal cell adhesion and biofilm formation.

5.3.3.2. Effect of hydrophobicity and surface roughness of membrane materials on adhesion of microalgae cells.

Figure 5.3 and Table 5.1 show that a more hydrophilic microalgae species (*Phormidium tenue*) had enhanced cell adhesion and biofilm formation on more hydrophobic membrane materials (PDMS). This is consistent with the observations from the literature [37, 43]. In general, hydrophilic microalgae prefers to adhere to hydrophobic substrate surfaces due to the water exclusion mechanism, which promotes the adhesion of microalgal cells [38, 44]. Many studies show that microalgae cells behave better in attachment on hydrophobic surfaces than on hydrophilic surfaces [45-47]. Ozkan and Berberoglu also suggested that biofouling can be mitigated by using hydrophilic coating over surfaces due to its weak adhesion performance [37]. Moreover, Cheah and Chan claimed that higher microalgae adhesion on hydrophobic surfaces could be attributed to some EPS components (proteins) with higher affinity to the hydrophobic surface than hydrophilic ones [48]. However, some literature argued that hydrophilic microalgae grow better on the hydrophilic substrate because hydrophobic hinders the diffusion of water and nutrients [49, 50]. The microalgae attachment on the hydrophobic membrane materials almost

follows the trends of PDMS > PTFE > PUR (except *Monoraphidium braunii*). In the case of *Phormidium tenue* and *Ankistrodesmus falcatus*, the microalgae prefer adhering to hydrophobic PDMS surface due to the water exclusion mechanism mentioned above. However, the attachment on PUR had less amount than the more hydrophilic PTFE revealing that the hydrophobicity did not affect the adhesion performance of these two materials. As presented in Table 5.1, the material's zeta potential follows the order from more negative charge to less negative charge: PTFE > PDMS > PUR. There is a common consensus that the negative substrate with a less absolute value of zeta potential provides higher adhesion strength to microalgae due to the weaker electrostatic repulsion [51]. However, the fact in this study is that higher attachments were usually achieved on the hydrophobic membrane substrate with a higher negative zeta potential. The PUR with the lowest zeta potential achieved the lowest attachment over all three microalgae species. Ignoring material charge density, it can only be confirmed from the literature that these three membrane materials are all negatively charged. As mentioned above, the occurrence of cell attachment and biofilm formation could be attributed to the ionic bridging with the existence of ionic particles, such as cations Ca^{2+}, Zn^{2+}, and Mg^{2+}. However, we cannot accurately analyze the influence of the zeta potential magnitude of the material in this research because some values we listed in Table 5.1 were obtained from the literature. In addition, some studies also claimed that the microalgae adhesion was enhanced by augmenting the absolute value of the negative zeta potential of the substrate [52, 53].

Literature reveals that surface roughness also positively affects the adhesion behaviour of the algal cell [46, 54, 55]. In the QCM test, the largest deposition was achieved on the PDMS sensors with the roughest surface. This phenomenon could be explained by the more stagnation areas caused by the rougher surface, which leads to a higher accumulation of microalgae cells than

the smoother ones [16, 54]. The surface roughness effect is more significant on the smaller microalgae cells because it can retain more microalgae [56]. Based on deposition profiles of microalgae, microalgae exhibited higher depositions on the PDMS surface, compared to the other two sensors, with higher roughness. The same tendencies were found in Zhang et al. research [14]. They pointed out that *Chlorella vulgaris* exhibited a higher adhesion strength on rougher pine sawdust carriers than on smoother rice husk carriers [14]. The exception is that *Monoraphidium braunii* didn't show better adhesion on rougher PDMS than PTFE, which might be attributed to other effects such as SFE. However, regarding PTFE and PUR sensors, the deposition of microalgae on these two sensors was not significantly affected by surface roughness. Although the PUR sensor (3.72 nm) had higher roughness than the PTFE sensor (3.53 nm), slightly lower depositions were observed on PUR sensors. Due to their close surface roughness, other factors (such as SFE) could play a more significant role in microalgae-substrate interaction between these two sensors. The roughness results in this study suggested that surface roughness has a positive effect on microalgae cells' initial adhesion, and it should be considered in future work.

5.3.3.3. Effect of interaction energy effect between microalgae and QCM sensors

As shown in Table 5.1, the adhesion of microalgal cells on the PTFE surface increased with the reduced difference of SFE between microalgae and the sensor. For the other two sensors, the deposition did not follow the same rule of PTFE. When it comes to the PDMS, the adhesion of microalgal cells increased with the decrease of the SFE. In constant, the deposition on the PUR surface increased with an augment of the SFE of microalgae. The different deposition results reveal that the attachments of microalgae on PDMS and PUR surfaces are attributed to different dominant factors, respectively. For PUR, the primary mechanism of cell-substrate adhesion could be focused on the SFE composition. Table 5.3 exhibited the interfacial Gibbs free energies determined from

the surface tension data. The EL free energy is considered negligible due to its lower magnitude than that of LW and AB free energy, which resulted in an extreme contribution to total Gibbs free energy [32, 57]. Thus, the ΔG^{Tol} was considered only equal to the sum of $\Delta G_{l_0}^{LW}$ and $\Delta G_{l_0}^{AB}$. As Li et al. mentioned, a negative value of ΔG^{Tol} is considered an attractive interaction, and a vice versa positive value represents a repulsive interaction [58]. Moreover, the higher absolute value of ΔG^{Tol}, the stronger either attractive or repulsive interaction will happen [6]. Table 5.3 shows that both PTFE and PDMS followed Gibbs free energy trends. However, the deposition on the PUR surface had not shown a higher value than that of PTFE, even though three microalgae all exhibited higher ΔG^{Tol} with PUR sensors. One explanation for this phenomenon is that the LW interaction became the dominant interaction because the higher deposition in these two sensors contained a higher absolute value of $\Delta G_{l_0}^{LW}$. However, when it comes to the more hydrophobic PDMS, the value of $\Delta G_{l_0}^{LW}$were positive, which represents the repulsive interaction of Lifshitz-van der Waals interactions. So, the negative $\Delta G_{l_0}^{AB}$ becoming dominant, led to a negative value of total Gibbs free energy.

In order to have a more comprehensive concept of interaction between microalgae and membrane material, predictions based on the XDLVO theory of EL, LW, AB and total interaction profiles have been made (Figure 5.4). Although these predictions were not entirely the same as the real experiment because some of the values were obtained from the literature (zeta potential of materials), they can still offer a compatible idea for the interaction study. As shown in Figure 5.4, the EL interaction energy value was constantly positive, indicating that EL interaction supplied a repulsive force to prevent the microalgal cells from attaching to the membrane materials' surface. On the contrary, the AB interaction energy in the prediction was always negative, validating that acid-base interaction was an attractive force that drove microalgae cells to adhere to the material

surface. In addition, EL interaction was negligible compared with the larger amount of the sum of LW and AB interaction energies when the microalgal cells completely adhered to the membrane material surfaces. Thus, the rationality of the neglection of EL interaction when calculating the interaction energy can also be verified.

Moreover, the total interaction energy G^{Tol} in PTFE and PUR material were all negative, which indicated the interaction between microalgae and material in these cases was dominant by attraction force. As interaction curves show (Figures 5.4a, 5.4c, 5.4d, 5.4f, 5.4g and 5.4i), the LW interaction in PTFE and PUR cases played a more important role in the microalgae adhesion because it exhibited a pretty larger value compared to AB and EL interaction energies. This finding also confirms the previous observation of Gibbs free energy in PTFE and PUR materials. For the PDMS material, the interaction force changed, followed by the changes in contact distance between microalgae and PDMS material. The total interaction force was close to zero when there was a large distance between the microalgae particle and PDMS. The EL interaction force was not increased until the distance between microalgae and PDMS was below 6 nm. However, LW interactions exhibited repulsive force (positive) and increased when the distance was below 16 nm. As Figure 5.4 displays, the G^{Tol} values were positive from 6 nm to 16 nm, representing a repulsion at that range. The dominant repulsion can be attributed to the combination of positive LW and EL interaction energies, which suppressed the negative AB interaction energy. From a distance of 6 nm to the PDMS surface, a dramatically increasing AB interaction force curve could be observed. The rate of augment of AB interaction was much higher than that of LW and EL interactions. Therefore, the total interaction became attraction (negative value) when the distance between microalgal cells and membrane material was smaller than 6 nm.

Furthermore, the G^{Tol} curves of three microalgae peaked at approximately 10 nm (*Phormidium tenue*: 27.46 KT, *Monoraphidium braunii*: 115.58 KT, and *Ankistrodesmus falcatus*: 55.79 KT, respectively). The highest positive total interaction energy between *Monoraphidium braunii* and PDMS indicated that *Monoraphidium braunii* cell suffered greater repulsive force when it moved close to the PDMS surface. This is probably why the *Monoraphidium braunii* achieved the least attachment on PDMS.

Table 5.3. Interfacial Gibbs free energies at a minimum microalgae-substrate distance between QCM sensor and microalgae.

Sample	QSX 331(PTFE)			QSX 900 (PDMS)			QSX 999 (PUR)		
	$\Delta G_{l_0}^{LW}$	$\Delta G_{l_0}^{AB}$	$\Delta G_{l_0}^{Tol}$	$\Delta G_{l_0}^{LW}$	$\Delta G_{l_0}^{AB}$	$\Delta G_{l_0}^{Tol}$	$\Delta G_{l_0}^{LW}$	$\Delta G_{l_0}^{AB}$	$\Delta G_{l_0}^{Tol}$
Phormidium tenue	-3.90	-5.00	-8.89	0.52	-4.92	-4.41	-3.45	-7.66	-11.11
Monoraphidium braunii	-3.69	-3.69	-7.38	0.49	-3.33	-2.84	-3.27	-6.59	-9.86
Ankistrodesmus falcatus	-3.11	-2.73	-5.84	0.41	-2.24	-1.83	-2.75	-5.53	-8.28

[*]**The contribution of ΔG^{EL} on ΔG^{Tol} is neglected, due to its small values, compared to the other two terms [32].**

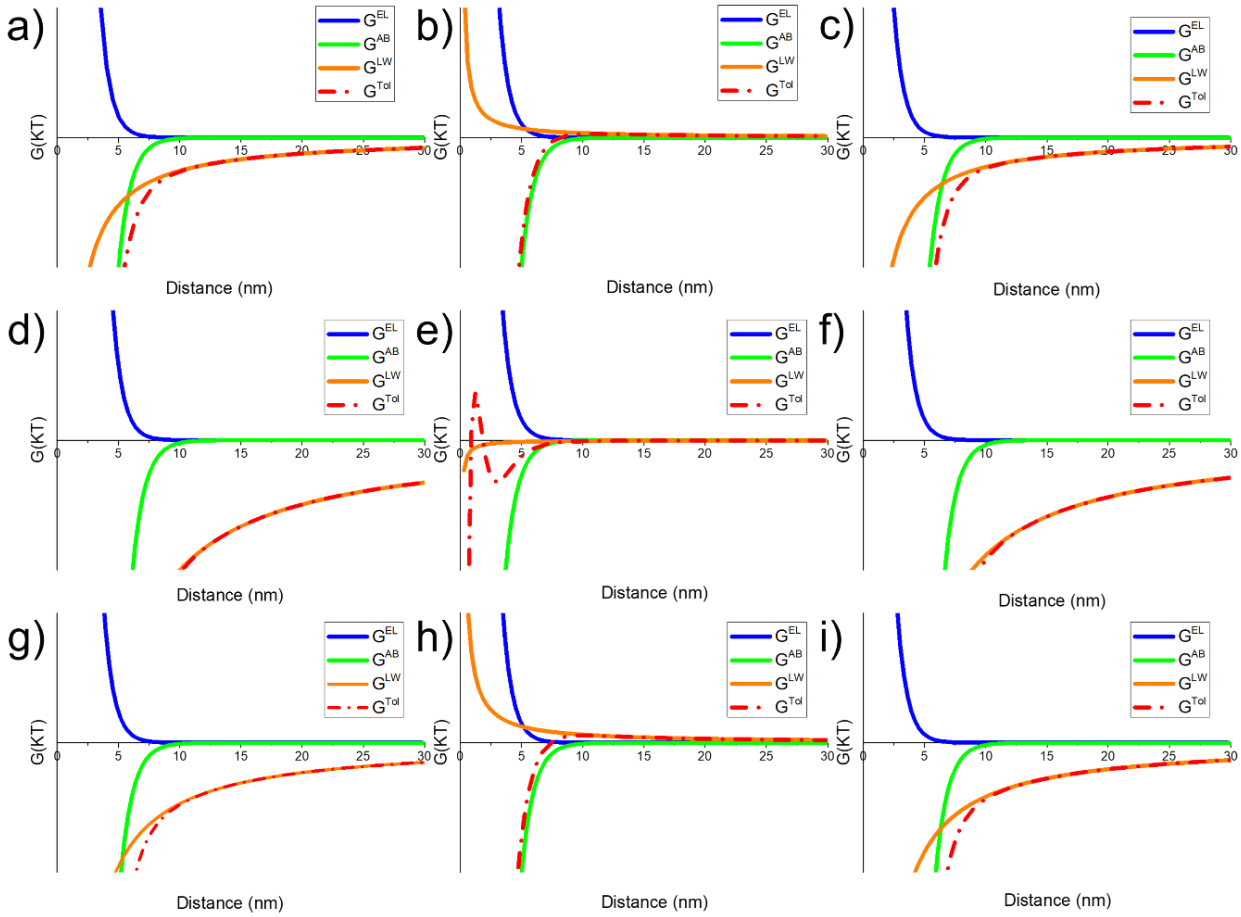

Figure 5.4. The interaction energy of *Phormidium tenue* with a) PTFE, b) PDMS, and c) PUR, *Monoraphidium braunii* with d) PTFE, e) PDMS, and f) PUR, *Ankistrodesmus falcatus* with g) PTFE, h) PDMS, and i) PUR, as predicted by the XDLVO theory.

5.3.4. Microalgae biofilm viscoelasticity

This study also investigated and discussed the dissipation deviation (ΔD) and frequency deviation (Δf) of adhesion processes and their relationship. The -ΔD/Δf value can indicate the viscoelasticity and rigidity of the microalgal layer adhered to the QCM sensors. In this study, we used 0.1×10^{-6} Hz^{-1} as the evaluation criterion to justify the rigidity of the microalgal layer, which is suggested by the literature [4]. The deposited microalgal layer was considered as a rigid layer when -ΔD/Δf below 0.1×10^{-6} Hz^{-1}, and vice versa was assumed as a viscoelastic layer. In this study, the -ΔD/Δf values of all the microalgal layers attached to the QCM sensors were above 0.1

$\times 10^{-6}$ Hz^{-1}, representing that deposited microalgal layers were considered viscoelastic layers (Figure 5.5). For a more in-depth analysis of the viscoelastic characteristics of the attached microalgal layers, the ratios of $\Delta f/\Delta D$ were also calculated and shown in Figure 5.6 to reflect the viscoelasticity of the layers.

Generally, a positive value of $\Delta f/\Delta D$ represents a higher elasticity of the microalgal layer, while a negative value means a more viscous layer [59, 60]. As Figure 5.6 shows, *Phormidium tenue* and *Monoraphidium braunii* exhibited dynamic adhesion in the sense of their viscoelasticity during the adhesion period. The viscoelastic properties of the microalgae-membrane bond of *Phormidium tenue* and *Ankistrodesmus falcatus* became more viscous with the overtone number increased due to its lower $\Delta f/\Delta D$ value. On the contrary, the $\Delta f/\Delta D$ value of *Ankistrodesmus falcatus* mostly remained relatively steady throughout the deposition experiments (except on PDMS sensors), which means a steadily viscous layer. As a result, the *Phormidium tenue* and *Monoraphidium braunii* might exhibit different attachment performances compared to those of *Ankistrodesmus falcatus* under different hydrodynamic conditions due to the dynamic viscoelasticity influence. Thus, the hydrodynamic conditions influence of viscosity of the microalgae should be considered in future work.

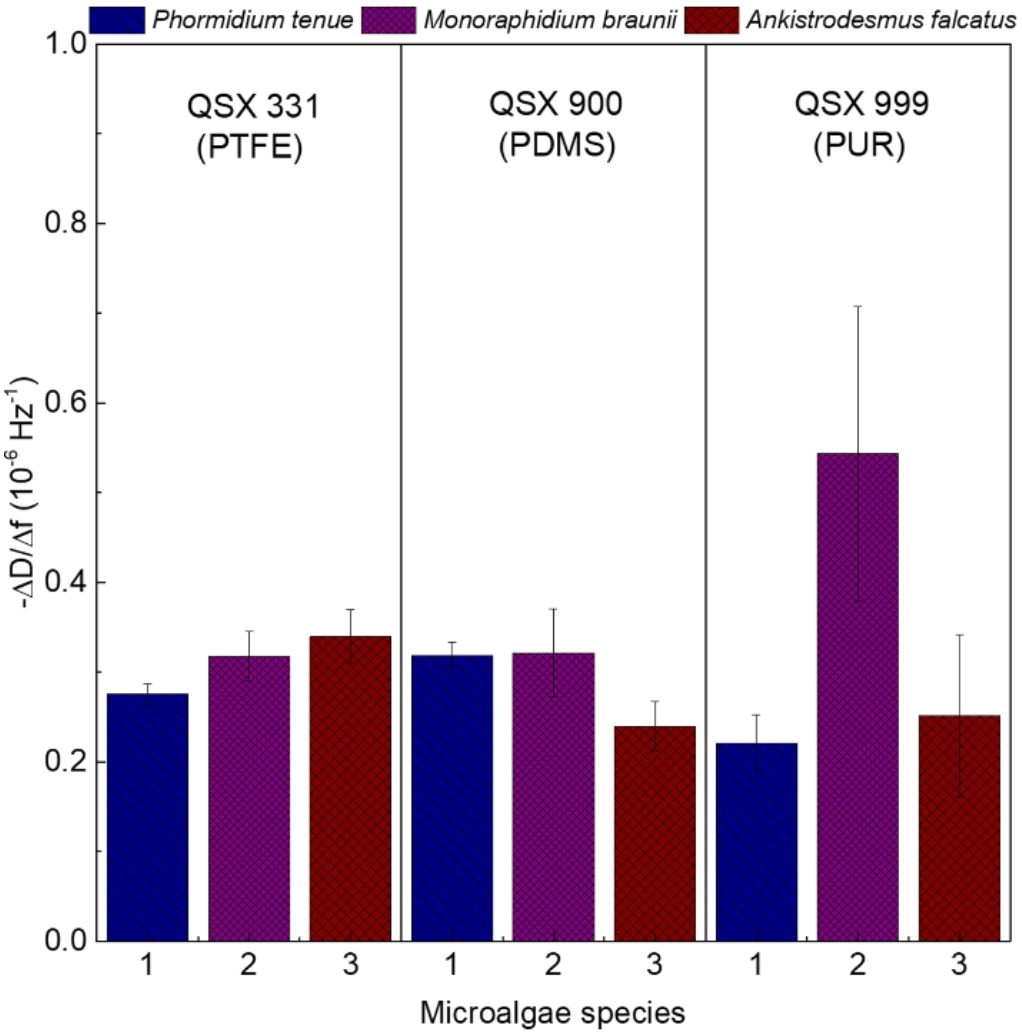

Figure 5.5. -ΔD/Δf ratios of the adlayers on the different QCM sensors under 20 °C (3rd overtone).

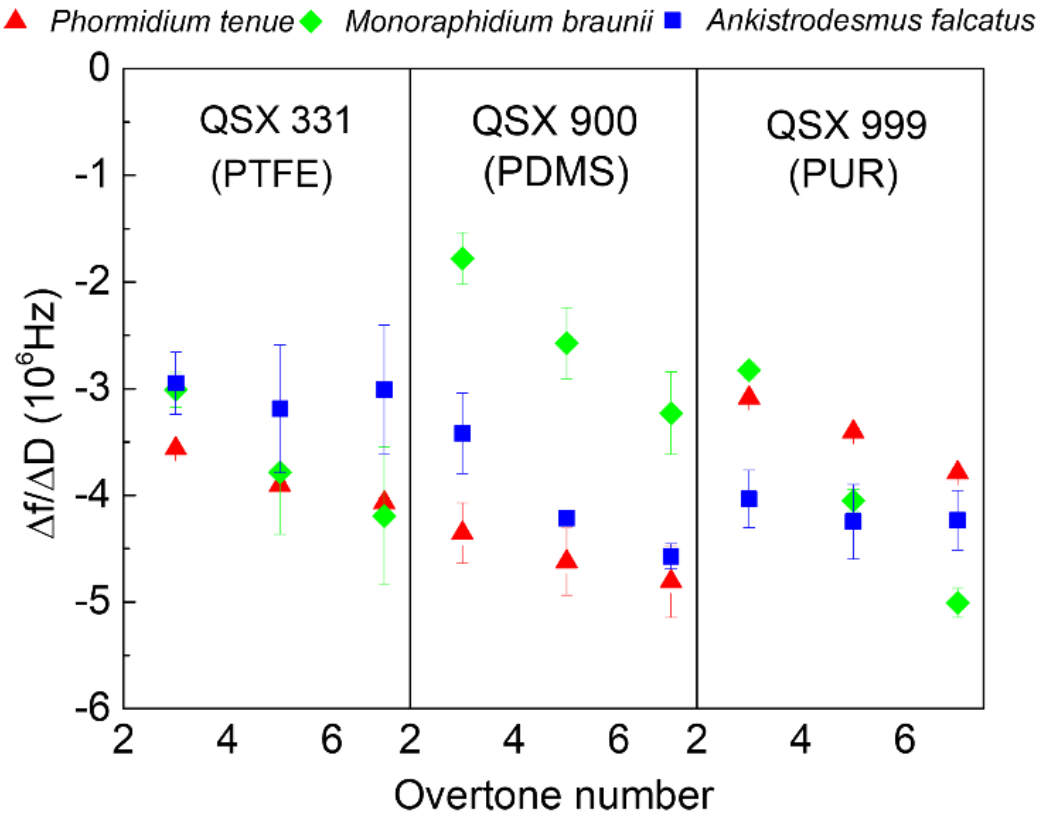

Figure 5.6. Δf/ΔD ratio at the stable state on QCM sensor surfaces as a function of the overtone number for a) *Phormidium tenue*, b) *Monoraphidium braunii*, and c) *Ankistrodesmus falcatus*.

5.3.5. Implications to the development of MCMBPR

As an emerging new concept for wastewater treatment, the success of the MCMBPR technology, which delivers molecular CO_2 for microalgal biofilm growth through hydrophobic membranes for enhanced higher process efficiency, depends on a fully fundamental understanding of the factors and mechanisms that determine the microalgae cell attachment and biofilm formation and its impact on biological performance and economic consideration. This study offers new insight into the role of morphology and surface properties of both microalgae species and hydrophobic membrane materials in determining microalgae cell attachment and biofilm formation. The results would guide the selection and screening of hydrophobic membrane materials for a fast molecular CO_2 transfer and quick microalgae biofilm formation in the

MCMPBR technology development. The results demonstrate that the relative importance of key factors, such as morphology, surface roughness, surface hydrophobicity, zeta potential, SFE, and interaction energy, that determine biofilm formation and biological performance would change under different situations and cases. Thus, an integration of analysis of all these properties and their relative importance in controlling the microalgae cell adhesion and biofilm should be considered.

5.4. Conclusions

This study investigated the three microalgae species' initial adhesion (*Phormidium tenue* (CPCC 424), *Monoraphidium braunii* (CPCC 625), and *Ankistrodesmus falcatus* (CPCC 669)) on different hydrophobic membrane materials (polytetrafluoroethylene, polydimethylsiloxane and polyurethane) by QCM-D testing. The *Phormidium tenue* exhibited the highest deposition throughout three materials, followed by *Monoraphidium braunii* in PTFE and PUR surfaces. In contrast, the second highest deposition on the PDMS sensor was *Ankistrodesmus falcatus*. The cell morphology and surface properties (surface roughness, hydrophobicity, zeta potential, SFE, interaction energy) of the sensors and microalgae cells had a crucial impact on the cell adhesion and biofilm formation during the QCM-D tests. The relative importance of these characteristics and mechanisms in controlling microalgae cell adhesion and biofilm formation would vary, depending on the specific microalgae species and hydrophobic membrane material involved. The higher the SFE and surface roughness, the higher the deposition was observed. Moreover, the Lewis acid-base interaction seems to play a positive role in the interactions between microalgae and sensors. The zeta potential of the microalgae strains and hydrophobic membrane materials could enhance microalgal cell adhesion through the ionic bridging mechanism. The microalgal layers exhibited viscoelastic properties in this study, while *Phormidium tenue* and *Monoraphidium*

braunii layers show a dynamic viscous characteristic compared to the *Ankistrodesmus falcatus* layer.

In conclusion, the QCM measurement proved a rapid, non-invasive and effective detection of microalgae initial adhesion in real-time, which could fulfill the fundamental knowledge of the microalgal biofilm membrane system. Moreover, many factors, such as ion strength and temperature, still haven't been investigated, which should be studied in future works.

5.5. Reference

[1] Shen, Y., Zhu, W., Chen, C., Nie, Y., Lin, X. (2016). Biofilm formation in attached microalgal reactors. Bioprocess and Biosystems Engineering, 39, 1281-1288.
[2] Dalirian, N., Najafabadi, H.A., Movahedirad, S. (2021). Surface attached cultivation and filtration of microalgal biofilm in a ceramic substrate photobioreactaor. Algal Research, 55, 102239.
[3] Guo, C., Duan, D., Sun, Y., Han, Y., Zhao, S. (2019). Enhancing *Scenedesmus obliquus* biofilm growth and CO_2 fixation in a gas-permeable membrane photobioreactor integrated with additional rough surface. Algal Research, 43, 101620.
[4] Peng, C., Fan, X., Xu, Y., Ren, H., Huang, H. (2021). Microscopic analysis towards rhamnolipid-mediated adhesion of *Thiobacillus denitrificans*: A QCM-D study. Chemosphere, 271, 129539.
[5] Moreno Osorio, J.H., De Natale, A., Del Mondo, A., Frunzo, L., Lens, P.N.L., Esposito, G., Pollio, A. (2020). Early colonization stages of fabric carriers by two *Chlorella* strains. Journal of Applied Phycology, 32, 3631-3644.
[6] Zhao, Z., Muylaert, K., Szymczyk, A., Vankelecom, I.F. (2021). Enhanced microalgal biofilm formation and facilitated microalgae harvesting using a novel pH-responsive, crosslinked patterned and vibrating membrane. Chemical Engineering Journal, 410, 127390.
[7] Shen, Y., Zhang, H., Xu, X., Lin, X. (2015). Biofilm formation and lipid accumulation of attached culture of *Botryococcus braunii*. Bioprocess and Biosystems Engineering, 38, 481-488.
[8] Chen, J.Y., Penn, L.S., Xi, J. (2018). Quartz crystal microbalance: Sensing cell-substrate adhesion and beyond. Biosensors and Bioelectronics, 99, 593-602.
[9] Yongabi, D., Jooken, S., Givanoudi, S., Khorshid, M., Deschaume, O., Bartic, C., Losada-Pérez, P., Wübbenhorst, M., Wagner, P. (2021). Ionic strength controls long-term cell-surface interactions–A QCM-D study of *S. cerevisiae* adhesion, retention and detachment. Journal of Colloid and Interface Science, 585, 583-595.
[10] Chen, M.Y., Chen, M.J., Lee, P.F., Cheng, L.H., Huang, L.J., Lai, C.H., Huang, K.H. (2010). Towards real-time observation of conditioning film and early biofilm formation under laminar flow conditions using a quartz crystal microbalance. Biochemical Engineering Journal, 53, 121-130.
[11] Yongabi, D., Khorshid, M., Gennaro, A., Jooken, S., Duwé, S., Deschaume, O., Losada-Pérez, P., Dedecker, P., Bartic, C., Wübbenhorst, M. (2020). QCM-D study of time-resolved cell

adhesion and detachment: Effect of surface free energy on eukaryotes and prokaryotes. ACS Applied Materials & Interfaces, 12, 18258-18272.
[12] Huang, R., Yi, P., Tang, Y. (2017). Probing the interactions of organic molecules, nanomaterials, and microbes with solid surfaces using quartz crystal microbalances: methodology, advantages, and limitations. Environmental Science: Processes & Impacts, 19, 793-811.
[13] Kreis, C.T., Grangier, A., Bäumchen, O. (2019). In vivo adhesion force measurements of Chlamydomonas on model substrates. Soft Matter, 15, 3027-3035.
[14] Zhang, Q., Yu, Z., Jin, S., Liu, C., Li, Y., Guo, D., Hu, M., Ruan, R., Liu, Y. (2020). Role of surface roughness in the algal short-term cell adhesion and long-term biofilm cultivation under dynamic flow condition. Algal Research, 46, 101787.
[15] Tsavatopoulou, V.D., Aravantinou, A.F., Manariotis, I.D. (2021). Comparison of *Botryococcus braunii* and *Neochloris vigensis* Biofilm Formation on Vertical Oriented Surfaces. Biointerface Research in Applied Chemistry, 11, 12843-12857.
[16] Tong, C., Derek, C. (2022). Membrane surface roughness promotes rapid initial cell adhesion and long term microalgal biofilm stability. Environmental Research, 206, 112602.
[17] Tonda-Turo, C., Carmagnola, I., Ciardelli, G. (2018). Quartz crystal microbalance with dissipation monitoring: a powerful method to predict the in vivo behavior of bioengineered surfaces. Frontiers in Bioengineering and Biotechnology, 6, 158.
[18] Subramanian, S., Huiszoon, R.C., Chu, S., Bentley, W.E., Ghodssi, R. (2020). Microsystems for biofilm characterization and sensing–a review. Biofilm, 2, 100015.
[19] Schofield, A.L., Rudd, T.R., Martin, D.S., Fernig, D.G., Edwards, C. (2007). Real-time monitoring of the development and stability of biofilms of *Streptococcus mutans* using the quartz crystal microbalance with dissipation monitoring. Biosensors and Bioelectronics, 23, 407-413.
[20] Walkowiak, J., Gradzielski, M., Zauscher, S., Ballauff, M. (2020). Interaction of Proteins with a Planar Poly (acrylic acid) Brush: Analysis by Quartz Crystal Microbalance with Dissipation Monitoring (QCM-D). Polymers, 13, 122.
[21] Rippka, R., Deruelles, J., Waterbury, J.B., Herdman, M., Stanier, R.Y. (1979). Generic assignments, strain histories and properties of pure cultures of cyanobacteria. Microbiology, 111, 1-61.
[22] Yang, C.C., Wen, R.C., Shen, C.R., Yao, D.J. (2015). Using a microfluidic gradient generator to characterize BG-11 medium for the growth of cyanobacteria *Synechococcus elongatus* PCC7942. Micromachines, 6, 1755-1767.
[23] Zeriouh, O., Reinoso-Moreno, J.V., López-Rosales, L., Cerón-García, M.D.C., Sánchez-Mirón, A., García-Camacho, F., Molina-Grima, E. (2017). Biofouling in photobioreactors for marine microalgae. Critical Reviews in Biotechnology, 37, 1006-1023.
[24] Švorčík, V., Řezníčková, A., Kolská, Z., Slepička, P., Hnatowicz, V. (2010). Variable surface properties of PTFE foils. e-Polymers, 10, 133.
[25] Wang, F., Zhu, H., Zhang, H., Tang, H., Chen, J., Guo, Y. (2015). Effect of surface hydrophilic modification on the wettability, surface charge property and separation performance of PTFE membrane. Journal of water process engineering, 8, 11-18.
[26] Emoto, K., Nagasaki, Y., Kataoka, K. (1999). Coating of Surfaces with Stabilized Reactive Micelles from Poly (ethylene glycol)− Poly (DL-lactic acid) Block Copolymer. Langmuir, 15, 5212-5218.

[27] Shirai, T., Takai, M., Ishihara, K. (2010). Simple and functional modification of PDMS surface for microchannel electropheresis.Proceedings of the 14th International Conference on Miniaturized Systems for Chemistry and Life Sciences; Oct 3-7; Groningen.
[28] Wang, M., Mo, H., Liu, G., Qi, L., Yu, Y., Fan, H., Xu, X., Luo, T., Shao, Y., Wang, H. (2020). Impact of scaling on aeration performance of fine-pore membrane diffusers based on a pilot-scale study. Scientific Reports, 10, 1-10.
[29] Bezdadea, M., Bourceanu, M., Zavastin, D. (2006). The permeation of protein solution at ultrafiltration through indigenous polyurethane membranes. ROMANIAN BIOTECHNOLOGICAL LETTERS, 11, 2979.
[30] Yuan, H., Zhang, X., Jiang, Z., Chen, X., Zhang, X. (2018). Quantitative criterion to predict cell adhesion by identifying dominant interaction between microorganisms and abiotic surfaces. Langmuir, 35, 3524-3533.
[31] Hoek, E.M., Agarwal, G.K. (2006). Extended DLVO interactions between spherical particles and rough surfaces. Journal of Colloid and Interface Science, 298, 50-58.
[32] Zhao, F., Chu, H., Su, Y., Tan, X., Zhang, Y., Yang, L., Zhou, X. (2016). Microalgae harvesting by an axial vibration membrane: The mechanism of mitigating membrane fouling. Journal of Membrane Science, 508, 127-135.
[33] Brant, J.A., Childress, A.E. (2002). Assessing short-range membrane–colloid interactions using surface energetics. Journal of Membrane Science, 203, 257-273.
[34] Wang, F., Zhang, M., Peng, W., He, Y., Lin, H., Chen, J., Hong, H., Wang, A., Yu, H. (2014). Effects of ionic strength on membrane fouling in a membrane bioreactor. Bioresource Technology, 156, 35-41.
[35] Ozkan, A., Berberoglu, H. (2013). Physico-chemical surface properties of microalgae. Colloids and Surfaces B: Biointerfaces, 112, 287-293.
[36] Wegener, J., Janshoff, A., Steinem, C. (2001). The quartz crystal microbalance as a novel means to study cell-substrate interactions in situ. Cell Biochemistry and Biophysics, 34, 121-151.
[37] Ozkan, A., Berberoglu, H. (2013). Cell to substratum and cell to cell interactions of microalgae. Colloids and Surfaces B: Biointerfaces, 112, 302-309.
[38] Ji, C., Wang, H., Cui, H., Zhang, C., Li, R., Liu, T. (2023). Characterization and evaluation of substratum material selection for microalgal biofilm cultivation. Applied Microbiology and Biotechnology, 107, 2707-2721.
[39] Krienitz, L., Ustinova, I., Friedl, T., Huss, V.A. (2001). Traditional generic concepts versus 18S rRNA gene phylogeny in the green algal family *Selenastraceae* (*Chlorophyceae*, *Chlorophyta*). Journal of Phycology, 37, 852-865.
[40] Jayanta, T., Chandra, K.M., Chandra, G.B. (2012). Growth, total lipid content and fatty acid profile of a native strain of the freshwater oleaginous microalgae *Ankistrodesmus falcatus* (Ralf) grown under salt stress condition. International Research Journal of Biological Sciences, 1, 27-35.
[41] Hoshiba, T., Yoshikawa, C., Sakakibara, K. (2018). Characterization of initial cell adhesion on charged polymer substrates in serum-containing and serum-free media. Langmuir, 34, 4043-4051.
[42] Ndikubwimana, T., Zeng, X., He, N., Xiao, Z., Xie, Y., Chang, J.S., Lin, L., Lu, Y. (2015). Microalgae biomass harvesting by bioflocculation-interpretation by classical DLVO theory. Biochemical Engineering Journal, 101, 160-167.

[43] Hanaor, D., Michelazzi, M., Leonelli, C., Sorrell, C.C. (2012). The effects of carboxylic acids on the aqueous dispersion and electrophoretic deposition of ZrO_2. Journal of the European Ceramic Society, 32, 235-244.
[44] Yuan, H., Zhang, X., Jiang, Z., Wang, X., Chen, X., Cao, L., Zhang, X. (2019). Analyzing the effect of pH on microalgae adhesion by identifying the dominant interaction between cell and surface. Colloids and Surfaces B: Biointerfaces, 177, 479-486.
[45] Finlay, J.A., Callow, M.E., Ista, L.K., Lopez, G.P., Callow, J.A. (2002). The influence of surface wettability on the adhesion strength of settled spores of the green alga *Enteromorpha* and the diatom *Amphora*. Integrative and Comparative Biology, 42, 1116-1122.
[46] Sekar, R., Venugopalan, V., Satpathy, K., Nair, K., Rao, V. (2004). Laboratory studies on adhesion of microalgae to hard substrates. Hydrobiologia, 512, 109-116.
[47] Cui, Y., Yuan, W.W., Pei, Z. (2010). Effects of carrier material and design on microalgae attachment for biofuel manufacturing: a literature review.Proceedings of the International Manufacturing Science and Engineering Conference; Oct 12-15; Erie. pp. 525-540.
[48] Cheah, Y.T., Chan, D.J.C. (2021). Physiology of microalgal biofilm: a review on prediction of adhesion on substrates. Bioengineered, 12, 7577-7599.
[49] Genin, S.N., Aitchison, J.S., Allen, D.G. (2014). Design of algal film photobioreactors: material surface energy effects on algal film productivity, colonization and lipid content. Bioresource Technology, 155, 136-143.
[50] Zhuang, L., Yu, D., Zhang, J., Liu, F., Wu, Y., Zhang, T., Dao, G., Hu, H. (2018). The characteristics and influencing factors of the attached microalgae cultivation: a review. Renewable and Sustainable Energy Reviews, 94, 1110-1119.
[51] Zeng, W., Li, P., Huang, Y., Xia, A., Zhu, X., Zhu, X., Liao, Q. (2022). How Interfacial Properties Affect Adhesion: An Analysis from the Interactions between Microalgal Cells and Solid Substrates. Langmuir, 38, 3284-3296.
[52] Tang, J., Liu, B., Gao, L., Wang, W., Liu, T., Su, G. (2021). Impacts of surface wettability and roughness of styrene-acrylic resin films on adhesion behavior of microalgae *Chlorella sp*. Colloids and Surfaces B: Biointerfaces, 199, 111522.
[53] Teixeira, P., Oliveira, R. (1999). Influence of surface characteristics on the adhesion of *Alcaligenes denitrificans* to polymeric substrates. Journal of Adhesion Science and Technology, 13, 1287-1294.
[54] Huang, Y., Zheng, Y., Li, J., Liao, Q., Fu, Q., Xia, A., Fu, J., Sun, Y. (2018). Enhancing microalgae biofilm formation and growth by fabricating microgrooves onto the substrate surface. Bioresource Technology, 261, 36-43.
[55] Zhang, Q., Liu, C., Li, Y., Yu, Z., Chen, Z., Ye, T., Wang, X., Hu, Z., Liu, S., Xiao, B. (2017). Cultivation of algal biofilm using different lignocellulosic materials as carriers. Biotechnology for Biofuels and Bioproducts, 10, 1-16.
[56] Sun, J., Yu, Z., Yang, L., Chu, H., Jiang, S., Zhang, Y., Zhou, X. (2023). New insight in algal cell adhesion and cake layer evolution in algal-related membrane processes: Size-fractioned particles, initial foulant seeds and EDEM simulation. Environmental Research, 220, 115162.
[57] Cao, H., Habimana, O., Semião, A.J., Allen, A., Heffernan, R., Casey, E. (2015). Understanding particle deposition kinetics on NF membranes: A focus on micro-beads and membrane interactions at different environmental conditions. Journal of Membrane Science, 475, 367-375.
[58] Li, L., Wang, Z., Rietveld, L.C., Gao, N., Hu, J., Yin, D., Yu, S. (2014). Comparison of the effects of extracellular and intracellular organic matter extracted from Microcystis aeruginosa on

ultrafiltration membrane fouling: dynamics and mechanisms. Environmental Science & Technology, 48, 14549-14557.
[59] Marcus, I.M., Herzberg, M., Walker, S.L., Freger, V. (2012). Pseudomonas aeruginosa attachment on QCM-D sensors: the role of cell and surface hydrophobicities. Langmuir, 28, 6396-6402.
[60] Gutman, J., Walker, S.L., Freger, V., Herzberg, M. (2013). Bacterial attachment and viscoelasticity: physicochemical and motility effects analyzed using quartz crystal microbalance with dissipation (QCM-D). Environmental Science & Technology, 47, 398-404.

Chapter 6: A study of theoretical analysis and modelling of microalgae membrane photobioreactors

Abstract

This study presents a theoretical analysis and modelling of microalgal membrane photobioreactors (MPBRs) for wastewater treatment. A mathematical model was developed to describe the biological performances of MPBRs in mono-microalgae systems. The model takes into account the effects of hydraulic retention time (HRT), solid retention time (SRT), and N/P ratio of influent on the biological performance of MPBRs, such as biomass production and pollutant removal (N and P removals). The model was calibrated and validated using experimental data from the literature. The modelling results are in good agreement with the experimental results from the literature. The findings suggest that the proposed mathematical models can be used to optimize these parameters to improve the removal of nutrients (N and P) and the productivity of biomass and bioenergy in MPBRs. This study provides new insights into using mathematical models for the optimal design and operation of MPBRs for sustainable wastewater treatment.

Keywords: Modeling; Microalgae; Membrane photobioreactor; Wastewater treatment.

6.1. Introduction

Microalgae are photo-autotrophic microorganisms that can consume nutrients such as nitrogen and phosphorus in the aqueous system. The microalgae photobioreactor has been studied for decades, and the microalgae biomass has been applied to a wide range of areas such as nutrient, cosmetic and pigment applications [1-3]. As a traditional biological process in wastewater treatment, activated sludge faces challenges such as the production of large amounts of harmful sludge and low-efficiency removal of nutrients (nitrogen, phosphorus) [4-6]. Compared to

traditional activated sludge biological treatment, microalgae-based wastewater treatment could achieve effective nutrient removal and produce high-lipid content feedstock for downstream applications such as biofuel or biodiesel production to alleviate the pressure of energy shortage [7-9]. Microalgae cultivation hasn't been industrialized into wastewater treatment due to handicaps such as diluted suspended microalgae concentration, difficult lipid extraction, and limitation of water purification [10-12].

Compared to conventional photobioreactor (either open pone or closed bioreactor), the concept that involving membrane technology in microalgae-based biological process guarantees better effluent quality, concentrated microalgae biomass, and decoupling of hydraulic retention time (HRT) and solid retention time (SRT) [13]. However, serious problems such as membrane fouling, the high maintenance cost and the short life cycle of the membrane are also followed by the application of membrane technology [13]. As the literature mentioned, adjusting the operating conditions of the membrane photobioreactor (MPBR) contributed to mitigating severe membrane fouling and improving reactor performance [14, 15]. Even though the effects brought by operating parameters could be diverse, the adjustment of those parameters should focus on the improvements of pollutant removals (N and P removals) and microalgae biomass production for the purposes of wastewater treatment and biomass harvesting for biofuels and feedstocks. Zhao et al. mentioned that HRT is a key condition that affects biomass productivity and wastewater treatment efficiency. They claimed that short HRTs facilitate microalgae growth due to the higher nutrient loading, while long HRTs contribute to better nutrient removal efficiency but sometimes cause nutrient limitations [16]. Xu et al. revealed that the *C. vulgaris* concentration increased from 895 mg COD/L to 1473 mg COD/L when the HRT of MPBR reduced from 24 h to 12 h [17]. However, they also found that higher HRT (24 h) achieved higher removal of nitrogen (66%) and phosphorus

(91%) in the same study [17]. Another parameter related to the biomass concentration and pollutant removal is SRT. As literature mentioned, the uncoupled HRT and SRT in MPBR system could remain a high concentration of biomass in the system (long SRT) while dealing with a high nutrient loading (short HRT) [18]. Thus, this high biomass concentration can result in faster and more stable nutrient removal. A previous study by Honda et al. mentioned that the concentration of *Chlorella* increased with the SRT rising from 9 d to 18 d [19]. As vital nutrients for microalgal biomass production, nitrogen and phosphorus loading are also considered to improve MPBR performance, especially in microalgal biomass concentration [13]. The higher nutrient loading could promote microalgae growth, but the growth declination might happen at a higher level due to the inhibition caused by excessive nutrients [20]. Some studies reported a similar phenomenon that microalgal biomass concentration increased with the augment of nutrient concentrations in influent, but a dramatic drop occurred at an extremely high level of nutrients (both nitrogen and phosphorus) [21, 22]. Despite the various factors (light intensity, temperature, and so on) that influence MPBR performance, these factors are the most cost effective and easiest to control during the microalgae cultivation period.

Many studies have been done to investigate the optimal operating conditions to take full advantage of MPBR in wastewater treatment and the following downstream product economic potential [23-25]. However, the optimal conditions could vary due to the microalgae species, MPBR configuration, and industrial requirements. Thus, the optimization of operating conditions and wastewater characteristics is still under examination, and it is time-consuming and expensive because it requires considerable amounts of laboratory experiments. The introduction of mathematical modelling work to predict the MBPR performance is thus suggested before the experiment work [26]. The mathematical model could simulate the specific microorganism activity

in MPBR by setting the correlated kinetic parameters. As a result, the time spent on following experiment work for optimization could be shortened. Several mathematical models have been proposed to investigate the different species under different types of conventional photobioreactors [18, 27, 28]. However, no mathematical models and modelling work were published for the MPBR systems in the literature.

This work aimed to investigate how process conditions (SRT and HRT) and wastewater characteristics would affect the biological performance (N and P removals and microalgae biomass production) of MPBRs by using mathematical models that integrate the mass balance concept and microbial kinetic models. The proposed mathematical models were calibrated and validated using experimental data from previous studies published in the literature. The mathematical models presented here are a powerful tool to optimize the design and operation of microalgae MPBRs.

6.2. Methods –model design and model variables

6.2.1. Model design

The model development proceeded through the steps indicated in Figure 6.1. The mathematical model we used in this study to simulate microalgae growth in microalgae MPBRs was based on the mass balance concept and microbial kinetic models. Biomass and nutrients (N and P) mass balances are in the form of ordinary differential for lumped systems. Biological and liquid phases were considered in the microalgae MPBRs, and the mass balance equations were derived according to the following assumptions:

The model only predicts the biological performance of microalgae MPBRs under the steady state, which would not provide the details of performance development during the transit period.

The illumination and gas (CO_2) supply are continuous in the cultivation system of microalgae; thus, they are assumed not to be limiting factors of microalgae growth in the model.

The nutrient consumption mechanism (nitrogen and phosphorus) is dominated by microalgae uptake; other nutrient removal mechanisms, such as the nitrification interaction between the bacteria and microalgae, are not taken into account.

The HRT and SRT are decoupled as individual factors for the microalgae MPBR.

$$\text{HRT} = \frac{V}{Q}\ (\text{d}) \tag{6.1}$$

$$\text{SRT} = \frac{VX}{Q^w X} = \frac{V}{Q^w}\ (\text{d}) \tag{6.2}$$

V-effective volume of microalgae MPBR, L

Q-Flow rate of influent, $L \cdot d^{-1}$

Q^w- Waste rate of microalgae suspension, $L \cdot d^{-1}$

X- Microalgae biomass concentration, $g \cdot L^{-1}$

In the microalgae MPBR, current microalgae biomass is equal to the sum of all biomass changes, including the initial amount of inoculum, the increasing biomass caused by microalgal growth over time, and the deduction of the loss of cell death and daily discard biomass. Biomass mass balance can be expressed as the following equation:

$$V\frac{dX_m}{dt} = QX_m^0 - Q^w X_m + V(\frac{\mu_m X_m S_N S_P}{(K_N+S_N)(K_P+S_P)} - X_m k_{d-m}) \quad (6.3)$$

X_m^0-initial concentration of microalgae in MPBR, gL^{-1}

X_m-microalgae concentration in discard suspension, gL^{-1}

μ_m-maximum growth rate of microalgae, day^{-1}

S_N-total nitrogen concentration in membrane photobioreactor and effluent, mgL^{-1}

S_P-total phosphorus concentration in membrane photobioreactor and effluent, mgL^{-1}

K_N-half saturation constant of NH_4^+-N, mg N L^{-1}

K_P- half-saturation constant of HPO_4^{2-}-P, mg P L^{-1}

k_{d-m}-decay coefficient of microalgae, d^{-1}

Under the steady state, biomass maintains a relatively stable value, which means the changing rate $V\frac{dX_m}{dt} = 0$, and the initial biomass X_m^0 is assumed as zero,

Thus, the equation can be simplified to:

$$0 = -Q^w X_m + VX_m(\frac{\mu_m S_N S_P}{(K_N+S_N)(K_P+S_P)} - k_d) \quad (6.4)$$

Equation (6.4) divided by $Q^w X_m$, then we can have the following equation:

$$-1 + \frac{V}{Q^w}(\frac{\mu_m X_m S_N S_P}{(K_N+S_N)(K_P+S_P)} - k_{d-m}) = 0 \quad (6.5)$$

Based on equation (6.2), equation (6.5) can be further simplified:

$$SRT(\frac{\mu_m S_N S_P}{(K_N+S_N)(K_P+S_P)} - k_{d-m}) = 1 \quad (6.6)$$

Moreover, the nutrient concentration in the MPBR is equal to the sum of the initial medium concentration (QS_i^0) and the deduction of nutrients in the effluent (QS_i) and consumption of microalgal metabolism ($\gamma_{\omega t_i}$) Thus, the nutrient (N and P) mass balance can be expressed as the following equation:

$$V\frac{dS_i}{dt} = QS_i^0 - QS_i + \gamma_{\omega t_i} \quad (6.7)$$

S_i^0- Initial nutrient concentration in MPBR, i = N, P; mgL^{-1}

S_i- Nutrient concentration in effluent, i = N, P; mgL^{-1}

$\gamma_{\omega t_i}$- nutrient consumption of microalgal metabolism, i=N, P; which:

$$\gamma_{\omega t_i} = -\frac{\mu_m X_m V S_N S_P}{Y_i(K_N+S_N)(K_P+S_P)} \quad (6.8)$$

Where Y_i- removal coefficient of nutrient, i = N, P; g algae · g $nutrient^{-1}$

Under the steady state, the nutrient consumption should be stable, which means the $V\frac{dS_i}{dt} = 0$

Thus,

$$QS_i^0 - QS_i + \gamma_{\omega t_i} = QS_i^0 - QS_i - \frac{\mu_m X_m V S_N S_P}{Y_i(K_N+S_N)(K_P+S_P)} = 0 \quad (6.9)$$

Equation (6.9) divided by Q and we got:

$$S_i^0 - S_i - \frac{V}{Q}X_m \cdot \frac{\mu_m S_N S_P}{Y_c(K_N+S_N)(K_P+S_P)} = 0 \quad (6.10)$$

Based on equation (6.1), equation (6.10) can be simplified to

$$S_i^0 - S_i - HRT\frac{X\mu_m S_N S_P}{Y_i(K_N+S_N)(K_P+S_P)} = 0 \quad (6.11)$$

$S^0_{i\ i=\ N\ and\ P}$ – influent concentration nitrogen and phosphorus, respectively, mgL^{-1}.

$S_{i=N\ and\ P}$ – effluent concentration nitrogen and phosphorus, respectively, mgL^{-1}.

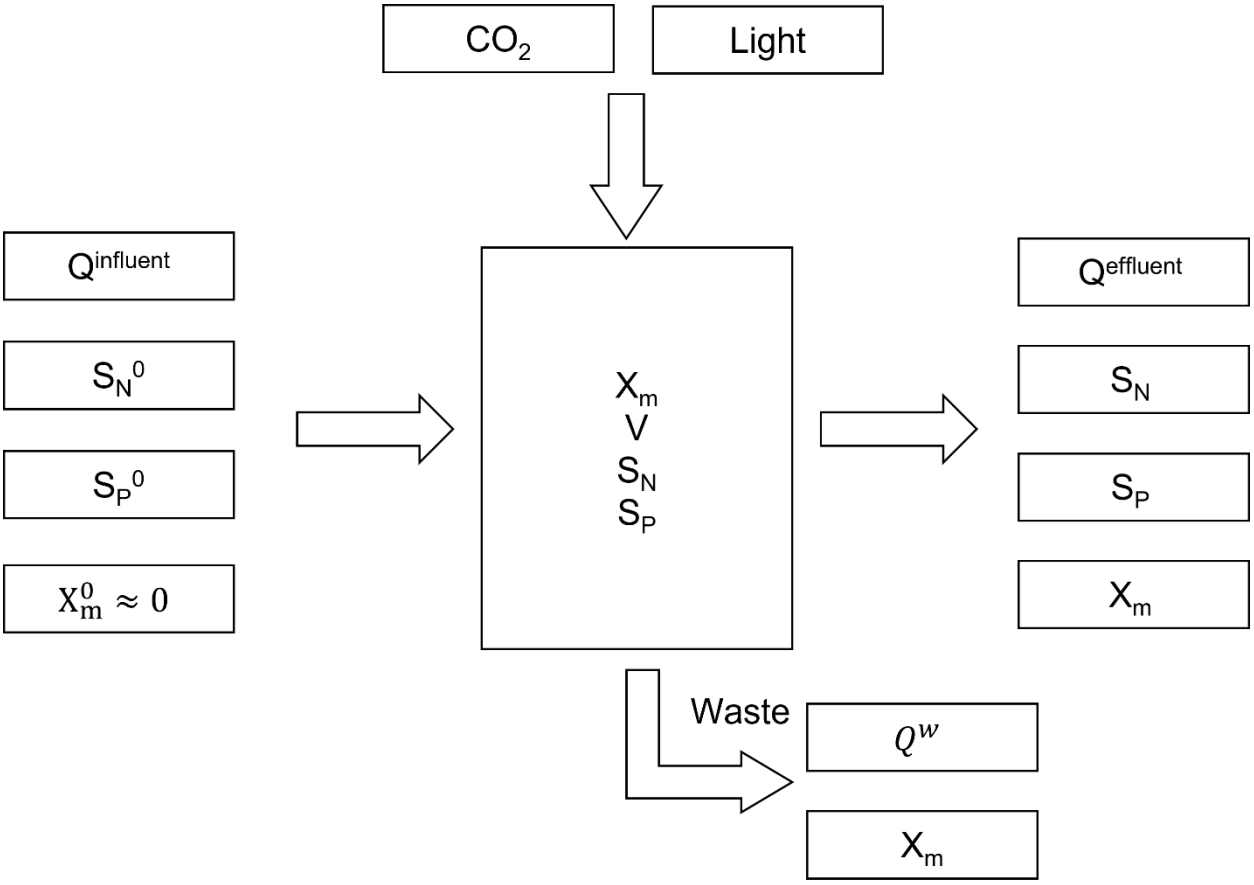

Figure 6.1. The a) microalgae and b) microalgae-bacteria model process development.

6.2.2. Model variables

The model variables were employed based on the general microorganism growth kinetics from previous studies and are listed in the following table:

Table 6.1. Growth kinetic parameters for the modelling study.

Kinetic parameters	Value	Ref
μ_m (d^{-1})	1.68	[29, 30]
k_{d-m} (d^{-1})	0.06	[29, 30]
Y_{N-M} (mg biomass·mg nitrogen^{-1})	15.8	[29, 30]
Y_{P-M} (mg biomass·mg phosphorus^{-1})	114	[29, 30]
K_N (mg nitrogen·L^{-1})	24.5	[29, 30]
K_P (mg phosphorus·L^{-1})	3.39	[29, 30]

The variables (microalgal biomass concentration Xm, effluent N (S_N) and P (S_P) concentrations in the models (Equations (6.6), (6.10), and (6.11)) were solved by using Microsoft Excel 2019 with a solver function.

6.3. Result and discussion

6.3.1. Mono-microalgae on membrane photobioreactor

Figures 6.2 and 6.3 show the biomass concentration in the bioreactor and nutrient profiles in the effluent under the different operating conditions (HRT: 1 to 5 d, SRT: 10 to 40 d, and influent N concentration: 20 to 60 mg/L, and influent P= 5 mg/L). As shown in Figure 6.2, the microalgal biomass concentration increased with the augment of SRT and influent N concentration while decreasing with the rise of HRT. The maximum microalgal biomass concentration is 5694 mg/L when HRT = 1 d and SRT = 40 d with the influent N concentration = 40 mg/L. In comparison, the maximum microalgal biomass concentration in Figure 6.2b is 6214 mg/L when SRT = 40 d and

influent N concentration = 60 mg/L at HRT = 1 d. From Figure 6.3, it is clear that an increase in SRT led to a decrease in both effluent N and P concentration at a fixed influent N concentration. Furthermore, an increase in influent N concentration resulted in an increase in effluent N concentration at the same SRT and influent P concentration (5 mg/L). The maximum effluent N concentration is 29 mg/L when SRT = 10 d and influent N concentration = 60 mg/L at HRT = 1 d. The effluent P concentration increased with the decrease of influent N concentration and SRT. The maximum effluent P concentration, 3.08 mg/L, was achieved at SRT = 10 d and influent N concentration = 20 mg/L at HRT = 1 d. The general trends of changes in effluent N and P concentrations under different SRT, HRT, and influent N and P concentrations are consistent with the ones predicted by microbial kinetics models and mass balance equations for conventional CSTR photobioreactors [31].

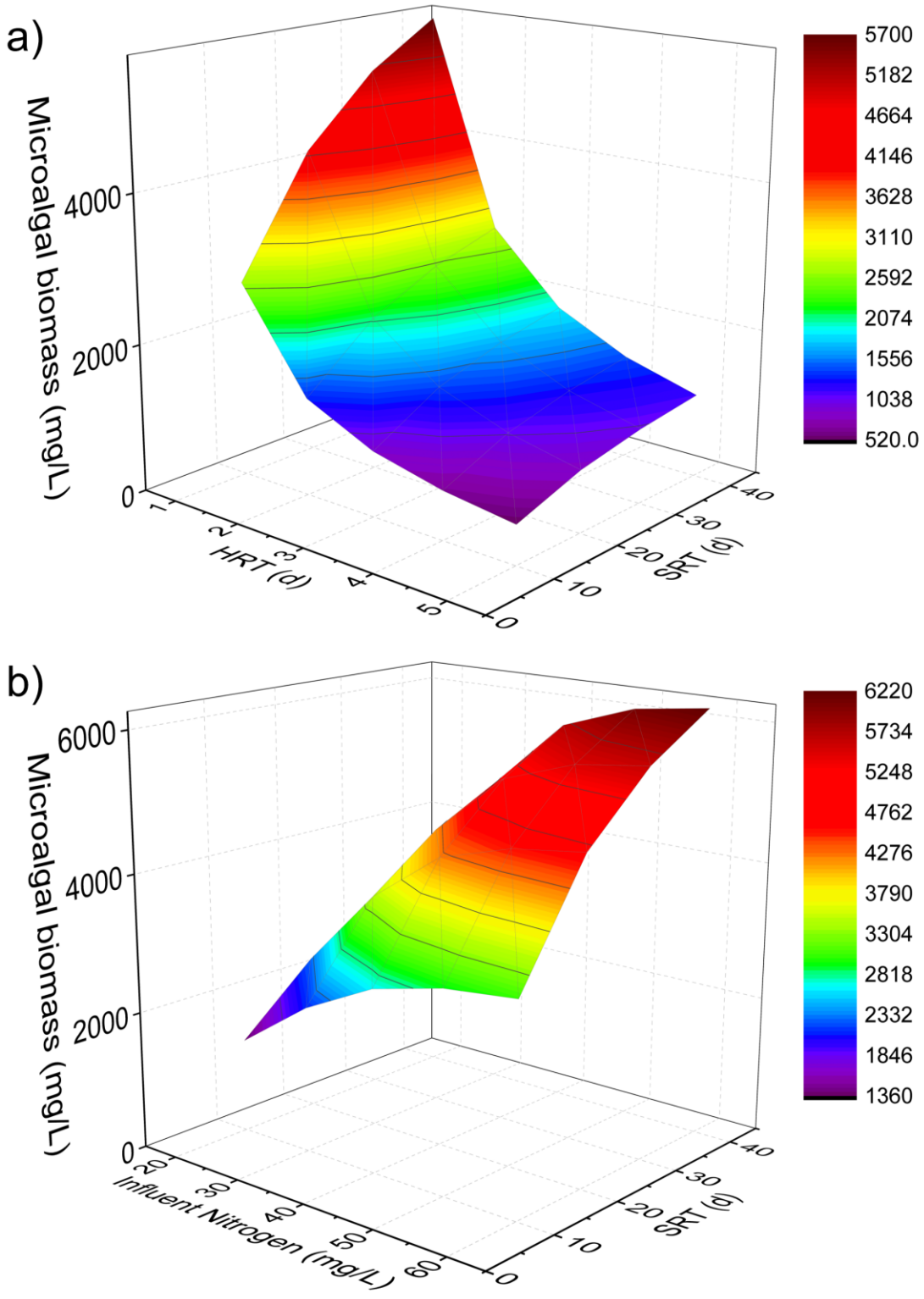

Figure 6.2. a) Microalgae biomass concentration under different SRT and HRT at influent N = 40 mg/L and P = 5 mg/L; and b) Microalgae biomass concentration under different SRTs and influent nitrogen concentrations at HRT = 1 d, P = 5 mg/L.

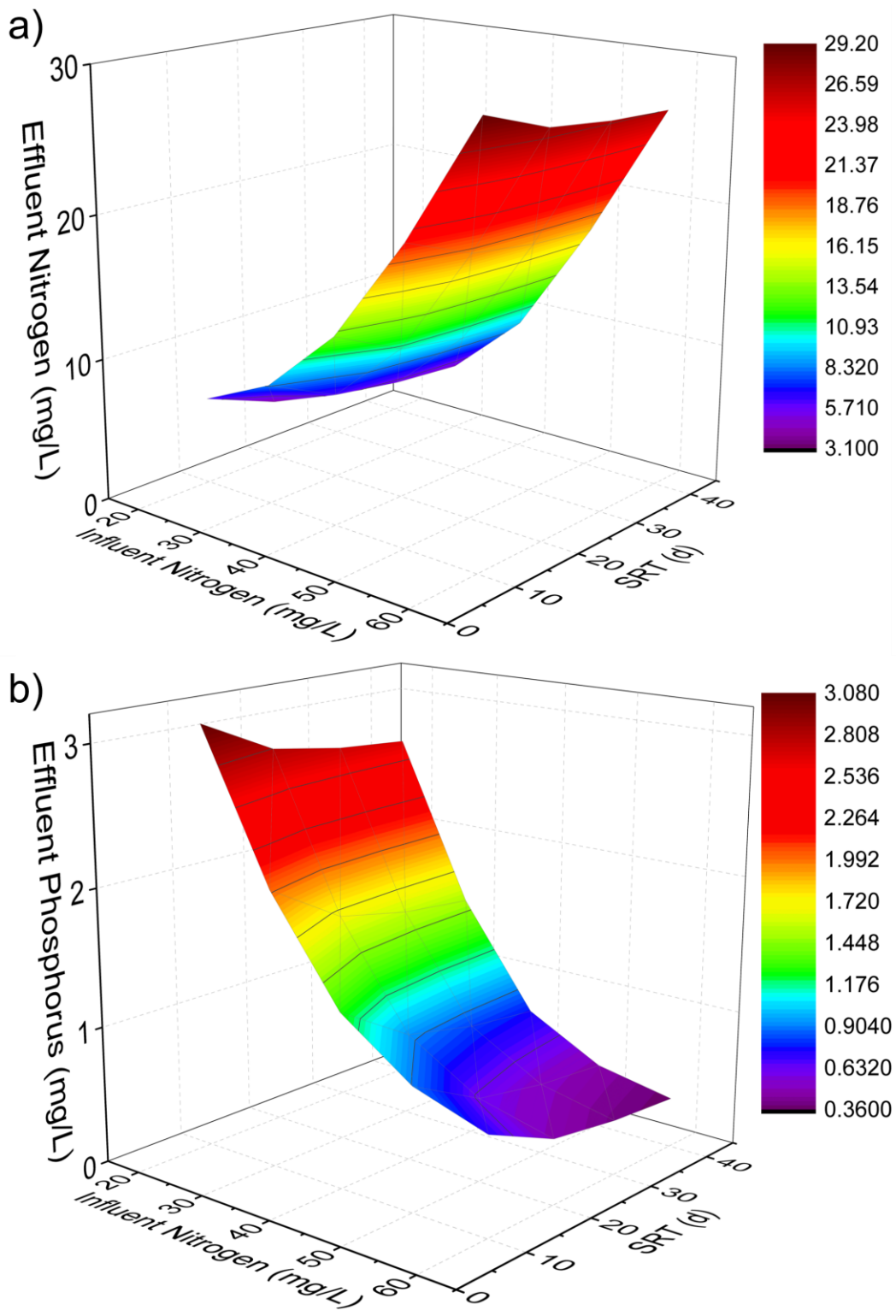

Figure 6.3. a) Nitrogen and b) phosphorus concentrations of effluent under different SRTs and influent N concentrations at HRT = 1 d, influent P= 5 mg/L.

6.3.1.1. HRT effect

As the literature mentioned, HRT is an important parameter of membrane photobioreactor operation, affecting pollutant removal and microalgae production [13, 14, 23]. In general, a short HRT corresponds to a high nutrient loading rate, which could provide sufficient nutrients for microalgae growth in the bioreactor, especially in low-medium strength wastewater cases [23]. Some studies reported that longer SRT can promote microalgae biomass production because it prolongs the contact between microalgae and suspended nutrients, thus increasing the metabolism period [32]. Lee et al. found that the *Chlorella vulgaris* biomass concentration decreased from 0.8 g/L to 0.4 g/L when the HRT decreased from 6 days to 3 days on chromium (VI) wastewater treatment [32]. This reduction of biomass production was ascribed to the high loading rate of toxic chromium (VI) under the short HRT, which was out of the limitation of microalgae degradation, thus causing the decay of microalgae. Their research revealed that long HRT is beneficial for microalgae cultivation during wastewater with high concentration of toxic compounds [32]. There is also an argument that longer HRT contributes to the reduction of microalgae biomass due to the lower nutrients loading and higher decay rate caused by the nutrient shortage [33]. Ashadullah et al. investigated the HRT effect on microalgal membrane photobioreactor, revealing that longer HRT exhibited better nutrient removal performance [24]. They found total N removal increased from 61.3% to 67.5% when HRT increased from 2 days to 7 days. However, the nutrient profiles in this study haven't shown a very obvious correlative varying trend with HRT changing compared to the experimental case. The reason might be that nutrient removal involves multiple mechanisms (microalgae assimilation, ammonia volatilization,) and nutrients in suspended solids need a long time for hydrolysis which also are influenced by HRT except for biomass production [34]. But in

this study, the mono-microalgal model only considered the soluble nutrients (N and P) consumed by biomass production.

Despite worldwide acceptance that longer HRT improves the microorganism processes such as biodegradation, photodegradation and sorption, leading to higher consumption of pollutants [35], it does not mean the photobioreactor would benefit from a very long HRT condition if the biodegradation rate is fast enough. The low organic loading rate traced back to long HRT restricted the microalgae biomass production even though long HRT provides a longer biodegradation period to improve the effluent quality [33, 36]. The long HRT and low biomass production are not applicable for industrial applications due to the high energy and capital costs.

6.3.1.2. SRT effect

Another important parameter that affects the biological performance of M-MSPBR is solid retention time (SRT). The literature claimed that longer SRT could enhance nutrient recovery and facilitate microalgae accumulation, increasing biomass production [16, 37, 38]. As a result, the microalgae biomass concentration increased (2661.26 mg/L to 5693.76 mg/L at HRT = 1 d with influent N concentration = 40 mg/L) with the increase of SRT (Figure 6.3). Wang et al. also reported that the osmotic photobioreactor's total N and P concentrations decreased when the SRT increased from 9.41 d to 25.26 d [39]. However, when the longer SRT is used, the biomass concentration could be limited to a steady state in real cases by other parameters such as living area, light, and nutrients [28, 40]. This might be other factors, such as light intensity, to be considered in the models in future work.

Nutrient removal also could be affected by the SRT. The effluent N and P concentration decreased (from 13.10 mg/L to 9.37 mg/L and 1.27 mg/L to 0.76 mg/L, respectively) with the

rising of SRT at HRT = 1 d with influent N and P concentration = 40 mg/L and 5 mg/L, respectively (Figure 6.4). Previous studies have found a linear correlation between microalgae biomass production and nutrient (nitrogen and phosphorus) uptake in batch or photobioreactor studies [41, 42]. Briefly, longer SRT contributes to higher microalgae biomass accumulation due to its lower discharge rate and longer harvest interval [43]. Xu et al. reported that the biomass concentration increased from 690 mg/L to 1473 mg/L when the SRT rose from 5 days to 10 days [17]. Ignoring the limitation of other impact factors (such as light and carbon dioxide), higher SRT indeed results in a higher microalgae biomass concentration, which usually comes with high nutrient removal due to the more significant nutrient consumption caused by more microalgae accumulation. The longer SRT might be more acceptable at this point due to high biomass amount and high nutrient removal. However, the positive effect brough by SRT could be restrict by other factors in real nature, such as the limitation of light penetration distance in microalgae suspension. As Discart et al. mentioned, the light attenuation and carbon dioxide shortage would happen when the biomass concentration reach a high level which will cause higher decay efficiency thus decrease the biomass productivity [44]. As a result, poor N removal could be obtained because the majority of N removal relied on algal biomass wasting [17]. Some experimental studies also reported similar behaviours that N removal decreased with the increase of SRT [45, 46]. Regarding this study, the mono-microalgal model results haven’t shown that similar trends could be attributed to the majority of N removal being carried out by the microalgae uptake, which only correlated to the microalgae biomass.

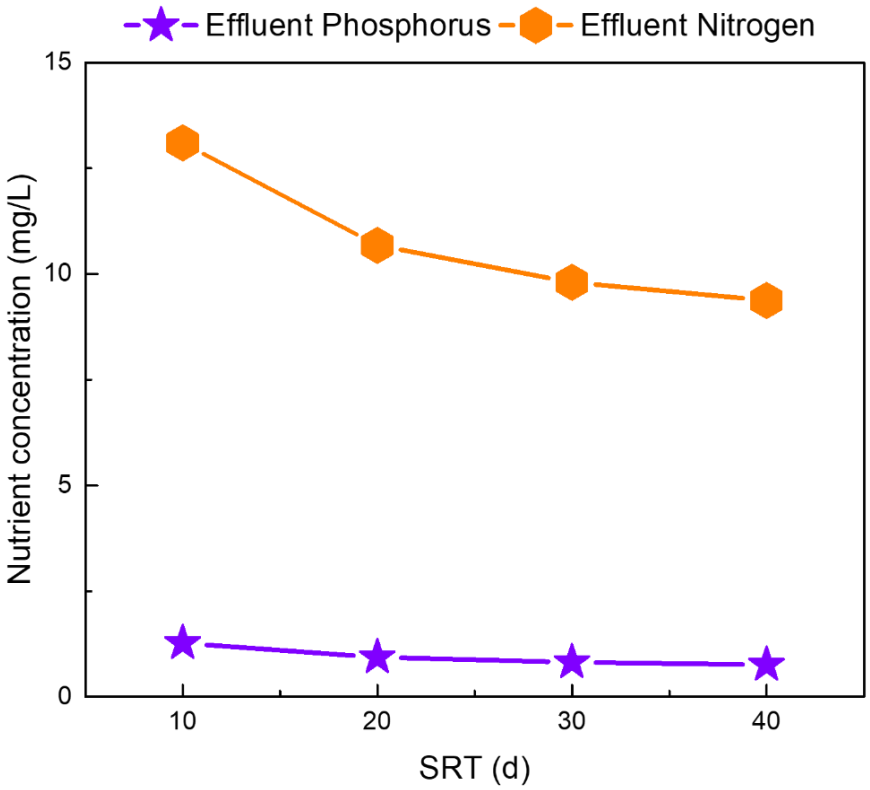

Figure 6.4. Nutrient profiles of effluent under different SRT at HRT = 1 d with influent nitrogen concentration = 40 mg/L.

6.3.1.3. Influent nitrogen concentration effect

Literature also mentioned that the ratio of nutrients in influent also affects M-MSPBR performance, especially in microalgal biomass production [13]. As shown in Figure 6.2, the microalgae biomass concentration increased from 3124 mg/L to 6214 mg/L when the nitrogen concentration of influent increased from 20 mg/L to 60 mg/L at HRT = 1 d and SRT = 40 d. As a key factor of microalgae growth, the augment of influent N concentration promotes microalgae productivity [47]. When the HRT and SRT were constant, the only effect of microalgae biomass concentration was brought from the wastewater characteristics, such as influent N concentration. As shown in this model, the microalgae biomass concentration on the right side of nutrient mass balance equations increased with the rising of nutrient concentration of influent to maintain the

mass balance at the steady state. When it came to the nutrient profile, the situation became a little bit complex. The effluent N concentration increased from 3.18 mg/L to 26.55 mg/L with an increase of influent N concentration (from 20 mg/L to 60 mg/L), while the effluent P concentration decreased from 2.67 mg/L to 0.37 mg/L at the HRT = 1 d and SRT = 40 d. This phenomenon could be attributed to the effect of nutrient limitation [48]. At a low influent N concentration, insufficient nitrogen content in the influent could not support microalgae to consume all remaining P in the influent. As a result, the M-MSPBR had a high N removal (84.1 %) but low P removal (46.7 %) efficiency.

Moreover, when the influent N concentration increased, more N could be utilized to support the P uptake. So, the P removal increased with an increase in the influent N concentration. However, the P content would become the limitation restricting N consumption if a high influent N concentration is further increased. Thereby, the M-MSPBR system had a low N removal (55.8 %) but high P removal (92.7 %). Thus, it appears that there is an optimal N/P ratio that would benefit the growth and microalgae and achieve the discharge standard of both effluent N and P after treatment. Wang et al. also claimed that an extremely high or low N/P ratio of influent contributed to the microalgae growth decline [49]. Their study reported that the optimal N/P ratio for algal growth was suggested around 6.8-10, which also agrees with the result in this study (Figures 6.2 and 6.3). Moreover, this N/P ratio is also close to the ratio in domestic wastewater and secondary effluent (7.5-9.6) [50], indicating that the microalgae-based MSPBR has a high potential in wastewater treatment applications.

In summary, suitable operating conditions can improve the biological performance of M-MSPBR. According to this model, an influent N concentration = 40 mg/L, P concentration =5 mg/L, HRT = 1 day, and SRT = 40 days seems to be the optimal operating condition for high

biomass production and nutrient removal. The mathematical models proposed in this study can predict the changes in the biological performance of M-MSPBR under different process conditions (SRT and HRT) and wastewater characteristics (N/P ratio).

6.3.2. Model validation of microalgae system

For this validation process, the accuracy of model prediction was validated with the experimental results from the literature [14, 51]. Figure 6.5 shows the validation of total biomass concentration and the profile of effluent pollutant or pollutant removal at the steady state period, which were obtained by mathematical modelling prediction and experiment, respectively. The maximum difference between the modelling and experimental results was less than 45 %, while most of the differences between the modelling and experimental results were less than 20 %. This suggests that the mathematical models proposed in this study can effectively predict the impacts of process variables and wastewater characteristics on the biological performance of M-MSPBR. The accuracy of model prediction can be further improved, if more suitable kinetic parameters and stoichiometric coefficients are used for these specific (species) experimental systems. The kinetic parameters and stoichiometric coefficients used in this study are the typical values for microalgae but may not be perfect for the microalgae species used in the literature [14, 51].

Except for the nutrient profiles in Luo et al. work [14], the validation shows a reasonably good fit between the experimental and modelling data was achieved. The nutrient profiles in Luo et al. work [14] were lower than the model data, which might be attributed to the contamination of bacteria in the late period of their work [14]. They reported that the bacteria proportion reached 3.5% under the period of SRT = 30 d. As a result, those increased portions of bacteria interrupt microalgae's nutrient uptake, leading to a lower removal efficiency than the results of the model

simulation. The reason might be attributed to the complex consumption mechanism of nutrients in natural cases. The model validation indicated the real situation is a more complicated situation than the mathematic model. Unlike this model, in which phosphorus only consumed by microorganisms, the nutrient removal routes are diverse (biological and physicochemical) and would happen together simultaneously to affect the nutrient profile thus making it is complicated to predict [52, 53]. Moreover, the mono-microalgae system in wastewater is facing the risk of contamination by bacteria, which could impact biomass production and nutrient removal [54]. Thereby, more considerations such as interaction with bacteria should be taken into account in future model development.

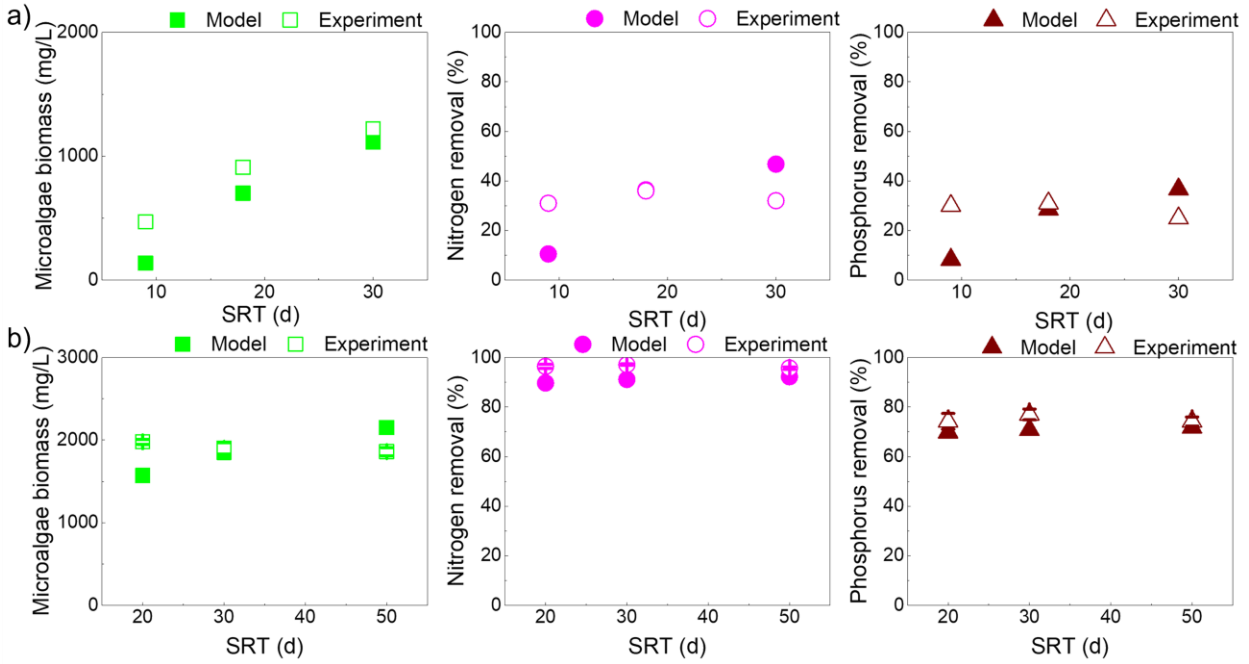

Figure 6.5. Model validation with experimental results of a) Luo et al.[14]work and b) Praveen et al.[51]work.

6.4. Conclusion

The modelling study can shorten the experiment setting time and provide ideal operating parameters for the design and operation of M-MSPBR. This study investigated the effects of SRT,

HRT and wastewater characteristics (N/P ratio) on the biological performance (microalgal biomass production, N and P removals) of M-MSPBR using mathematical modelling. The proposed mathematical models can effectively predict the impacts of process variables and wastewater characteristics on the biological performance of M-MSPBR. The modelling results suggest that there is an optimal SRT and N/P ratio that would enhance the microalgal biomass production and N and P removal. The modelling results are in good agreement with experimental results from the literature. For the mono-microalgal-based system, biomass production and nutrient removal increased with an increase in SRT and a decrease in HRT. When it comes to the nutrient concentration of the influent, biomass production increased with the influent N concentration increased. At the same time, pollutant removal could be restricted in extreme conditions (either high or low N concentration of influent). The optimal conditions are considered HRT = 1 day, SRT = 40 days, and influent of nitrogen concentration = 40 mg/L based on the high biomass production, acceptable pollutant removal, and frequent harvesting period.

In conclusion, this model inspires the future setting parameters for real-time M-MSPBR research and could contribute to the shortening of the expanded cost in the early period for optimization of operating parameters. However, microalgae cultivation in real nature is influenced by factors such as competition from other species, CO_2 concentration, temperature, pH, and light intensity besides HRT and SRT. A more complicated model that includes the impacts of other factors should be considered in future studies.

6.5. Reference

[1] Sathinathan, P., Parab, H., Yusoff, R., Ibrahim, S., Vello, V., Ngoh, G. (2023). Photobioreactor design and parameters essential for algal cultivation using industrial wastewater: A review. Renewable and Sustainable Energy Reviews, 173, 113096.

[2] Ting, H., Haifeng, L., Shanshan, M., Zhang, Y., Zhidan, L., Na, D. (2017). Progress in microalgae cultivation photobioreactors and applications in wastewater treatment: A review. International Journal of Agricultural and Biological Engineering, 10, 1-29.
[3] Gupta, P.L., Lee, S., Choi, H. (2015). A mini review: photobioreactors for large scale algal cultivation. World Journal of Microbiology and Biotechnology, 31, 1409-1417.
[4] Xu, Q., Huang, Q.S., Wei, W., Sun, J., Dai, X., Ni, B.J. (2020). Improving the treatment of waste activated sludge using calcium peroxide. Water Research, 187, 116440.
[5] Wang, L., Liu, J., Zhao, Q., Wei, W., Sun, Y. (2016). Comparative study of wastewater treatment and nutrient recycle via activated sludge, microalgae and combination systems. Bioresource technology, 211, 1-5.
[6] Aditya, L., Mahlia, T.I., Nguyen, L.N., Vu, H.P., Nghiem, L.D. (2022). Microalgae-bacteria consortium for wastewater treatment and biomass production. Science of The Total Environment, 838, 155871.
[7] Abdelfattah, A., Ali, S.S., Ramadan, H., El-Aswar, E.I., Eltawab, R., Ho, S.H., Elsamahy, T., Li, S., El-Sheekh, M.M., Schagerl, M. (2023). Microalgae-based wastewater treatment: Mechanisms, challenges, recent advances, and future prospects. Environmental Science and Ecotechnology, 13, 100205.
[8] Wollmann, F., Dietze, S., Ackermann, J.U., Bley, T., Walther, T., Steingroewer, J., Krujatz, F. (2019). Microalgae wastewater treatment: Biological and technological approaches. Engineering in Life Sciences, 19, 860-871.
[9] Sial, A., Zhang, B., Zhang, A., Liu, K., Imtiaz, S.A., Yashir, N. (2021). Microalgal–bacterial synergistic interactions and their potential influence in wastewater treatment: A review. BioEnergy Research, 14, 723-738.
[10] Morillas-España, A., Lafarga, T., Sánchez-Zurano, A., Acién-Fernández, F.G., González-López, C. (2022). Microalgae based wastewater treatment coupled to the production of high value agricultural products: Current needs and challenges. Chemosphere, 291, 132968.
[11] Moshood, T.D., Nawanir, G., Mahmud, F. (2021). Microalgae biofuels production: A systematic review on socioeconomic prospects of microalgae biofuels and policy implications. Environmental Challenges, 5, 100207.
[12] Mishra, N., Mishra, S., Prasad, R. (2021). Current Status and Challenges of Microalgae as an Eco-Friendly Biofuel Feedstock: A Review. Present Environment & Sustainable Development, 15, 179-189.
[13] Zhang, M., Yao, L., Maleki, E., Liao, B., Lin, H. (2019). Membrane technologies for microalgal cultivation and dewatering: Recent progress and challenges. Algal Research, 44, 101686.
[14] Luo, Y., Le-Clech, P., Henderson, R.K. (2018). Assessment of membrane photobioreactor (MPBR) performance parameters and operating conditions. Water Research, 138, 169-180.
[15] Gonzalez-Camejo, J., Jiménez-Benítez, A., Ruano, M., Robles, A., Barat, R., Ferrer, J. (2019). Optimising an outdoor membrane photobioreactor for tertiary sewage treatment. Journal of Environmental Management, 245, 76-85.
[16] Zhao, Z., Muylaert, K., Vankelecom, I.F. (2023). Applying membrane technology in microalgae industry: A comprehensive review. Renewable and Sustainable Energy Reviews, 172, 113041.
[17] Xu, M., Li, P., Tang, T., Hu, Z. (2015). Roles of SRT and HRT of an algal membrane bioreactor system with a tanks-in-series configuration for secondary wastewater effluent polishing. Ecological Engineering, 85, 257-264.

[18] Barbera, E., Sforza, E., Grandi, A., Bertucco, A. (2020). Uncoupling solid and hydraulic retention time in photobioreactors for microalgae mass production: A model-based analysis. Chemical Engineering Science, 218, 115578.
[19] Honda, R., Boonnorat, J., Chiemchaisri, C., Chiemchaisri, W., Yamamoto, K. (2012). Carbon dioxide capture and nutrients removal utilizing treated sewage by concentrated microalgae cultivation in a membrane photobioreactor. Bioresource Technology, 125, 59-64.
[20] Luo, Y., Le-Clech, P., Henderson, R.K. (2017). Simultaneous microalgae cultivation and wastewater treatment in submerged membrane photobioreactors: a review. Algal Research, 24, 425-437.
[21] Chen, X., Li, Z., He, N., Zheng, Y., Li, H., Wang, H., Wang, Y., Lu, Y., Li, Q., Peng, Y. (2018). Nitrogen and phosphorus removal from anaerobically digested wastewater by microalgae cultured in a novel membrane photobioreactor. Biotechnology for Biofuels, 11, 1-11.
[22] Chang, H., Fu, Q., Zhong, N., Yang, X., Quan, X., Li, S., Fu, J., Xiao, C. (2019). Microalgal lipids production and nutrients recovery from landfill leachate using membrane photobioreactor. Bioresource Technology, 277, 18-26.
[23] Honda, R., Teraoka, Y., Noguchi, M., Yang, S. (2017). Optimization of hydraulic retention time and biomass concentration in microalgae biomass production from treated sewage with a membrane photobioreactor. Journal of Water and Environment Technology, 15, 1-11.
[24] Ashadullah, A., Shafiquzzaman, M., Haider, H., Alresheedi, M., Azam, M.S., Ghumman, A.R. (2021). Wastewater treatment by microalgal membrane bioreactor: evaluating the effect of organic loading rate and hydraulic residence time. Journal of Environmental Management, 278, 111548.
[25] Zou, H., Rutta, N.C., Chen, S., Zhang, M., Lin, H., Liao, B. (2022). Membrane Photobioreactor Applied for Municipal Wastewater Treatment at a High Solids Retention Time: Effects of Microalgae Decay on Treatment Performance and Biomass Properties. Membranes, 12, 564.
[26] Eze, V.C., Velasquez-Orta, S.B., Hernández-García, A., Monje-Ramírez, I., Orta-Ledesma, M.T. (2018). Kinetic modelling of microalgae cultivation for wastewater treatment and carbon dioxide sequestration. Algal Research, 32, 131-141.
[27] Bello, M., Ranganathan, P., Brennan, F. (2017). Dynamic modelling of microalgae cultivation process in high rate algal wastewater pond. Algal Research, 24, 457-466.
[28] Feng, F., Li, Y., Latimer, B., Zhang, C., Nair, S.S., Hu, Z. (2021). Prediction of maximum algal productivity in membrane bioreactors with a light-dependent growth model. Science of The Total Environment, 753, 141922.
[29] Lee, E., Jalalizadeh, M., Zhang, Q. (2015). Growth kinetic models for microalgae cultivation: A review. Algal research, 12, 497-512.
[30] Bekirogullari, M., Figueroa-Torres, G.M., Pittman, J.K., Theodoropoulos, C. (2020). Models of microalgal cultivation for added-value products-A review. Biotechnology Advances, 44, 107609.
[31] Rittmann, B.E., McCarty, P.L. (2020). Environmental biotechnology: principles and applications. McGraw-Hill Education: New York.
[32] Lee, L., Hsu, C.Y., Yen, H.W. (2017). The effects of hydraulic retention time (HRT) on chromium (VI) reduction using autotrophic cultivation of *Chlorella vulgaris*. Bioprocess and Biosystems Engineering, 40, 1725-1731.
[33] Wang, Y.N., Pang, H., Yu, C., Li, C., Wang, J.H., Chi, Z.Y., Xu, Y.P., Li, S.Y., Zhang, Q., Che, J. (2022). Growth and nutrients removal characteristics of attached *Chlorella sp*. using

synthetic municipal secondary effluent with varied hydraulic retention times and biomass harvest intervals. Algal Research, 61, 102600.
[34] Vu, M.T., Nguyen, L.N., Mofijur, M., Johir, M.A.H., Ngo, H.H., Mahlia, T., Nghiem, L.D. (2022). Simultaneous nutrient recovery and algal biomass production from anaerobically digested sludge centrate using a membrane photobioreactor. Bioresource technology, 343, 126069.
[35] Matamoros, V., Rodriguez, Y. (2016). Batch vs continuous-feeding operational mode for the removal of pesticides from agricultural run-off by microalgae systems: A laboratory scale study. Journal of Hazardous Materials, 309, 126-132.
[36] Solís-Salinas, C.E., Patlán-Juárez, G., Okoye, P.U., Guillén-Garcés, A., Sebastian, P., Arias, D.M. (2021). Long-term semi-continuous production of carbohydrate-enriched microalgae biomass cultivated in low-loaded domestic wastewater. Science of The Total Environment, 798, 149227.
[37] Valigore, J.M. (2011). Microbial (microalgal-bacterial) biomass grown on municipal wastewater for sustainable biofuel production [Doctoral dissertation]. University of Canterbury.
[38] Lai, Y.S., McCaw, A., Ontiveros-Valencia, A., Shi, Y., Parameswaran, P., Rittmann, B.E. (2016). Multiple synergistic benefits of selective fermentation of *Scenedesmus* biomass for fuel recovery via wet-biomass extraction. Algal Research, 17, 253-260.
[39] Wang, Z., Lee, Y.Y., Scherr, D., Senger, R.S., Li, Y., He, Z. (2020). Mitigating nutrient accumulation with microalgal growth towards enhanced nutrient removal and biomass production in an osmotic photobioreactor. Water Research, 182, 116038.
[40] Pastore, M., Primavera, A., Milocco, A., Barbera, E., Sforza, E. (2022). Tuning the Solid Retention Time to Boost Microalgal Productivity and Carbon Exploitation in an Industrial Pilot-Scale LED Photobioreactor. Industrial & Engineering Chemistry Research, 61, 7739-7747.
[41] Martınez, M., Sánchez, S., Jimenez, J., El Yousfi, F., Munoz, L. (2000). Nitrogen and phosphorus removal from urban wastewater by the microalga *Scenedesmus obliquus*. Bioresource Technology, 73, 263-272.
[42] Di Termini, I., Prassone, A., Cattaneo, C., Rovatti, M. (2011). On the nitrogen and phosphorus removal in algal photobioreactors. Ecological Engineering, 37, 976-980.
[43] Gao, F., Yang, Z.H., Li, C., Wang, Y., Jin, W., Deng, Y. (2014). Concentrated microalgae cultivation in treated sewage by membrane photobioreactor operated in batch flow mode. Bioresource Technology, 167, 441-446.
[44] Discart, V., Bilad, M., Van Nevel, S., Boon, N., Cromphout, J., Vankelecom, I. (2014). Role of transparent exopolymer particles on membrane fouling in a full-scale ultrafiltration plant: feed parameter analysis and membrane autopsy. Bioresource technology, 173, 67-74.
[45] Dang, B.T., Tran, C.S., Le, T.S., Nguyen, V.T., Nguyen, T.B., Lin, C., Varjani, S., Dao, T.S., Bui, T.V., Bui, X.T. (2022). Influence of nitrogen species and biomass retention time on nutrient removal and biomass productivity in a microalgae-based bioreactor. Environmental Technology & Innovation, 28, 102880.
[46] Solmaz, A., Işik, M. (2019). Effect of sludge retention time on biomass production and nutrient removal at an algal membrane photobioreactor. BioEnergy Research, 12, 197-204.
[47] Xin, L., Hong-Ying, H., Ke, G., Ying-Xue, S. (2010). Effects of different nitrogen and phosphorus concentrations on the growth, nutrient uptake, and lipid accumulation of a freshwater microalga *Scenedesmus sp*. Bioresource Technology, 101, 5494-5500.

[48] Gao, F., Peng, Y.Y., Li, C., Cui, W., Yang, Z.H., Zeng, G.M. (2018). Coupled nutrient removal from secondary effluent and algal biomass production in membrane photobioreactor (MPBR): Effect of HRT and long-term operation. Chemical Engineering Journal, 335, 169-175.
[49] Wang, L., Min, M., Li, Y., Chen, P., Chen, Y., Liu, Y., Wang, Y., Ruan, R. (2010). Cultivation of green algae *Chlorella sp*. in different wastewaters from municipal wastewater treatment plant. Applied Biochemistry and Biotechnology, 162, 1174-1186.
[50] Bilad, M., Discart, V., Vandamme, D., Foubert, I., Muylaert, K., Vankelecom, I.F. (2014). Coupled cultivation and pre-harvesting of microalgae in a membrane photobioreactor (MPBR). Bioresource Technology, 155, 410-417.
[51] Praveen, P., Xiao, W., Lamba, B., Loh, K.C. (2019). Low-retention operation to enhance biomass productivity in an algal membrane photobioreactor. Algal Research, 40, 101487.
[52] Cuellar-Bermudez, S.P., Aleman-Nava, G.S., Chandra, R., Garcia-Perez, J.S., Contreras-Angulo, J.R., Markou, G., Muylaert, K., Rittmann, B.E., Parra-Saldivar, R. (2017). Nutrients utilization and contaminants removal. A review of two approaches of algae and cyanobacteria in wastewater. Algal Research, 24, 438-449.
[53] Luo, G. (2022). Review of waste phosphorus from aquaculture: Source, removal and recovery. Reviews in Aquaculture, 15, 1058-1082.
[54] Wang, H., Deng, L., Qi, Z., Wang, W. (2022). Constructed microalgal-bacterial symbiotic (MBS) system: Classification, performance, partnerships and perspectives. Science of The Total Environment, 803, 150082.

Chapter 7: A study of theoretical analysis and modelling of microalgal-bacterial membrane photobioreactor

Abstract

This study presents a theoretical analysis and modelling of microalgae-bacterial membrane photobioreactors (MB-MPBRs) for wastewater treatment. A set of mathematical models was developed to describe the membrane photobioreactor performances in a microalgae-bacteria system, respectively. These models were used to study the effects of process conditions (hydraulic retention time (HRT) and solid retention time (SRT)) and wastewater characteristics (substrate/COD concentrations and COD/N ratio in influent) on the biological performance such as biomass production (bacteria and microalgae) and pollutants (COD, N and P) removals. The model was calibrated and validated using experimental data from laboratory studies in the literature. The results showed that the model can accurately predict the performance of the microorganism system except for some nutrient profiles due to their complicated consumption mechanisms in real cases. The findings suggest that optimizing these parameters can significantly improve the removal of organic matter and nutrients and the productivity of biomass and bioenergy in MBMPBRs. This study uses mathematical modelling tools to provide new insights into the design and operation of MBMPBRs for sustainable wastewater treatment.

Keywords: Modeling; Microalgae; Bacteria; Microalgal-bacterial consortium; Membrane photobioreactor; Wastewater

7.1. Introduction

The activated sludge process is a traditional biological wastewater treatment technology that could deal with high organic pollutant influents such as municipal wastewater [1]. Despite the activated sludge process being applied worldwide in wastewater treatment; activated sludge is still facing the challenges, such as an energy-intensive process and low-efficiency removal of nutrients (nitrogen, phosphorus) [2-4]. In order to further improve the biological wastewater treatment process, microalgal-based wastewater treatment is suggested to replace the activated sludge [5]. Compared to conventional activated sludge biological treatment, microalgae-based wastewater treatment not only has effective nutrient removal but also could provide microalgal feedstock for downstream applications such as biofuel or biodiesel production to alleviate the pressure from energy crisis and to earn more economic benefits [6-8]. However, microalgae process application has been hindered in the laboratory stage due to shortages such as diluted suspended microalgae concentration, difficult lipid extraction, and limitation of water purification [5, 9, 10]. Literature also argued that the effluent obtained from individual microalgae strains treatment might not reach the treatment standard for discharge [11, 12]. As a result, a muti-microsystem would be better for bioreactor cultivation in wastewater treatment due to benefits from symbiotic interactions, such as higher production yield, lower risk of contamination, lower operation maintenance, and capacity of multiple-pollutant removal [13-15], between microalgae and bacteria.

Moreover, it is hard to maintain the purity of individual microalgae strains in wastewater because of the open system and contamination from real wastewater [11, 16, 17]. Thus, an alternative solution suggested by some literature is to develop a microalgae-bacterial co-culture in the bioreactor to take full advantage of these two kinds of microorganisms. On the one hand,

bacteria have a very high removal efficiency of organic matter from wastewater [18] and produce CO_2 as an inorganic carbon source for microalgae growth. Moreover, the bacteria could be a flocculant to promote the aggregation of microalgae cells through their extracellular polymeric substances (EPSs), which could further increase the microorganism biomass harvest yield [19, 20]. On the other hand, microalgae in the system could not only fill the nutrient limitation in activated sludge treatment but also reduce the oxygen supply due to the oxygen production from the photosynthesis of microalgae [12]. Thus, the microalgal-bacterial consortium can potentially develop a self-sustainable ecosystem for simultaneous COD, and N and P removal in a single step. Indeed, even though the microalgae-bacterial combination achieves high removal efficiency of either COD or nutrients, the industrial application hasn't been achieved due to the lack of fundamental knowledge and the challenge of racing competition between microalgae and bacteria. As Wang et al. mentioned, bacteria will secret some biotoxin to inhibit the growth of nearby ethnic groups [21]. Mayali and Azam found that microalgae growth inhibition was induced by extracellular algicidal compounds released from bacteria such as *Alteromonas* and *Pseudoaltermonas* [22]. Overall, microalgae-bacterial cultivation is a double-edged sword. We could benefit from this combination in many aspects, such as better removal efficiency, cost and energy reduction, and higher production yield [11]. However, the system could collapse if the setting parameters are inappropriate [13]. Thus, more and more laboratory experiments were carried out to determine the optimal operational conditions.

However, multiple factors affect microalgae-bacterial cultivation, such as process conditions (solids retention time (SRT) and hydraulic retention time (HRT)), species, influent composition (COD/N/P ratios), O_2 and CO_2 concentrations, temperature, and illumination intensity [23]. It is a time-consuming and high-cost requirement to determine the optimal conditions. In

order to shorten the time spent on optimizing microalgae-bacterial cultivation, several mathematical models were introduced to develop a more comprehensive understanding of the development of the conventional microalgae-bacterial ecosystem [24-27]. We are aware of no reported modelling studies on the impact of process conditions and wastewater characteristics on the biological performance of the novel and emerging MB-MSPBR.

This work aims to develop a set of mathematical models to simulate and model the impact of process variables (SRT and HRT) and wastewater characteristics (COD/N/P ratios) on the biological performance (bacteria production, microalgae production, COD, total N and total P removals) of the MB-MSPBR systems and validate the accuracy of the modelling results with experimental results from the literature. The model allows for predicting the evolution of the main variables of the microalgae-bacterial system, such as biomass concentrations, effluent nutrients (N and P) and substrate (COD) concentrations. The model has been calibrated and validated using experimental data from previous studies in the literature. This model has proved to be a powerful tool for optimizing the design and operation of MB-MSPBR systems.

7.2. Methods –model design and model variables

7.2.1. Model design

The microalgal-bacterial system model was inherited from the previous mono-microalgae system, and the development proceeded through the steps indicated in Figure 7.1. In the mono-microalgae MPBR system, the microalgal biomass and nutrients mass balance under the steady state could be expressed in the following equations [28]:

$$SRT\left(\frac{\mu_m S_N S_P}{(K_N+S_N)(K_P+S_P)} - k_{d-m}\right) = 1 \qquad (7.1)$$

$$S_i^0 - S_i - HRT\frac{X_m\mu_m S_N S_P}{Y_i(K_N+S_N)(K_P+S_P)} = 0 \qquad (7.2)$$

S_i^0- Initial nutrient concentration in MPBR, i = N, P; mgL^{-1}

S_i- Nutrient concentration in effluent, i = N, P; mgL^{-1}

X_m-microalgae concentration in discard suspension, gL^{-1}

μ_m-maximum growth rate of microalgae, day^{-1}

S_N-total nitrogen concentration in membrane photobioreactor, mgL^{-1}

S_P-total phosphorus concentration in membrane photobioreactor, mgL^{-1}

K_N-half saturation constant of NH_4^+ and NO_3^-, mgL^{-1}

K_P- half-saturation constant of HPO_4^{2-}, mgL^{-1}

k_{d-m}-decay coefficient of microalgae, d^{-1}

Y_i- removal coefficient of nutrient, i = N,P; g algae · g $nutrient^{-1}$

Based on microalgae mass balance, the bacterial performance in MPBR was introduced into the system. Thus, the microalgal-bacterial system in MPBR could be divided into two parts. For bacterial, the biomass growth is assumed only be limited by substrate/COD uptake; thus the mass balance equation could be expressed as:

$$V\frac{dX_b}{dt} = QX_b^0 - Q^w X_b + V(\frac{\mu_b X_b S_S}{(K_S+S_S)} - X_b k_{d-b}) \qquad (7.3)$$

Where X_b^0-initial concentration of bacteria in MPBR, gL^{-1}

X_b-bacteria concentration in discard suspension, gL^{-1}

μ_b-maximum growth rate of bacteria, day^{-1}

S_s-Substrate concentration in MPBR gL^{-1}

K_S- half-saturation constant of the substrate, mgL^{-1}

$k_{d\text{-}b}$-decay coefficient of bacteria, d^{-1}

Q-Flow rate of influence, $L \cdot d^{-1}$

Q^w- Discard rate of the biomass suspension, $L \cdot d^{-1}$

V-effective volume of membrane photobioreactor, L

Under the steady state, biomass maintains a relatively stable value, which means the changing rate $V\frac{dX_b}{dt} = 0$, and the initial bacteria biomass $X_b{}^0$ is assumed as zero,

Thus, the equation for bacteria could be changed to:

$$-Q^w X_b + V(\frac{\mu_b X_b S_S}{(K_S+S_S)} - X_b k_{d-b}) = 0 \qquad (7.4)$$

Divided by $Q^w X_b$, equation (7.4) can be simplified to:

$$-1 + \frac{VX_b}{Q^w X_b}(\frac{\mu_b S_S}{(K_S+S_S)} - k_{d-b}) = 0,$$

Since SRT $=\frac{VXb}{Q^w Xb}$, we can get the equation:

$$SRT(\frac{\mu_b S_S}{(K_S+S_S)} - k_{d-b}) = 1 \qquad (7.5)$$

Similarly, biomass mass balance for microalgae can be derived from the microalgae part without substrate component:

$$SRT\left(\frac{\mu_m S_N S_P}{(K_N+S_N)(K_P+S_P)} - k_{d-m}\right) = 1 \quad (7.6)$$

Similar to nutrient mass balance, the substrate/COD concentration in the MPBR is equal to the sum of the influent medium concentration (QS_S^0) and the deduction of nutrients in the effluent (QS_S) and consumption of bacterial metabolism ($\gamma_{\omega t_S}$) Thus, the substrate/COD mass balance can be expressed as the following equation: substrate mass balance for bacterial, we can know that:

$$V\frac{dS_S}{dt} = QS_S^0 - QS_S + \gamma_{\omega t_S} \quad (7.7)$$

$\gamma_{\omega t_S}$-Substrate/COD consumption of bacterial metabolism, which:

$$\gamma_{\omega t_S} = -\frac{\mu_b X_b V S_S}{Y_s(K_S+S_S)} \quad (7.8)$$

Where Y_s- bacterial cell yield, mg bacteria · mg substrate^{-1}

Under steady state, $V\frac{dS_S}{dt} = 0$,

Thus, $0 = Q(S_S^0 - S_S) - \frac{\mu_b X_b V S_S}{Y_s(K_S+S_S)}$, divided Q, we can simplify the equation to:

$$(S_S^0 - S_S) - HRT \cdot \frac{\mu_b X_b S_S}{Y_s(K_S+S_S)} = 0 \quad (7.9)$$

For the microalgal part, the microalgal biomass production is assumed to be only limited by the nutrients (nitrogen and phosphorus). So, the microalgal biomass mass balance equation (Equation (7.1)) doesn't change. When it comes to nutrient profile, the nitrogen concentration in the MB-MSPBR in the microalgal-bacterial system is equal to the sum of the influent medium concentration (QS_N^0) and the deduction of nutrients in the effluent (QS_N) and consumption of

microalgal metabolism ($\gamma_{\omega t_N}$) and the uptake from bacteria metabolism ($\gamma_{\omega t_S} Y_b \cdot 0.125$). Thus, the nutrient (N and P) mass balance equation will be modified as the following equation:

$$V\frac{dS_N}{dt} = QS_N^0 - (QS_N + \gamma_{\omega t_S} Y_b \cdot 0.125 + \gamma_{\omega t_N}) \qquad (7.10)$$

$\gamma_{\omega t_N}$ -Nitrogen consumption of microalgae metabolism in the Microalgal-Bacterial system,

$$\gamma_{\omega t_N} = -\frac{\mu_m X_m V S_N S_P}{Y_{N-M}(K_N+S_N)(K_P+S_P)} \qquad (7.11)$$

$Y_{N\text{-}M}$- microalgae cell yield based on nitrogen, mg microalgae · mg Nitrogen^{-1}

Under steady state, $V\frac{dS_N}{dt} = 0$,

The equation can be changed and simplified to:

$$S_N^0 - S_N - HRT \cdot \frac{X_b}{SRT} \cdot 0.125 - HRT\left(\frac{S_N S_P}{(K_N+S_N)(K_P+S_P)} \cdot \frac{\mu_m X_m}{Y_{N-M}}\right) = 0 \qquad (7.12)$$

Similarly, the phosphorus concentration in the MB-MSPBR system is equal to the sum of the influent medium concentration (QS_P^0) and the deduction of nutrients in the effluent (QS_P) and consumption of microalgal metabolism ($\gamma_{\omega t_P}$) and the uptake of bacteria metabolism ($\gamma_{\omega t_S} Y_b \cdot 0.025$), which is expressed as the following equation:

$$V\frac{dS_P}{dt} = QS_P^0 - (QS_P + \gamma_{\omega t_S} Y_b \cdot 0.025 + \gamma_{\omega t_P}) \qquad (7.13)$$

$\gamma_{\omega t_P}$-Phosphorus consumption of microalgae metabolism in the Microalgal-Bacterial system,

$$\gamma_{\omega t_P} = -\frac{\mu_m X_m V S_N S_P}{Y_{P-M}(K_N+S_N)(K_P+S_P)} \qquad (7.14)$$

$Y_{P\text{-}M}$- microalgae cell yield based on phosphorus, mg algae · mg Phosphorus^{-1}

Furthermore, the equation (7.11) can be simplified to:

$$S_P^0 - S_P - HRT \cdot \frac{X_b}{SRT} \cdot 0.025 - HRT\left(\frac{S_N S_P}{(K_N+S_N)(K_P+S_P)} \cdot \frac{\mu_m X_m}{Y_{P-M}}\right) = 0 \qquad (7.15)$$

$S^0_{i\ i=S,N,and\ P}$ – influent concentration of substrate, nitrogen and phosphorus, respectively, mgL^{-1}.

$S_{\ i=S,N,and\ P}$ – effluent concentration of substrate, nitrogen and phosphorus, respectively, mgL^{-1}.

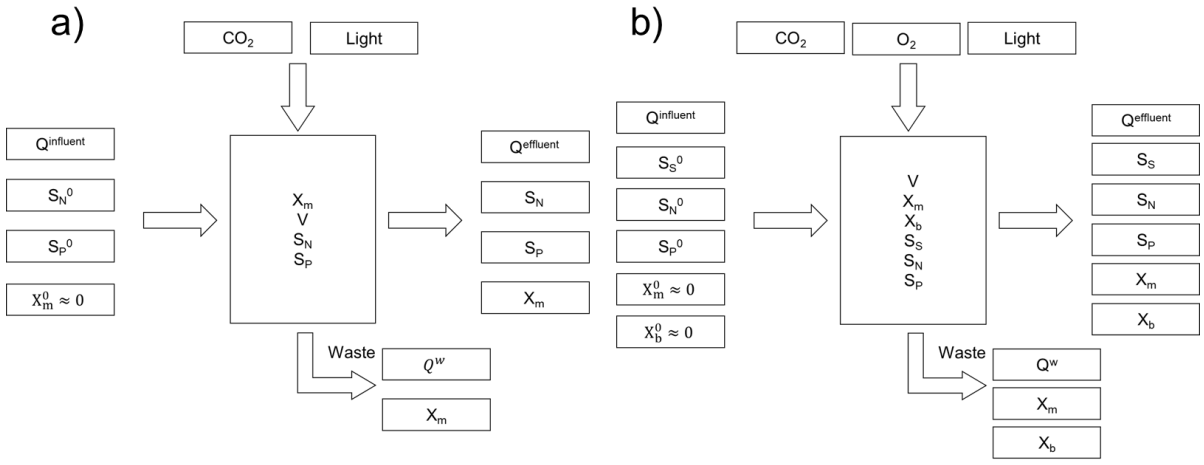

Figure 7.1. The a) microalgae and b) microalgae-bacteria model process development.

7.2.2. Model variables

The model variables were employed based on the general microorganism growth kinetics from previous studies and are listed in the following table:

Table 7.1. Growth kinetic parameters for the modelling study.

Kinetic parameters	Value	Ref
μ_b (d^{-1})	5	[29-31]
μ_m (d^{-1})	1.68	[29-31]
k_{d-b} (d^{-1})	0.10	[29-31]
k_{d-m} (d^{-1})	0.06	[29-31]
Y_s (mg biomass·mg substrate^{-1})	0.5	[29-31]
Y_{N-M} (mg biomass·mg nitrogen^{-1})	15.8	[29-31]
Y_{P-M} (mg biomass·mg phosphorus^{-1})	114	[29-31]
K_S (mg substrate·L^{-1})	25	[29-31]
K_N (mg nitrogen·L^{-1})	24.5	[29-31]
K_P (mg phosphorus·L^{-1})	3.39	[29-31]

There are five variables X_b, X_m, S, S_N, and S_P and five independent equations (Equations (7.5), (7.6), (7.9), (7.12), and (7.15)). Microsoft Excel Solver was used to solve these five equations and get the five variables' results under different SRT, HRT, and COD/N/P ratio conditions.

7.3. Result and discussion

7.3.1. Microalgae-bacteria system

The microalgae-bacteria photobioreactor is more complicated than the mono-specie system. It needs to consider the interaction between the microalgae and bacteria. As Gao et al. mentioned, the COD concentration of influent influences the M-B system [32].

Figures 7.2, 7.3 and 7.4 show the performances of the MB-MSPBR with the condition of microalgae-bacteria co-system under different SRTs (20, 30, and 40 days), HRTs (1-5 days), and influent COD concentrations (300-600 mg COD/L) conditions. As shown in Figure 7.2, the bacterial, microalgal and total biomass concentrations reduced with the increase of HRT while increasing with the increase of SRT. The maximum bacterial, microalgal and total biomass concentration was 1597 mg/L. 5707 mg/L, and 7305 mg/L respectively when HRT = 1 d and SRT = 40 d with the influent COD concentration = 400 mg/L. Moreover, the microalgae exhibited a high biomass concentration compared to bacterial (5707 mg/L vs 1598 mg/L at HRT = 1 d, SRT = 40 d, and influent COD = 400 mg/L), which indicated that microalgae are the dominant part in this system. Accordingly, the changes in total biomass production are very similar to that of one of the microalgae biomass curves, which also achieved the highest level at HRT = 1 d and SRT = 40 d with the influent COD concentration = 400 mg/L.

Moreover, Figure 7.3 displayed the biomass concentration profiles under different influent COD concentrations and SRT at HRT = 1 d. The bacterial biomass concentration increased with an increase of influent COD concentration, while the microalgae concentration decreased with the rise of influent COD concentration. The bacterial increased from 1197.54 mg/L to 2396.41 mg/L with the rising of influent COD concentration from 300 mg/L to 600 mg/L. In comparison, the

microalgae biomass concentration decreased from 5967.39 mg/L to 5202.10 mg/L at the conditions of HRT =1 d and SRT = 40 d. This could be due to the competition of bacteria produced by the increased COD for nutrients (N and P), and thus, there was less N and P for microalgae growth. The total biomass concentration slightly increased with the increase of influent COD concentration at high SRT (SRT = 30 d and 40 d) while slightly decreased with the augment of influent COD concentration at low SRT level (SRT = 10 d and 20 d). These results suggest that N and P rather than COD levels are the limited nutrients for both bacteria and microalgae growth. As the growth of bacteria (with a larger $\mu_{max\text{-}b}$) is larger than that of microalgae (with a smaller $\mu_{max\text{-}m}$); thus, the increased COD would favor the growth of bacteria taking additional N and P and reduce the availability of N and P for slower growth of microalgae. This explains the increase in bacteria concentration and decrease in microalgae concentration with an increase in the COD level, as shown in Figure 7.3.

As shown in Figure 7.4, the COD concentration of effluent decreased with an increase of SRT. The COD concentration of effluent was extremely low (below 2 mg/L) and exhibited a relatively high removal efficiency (above 99%). The N and P concentrations of effluent decreased with an increase in SRT. The N concentration of effluent increased with an increase of influent COD concentration while the P concentration of effluent decreased. The maximum N concentration, as shown in Figure 7.4, was 9.91 mg/L when SRT = 10 and influent COD concentration = 600 mg/L at HRT = 1 d. The maximum P concentration of effluent in Figure 7.4 was 2.04 mg/L when the SRT = 10 d and influent COD concentration = 300 mg/L at HRT = 1 d.

The modelling results suggest that with appropriate selections of SRT, HRT, and wastewater characteristics (COD/N/P ratio), it is feasible to achieve simultaneous COD/BOD and nutrients (N and P) removals in a single step of MB-MSPBR system.

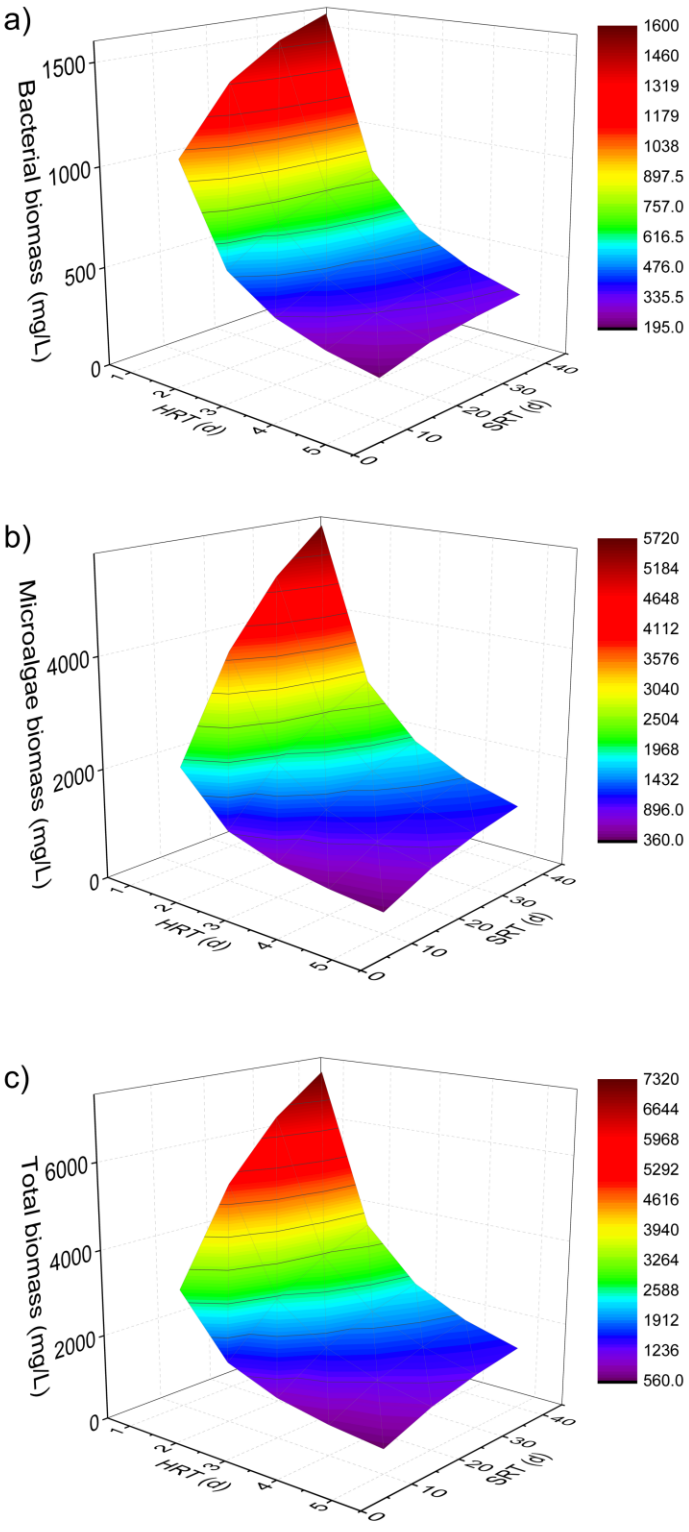

Figure 7.2. a) Bacteral, b) microalgal, and c) total biomass concentration under different HRT and SRT with influent COD concentration = 400 mg/L.

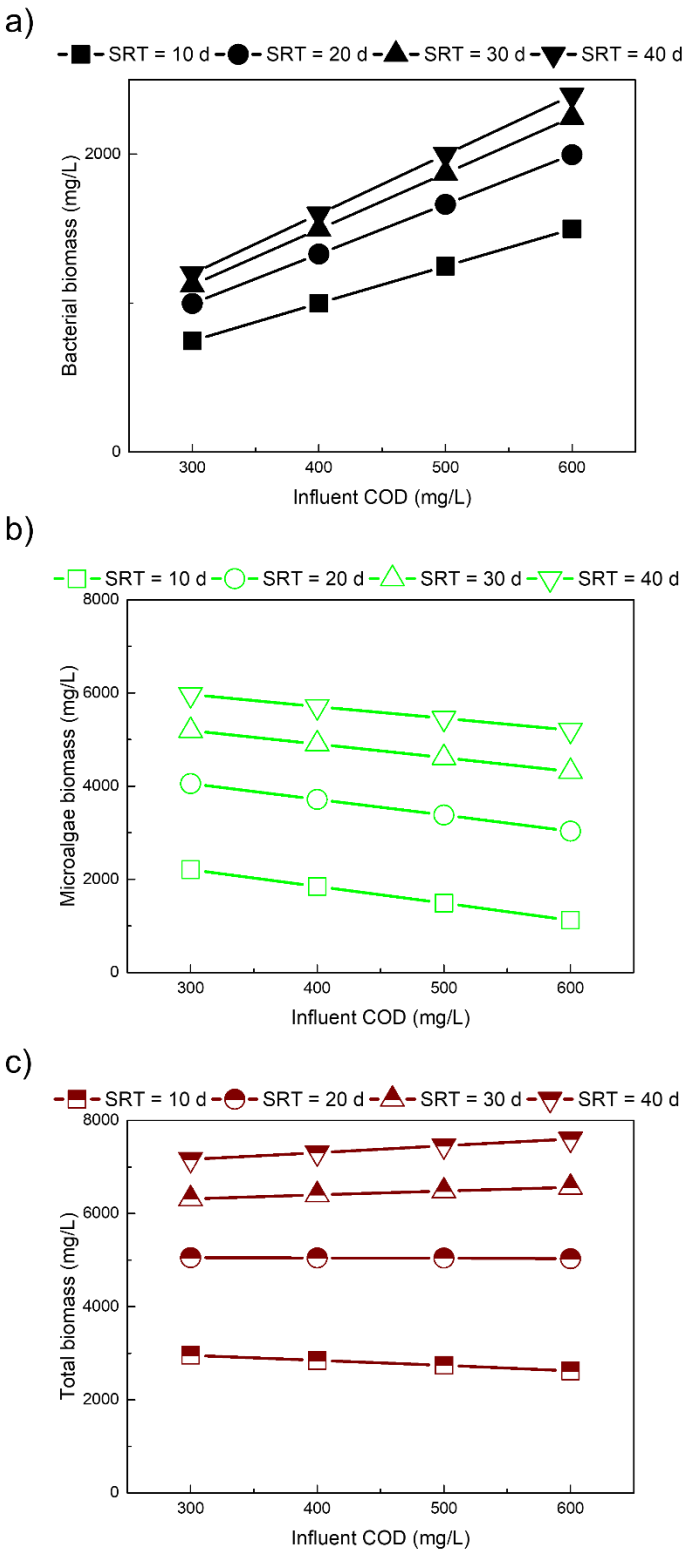

Figure 7.3. a) Bacteral, b) microalgal, and c) total biomass concentration under different SRT and COD concentrations of influent at HRT = 1 d.

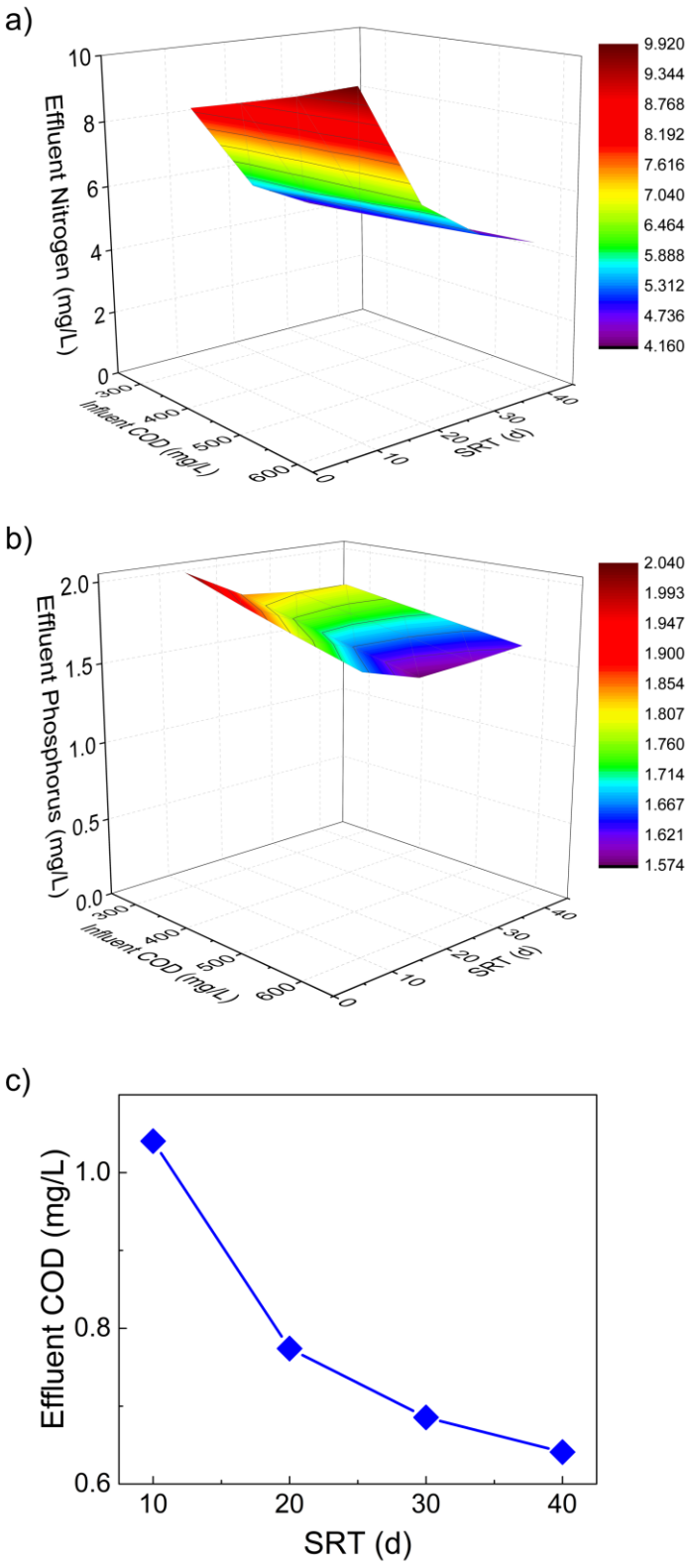

Figure 7.4. a) Nitrogen, b) Phosphorus, and c) COD concentration of effluent under different SRT and influent COD concentration at HRT = 1 d.

7.3.1.1. HRT effect

7.3.1.1.1. Biomass concentration

In this model, the bacteria and microalgae biomass concentration is directly related to the consumed nutrient (COD, nitrogen, or phosphorus) amount which is determined by their loading rates. As Figure 7.2 shows, a decrease in microorganism (both bacteria and microalgae) biomass concentration caused by the increase of HRT could be attributed to the insufficient nutrient loading that limits the microorganism biomass production, thus reducing the biomass concentration. In this model, the biomass concentration is indirectly negatively correlated to HRT. Firstly, the prolonged HRT caused the rising of nutrients (COD, nitrogen, or phosphorus) consumption efficiency ($\gamma_{\omega t_i}$, i = S, N, P) based on the mass balance. As a result, the biomass concentration decreased with the increase of nutrient uptake due to it being negatively correlated to the nutrient consumption efficiency. Similar phenomena were also found in other experimental studies. Zhang et al. reported that the membrane photobioreactor yielded higher microorganism biomass concentration under the same N/P ratio when decreasing HRT from 3 d to 2 d [33]. Furthermore, the bacterial biomass production became very low at a long HRT (149.35 mg/L at HRT =5 d, SRT = 10 d, and influent COD = 300 mg/L), which indicated that longer HRT is not suitable for bacterial biomass accumulation. Even though the microalgae biomass concentration also exhibited a similar decline tendency with an increase of HRT, the microalgae biomass still maintained a higher biomass concentration than bacteria (441.36 mg/L at the same conditions) under a long HRT. This could be ascribed to the higher decay rate of bacteria ($k_{d\text{-}b}$ = 0.1 d^{-1}), leading to a lower tolerance of low nutrient loading when compared to microalgae ($k_{d\text{-}m}$ = 0.06 d^{-1}).

7.3.1.1.2. Pollutant removal

There was no significant change in pollutant removal was found with the variation of HRT. As shown in Figure 7.4, the COD removal efficiency was above 99% (residual nutrient concentrations were below 2 mg/L). The COD removal was too high to show a significant correlation to HRT. This could be attributed to the fact that COD consumption in the M-B model was not limited in this range, which resulted in a maximal removal efficiency (above 99 %). Regarding N or P removal, the removal efficiency was also kept constant with HRT increased. These phenomena could be ascribed to the fact that the pollutant concentration of effluent in the mass balance equation was only controlled by SRT, kinetic constants, and stoichiometric coefficients but not the HRT [34]. In the premise of the SRT constant, the nutrient concentration would remain constant based on the mass balance (Equations (7.5) and (7.6)). As a result, the variation of HRT only causes the changing of biomass concentration (Equations (7.9), (7.12), and (7.15)), not the effluent COD, N and P concentrations and removals.

7.3.1.2. SRT effect

7.3.1.2.1. Biomass concentration

Regarding SRT, the biomass concentrations were positively correlated with the SRT. Unlike HRT, the influence of SRT on biomass concentration is indirect. Firstly, the pollutant concentration of effluent would decrease to maintain the steady state when the SRT on the right side of the biomass mass balance equation increases (Equations (7.5) and (7.6)). Next, the right side of the pollutant mass balance equations (Equations (7.9), (7.12), and (7.15)) would increase the biomass concentration with the reduction of pollutant concentration of effluent to maintain the steady state. As a result, biomass concentration became larger with the rising of SRT (Figures 7.2

and 7.3). In the experimental case, this could be attributed to the longer SRT resulting in higher biomass accumulation due to the smaller biomass waste rate [35].

7.3.1.2.2. Pollutant removal

As shown in the mass balance of biomass (Equations (7.5) and (7.6)), the SRT directly negatively affects the pollutant (substrate/COD and nutrients (N and P)) concentrations. Similarly, the substrate/COD removal was still at a very high level (above 99%) due to the fact that it reached the maximal consumption (minimal substrate/COD concentration of effluent). Despite the N and P removals also being high (above 75% and 70%, respectively), the effect brought from SRT could still be recognized. The N removal increased from 78% to 89% (effluent concentration from 8.81 mg/L to 4.29 mg/L) when the SRT increased from 10 d to 40 d (HRT = 1 d, influent COD = 400 mg/L). P removal also showed a similar trend under the same conditions (from 72% to 75%). In the biomass mass balance equations (Equations (7.5) and (7.6)) of this model (both microalgae and bacteria), the augment of SRT caused the reduction of the pollutant concentration of effluent on the right side of the equation to maintain the constant state. From the view of biomass concentration, the prolonged SRT increases the accumulation of microorganisms, resulting in higher pollutant uptake. Thus, the pollutants (COD, N, and P) concentrations of effluent decreased (Figure 7.4). The experimental study also reported a similar performance in that pollutant removal efficiency increased when the SRT rose from 2 d to 10 d [36]. Unlike the experimental studies, the microorganism growth rate was kept constant. The variables in this model were only affected by the limited parameters (HRT, SRT, COD concentration), which suggested employing SRT as long as possible. However, the extremely long SRT was not suggested in real wastewater treatment because it will increase the microorganism decay and decrease the effluent quality [37]. The light limitation in a high biomass concentration is also a concern. One possible explanation might be

microorganism decay increases due to the increasing competition potential between the species caused by the higher biomass amount, leading to cell breakage and worsening nutrient consumption [38]. Segredo-Morales et al. also claimed that the effluent has higher COD and nutrient concentrations at a prolonged SRT when using a microalgal-bacterial membrane photobioreactor to treat secondary wastewater [35].

7.3.1.3. COD concentration effect

7.3.1.3.1. Biomass concentration

The COD concentration of influent showed significant effects on bacterial and microalgae biomass concentrations. This could be ascribed to the promoted bacterial biomass by rising influent COD concentration restricting the microalgae growth by competing for the fixed amount of nutrients (N and P). As Equation (7.9) shows, the COD mass balance was controlled by the changing between effluent concentration and bacterial biomass concentration under the same conditions (HRT was considered constant in this case). The stable COD/substrate profile of effluent indicated that the COD consumption was not limited and reached maximal at this range (influent COD around 300 mg/L to 600 mg/L). Thus, the effluent COD concentration could be assumed to be constant with minimal changes. Therefore, the bacterial biomass concentration (X_b) on the right side of Equation (7.9) increased with the augment of influent COD concentration (S_0).

Moreover, the nutrient (N and P) concentrations of effluent were only affected by the SRT (Equation (7.6)); there should not be any significant shift of nutrient concentrations of effluent under different influent COD concentrations. So, the microalgae biomass concentration (X_m) on the left side of the nutrient mass balance (Equations (7.12) and (7.15)) would decrease due to the increase of X_b, which competes for the limited nutrients (N and P). The total biomass concentration

decreased with the influent COD concentration increased at a low SRT level but increased with the increase of influent COD concentration at a high SRT level, which indicated that high SRT was beneficial to microbial biomass production in this system. This phenomenon could be ascribed to the bacterial biomass concentration affected by influent COD concentration contributing more significantly to the microalgal biomass concentration reduction at low SRT level in the mass balance equations, thus affecting the total biomass concentration.

7.3.1.3.2. Pollutant removal

The pollutant profiles of effluent didn't exhibit an obvious correlation with the influent COD concentration. The stable COD removal could be attributed to the previously mentioned maximal COD consumption leading to the changing of effluent COD concentration being too small to be observed. For nutrients, the N concentration of effluent increased with the influent COD concentration, while the P concentration of effluent decreased. This might be attributed to the high microalgae cell yield based on P compared to the one based on N (114 mg biomass/mg P vs 15.8 mg biomass/mg N). Compared to the P concentration of effluent, the N concentration of effluent was more significantly affected by the changing of the microalgal biomass uptake part than the bacterial consumption part (Equations (7.12) and (7.15)). As a result, the N concentration of effluent increased with the decrease of the microalgal biomass (less consumption due to the less microalgal biomass). Furthermore, the N and P concentrations in effluent under different influent COD concentrations showed more stability at high SRT levels (4.17 mg/L to 4.53 mg/L and 1.81 mg/L to 1.63 mg/L at HRT =1 and SRT = 40 d, respectively) compared to that at low SRT level (from 8.32 mg/L to 9.91 mg/L and 2.04 mg/L to 1.68 mg/L at HRT =1 and SRT = 10 d, respectively). This could be ascribed to the following reasons: a) the nutrient concentrations of effluent were dominated by the SRT (Equation (7.6)), especially at high SRT level; b) at the low

SRT level, the variation of bacterial biomass concentration controlled by influent COD concentration contributed more on nutrients concentrations of effluent in mass balance equations thus the changes of effluent nutrients concentration became more obvious.

In summary, the COD concentration of influents from 300 mg/L to 600 mg/L did not significantly influence COD removal, nutrient removal, and microalgae biomass concentration except for bacterial biomass concentration at the high SRT level. This indicated that the MB-MSPBR system might have a high potential for high-organic matter and nutrient wastewater treatment.

7.3.2. Model validation of microalgae-bacteria system

The accuracy of the model prediction results was validated by using experimental results from the literature [33, 39]. Figure 7.5 shows the validation of total biomass concentration and the profile of effluent pollutants removal at the steady state period. The modelling results are in good agreement with the experimental results. The maximal relative difference between modelling results and experimental results is less than 40 %, with most of them less than 20 %.

Except for some examples of the nutrient profile, the validation was a reasonable fit between the rest of the experimental and model data. The reason might be attributed to the complex consumption mechanism of nutrients in nature case. As the literature mentioned, the nutrient removal mechanism includes biological (biomass accumulation and microorganism uptake) and physicochemical (chemical precipitation and adsorption) routes [40, 41]. Unlike this model in which nutrients are only consumed by microorganisms, those removal routes would happen together simultaneously to affect the nutrient profiles, thus making them too complicated to predict. As a result, the validation of the nutrient profile didn't exhibit a perfect fit between every model

and experimental data. The results can be further refined by using the kinetic constants and stoichiometric coefficients more suitable for these MB-MSPBR systems (microalgae species), if available, as these parameter values used in the study here are the typical ones but not necessarily perfectly fit for these microalgae species.

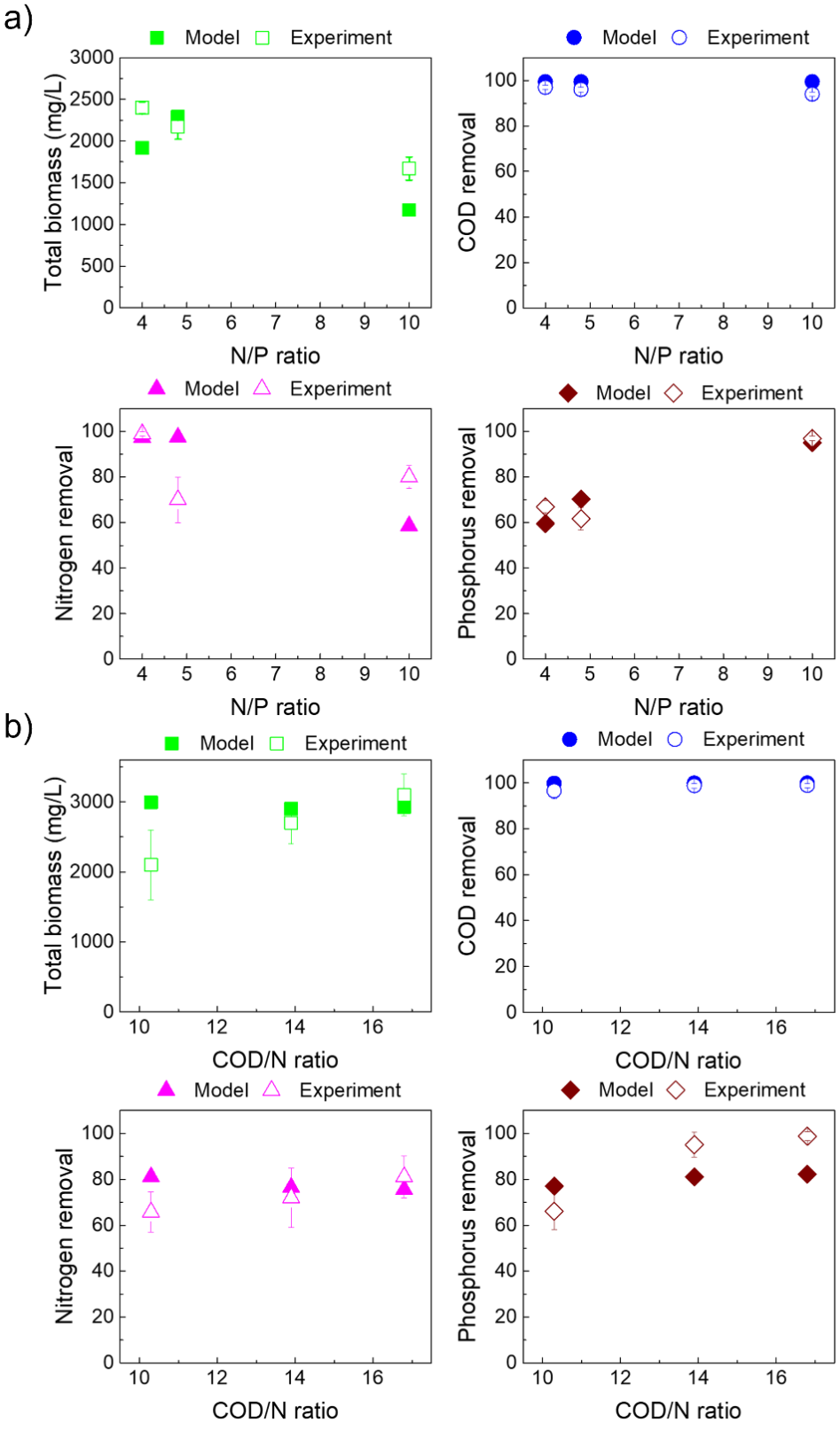

Figure 7.5. Model validation with experimental results of a) Zhang et al.[33] work and b) Lafi et al.[39] work.

7.4. Conclusion

This modelling study investigated the effects of SRT, HRT, and wastewater characteristics (COD level and COD/N ratio) on the biological performance of MB-MSPBR. The model showed that microorganisms prefer shorter HRT for high organic loading and longer SRT for larger biomass accumulation. When it comes to substrate/COD concentration of influent, the substrate/COD didn't show a significant effect on the pollutants (COD, N and P) removal. The reason might be the employed substrate/COD value still does not reach the limitation thus all show the maximum removal efficiency, which may indicate that the microalgae-bacterial system has a high potential for dealing wastewater with concentrated substrate/COD. Moreover, bacterial growth could be promoted by higher substrate/COD concentration of influent. In contrast, the microalgal growth could be restricted, and this behaviour became more evident at low SRT levels. The comparison of experimental results under the same operating conditions also validated the model. The validation showed that the model data reasonably fit with experimental data except for some nutrient profiles. This could be attributed to the complex nutrient removal mechanisms in nature case.

This study has demonstrated that the proposed mathematical models can be used to design of the novel and emerging MB-MSPBR and optimize the biological performance of the MB-MSPBR. And provide new insight into the MB-MSPBR design and operation. Thus, the proposed mathematical models are a powerful tool for optimizing the processes of MB-MSPBR. Further studies can include more parameters, like light intensity, CO_2, and O_2 limitations to refine these models.

7.5. Reference

[1] Sikosana, M.L., Sikhwivhilu, K., Moutloali, R., Madyira, D.M. (2019). Municipal wastewater treatment technologies: A review. Procedia Manufacturing, 35, 1018-1024.
[2] Xu, Q., Huang, Q.S., Wei, W., Sun, J., Dai, X., Ni, B.J. (2020). Improving the treatment of waste activated sludge using calcium peroxide. Water Research, 187, 116440.
[3] Wang, L., Liu, J., Zhao, Q., Wei, W., Sun, Y. (2016). Comparative study of wastewater treatment and nutrient recycle via activated sludge, microalgae and combination systems. Bioresource technology, 211, 1-5.
[4] Aditya, L., Mahlia, T.I., Nguyen, L.N., Vu, H.P., Nghiem, L.D. (2022). Microalgae-bacteria consortium for wastewater treatment and biomass production. Science of The Total Environment, 155871.
[5] Morillas-España, A., Lafarga, T., Sánchez-Zurano, A., Acién-Fernández, F.G., González-López, C. (2022). Microalgae based wastewater treatment coupled to the production of high value agricultural products: Current needs and challenges. Chemosphere, 291, 132968.
[6] Abdelfattah, A., Ali, S.S., Ramadan, H., El-Aswar, E.I., Eltawab, R., Ho, S.H., Elsamahy, T., Li, S., El-Sheekh, M.M., Schagerl, M. (2023). Microalgae-based wastewater treatment: Mechanisms, challenges, recent advances, and future prospects. Environmental Science and Ecotechnology, 13, 100205.
[7] Wollmann, F., Dietze, S., Ackermann, J.U., Bley, T., Walther, T., Steingroewer, J., Krujatz, F. (2019). Microalgae wastewater treatment: Biological and technological approaches. Engineering in Life Sciences, 19, 860-871.
[8] Sial, A., Zhang, B., Zhang, A., Liu, K., Imtiaz, S.A., Yashir, N. (2021). Microalgal–bacterial synergistic interactions and their potential influence in wastewater treatment: A review. BioEnergy Research, 14, 723-738.
[9] Moshood, T.D., Nawanir, G., Mahmud, F. (2021). Microalgae biofuels production: A systematic review on socioeconomic prospects of microalgae biofuels and policy implications. Environmental Challenges, 5, 100207.
[10] Mishra, N., Mishra, S., Prasad, R. (2021). Current Status and Challenges of Microalgae as an Eco-Friendly Biofuel Feedstock: A Review. Present Environment & Sustainable Development, 15, 179-189.
[11] Quijano, G., Arcila, J.S., Buitrón, G. (2017). Microalgal-bacterial aggregates: applications and perspectives for wastewater treatment. Biotechnology Advances, 35, 772-781.
[12] Zhang, B., Li, W., Guo, Y., Zhang, Z., Shi, W., Cui, F., Lens, P.N., Tay, J.H. (2020). Microalgal-bacterial consortia: from interspecies interactions to biotechnological applications. Renewable and Sustainable Energy Reviews, 118, 109563.
[13] Wang, H., Deng, L., Qi, Z., Wang, W. (2022). Constructed microalgal-bacterial symbiotic (MBS) system: Classification, performance, partnerships and perspectives. Science of The Total Environment, 803, 150082.
[14] Unnithan, V.V., Unc, A., Smith, G.B. (2014). Mini-review: a priori considerations for bacteria–algae interactions in algal biofuel systems receiving municipal wastewaters. Algal Research, 4, 35-40.
[15] Posadas, E., García-Encina, P.-A., Soltau, A., Domínguez, A., Díaz, I., Muñoz, R. (2013). Carbon and nutrient removal from centrates and domestic wastewater using algal–bacterial biofilm bioreactors. Bioresource Technology, 139, 50-58.

[16] Solimeno, A., Parker, L., Lundquist, T., García, J. (2017). Integral microalgae-bacteria model (BIO_ALGAE): Application to wastewater high rate algal ponds. Science of the Total Environment, 601, 646-657.
[17] Ramanan, R., Kim, B.H., Cho, D.H., Oh, H.M., Kim, H.S. (2016). Algae–bacteria interactions: evolution, ecology and emerging applications. Biotechnology Advances, 34, 14-29.
[18] Olapade, O.A., Leff, L.G. (2006). Influence of dissolved organic matter and inorganic nutrients on the biofilm bacterial community on artificial substrates in a northeastern Ohio, USA, stream. Canadian Journal of Microbiology, 52, 540-549.
[19] Subashchandrabose, S.R., Ramakrishnan, B., Megharaj, M., Venkateswarlu, K., Naidu, R. (2011). Consortia of cyanobacteria/microalgae and bacteria: biotechnological potential. Biotechnology Advances, 29, 896-907.
[20] Devi, N.D., Tiwari, R., Goud, V.V. (2023). Cultivating *Scenedesmus sp*. on substrata coated with cyanobacterial-derived extracellular polymeric substances for enhanced biomass productivity: a novel harvesting approach. Biomass Conversion and Biorefinery, 13, 2971-2983.
[21] Wang, H., Hill, R.T., Zheng, T., Hu, X., Wang, B. (2016). Effects of bacterial communities on biofuel-producing microalgae: stimulation, inhibition and harvesting. Critical Reviews in Biotechnology, 36, 341-352.
[22] Mayali, X., Azam, F. (2004). Algicidal bacteria in the sea and their impact on algal blooms 1. Journal of Eukaryotic Microbiology, 51, 139-144.
[23] Fuentes, J.L., Garbayo, I., Cuaresma, M., Montero, Z., González-del-Valle, M., Vílchez, C. (2016). Impact of microalgae-bacteria interactions on the production of algal biomass and associated compounds. Marine Drugs, 14, 100.
[24] Buhr, H., Miller, S. (1983). A dynamic model of the high-rate algal-bacterial wastewater treatment pond. Water Research, 17, 29-37.
[25] Sánchez-Zurano, A., Rodríguez-Miranda, E., Guzmán, J.L., Acién-Fernández, F.G., Fernández-Sevilla, J.M., Molina Grima, E. (2021). ABACO: a new model of microalgae-bacteria consortia for biological treatment of wastewaters. Applied Sciences, 11, 998.
[26] Sanchez Zurano, A., Gomez Serrano, C., Acién‐Fernández, F.G., Fernández‐Sevilla, J.M., Molina‐Grima, E. (2021). Modeling of photosynthesis and respiration rate for microalgae–bacteria consortia. Biotechnology and Bioengineering, 118, 952-962.
[27] Xiao, Z., Zheng, Y., Gudi, C.R., Liu, Y., Liao, W., Tang, Y.J. (2021). Development of a kinetic model to describe six types of symbiotic interactions in a formate utilizing microalgae-bacteria cultivation system. Algal Research, 58, 102372.
[28] Y Liao, P Fatehi, Liao, B. (2023). A study of theoretical analysis and modelling of microalgal membrane photobioreactors Not published yet.
[29] Lee, E., Jalalizadeh, M., Zhang, Q. (2015). Growth kinetic models for microalgae cultivation: A review. Algal research, 12, 497-512.
[30] Bekirogullari, M., Figueroa-Torres, G.M., Pittman, J.K., Theodoropoulos, C. (2020). Models of microalgal cultivation for added-value products-A review. Biotechnology Advances, 44, 107609.
[31] Solimeno, A., García, J. (2017). Microalgae-bacteria models evolution: from microalgae steady-state to integrated microalgae-bacteria wastewater treatment models–a comparative review. Science of the Total Environment, 607, 1136-1150.
[32] Gao, S., Hu, C., Sun, S., Xu, J., Zhao, Y., Zhang, H. (2018). Performance of piggery wastewater treatment and biogas upgrading by three microalgal cultivation technologies under different initial COD concentration. Energy, 165, 360-369.

[33] Zhang, M., Leung, K.-T., Lin, H., Liao, B. (2020). The biological performance of a novel microalgal-bacterial membrane photobioreactor: Effects of HRT and N/P ratio. Chemosphere, 261, 128199.
[34] Rittmann, B.E., McCarty, P.L. (2001). Environmental biotechnology: principles and applications. McGraw-Hill Education: New York.
[35] Segredo-Morales, E., González, E., González-Martín, C., Vera, L. (2022). Secondary wastewater effluent treatment by microalgal-bacterial membrane photobioreactor at long solid retention times. Journal of Water Process Engineering, 49, 103200.
[36] Katam, K., Bhattacharyya, D. (2020). Effect of solids retention time on the performance of alga-activated sludge association in municipal wastewater treatment and biofuel production. Journal of Applied Phycology, 32, 1803-1812.
[37] Zou, H., Rutta, N.C., Chen, S., Zhang, M., Lin, H., Liao, B. (2022). Membrane Photobioreactor Applied for Municipal Wastewater Treatment at a High Solids Retention Time: Effects of Microalgae Decay on Treatment Performance and Biomass Properties. Membranes, 12, 564.
[38] Zhang, M., Leung, K.T., Lin, H., Liao, B. (2021). Effects of solids retention time on the biological performance of a novel microalgal-bacterial membrane photobioreactor for industrial wastewater treatment. Journal of Environmental Chemical Engineering, 9, 105500.
[39] Lafi, H., Panu, U., Liao, B. (2023). Effect of the organic carbon to nutrient (N and P) ratio on the biological performance of a microalgal–bacterial membrane photobioreactor. Environmental Science: Water Research & Technology, 9, 2021-2030.
[40] Daigger, G.T., Littleton, H.X. (2014). Simultaneous biological nutrient removal: A state-of-the-art review. Water Environment Research, 86, 245-257.
[41] Fallahi, A., Rezvani, F., Asgharnejad, H., Nazloo, E.K., Hajinajaf, N., Higgins, B. (2021). Interactions of microalgae-bacteria consortia for nutrient removal from wastewater: A review. Chemosphere, 272, 129878.

Chapter 8: Conclusion and future studies recommendations

8.1. Conclusions

In conclusion, the fundamental studies of microalgal biofilm formation and microalgal/microalgal-bacterial membrane photobioreactors (M-MSPBR and MB-MSPBR) provide valuable new insights into the development of sustainable and efficient MPBR systems for microalgae cultivation and wastewater treatment. The studies have revealed that biofilm formation can enhance microalgae growth rate, biomass productivity, and nutrient uptake. Additionally, using bacteria in microalgal membrane photobioreactors can improve light utilization efficiency, reduce biomass loss, and mitigate contamination issues associated with traditional photobioreactors. This study has investigated the microalgal biofilm formation mechanism by examining the interactions between cell substrate and environmental conditions. The results were discussed in the following sections:

(1) Among the five tested materials (nylon, polypropylene, polyurethane rubber, polytetrafluoroethylene, and silicone rubber), nylon exhibited the highest wet biofilm attachment of *Chlorella vulgaris*, reaching up to 514.3 g/m^2 over 16 days of cultivation. The hydrophilic *Chlorella vulgaris* did not adhere better to the highest hydrophobic silicone rubber. On the contrary, the thickest biofilm is achieved on nylon coupons with the lowest difference between the SFE and the *Chlorella vulgaris* cells. These results showed that the contact angle and hydrophobicity did not play the main role in the cell attachment of *Chlorella vulgaris*. Moreover, bounded EPS positively impacted the initial adhesion of microalgae biofilm and served a role in maintaining the biofilm matrix in the thickening period. As a result, bounded EPS productivity increased with

biofilm growth. For almost all materials (except polypropylene), SFE plays a significant role in biofilm adhesion. Based on this argument, nylon comes first in selectivity for the further extractive microalgal biofilm membrane reactor study to optimize microalgae cells' adhesion during the early cultivation period.

(2) Among the three test microalgae species (*Phormidium tenue*, *Monoraphidium braunii*, and *Ankistrodesmus falcatus*), *Monoraphidium braunii* exhibited the highest wet biofilm attachment on nylon material surface at 125 rpm (187.40 g/m^2) over 16 days of cultivation due to its lowest difference of surface free energy between cell-substrate interaction, which again proved SFE plays a significant role at microalgal adhesion performance. Moreover, the hydrodynamic condition also has an influential role in cell-substrate interaction. When the stirring speed of the reactor decreased to 60 rpm, the highest attachment showed on *Ankistrodesmus falcatus* biofilm (144.23 g/m^2). The effects of the hydrodynamic condition of the cultivation environment depended on the microalgae species due to their tolerance of shear force. Higher shear stress below critical limitation can promote biofilm formation due to higher mass transfer interaction. Once the shear stress is over the critical value, biofilm detachment happens.

(3) The investigation of the three microalgae species' initial adhesion (*Phormidium tenue* (CPCC 424), *Monoraphidium braunii* (CPCC 625), and *Ankistrodesmus falcatus* (CPCC 669)) on different materials (polytetrafluoroethylene, polydimethylsiloxane and polyurethane) were run by QCM-D testing. The *Phormidium tenue* exhibited the highest deposition throughout three materials, followed by *Monoraphidium braunii* in PTFE and PUR surfaces. In contrast, the second highest deposition on the PDMS sensor was *Ankistrodesmus falcatus*. The surface properties of the sensor and microalgae cells affected the adhesion performance during the QCM test. The higher the surface free energy, the higher the deposition should be. Moreover, the Lewis acid-base

interaction seems to play a major positive role in the interactions between microalgae and sensors. The microalgal layers exhibited viscoelastic properties in this study, while *Phormidium tenue* and *Monoraphidium braunii* layers show a dynamic viscous characteristic compared to the *Ankistrodesmus falcatus* layer. The result obtained from the QCM test exhibited similar trends to those of reactor experiments, which implied that QCM could be used as a rapid and effective tool to simulate the real-time adhesion behaviours between microalgal cells and substratum.

(4) The modelling studies investigated the operating parameters (HRT, SRT, and influent pollutants ratio) effects on membrane photobioreactor performance (microorganism biomass concentration and pollutant removal). For the mono-microalgal-based system, biomass production and nutrient removal increased with the increase of HRT and SRT. At the same time, they declined in either extremely low or high N/P ratio of influent. The best conditions in this study are considered HRT = 1 day, SRT = 40 days and N/P ratio around 8 based on the high biomass production and frequent harvesting period. In the microalgal-bacterial-based system, the model was processed under the effects of HRT, SRT and substrate/COD concentration of influent. The HRT and SRT exhibited a similar trend as the mono-microalgae system. The substrate/COD didn't exhibit a significant effect on the pollutant removal in this model, which could be ascribed to the high tolerance of this model system on high COD concentration influent. Moreover, COD positively affects bacterial biomass production but has a minor negative on microalgal biomass production. The model was also validated by comparing experimental results under the same operating conditions and shows a reasonable fitting with experimental studies. This model can shorten the experiment setting time and provide ideal operating parameters for laboratory research., leading to a more efficient investigation during the laboratory work.

In conclusion, the studies on microalgal biofilm formation have shown promising results for developing sustainable and efficient methods for wastewater treatment and biofuel production. The formation of biofilms by microalgae on surfaces can enhance their growth and productivity and provide a natural method for water filtration and purification. Moreover, using bacterial co-cultures in membrane photobioreactors can further improve the performance of microalgal systems by increasing nutrient uptake and providing additional metabolic pathways. A holistic approach that combines engineering, microbiology, and bioprocess optimization is necessary to develop sustainable microalgal cultivation systems. These findings can be applied to designing and optimizing emerging microalgal biofilm MPBR such as membrane carbonated microalgal biofilm reactor (MCMBR) and extractive membrane microalgal biofilm (EMMBR) reactor for wastewater treatment and bioremediation.

8.2. Future Research Suggestions

Based on the fundamental studies of microalgal biofilm formation and microalgal-bacterial membrane photobioreactors, future research directions could further advance these technologies.

First, more research could investigate the synergy effect by multiple conditions for microalgal biofilm formation, which will be more complicated than individual effect systems. In addition, further research could also consider the genetic and metabolic mechanisms underlying biofilm formation in microalgae, which could lead to developing strategies for enhancing biofilm growth and productivity.

Second, there is a need for more research on the use of bacterial co-cultures in microalgal-bacterial membrane photobioreactors. These investigations could focus on beneficial bacteria, such as nitrifying and photosynthetic bacteria, further promoting microalgal biofilm production.

Furthermore, more research could be conducted on the interactions from the genetic aspect between microalgae and bacteria in these systems, which could help to identify novel metabolic pathways and optimize biomass and product yields.

Third, further research could be conducted on the scale-up and commercialization of microalgal biofilm membrane photobioreactor systems. This could involve the development of engineering approaches for large-scale cultivation and harvesting of microalgae, as well as optimizing downstream processing for biofuel production and high-value bioproducts. Additionally, more research could be conducted on the economic feasibility of these technologies, including evaluating their environmental and social impacts and identifying potential market opportunities and barriers to adoption.

Overall, future research in these areas could further advance the development of sustainable and efficient methods for wastewater treatment, biofuel production, and bioremediation, which are critical for addressing the challenges of global environmental sustainability.